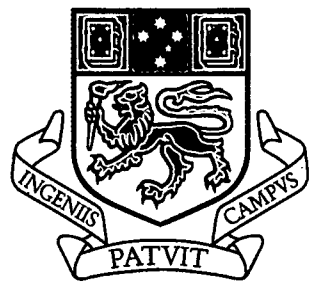

UNIVERSITY
OF TASMANIA

N,E Heteroleptic Ligands in the Heck Reaction and Other Carbon – Carbon Bond Formation Processes

By

Roderick Charles Jones, BSc, BSc(Hons)

Submitted in fulfillment of the requirements for the Degree of

Doctor of Philosophy

School of Chemistry
University of Tasmania
Hobart, Tasmania

September, 2009

Declaration

This thesis contains no material which has been accepted for a degree or diploma by the University of Tasmania or any institution and, to the best of my knowledge and belief, contains no material previously published or written by another person except where due acknowledgement is made in the text of the thesis.

This thesis may be made available for loan and limited copying in accordance with the Copyright Act, 1968.

Roderick C. Jones

May 2009

Abstract

The development of a simple 'one-pot' synthesis for the preparation of substituted 2-organothiomethyl- and 2-organoselenomethylpyridines has allowed the synthesis of six new ligands (4-MepyCH$_2$SMe, 6-PhpyCH$_2$SMe, 4-MepyCH$_2$SPh, 6-PhpyCH$_2$SPh, 4-MepyCH$_2$SePh, and 6-PhpyCH$_2$SePh), together with an improved and more direct route to known ligands (pyCH$_2$SMe, 6-MepyCH$_2$SMe, pyCH$_2$SPh, 6-MepyCH$_2$SPh, pyCH$_2$SeMe, pyCH$_2$SePh, and 6-MepyCH$_2$SePh). These bidentate heteroleptic ligands were successfully used in the synthesis of dihalogenopalladium(II) and platinum(II) complexes, which were isolated in high yield and were characterised as predominantly square planar complexes of the form *cis*-MX$_2$(*N*,*E*) (X = halogen, E = S, Se).

X-ray diffraction techniques allowed a systematic structural study of the dihalogenopalladium(II) and platinum(II) complexes formed, producing several sets of isomorphous complexes giving a detailed insight into the coordination chemistry of palladium(II) and platinum(II). The structural studies confirm the formulation of new ligands and complexes, and identified bond length trends Pd–N > Pt–N and Pd–E > Pt–E matching earlier reports of isomorphous organometallic complexes of palladium and platinum, but the observed trend Pd–Cl$_N$ < Pt–Cl$_N$ is opposite to a literature report for an organometallic complex.

The influence of a 6-substituent in the pyridine ring on structural chemistry is evident. Replacement of hydrogen by methyl results in a significant Me···X steric interaction which can be relieved by formation of a larger dihedral angle between the pyridine ring and the coordination plane for *cis*-PtX$_2$(*N*,*S*), but formation of an array of different structures for palladium involving *trans*-PdX$_2$(*N*,*E*) motifs in the dimer [PdI$_2$(μ-*N*,*Se*)]$_2$ (N~Se = 6-methyl-2-phenylselenomethylpyridine), the trimer [PdCl$_2$(*N*,*S*)]$_3$, and *trans*-PdI$_2$*N*$_2$ (monodentate ligand) in PdI$_2$(*N*,*S*) (*N*,*S* = 6-methyl-2-phenylthiomethylpyridine). If the substituent on the 6-position of the pyridyl ring is a phenyl group, *ortho*-metallation of the ligand occurs producing complexes in which a tridentate heteroleptic ligand [*C*,*N*,*S*]$^-$ is present.

The catalytic performance of the dichloropalladium(II) complexes synthesised in this study were tested in the Heck and Suzuki reactions. The structurally simple and chemically stable pre-catalyst $PdCl_2(pyCH_2SMe)$ gave the highest yields achieving TONs up to 10^6 for aryl iodides and bromides in the Heck reaction. Closely related selenium containing ligands, or ligands with a 6-methyl substituent on the pyridyl ring, or cyclopalladated species, are much less active. Activation of aryl chlorides using $PdCl_2(pyCH_2SMe)$ was also achieved using Bu^n_4NCl as a solvent, giving higher yields for both 4-chloroacetophenone and chlorobenzene than that obtained under the same conditions using *N,N*-dimethylacetamide as a solvent.

Ligand synthesis for the *N,S*-system was developed to include a ligand able to be readily attached to organic polymers via reaction of the hydroxyl group in 4-(4-hydroxyphenyl)-2-methylthiomethylpyridine with benzyl halide groups of organic polymers. This ligand was anchored to Merrifield and Wang beads, and a porous monolith of similar formulation, poly(chloromethyl-*co*-divinylbenzene), followed by coordination to dichloropalladium(II). These three heterogeneous catalysts were successfully tested in Heck and Suzuki reactions and were shown to be highly active for aryl iodides and bromides, including double Heck products with a >99% stereoselectivity in product formation. Under similar conditions, the heterogeneous catalyst displayed higher activity than the model complex $PdCl_2(4\text{-}(4\text{-}BnOC_6H_4)pyCH_2SMe)$. A flow-through microreactor was developed, based upon a 250 μm internal diameter capillary containing monolith synthesized *in situ* and funtionalised with precatalyst in the same manner as beads and bulk monolith, and successfully trialled in the Heck and Suzuki reactions.

"Tetraaryl" products are synthesised in the catalytic reaction of aryl iodides and terminal aryl acetylenes at 120 °C using $PdCl_2(pyCH_2SMe)$ as a palladium(II) pre-catalyst, *apparently* the first reported case of such products synthesised using Sonogashira conditions. Although a full and extensive study of the identity of the formed products, and possible mechanism for the reaction, are yet to be undertaken, it is of interest that 4-iodonitrobenzene and phenylacetylene gave 1,3,5-triphenyl-2-(4-nitrophenyl)benzene as the sole product in appreciable yield, with X-ray structure analysis confirming the structure and identity of the compound.

Acknowledgements

To my supervisors, Prof. Allan Canty and Dr. Michael Gardiner, thankyou for your constant support, enthusiasm and guidance throughout my canditure, I feel privileged to have been part of your research groups. Special thanks must to Dr. Vicki-Anne Tolhurst without whom I would not be doing this project.

Thanks must go to Dr. Thomas Rodemann without your help as a teacher and a mentor, particularly in the laboratory, I would not be completing this thesis. You made the lab a fun and enjoyable, if not confusing place to work. A thank you must also go to the other members and visitors to the Canty research group past and present who have given input and guidance over the years.

To the collective research groups of Prof Allan Canty, Dr. Michael Gardiner, Dr. Jason Smith and Prof. Brian Yates I greatly appreciate all the help you have given me over the years.

Thank you to the staff of the Central Science Laboratory for analysis of samples and providing expert technical advice. In particular, thank you Dr. Noel Davies, Mr. Marshall Hughes, Dr. Ashley Townsend and Dr. Graham Rowbottom.

Thank you to Prof. Allan White and Dr. Brian Skelton of the University of Western Australia for X-ray structure determinations.

To the staff and students of the School of Chemistry who have made it a fantastic environment to work in and have been supportive and helpful in the last few years. Thank you all.

Special thanks must go to the Australian Research Council and the University of Tasmania for project funding and scholarship funding.

To Dr. Éadaoin Tyrrell, without whose help I would not have survived the PhD experience, go raibh míle maith agat.

Finally, my biggest thank you to my family especially to my parents, whose endless support has made achieving this degree possible.

List of Abbreviations

APCIMS	atmospheric pressure chemical ionization quadrupole mass spectrometry
Ar	aryl
Bu	butyl
Bz	benzyl
CMS	(chloromethyl)styrene
CO	carbon monoxide
DMA	*N*,*N* – dimethylacetamide
DMF	dimethylformamide
DMSO	dimethylsulfoxide
DVB	divinyl benzene
EI	electron ionization
FID	flame ionisation detection
GC	gas chromatography
Hz	Hertz
LSIMS	liquid secondary ionization mass spectrometry
M^+	molecular ion
Me	methyl
MS	mass spectrometry
Na/K	sodium/potassium alloy
NMR	nuclear magnetic resonance
OAc^-	acetate anion
Ph	phenyl
Pr	propyl
Py	pyridyl
SEM	scanning electron micrograph
THF	tetrahydrofuran
TMS	trimethylsilyl
Tol	4-methylphenyl
TON	turn over number

Table of Contents

Chapter One

The Role of Heteroleptic Ligands in Catalysis

1.1 Heteroleptic Ligands

In recent years there have been great advances in the development of palladium catalysed carbon-carbon and carbon-heteroatom bond formation processes. In particular, Sonogashira, Heck, Suzuki, and Stille coupling reactions have been utilised to contribute significant advances in synthetic chemistry, in no small part in the fields of natural products and materials.[1-4] These and other advances have shown that ligand design is becoming an increasingly important part of synthetic coordination chemistry, organotransition metal chemistry and catalytic applications.[5-16]

The chemistry of bidentate ligands which contain donor groups with differing lability is being increasingly studied in synthetic and catalytic chemistry.[17-20] These ligands are known as bidentate heteroleptic ligands. The differing properties of the constituent donor atoms often leads to quite different behaviour in their complexes as compared with the analogous symmetrical homoleptic systems.[8,12,22] The ligands are often hemilabile in nature if they contain two significantly different donor atoms or groups, *e.g.*, "hard" and "soft" donors. One of the donor atoms can reversibly provide open coordination sites at the metal during reactions, or in a catalytic cycle. This usually occurs by a dissociative process or is initiated by coordination of other ligands or a solvent molecule.[21] Coordination by both donor atoms simultaneously can act to stabilise species occurring in the cycle.[11,22] Transition metal complexes containing a variety of phosphorus-, nitrogen- and carbon-based heteroleptic ligands have been utilised in a wide range of homogeneous catalysis coupling reactions, and continue to be a focus of research.[23,24]

The concept of hemilability of heteroleptic ligands was introduced 20 years ago by Jeffery and Rauchfuss in reporting the synthesis and reactivity of ruthenium complexes containing bidentate neutral *P,O* donor ligands with CO and Bu^{t}NC.[25] Although the

phenomenon of hemilability itself was observed earlier,[26-30] the oxygen donor of the ligand was shown to reversibly coordinate to the metal centre to allow the coordination of either CO or Bu^{t}NC. The concept of hemilabile heteroleptic ligands has since grown to encompass various situations involving polydentate ligands containing at least two different types of chemical functionality capable of binding to metal centres,[20] **Figure 1.1.**

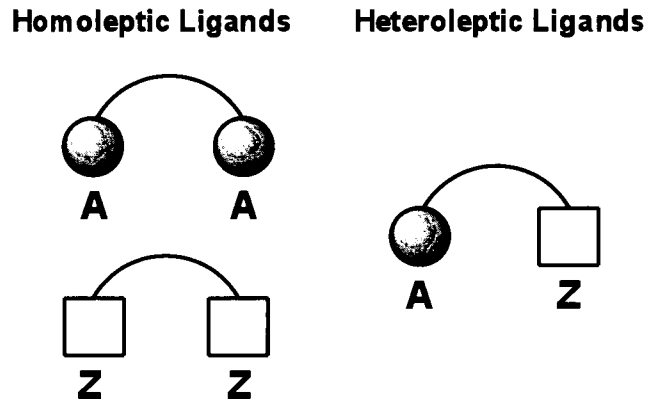

Figure 1.1 Homoleptic ligands contain donor atoms of the same type (**A~A**, **Z~Z**), while heteroleptic ligands contain two chemically different donor atoms (**A~Z**), where A is the stronger donor.

Hemilabile heteroleptic ligands were first encountered in mononuclear complexes, with numerous examples now reported. The concept has since been extended to include dinuclear complexes and metal clusters, where the labile coordination site does not need to be at the metal ligated by the strong donor **A**, **Figure 1.2.**[20] This concept was illustrated by Manzano in which ruthenium derivatives were synthesised containing the heteroleptic ligand 2-(diphenylphosphanyl)-1-methyl-1*H*-imidazole in two different possible coordination modes, *P,P* and *P,N*.[31] However, for this study the focus is on mononuclear complexes.

Typically, the donor atoms of heteroleptic ligands are chosen to be as different from each other as possible if hemilability is desired. This increases the differences in the chemoselectivity of the constituent donor atoms and subsequent interactions with the metal centre(s).[18] Furthermore, these differences will influence the bonding/reactivity of

other ligands bound to the metal, particularly in the *trans* position to each donor, allowing the possibility of novel and unprecedented properties and reactivity for the resulting metal complexes.[18]

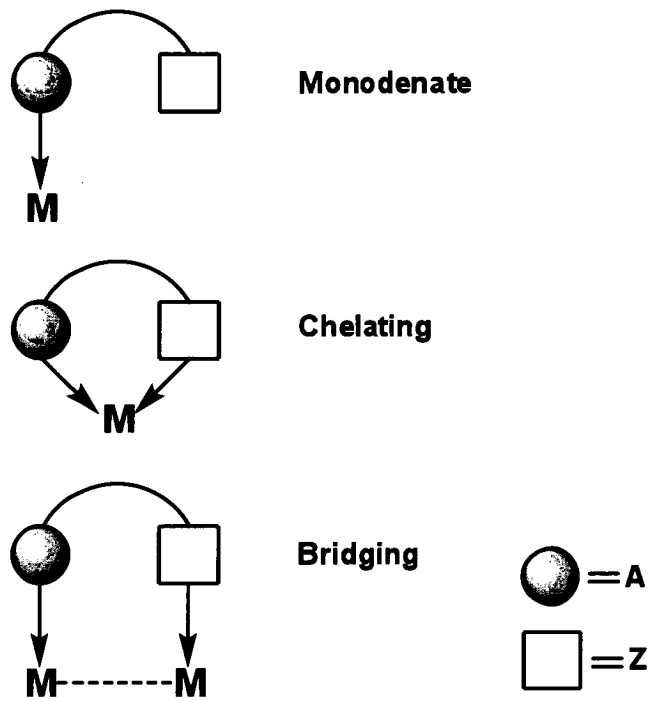

Figure 1.2 Binding modes of heteroleptic ligands where, in the bridging case, it can be with or without the presence of metal-metal bonding.

1.2 Types of Hemilability

In order for a heteroleptic ligand to exhibit pronounced hemilability it must have one substantially labile donor function (**Z**) which can reversibly bind to the metal centre, while the other donor group (**A**) remains firmly bound at all times, **Scheme 1.1**. Recoordination of **Z** to the metal centre may restore the complex to its original state, as in an equilibrium process, or recoordination may take place after a chemical transformation at the metal centre, such as an oxidative addition reaction.[18,20,21]

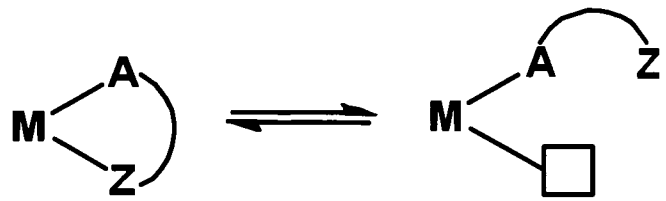

Scheme 1.1 Dissociation and re-coordination of the more labile donor **Z** to the metal centre gives the ligand a hemilabile nature.

The equilibrium shown in **Scheme 1.1** is typically encountered with metal centres which have easily variable coordination numbers: 4 ⇋ 3 (eg. d^{10} ML_4/ML_3 complexes),[16] 5 ⇋ 4 (e.g. d^8 ML_5/ML_4 complexes),[32] 6 ⇋ 5 (e.g. d^6 ML_6/ML_5 complexes).[33]

Braunstein[18] differentiated three types of hemilabile behaviour. **Type I** hemilability involves the spontaneous formation of a vacant coordination site after a partial dissociation of the hemilabile ligand, **Scheme 1.1**. This form of hemilabile behaviour is exemplified in ruthenium complexes in which the oxygen donors of *P,O* heteroleptic ligands reversibly dissociate to allow incoming acetylenes to interact, forming vinylideneruthenium complexes, **Scheme 1.2**.[34]

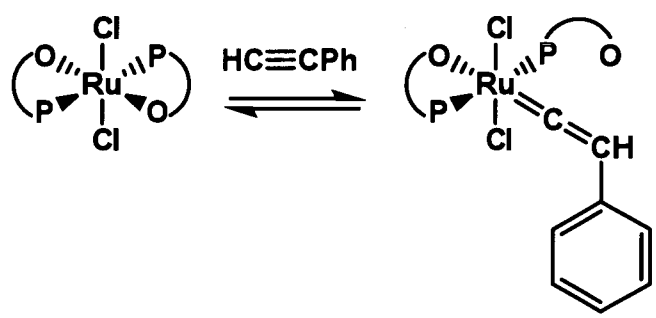

Scheme 1.2 Dissociation of the more labile donor oxygen donor in $Pr^i_2PCH_2CH_2OMe$, allows a vacant coordination site for phenylacetylene to interact with the metal centre.

Type II hemilability involves intramolecular competition between donor functions on the same ligand, **Scheme 1.3**.

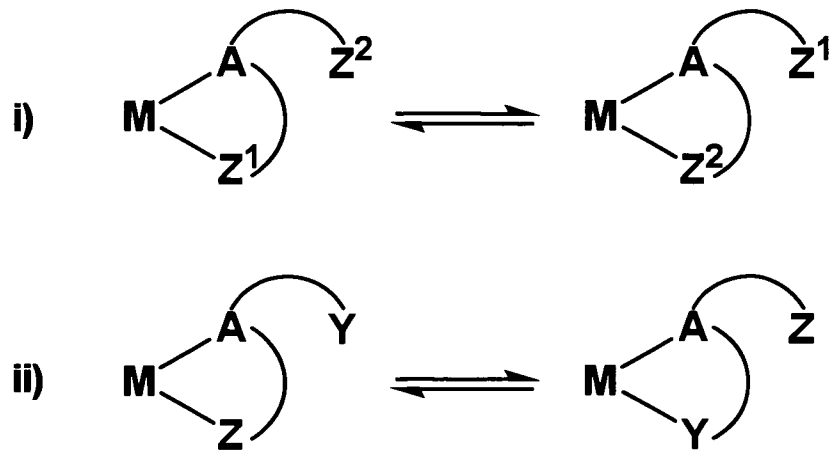

Scheme 1.3 Type II hemilability involves intramolecular competition between two donor functions that are (**i**) chemically equivalent, or (**ii**) chemically inequivalent.

An example of **Type II** (**i**) hemilabile behaviour is seen in a fluxional process involving chemically equivalent pyridine donor groups of terpyridine ligands in tetracarbonyl complexes of Cr, Mo and W,[35] **Scheme 1.4**.

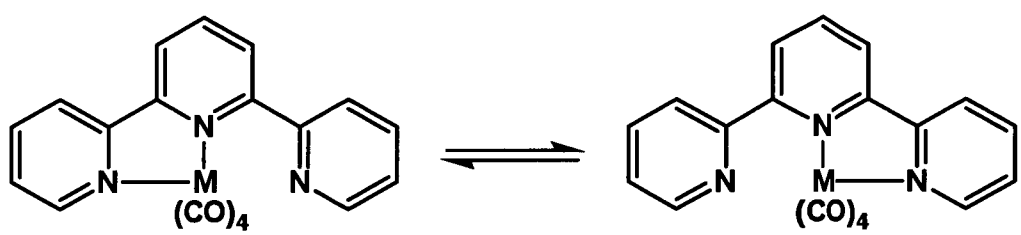

Scheme 1.4 Hemilability involving pyridine-group exchange.

An example of **Type II** (**ii**) behaviour is displayed by cationic methallylnickel complexes in which the nickel centre is bound by a chelating phosphine and interchanging pyridine and carbonyl donor functionalities, **Scheme 1.5**.[36]

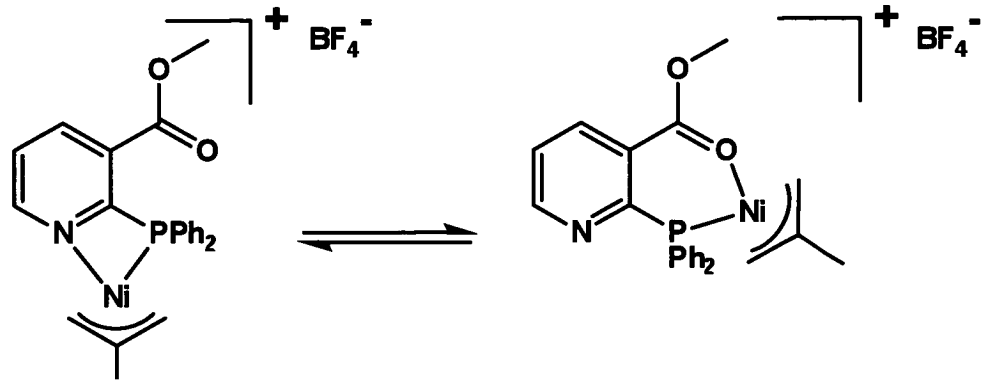

Scheme 1.5 Hemilability involving pyridine/ester group exchange.

For **Type III** hemilability, the coordination of an external ligand or reduction takes place, thereby breaking the labile ligand-metal bond, **Scheme 1.6**. The nature of the external ligand, **Y**, can be a small molecule, such as CO, a solvent molecule, or electrons in the case of redox reactions.[11,22]

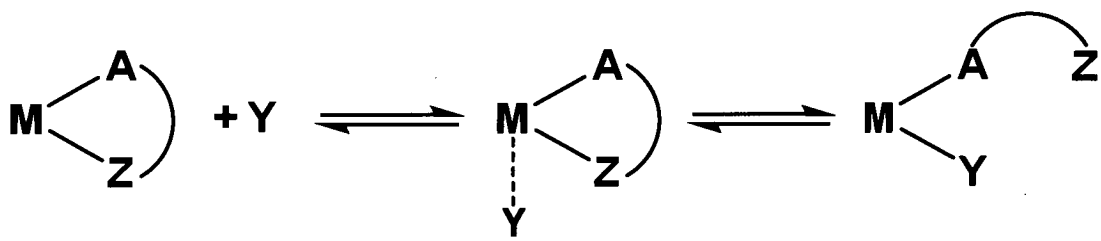

Scheme 1.6 Hemilability induced by coordination of an external ligand or solvent molecule (**Y**).

Jutzi and Siemeling showed that the more labile amine donor of dimethylaminoethyl-tetramethylcyclopentadienyl is reversibly displaced by an incoming *t*-butylisocyanide, **Scheme 1.7**.[37]

Heteroleptic ligands may, *via* various types of hemilability, stabilise reactive transition metal centres throughout catalytic cycles. This behaviour provides a strong rationale for the exploration of this class of ligand in coordination chemistry, and particularly in catalytic chemistry. Complexes containing heteroleptic ligands have been successfully utilised in a range of catalytic reactions including hydrogenation,[38-40] methanol carbonylation,[41,42] hydroformylation,[43,44] epoxidation of alkenes,[45] allylation,[46]

codimerisation of ethene and styrene,[47,48] and cyclotrimerisation of dimethyl acetylenedicarboxylate.[49] Further to this, as the labile donor atoms are easily and reversibly displaced from a metal centre by small donor molecules, heteroleptic ligands are useful for small molecule activation[50] and in some cases small molecule sensing.[51] Also, the often weak chelating ability of a heteroleptic ligand has been shown to stabilise certain transition metal complexes relative to their more reactive, non-chelated analogues.[52-54] Examples of transition metal complexes and their respective coordination chemistry displaying all three types of hemilabile behaviour can be found in the extensive review by Slone, Wienberger, and Mirkin.[20]

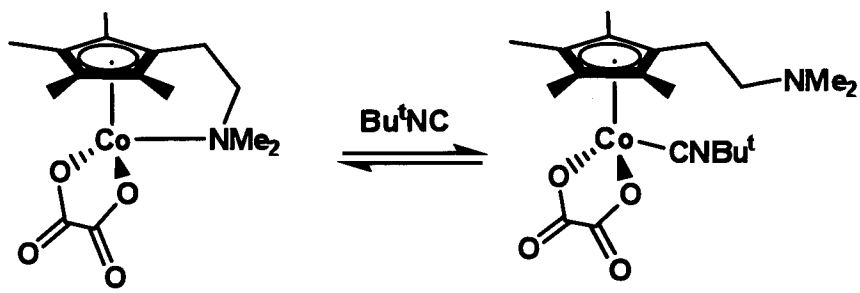

Scheme 1.7 Hemilability induced by coordination of an isocyanide functionality.

1.3 Types of Heteroleptic Ligands

There are many different types of heteroleptic ligands containing carbon, nitrogen, oxygen, phosphorus and, to a much lesser extent, chalcogen and arsenic donor atoms.[20] Of these, it is the heteroleptic ligand systems based upon phosphorus and/or nitrogen donor functionalities that are most common. In fact, the application of transition metal complexes for homogeneous catalysis has been established for a wide variety of heteroleptic ligands containing *P,O*,[55] *P,N*,[56] *P,S*,[21] and [*N*,O]$^{-}$[57] donor atoms. For more examples of heteroleptic ligands in catalysis see Slone, Wienberger, and Mirkin.[20] Heteroleptic ligands based upon pyridine moieties and various weakly donating groups are well established and have found great success in coordination and catalytic chemistry,[20] *e.g.*, rhenium(I) complexes of 2,6-diacetylpyridine which exhibit a "tick-tock-twist" mechanism for a 1,4-metallotropic shift, **Scheme 1.8**.[58]

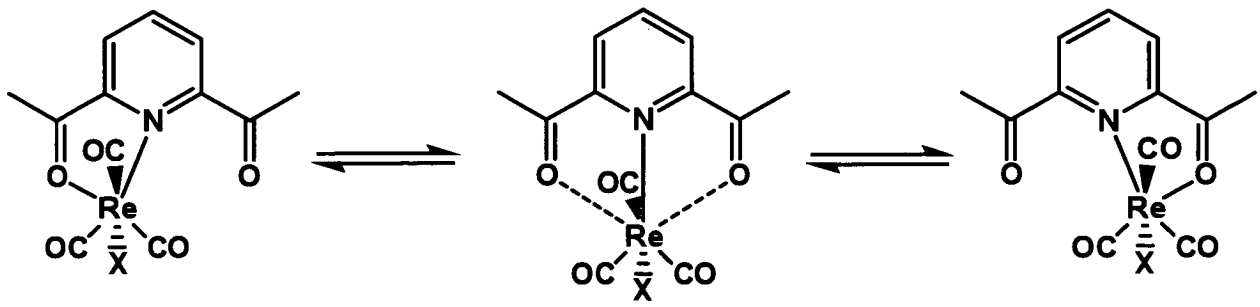

Scheme 1.8 Fluxional behaviour of a pyridine-ketone ligand on a rhenium centre.

1.4 Palladium Catalysed Reactions - The Heck Reaction

1.4.1 Definition and Applications

The Heck reaction that is in use today has evolved considerably from its original guise as the stoichiometric arylation of alkenes with arylmercury(II) compounds.[59-61] Mizoroki[62] and Heck[63] discovered independently that aryl iodides could be used as substitutes for arylmercury(II) compounds in the reaction. This significant breakthrough allowed the reaction to become a viable process for C–C bond formation as it permitted the use of catalytic amounts of palladium by oxidation of the Pd^0 product by the aryl iodide reagent. The reaction has been further developed over subsequent years to allow the coupling of related reagents such as aryl bromides,[64] chlorides,[65] triflates,[66] tosylates,[67] mesylates[68] and aryldiazonium salts[69] (**Scheme 1.9**) in both inter- and intramolecular reactions, **Scheme 1.10**. This strategy can also be used to couple vinyl halides to alkenes.[70]

An important advance in the Heck reaction has been the synthesis of chiral ligands for the development of chiral palladium pre-catalysts leading to a high degree of enantiocontrol for certain substrates.[71-73] In most recent developments of the protocol, aryl halides are replaced with organoboron reagents in the presence of a stoichiometric amount of copper(II) acetate as a reoxidant for palladium(0).[74]

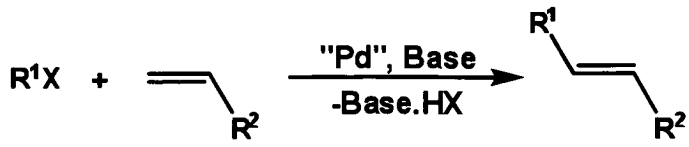

R¹ = aryl, vinyl
R² = Electron donating group, electron withdrawing group
X = Halide, OTf, OTs

Scheme 1.9 The generalised Heck coupling reaction

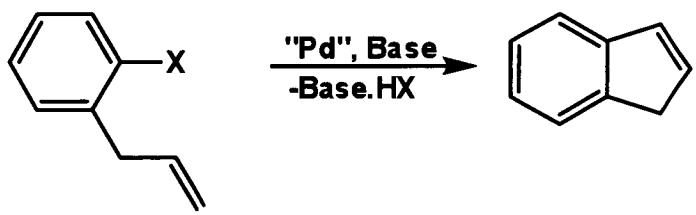

Scheme1.10 Intramolecular example of the Heck reaction

During the first two decades after its inception, the main direction of research for the Heck reaction was examination of its versatility as a synthetic tool.[75] With this proven, in the last ten years there has been a distinct focus upon mechanistic studies, and extension of the Heck reaction to carbon-heteroatom bond-forming reactions.[76] Recent studies include cross-coupling between sp^3–hybridised partners,[77] activation of aryl chlorides,[78,79] and a shift toward making the Heck reaction a more economical and practical tool of synthesis in order for it to be used industrially, where it is still rarely utilised.[80-82] From this versatility the Heck reaction is one of the simplest ways to obtain variously substituted alkenes, dienes and other unsaturated compounds, many of which are useful as pharmaceutical intermediates, *e.g.*, Taxol backbone (**I**),[83] UV sunscreens (**II**),[83] dyes[84] and herbicides such as Prosulfuron (**III**).[85]

Numerous current reports on new palladium pre-catalysts, mechanistic discoveries, or natural product synthesis. Extensive reviews of the field have appeared, *e.g.*, by Beletskaya,[84,86] Fu,[78,79] Farina,[75] and de Meijere.[87]

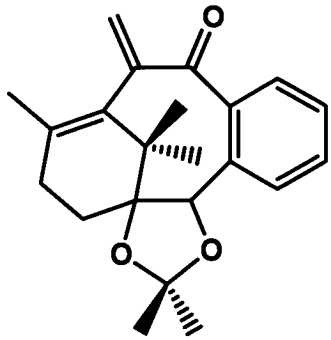

I

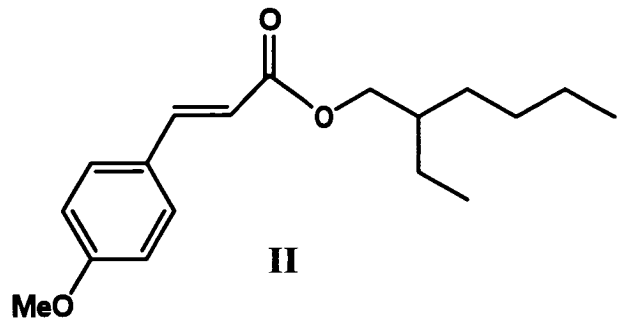

II

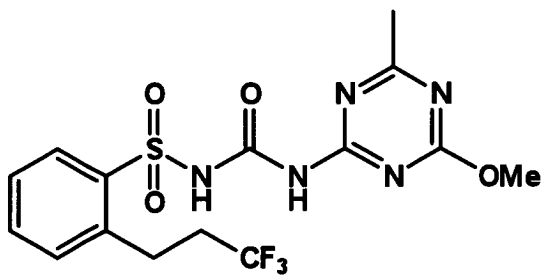

III

One of the most important aspects of the Heck reaction that differentiates it from related palladium catalysed coupling reactions such as Negishi, Kumada, and Suzuki reactions, is the absence of organometallic reagents to facilitate a transmetallation step, rendering this synthetic protocol highly desirable in industrial and pharmaceutical synthesis.[80]

1.4.2 The Heck Reaction Mechanism

There have been two general mechanisms proposed for the Heck reaction over the years; a Pd(0)/(II) interconversion and a Pd(II)/(IV) interconversion for intramolecular coordination containing Pd^{II}–C pre-catalysts. There have been suggestions that a Pd(II)/(IV) mechanism may be present.[88,89] However, the evidence for this is poor as it has been shown that for the majority of cases the palladacycles involved, instead of proceeding *via* Pd(IV), act as reservoirs of palladium metal present as nanoparticles or proceed in some other way *via* a Pd(0)/(II) cycle.[90-95] The Pd(0)/(II) cycle however, is the generally accepted mechanism for the Heck reaction and involves an initial oxidative addition of an organohalide to a palladium(0) catalyst.

Molecular pre-catalysts for the Heck reaction may be either Pd(0) complexes, *e.g.*, $Pd(PPh_3)_4$, or Pd(II) complexes, *e.g.*, $PdCl_2(PPh_3)_2$. In the case of Pd(II) pre-catalysts, the first step in the Pd(0)/Pd(II) mechanism is reduction of the palladium(II) complex to give the catalytically active Pd(0) species, generally considered to be based on PdL_2 (L = monodentates or L_2 = bidentate ligand), **IV**, **Scheme 1.11**. Next, oxidative addition of the aryl halide occurs to form an organopalladium(II) intermediate, **V**. This is followed by a decoordination of one of the donor atoms leaving a vacant coordination site on the metal centre to which an incoming alkene can coordinate, **VI**, (Step 3). Migratory insertion (Step 4) is the product-forming step of the reaction cycle where the new C–C bond is formed via *syn*-migration of the aryl group, which is followed by recoordination of the ligand, **VII**. After internal rotation around the former C=C double bond, β–hydride elimination results in the formation of a hydridopalladium(II) species and dissociation of the coupled product (Step 5). The catalytically active palladium(0) species **IV** is regenerated by the reductive elimination of HX aided by the addition of an appropriate base (Step 6).

This mechanism is highly simplified as it does not rationalise some important aspects of the reaction cycle, *e.g.*, the accelerating effects of certain additives, solvent effects, differences in enantio- and regioselectivity, and ligand effects.[84,96] To help explain these effects, three reaction pathways have been proposed through which the Pd(0)/(II) mechanism is thought to proceed, dependent upon the additives and conditions used. Cabri and Candiani proposed that for the coordination-insertion process of alkenes a neutral pathway,[96] (**a**), or a cationic pathway,[96] (**b**), occurs for bidentate or monodentate ligands, while Amatore and Jutand proposed an anionic pathway involving the highly nucleophilic, formally coordinately unsaturated and negatively charged $[Pd^0(PPh_3)_2(OAc)]^-$ complex.[97,98] The rationale behind these differing pathways is significant, as different palladium pre-catalysts may generate not only different active Pd(0) complexes, but also different reaction intermediates.[96]

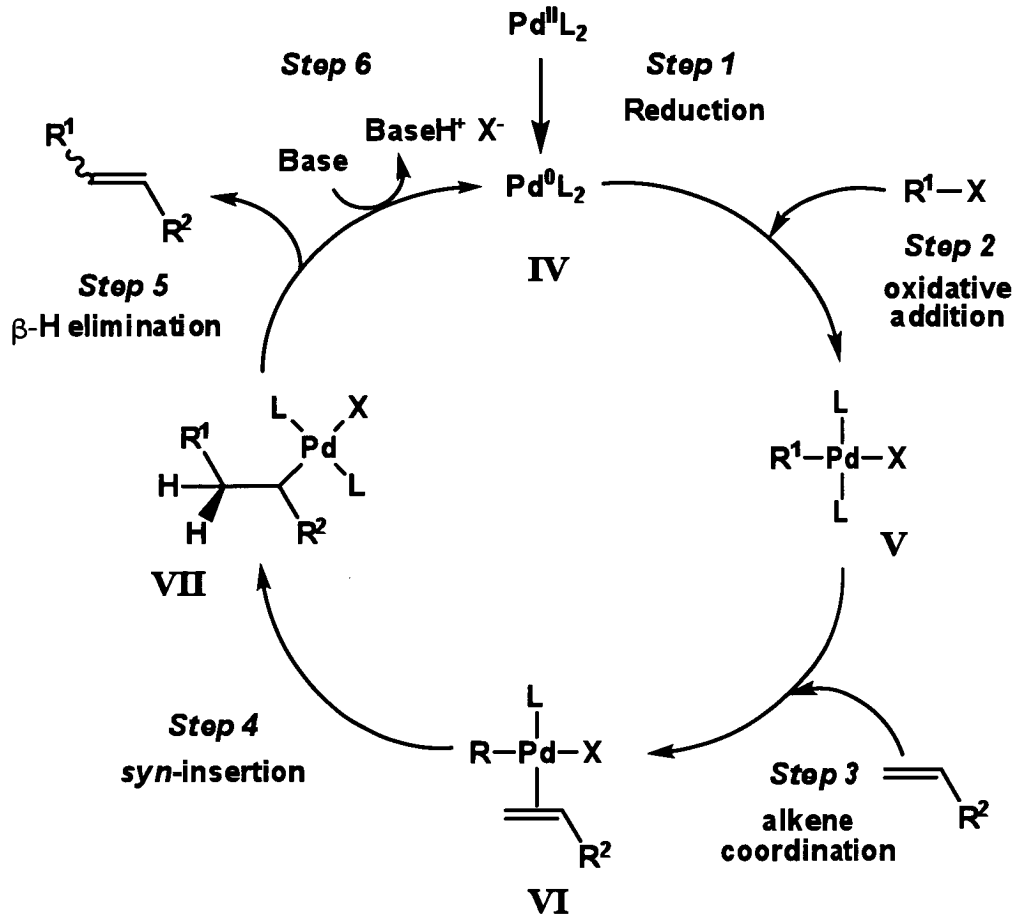

Scheme 1.11 The traditional generalised Pd(0)/(II) Heck reaction mechanism for monodentate ligands.

The neutral pathway is used to explain Heck systems where no Ag(I) or Tl(I) additives are present (**Scheme 1.12 (a)** where L···L represents a bidentate or two monodentate phosphine ligands). Such reactions have been found to show poorer enantioselectivity in asymmetric Heck reactions. This lack of selectivity is thought to be due to dissociation of one of the donor atoms during the reaction to afford a vacant coordination site for the incoming alkene to coordinate. This results in the π-system of the electron rich alkene being only weakly polarised, resulting in a significant mix of α- and β-arylated products.[96]

The cationic pathway (**Scheme 1.12 (b)**) is the accepted pathway when Ag(I) or Tl(I) additives are present in Heck systems. These additives enhance the enantioselectivity in

asymmetric Heck reactions of unsaturated aryl halides. Halide abstraction by Ag(I) or Tl(I) follows the oxidative addition of the aryl halide to the Pd(0) complex, leaving a vacant coordination site for the incoming alkene to coordinate and, therefore, forming a cationic intermediate. During this process the donor atoms of the ligand remain coordinated to the metal centre, enhancing enantioselectivity.[96] The fundamental difference between these two pathways is that in the cationic system the availability of a free site for an alkene to bind is due to the dissociation of an anion (X^-), whilst in the neutral system ligand dissociation (L) is necessary.

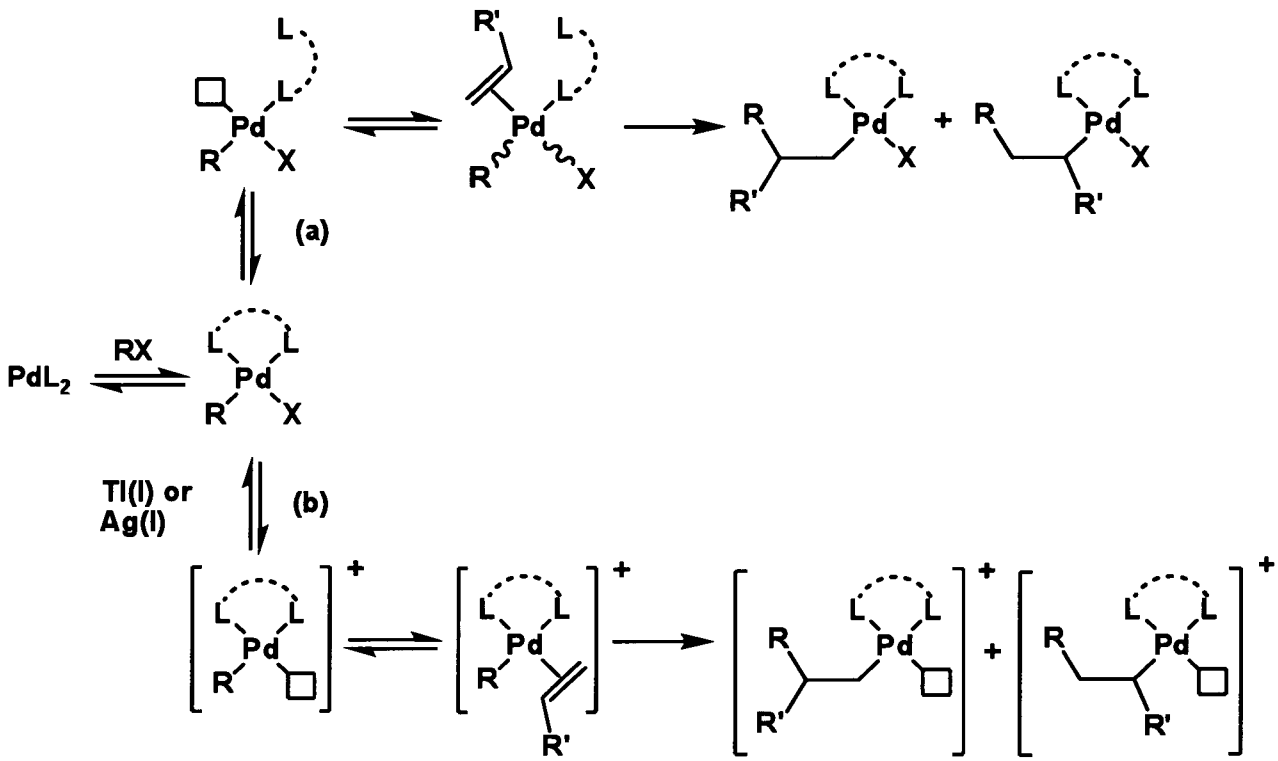

Scheme 1.12 Coordination-insertion process involving bidentate ligands via (a) the neutral pathway, and (b) the cationic pathway

The anionic pathway proposed by Jutand and Amatore (**Scheme 1.13**),[97] suggests that an increased reactivity of systems where additives such as Na_2CO_3 and NaOAc are used is due to anionic species being involved in the oxidative addition of the aryl halide. The pathway proposed involves reduction of the Pd(II) precatalyst, **VIII**, to form a three coordinate anionic Pd(0) catalyst $[Pd(X)(PR_3)_2]^-$ (X = [halide$^-$, CO_3^{-2}, or OAc^-), **IX**. This

species then undergoes oxidative addition to form a five coordinate species $[Pd(Ar)(X)(Y)(PR_3)_2]^-$ (Ar = aryl group and Y = halide), **X**, rather than the expected 4-coordinate species $Pd(Ar)(Y)(PR_3)_2$. An anionic ligand then rapidly dissociates to form the four coordinate Pd(II) complex $Pd(Ar)(X)(PR_3)_2$, **XI**, which undergoes increased reactivity relative to $Pd(Ar)(Y)(PR_3)_2$ in the dissociation of a phosphine donor atom to afford a vacant coordination site for the incoming alkene to coordinate.

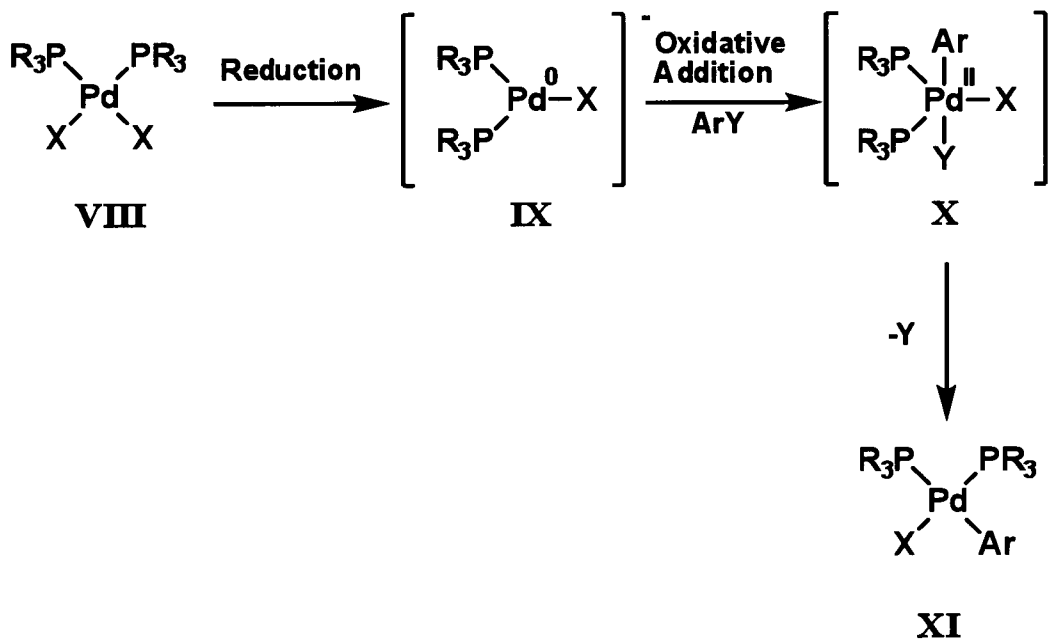

Scheme 1.13 The anionic pathway as proposed by Jutand and Amatore.[97]

1.4.3 The Rate Determining Step and Substrate Activity

It is generally agreed that there are two possible rate determining steps in the Heck reaction: the oxidative addition of the aryl halide, or the migratory insertion of the alkene.[84,97] The oxidative addition of the aryl halide is generally accepted to be the rate determining step for the overall reaction cycle for substrates other than aryl iodides.[99] The order of reactivity for aryl halides is Ar–I > Ar–Br >> Ar–Cl, in the same order as their relative C–X bond energies (272, 339, and 402 kJ mol^{-1}, respectively).[97,100-102] Electron withdrawing groups on the aryl ring (*e.g.*, –CHO, $–COCH_3$, $–NO_2$) activate the halide, making it easier to cleave the aryl halide bond and, therefore, accelerate the overall reaction. In contrast, electron-donating groups (*e.g.*, $–OCH_3$, $–NH_2$) deactivate

the aryl halide, impeding the reaction. The influence of aryl substitution is, however, secondary to the influence of the halide itself upon the speed of the overall reaction,[82,101] *i.e.*, a deactivated aryl bromide is considerably more reactive than an activated aryl chloride.

1.4.4 Industrial Limitations of Heck Catalysis

Since the mid-1980s the Heck reaction has been of specific interest to synthetic chemists, as it was discovered that selectivity could be controlled by using particular reaction conditions giving consistent and predictable results for selected substrates.[102] However, the reaction is currently not widely used by industry due to the lack of versatility of current systems and the substantially high costs involved in its use.[75,84,103]

Farina[75] has established five major challenges associated with the development of a catalytic process in order for it to be widely utilised on an industrial scale. **Scope**: the choice of electrophile may be affected by cost factors, *e.g.*, aryl chlorides may be the only substrates on hand due to expense, or synthetic availability of the more facile iodo-substituted electrophiles, and consequently catalysts which can activate C-Cl bonds are required. **Purity**: the purity of the electrophile or nucleophile may determine the viability of a catalytic system, *e.g.*, if crude starting materials can be used without affecting product quality then lower costs are achieved through fewer purification steps. **Impurity profile**: fewer side products or impurities lead to lower costs. **Throughput**: reactions on industrial scales tend to run under high concentration conditions in the shortest possible timeframe, such that reactions longer than 12 h are viewed as impractical and costly. **Time**: in all industrial applications there is a limited amount of time for a catalytic system to be developed and produce the desired product in high yield and purity. The longer a research and development department takes to produce a reliable and working catalyst, the process becomes less commercially attractive.

Currently, there is no single homogeneous palladium pre-catalyst in the literature which fulfils all of these criteria. Typically, most systems are only efficient when using aryl iodides or activated aryl bromides as substrates.[14] This problem limits the synthetic

scope and, consequently, limits commercial viability as aryl iodides and activated aryl bromides are considerably more expensive when compared to analogous aryl chlorides, while also containing fewer moles per unit mass.[84] There are examples in the literature, however, of new pre-catalysts which can activate deactivated aryl bromides, activated aryl chlorides and, in a few examples, deactivated aryl chlorides, as outlined in reviews by Fu.[78,79] However, these systems typically require much higher temperatures than those needed for aryl iodides, which can lead to catalyst degradation and low turnover numbers (TONs).[18] In those cases where low temperatures can be utilised, often poor selectivity of the product results in poor impurity profiles.

1.4.6 Ligands in the Heck Reaction

The lifetime of the catalyst can be improved by the addition of ligands whose presence is thought to stabilise the palladium centre and accelerate some steps in the catalytic cycle.[101] Traditionally, phosphine ligands (PR_3) have been used in this role but they have some major disadvantages. Phosphine ligands are toxic, expensive, often difficult to synthesise and usually non-recoverable.[84] Consequently, in catalytic applications the phosphine ligands themselves could become more of a serious economic challenge than even palladium itself, which if desired can be recovered from most stages of production or from waste.[84] Also, at the high temperatures required to react deactivated aryl bromides and aryl chlorides (typically 120 °C and above), phosphine-containing catalysts often undergo degradation via the breaking of P–C bonds of the ligand, forming unwanted by-products and resulting in low TONs.[104] To activate such systems at lower temperatures high catalyst loadings are usually required, thereby increasing cost.

The principle aims of this research are to improve catalyst stability and activate aryl chlorides while still achieving high TONs, and without the need for phosphorus containing ligands.[105] Currently in the literature there are many examples of phosphine-free ligand systems that have been developed for the Heck reaction, *e.g.*, palladacycles[105] (**XIII**), carbenes[79] (**XIV**), tridentate[106] (**XV**), and bidentate ligand systems[16] (**XVI**).

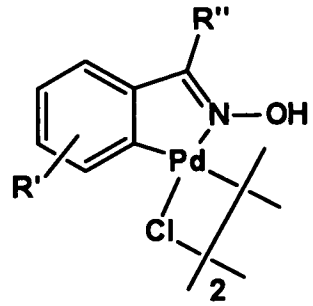

XIII

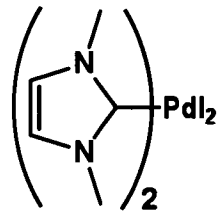

XIV

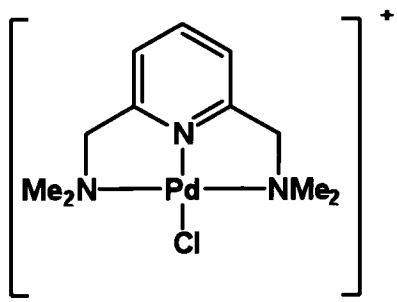

XV

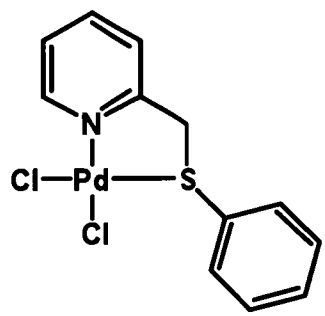

XVI

Palladium(II) pre-catalysts containing heteroleptic ligands such as **XVI** may be excellent for studies in the Heck reaction as they have shown activity in preliminary studies[16] and, if examined in a systematic manner, may advance the field of C–C bond formation catalysis and thereby provide a viable alternative for phosphine ligands in the Heck reaction.

Monosubstituted or 1,1-disubstituted (terminal) alkenes are easily coupled to aryl halides in Heck reactions due to their high reactivity, as well documented.[84] 1,2-Disubstituted (internal) alkenes are not often studied because of their low reactivity with most typical catalysts due to their increased bulk.[87] The use of 1,2-disubstituted alkenes to stereoselectively synthesise trisubstituted alkenes, however, would be of great benefit to the pharmaceutical industry in the production of drugs such as Tamoxifen, **XVII**, which is currently produced by methods which result in a mixture of isomers.[107]

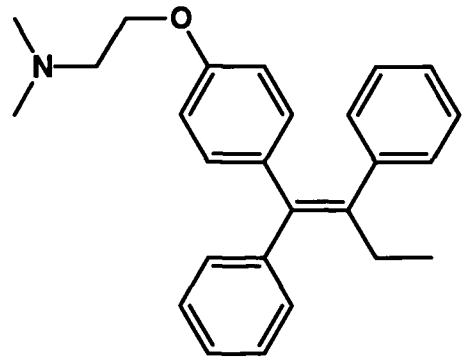

XVII

Our research group has recently achieved a 100% conversion after 3 hours at 80 °C with a product *E:Z* ratio >99:1 in the Heck reaction of ethyl *trans*-cinnamate and 4-bromoacetophenone (**Scheme 1.14**) using palladium pre-catalysts containing heteroleptic ligand systems, such as **XVI**.[16] The heteroleptic system performs much better than similar reactions containing the homoleptic bidentate nitrogen and sulfur ligands, such as 2,2-bipyridine (bipy) and 2,5-dithiahexane, which achieved 46 and 90% conversion after 6 hours, respectively, under the same conditions.[16]

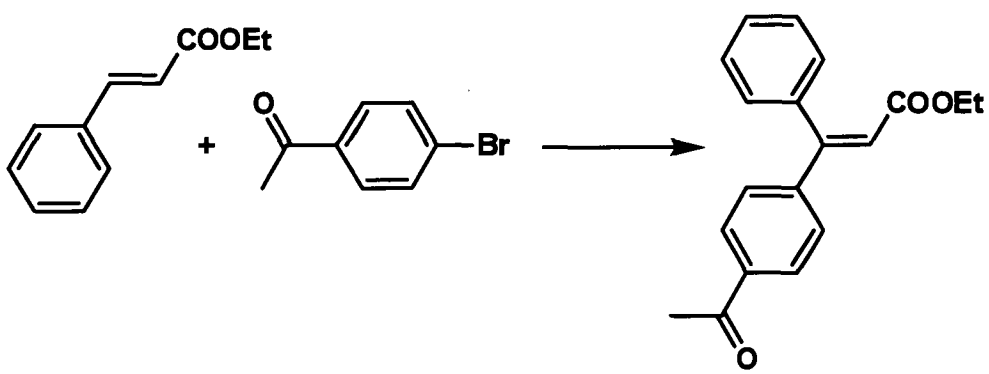

Scheme 1.14 Heck reaction of ethyl *trans*-cinnamate and 4-bromoacetophenone.

The optimised conditions that are used in the Heck reaction focus on three key elements: the choice of base, the addition of a phase transfer reagent, and a reducing agent. Previous research in our group has shown that, with **XVI** as a pre-catalyst, the addition of Na_2CO_3 to a Heck reaction was found to increase the level of conversion of the aryl halide to product, while NaOAc was found to increase the level of stereoselectivity of the products.[16,108] This indicated that, for trisubstituted alkenes where stereoselectivity may become problematic, NaOAc should be used so that only one product is formed. Aryl halide conversion and stereoselectivity is improved when Bu^n_4NX (X = halide) is

added to the Heck reaction.[108] In the coupling reaction of 4-bromoacetophenone and *n*-butyl acrylate, TONs of 1,000,000 were obtained using $PdCl_2(pyCH_2SPh)$ (where py = 2-C_5H_4N) a pre-catalyst.[16] The addition of a reducing agent such as sodium formate increases the rate of conversion, allowing the reaction to proceed at much lower temperatures (80 °C) than previously possible (140 °C) in the formation of trisubstituted alkenes,[16] and supporting the assumption that this system follows the Pd(0)/(II) mechanism.[108] This exploratory work illustrates the promise of heteroleptic ligand systems such as $pyCH_2SPh$ in **XVI**.

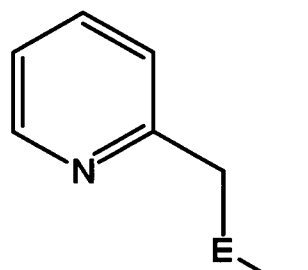

XVIII

Ligands containing pyridine and chalcogen (S, Se) donor atoms (**XVIII**) have not been comprehensively explored in catalysis. This particular class of heteroleptic ligand has been studied in coordination chemistry over the last fifty years;[15] *e.g.*, complexes of Ni(II), Co(II), Cu(II), Hg(II),[109] Ag(I),[109,110] Pd(II), Pt(II) [15,16,109] and Mn(I) carbonyl complexes.[111] Organometallic applications include studies of fluxionality and olefin exchange in Pd(0) complexes;[15,112-114] allene,[115,116] diene[117] and alkyne[118] insertion into Pd–C bonds; and allylic amination in Pd(II) complexes.[15,119-121] There are also reports of 2-(phenylthiomethyl)pyridine derivatives being used in drug testing, particularly as anti-inflammatory agents.[122] Despite this wide range of use in coordination, organometallic and drug studies, there are only a few reported examples in the literature of the deliberate use of ligands **XVIII** in the synthesis of palladium pre-catalysts in catalytic C–C bond formation reactions.

It is the work conducted by Canovese that is most prominent in the application of 2-organochalcogenomethylpyridine ligands in palladium chemistry. Canovese has shown that the versatility of these ligands allows the synthesis of a great number of different coordination compounds of palladium.[15,112-121] Utilising these ligands, Canovese

synthesised a number of allylpalladium(II) complexes and conducted reactivity studies of substituent effects on allylic amination and insertion of allenes into Pd-C bonds. This early work led to the synthesis of palladium(0) and platinum(0) olefin complexes and subsequent kinetic studies on the equilibria and rates of olefin exchange. Palladium catalysed addition of diethylzinc to benzaldehyde[123,124] and palladium catalysed allylic substitution was also trialled by Chelucci and co-workers.[123] More recently the palladium catalysed trimerisation of substituted alkynes bearing dimethylacetylene dicarboxylate functionalities has been investigated in the synthesis of hexasubstituted benzenes.[125] The synthesis of fluoranthenes[126,127] and 2,4-diene-6-ynes[128] have also been achieved in stoichiometric reactions.

1.4.7 Project Aims for the Heck Reaction

An aim of this project is to further develop the use of ligands of the type **XVIII** in catalytic applications, particularly the Heck reaction. This will be achieved by developing new ligands with varying substituents around the pyridyl ring, the chalcogen atom, and variation of the chalcogen and subsequently utilising these ligands in the synthesis of dichloropalladium(II) complexes which will be systematically tested as pre-catalysts in the Heck reaction.

1.5 Palladium Catalysed Cross-Coupling Reactions - The Suzuki Reaction

1.5.1 Definition and Applications

Palladium mediated cross-coupling reactions are readily accessible *via* a large variety of organometallic reagents providing simple and efficient methods for fine chemical synthesis,[129-131] **Scheme 1.15**.

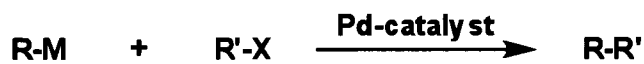

Scheme 1.15 General scheme for Pd mediated cross-coupling reactions involving organometallic reagents.

The first of these cross-coupling reactions was independently discovered by Kumada and Tamao[132,133] and Corriu[134] in 1972, in which the reaction of organomagnesium reagents with alkenyl or aryl halides could be markedly catalysed by Ni(II) complexes. Kochi[135,136] found that Fe(III) catalysts could increase the efficiency of the cross-coupling reaction of Grignard reagents with 1-halo-1-alkenes. The palladium catalysed reaction of Grignard reagents was first reported by Murahashi,[137] a synthetic protocol which was adapted and utilised by Negishi in reactions of organoaluminium,[138] zinc,[139] and zirconium reagents.[140] After these initial discoveries, many other organometallic reagents have been proven to be highly useful as reagents for palladium mediated cross-coupling reagents, *i.e.*, organolithiums by Murahashi,[141] organostannanes by Migita[142] and Stille,[143] organosilicons by Hiyama,[144] and organoboron compounds by Suzuki and Miyaura.[145,146] Negishi has summarised the history of the development of palladium catalysed cross-coupling reactions.[147]

Among palladium-catalysed cross-coupling reactions, it is the Suzuki reaction of aryl and vinyl halides with organoboron reagents which is emerging as a favoured process for carbon–carbon bond formation. Like the Heck reaction, the Suzuki reaction of today is very different to that originally developed. In 1978 Negishi reported that iodobenzene selectively couples with the 1-alkynyl group in lithium 1-hexynyl(tributyl)borate through a palladium-catalysed addition-elimination "Heck type" process.[148,149] However, it was Suzuki and Miyaura in 1979 who first reported a direct cross-coupling reaction of 1-alkenylboronic esters and 1-bromo- or 1-iodo-1-alkenes in the presence of a base and palladium catalyst.[145] This work was quickly expanded, with Suzuki and Miyaura showing that cross-coupling reactions of organoboron compounds (particularly aryl boronic acids and esters) proceed smoothly when these compounds are activated with an appropriate base in the presence of a palladium catalyst. This reaction, now known as the Suzuki reaction, has proven to be a general technique for a range of selective carbon-carbon bond formation reactions.[79] During the last decade the reaction has grown to encompass a wide variety of substrates, where the majority of coupling reactions are between aryl or vinyl halides/triflates and aryl, alkyl, or vinyl boronic acids or esters, **Scheme 1.16**.

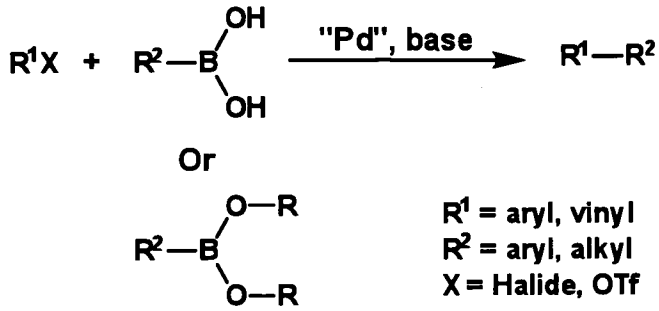

Scheme 1.16 General scheme for the Suzuki reaction involving boronic acids and esters.

The Suzuki reaction is typically regarded as the protocol of choice for the synthesis of biaryl or substituted aromatic moieties.[150] Compounds that contain these sub-structures constitute important building blocks of polymers,[151] ligands,[152] many natural products, and a large number of biologically active pharmaceuticals.[153] The key advantages of this protocol are the mild conditions under which the reaction can be conducted and the high tolerance toward functional groups. In addition, a range of boronic acid and ester substrates are commercially available, they are generally non-toxic, and stable to the presence of water, heat, and air. Also, the boron-containing by-products can be readily separated from the product.[154] This synthetic versatility has allowed the reaction to be employed in the industrial synthesis of pharmaceuticals and fine chemicals,[155] e.g. the antihypertensive drug Losartan (**IXX**);[156] the fine chemical **XX**, a key intermediate in the synthesis of the antidepressant SB-245570 (**XXI**);[157] and as a key step in a multikilogram synthesis of the potent endothelian receptor antagonist CI-1034 (**XXII**).[158]

The scope of the Suzuki reaction has been extensively surveyed in several excellent reviews which cover the work before 1998,[129-131,159] developments from 1999 to 2001,[153,160] and advances between 2001 to 2004.[161]

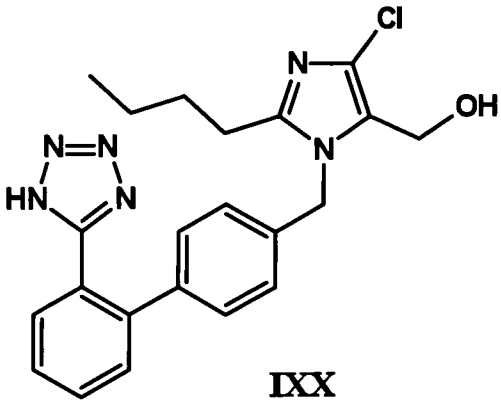

IXX

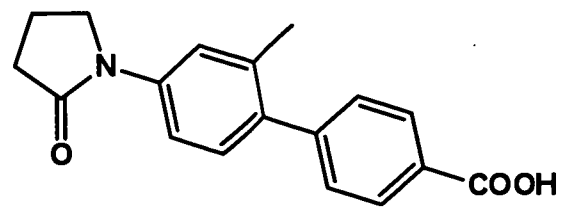

XX

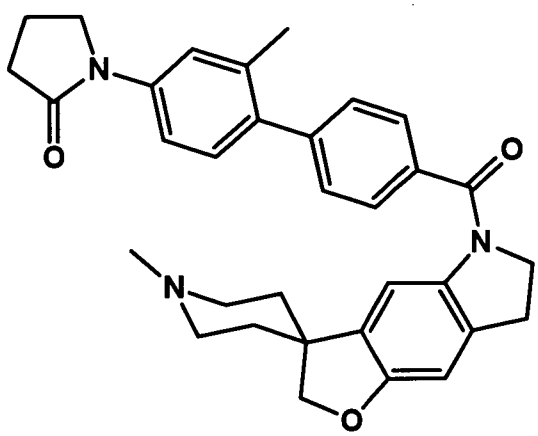

XXI

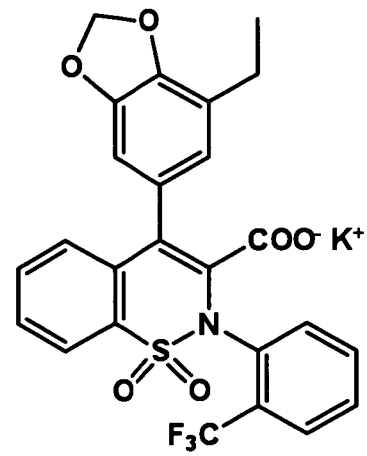

XXII

1.5.2 The Suzuki Reaction Mechanism

The general mechanism for the Suzuki reaction is similar to other palladium catalysed cross-coupling protocols involving organometallic reagents. A recent comprehensive study of mechanistic possibilities is presented in **Scheme 1.17**. Like the Heck reaction, precatalysts for the Suzuki reaction may be either Pd(0) or Pd(II) complexes. In the case of Pd(II) precatalysts, the first step in the mechanism is reduction to give the catalytically active Pd(0) species, generally considered to have the formula PdL_n (L = monodentate or bidentate ligands). After reduction, oxidative addition of the aryl halide occurs to form an organopalladium(II) intermediate. As for the Heck reaction, the oxidative addition step is generally considered to be the rate determining step in the catalytic cycle for substrates other than aryl iodides, with halide reactivity in the order of

I > Br >> Cl. Substrates containing electron withdrawing groups are more reactive in the Suzuki reaction, while substrates containing electron donating groups are less reactive (see **Section 1.5.3**).

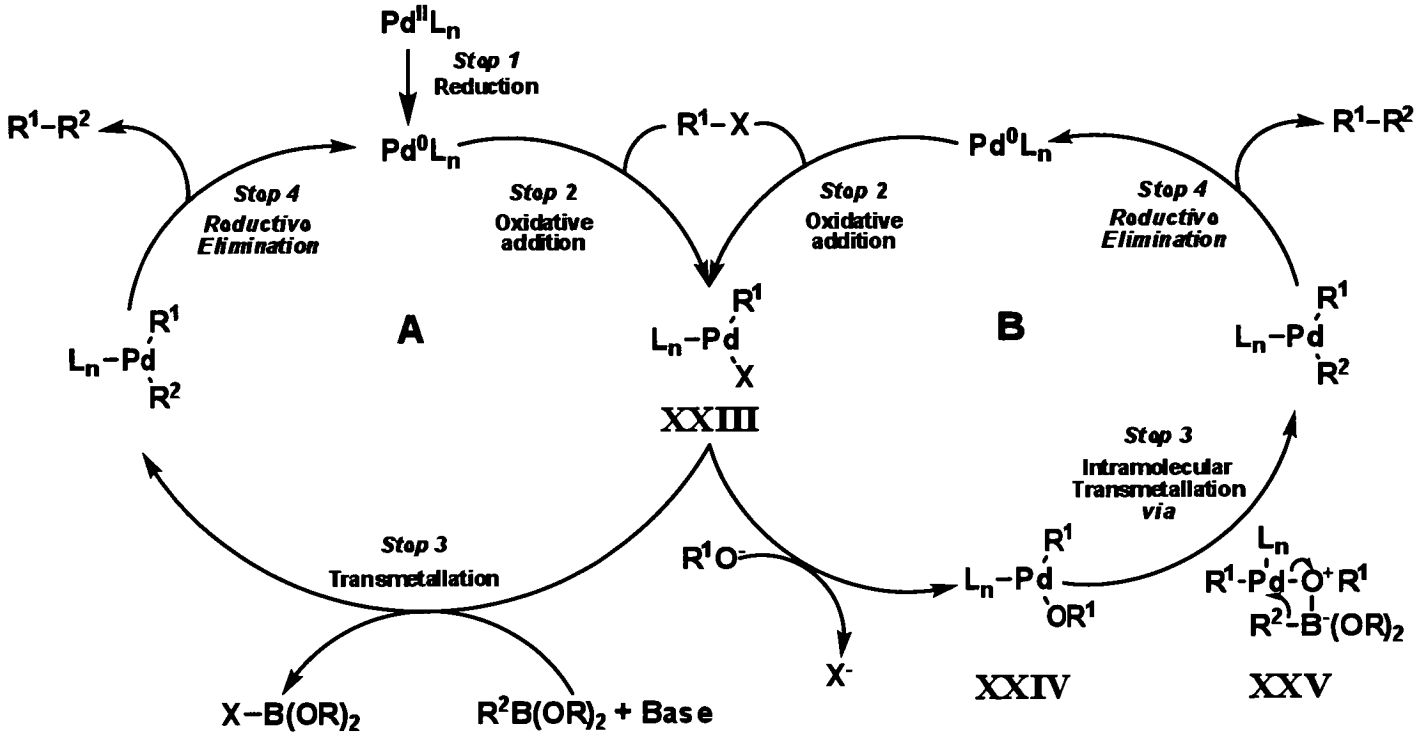

Scheme 1.17 General catalytic scheme for the Suzuki reaction involving boronic acids and esters.[150]

The next step in the catalytic cycle is the base assisted transmetallation of the palladium(II) species with the boron containing substrate. The transmetallation of organoboron compounds in an alkaline solution, although not widely understood, is thought to proceed *via* two different pathways. In **pathway A** the base facilitates the otherwise slow transmetallation of the boronic acid or ester by forming a more reactive boronate species which can interact with the palladium(II) species **XXIII** (not detailed in **Scheme 1.17**) and transmetallate in an intramolecular fashion.[162] In **pathway B** the base; replaces the halide moiety in the coordination sphere of the palladium(II) complex **XXIV**, facilitating an intramolecular transmetallation *via* **XXV**.[163] It is not known which pathway predominates, with the process dependent upon the substrates, conditions and base.[163] Although the role of the base is crucial for the transmetallation

process to occur, the choice of base is often arbitrary with selection largely dependent upon which substrates are used in the reaction.[161] Bases typically chosen are negatively charged species such as carbonates (Na_2CO_3, K_2CO_3), phosphates (K_3PO_4), or hydroxides (NaOH, LiOH, and $Ba(OH)_2$). Once transmetallation is complete, the final step in the catalytic cycle is reductive elimination to form the desired organic product and regeneration of the active palladium(0) species. This mechanism given in **Scheme 1.17** is highly simplified as it does not rationalise some important aspects of the reaction cycle, *e.g.*, the accelerating effects of certain additives, solvent effects, differences in enantio- and regioselectivity, and ligand effects.

1.5.3 Ligands in the Suzuki Reaction, and Project Aims

Like the Heck reaction, most of the early work in Suzuki catalysis was conducted using phosphines, particularly triarylphosphines. [129] During the last ten years, the use of phosphine ligands in the Suzuki reaction has grown rapidly with an emphasis on trialkylphosphines,[164] and more recently bulky dialkylbiarylphosphines.[165] These new ligands, particularly the electron rich bulky dialkylbiarylphosphines, have had a dramatic effect on improving reaction efficiency and selectivity.[150] However, as for studies of the Heck reaction, there has been a shift in the development of ligand systems to those which do not contain phosphine donor atoms. The most widely utilised and developed of these non-phosphine ligands are *N*-heterocyclic carbenes which have been very successful in the Suzuki reaction.[166] The development of heteroleptic ligand systems for the Suzuki reaction has also been reported, with various degrees of success for $[P,C]^-$ (**XXVI**),[167] *P,S* (**XXVII**),[168] $[O,S]^-$ (**XXVIII**),[169] and $[O,N,Te]^-$ (**IXXX**)[170] based ligands. There are no reports of palladium(II) pre-catalysts containing *N,E* ligands such as **XVIII**. This class of complex, exhibiting promising results in preliminary studies of Heck catalysis,[16] may provide a viable alternative for phosphines in the Suzuki reaction.

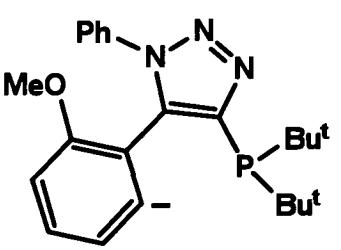

XXVI

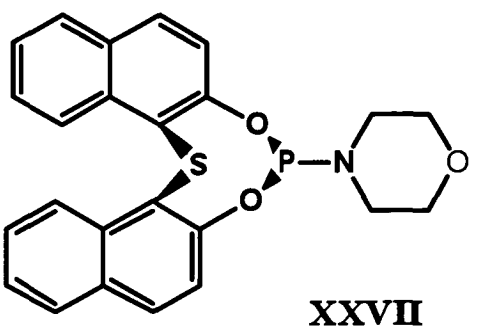

XXVII

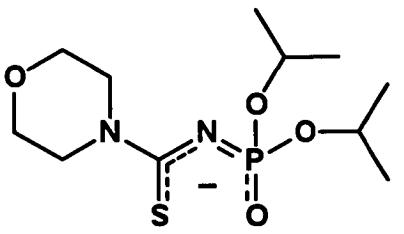

XXVIII

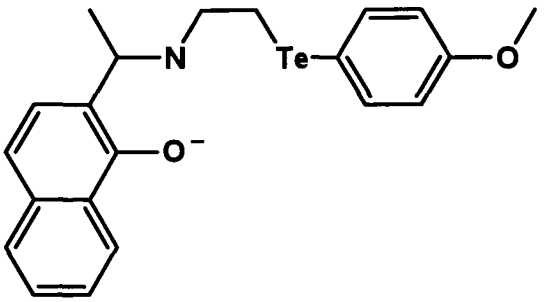

IXXX

Thus, another aim of this project is to explore in a preliminary manner the application of palladium(II) precatalysts containing *N,E* heteroleptic ligands for the Suzuki reaction, choosing pre-catalysts on the basis of activity in the Heck reaction.

1.6 Palladium Catalysed Reactions - The Sonogashira Reaction

1.6.1 Definition and Applications

There are currently two different types of palladium metal catalysed cross-coupling reactions of sp^2-C to *sp*-C atoms available for the synthesis of conjugated acetylenes, coupling of unsaturated organic halides with terminal acetylenes (Sonogashira reaction) and coupling of halides with alknyl metal reagents, (*e.g.*, Stille coupling (M = Sn), Suzuki coupling (M = B), Negishi coupling (M = AlR_2, and ZnX), and Kumada-Tamao-Corriu coupling (M = MgX). The Sonogashira reaction of terminal acetylenes with sp^2-C halides has provided the most useful method for synthesising conjugated acetylenic compounds.[171]

The Sonogashira reaction originated from early studies reported independently by Heck[172] and Cassar[173] in 1975. Heck's reaction, based upon the Heck protocol, consisted of performing an alkynylation of alkenes using a phosphine palladium complex as a catalyst and triethylamine or piperidine as a base and solvent. Cassar's procedure also used a phosphine palladium catalyst but differed to Heck's system by using sodium methoxide and dimethylformamide as a base and solvent. In both cases coupling was achieved utilising high temperatures. Following these early reports in the same year, Sonogashira and Hagihara reported that the addition of a catalytic amount of

copper(I) iodide greatly accelerates the reaction, therefore enabling the alkynylation to occur at room temperature[174] (this accelerating effect of copper(I) salts had already been reported for coupling reactions of copper(I) acetylides and phenyl or vinyl halides, labelled as the Stephens-Castro reaction).[175,176] This initial development has led to a highly versatile protocol which today is widely utilised in the coupling of aryl and alkenyl halides to alkynes, using both copper and copper-free conditions **Scheme 1.18**. More recently the Sonogashira reaction has been developed to include the reaction of primary alkyl iodides and bromides,[177] and secondary alkyl bromides,[178] however this form of coupling remains largely unexplored.

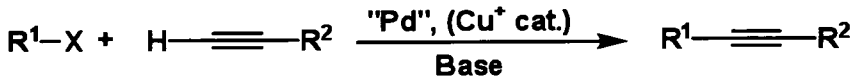

R^1 = aryl, heteroaryl, vinyl
R^2 = aryl, heteroaryl, alkenyl, alkyl, SiR_3
X = Halide, OTf^-

Scheme 1.18 General catalytic scheme for the Sonogashira reaction.

The Sonogashira reaction has been found to be highly versatile, allowing utilisation in the synthesis of molecules containing many different functional groups. The reaction itself is one of the simplest ways to obtain variously substituted alkynes, diynes, and other unsaturated compounds, many of which are useful as key intermediates in the synthesis of natural products, *e.g.*, alkaloids (**XXX**),[179] metabolites (**XXXI**),[180] electronic and electro-optical molecules (**XXXII**),[181] and nanostructure materials (**XXXIII**).[182] There are numerous current reports for the Sonogashira reaction utilising new palladium pre-catalysts, mechanistic discoveries, or natural product synthesis, and extensive reviews of the field have appeared, *e.g.*, by Chinchilla,[171] Sonogashira,[1,183] and Brandsma.[184]

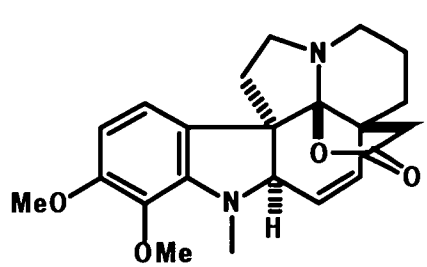

XXX

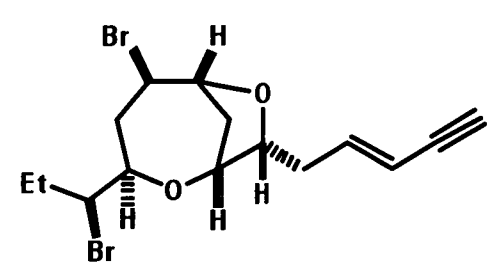

XXXI

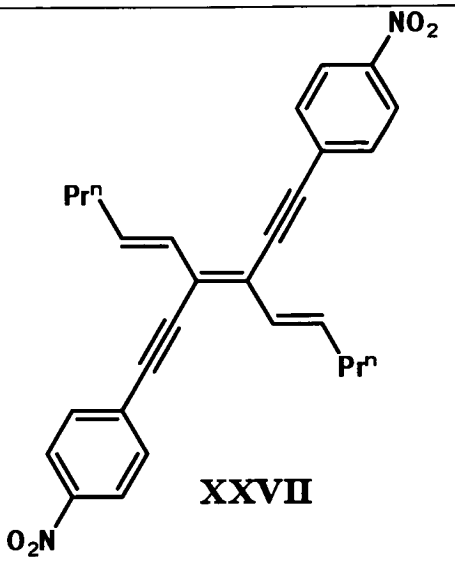

XXVII

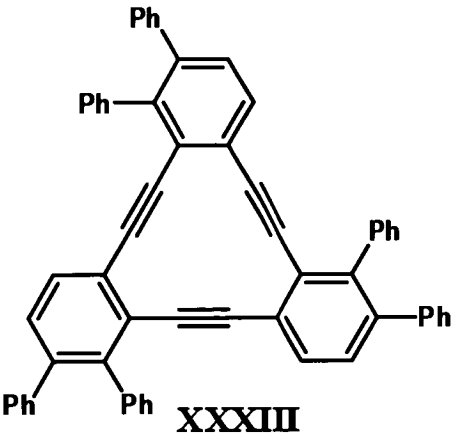

XXXIII

1.6.2 The Sonogashira Reaction Mechanism

The exact mechanism of the Songashira reaction is largely unknown consequently more recent studies on the coupling protocol are dedicated to the elucidation of the mechanistic pathways of both the copper co-catalysed[185] and copper free systems.[186]

The copper co-catalysed reaction is believed to take place through two linked catalytic cycles, **Scheme 1.19**.[1,183,184] The generalised mechanism begins by reduction of the palladium(II) pre-catalyst to the active palladium(0) species. This is quickly followed by the oxidative addition of aryl halide to the unsaturated Pd^0L_2 complex forming the 16 electron organopalladium(II) species **XXXIV**. Like the Heck and Suzuki reactions, the characteristics of the incoming organohalide are critical, with the general reactivity scheme for halides I > Br >> Cl. Again, electron withdrawing groups accelerate the process while electron donating groups retard the oxidative addition step in the cycle. The transmetallation reaction occurs next, where formation of the copper acetylide species occurs *via* a base assisted deprotonation of the terminal acetylene. Transmetallation of this species with **XXXIV** generates the $PdR^1(C{\equiv}CR^2)$ species (**XXXV**) which undergoes reductive elimination to produce the coupled alkyne and regeneration of the active palladium(0) species. The transmetallation of the copper acetylide is often the rate determining step of the cycle. The copper acetylene cycle (**B**) is still poorly understood.[171] In the generalised "textbook" copper cycle the base (generally an amine) abstracts the acetylenic proton of the terminal alkyne, thereby

forming the copper acetylide in the presence of a copper(I) salt. However, the amines usually employed, such as triethylamine, are not basic enough to deprotonate the alkyne in order to generate the anionic nucleophile that should form the copper acetylide. Bertus[187] has proposed that a π-alkyne-Cu complex (**XXXVI**, cycle **B**) could be involved, rendering the proton more acidic and easier to abstract. More recently, silver co-catalysed Sonogashira reactions have shown that π-alkyne-Ag complexes are formed before the generation of silver acetylides, providing support for Bertus' proposal.[188] However, there has been no direct evidence for the formation of a copper acetylide species.

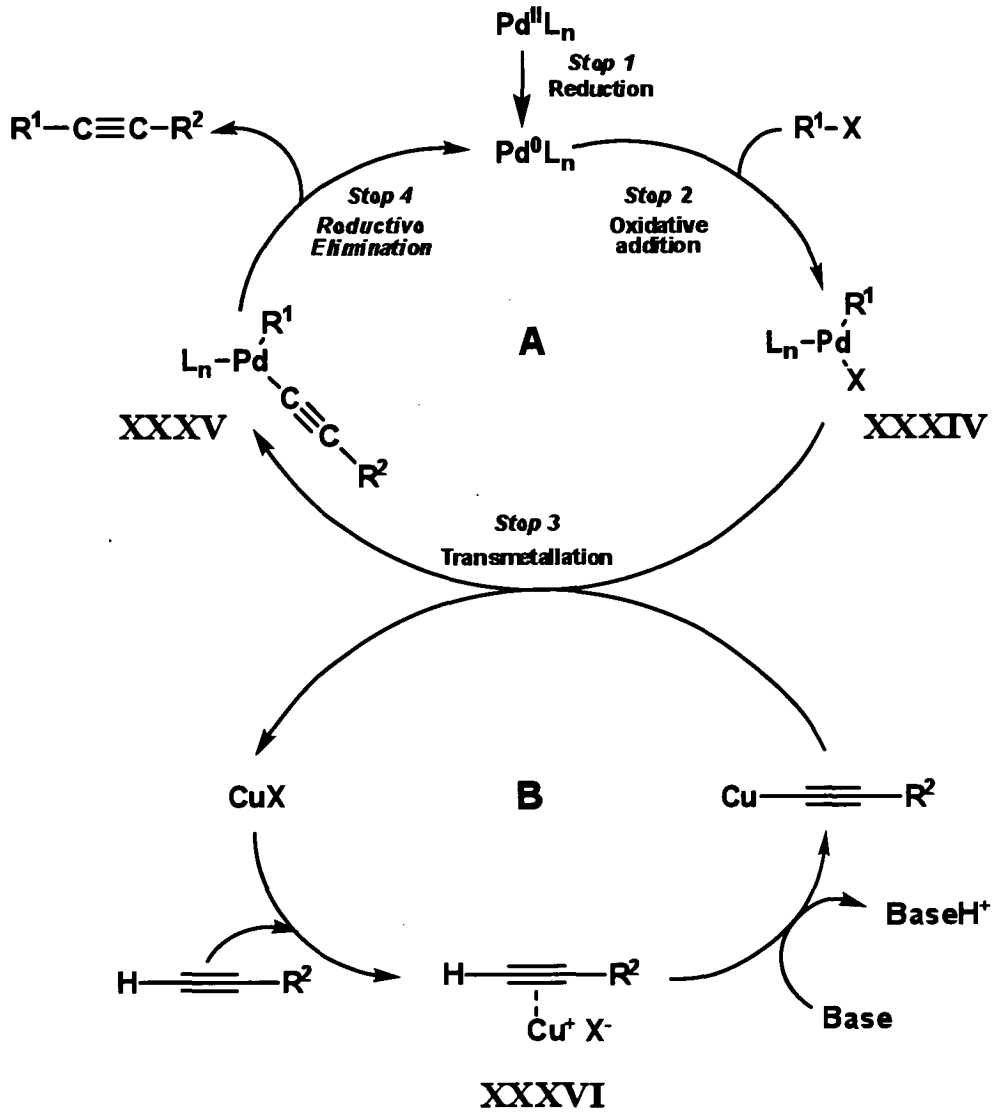

Scheme 1.19 General catalytic scheme for the copper-cocatalysed Sonogashira reaction.

The mechanism for the copper-free Sonogashira reaction is also not fully understood, **Scheme 1.20**.[186] The first step of the reaction cycle, after reduction of the Pd(II) species, is oxidative addition of R^1–X to the Pd(0) complex. The pathway for the incorporation of the alkyne is still under debate. As mentioned above, amines are generally not basic enough to deprotonate the alkyne. The generally accepted process for this transformation is displacement of one ligand to give an $PdXR^1(\eta^2\text{-}RC{\equiv}CH)L$ intermediate (**XXXVII**).[189] The ligated alkyne is then deprotonated by the amine, forming $PdR^1(C{\equiv}CR^2)L_2$ (**XXXVIII**), which then undergoes reductive elimination to give the coupled alkyne R^1–C≡C–R^2. If the base is not an amine, a carbopalladation step takes place.[190]

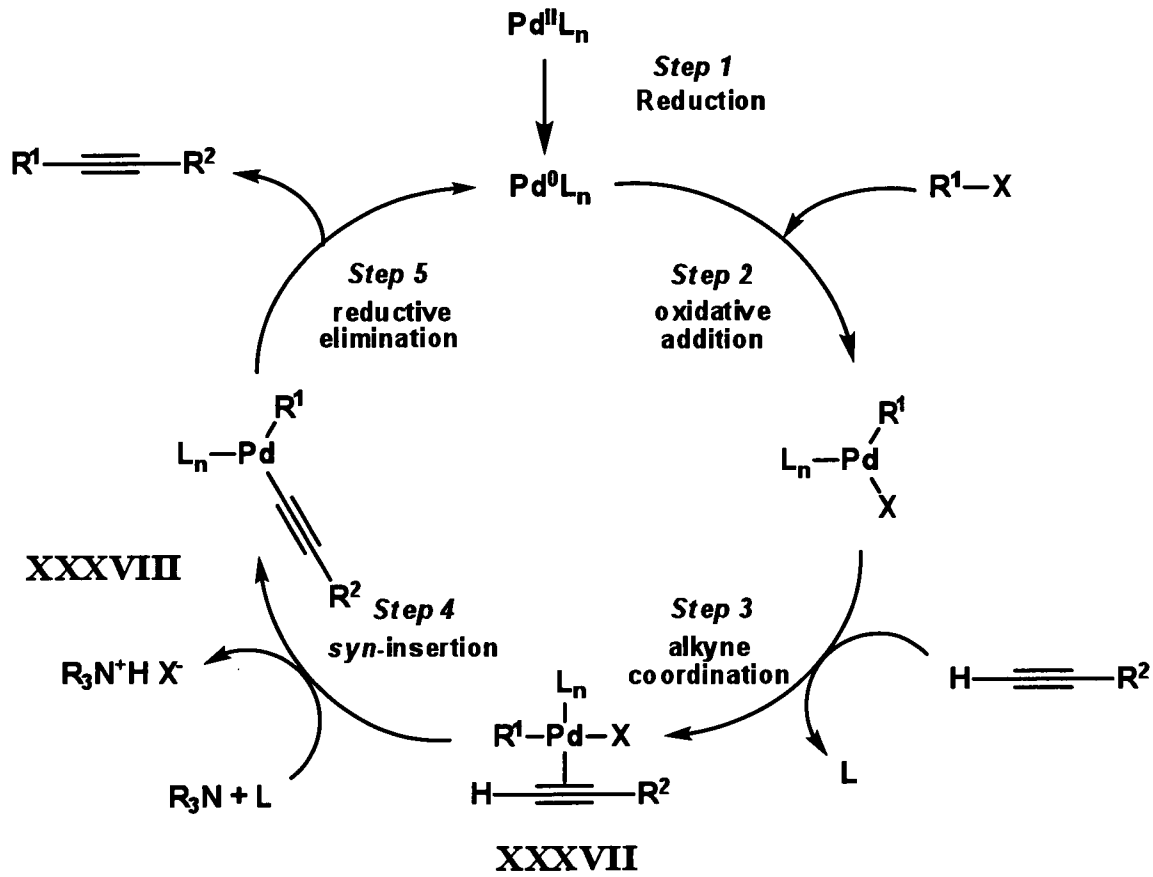

Scheme 1.20 General catalytic scheme for the copper free Sonogashira reaction.

For both the copper catalysed and copper free systems, the mechanisms described above are simplified and do not take into account important aspects such as the accelerating

effects of certain additives, solvent effects, base effects (crucial in the case of the copper free process), and ligand effects.

1.6.3 Ligands in the Sonogashira Reaction and Project Aims

Ligands used in the Sonogashira reaction are typically based upon phosphines, with traditional compounds used being $Pd(PPh_3)_4$ and the air-stable Pd(II) precatalyst, $PdCl_2(PPh_3)_2$. The bidentate ligand complexes $PdCl_2$(dppe), $PdCl_2$(dppp), and $PdCl_2$(dppf) have also been employed successfully in the cross-coupling protocol. However, typically high palladium loadings (5 mol%) and high copper loadings (10 - 30 mol%) are required when using the palladium complexes described above.[171] Consequently, there has been a recent shift in research aimed not just at extending the scope of the reaction itself, but finding more active catalysts for simpler, milder, and more effective reaction conditions which are, where possible, copper free. Initially the focus of this research has been on developing palladium catalysts containing bulky, electron rich phosphines, which have had extensive success in the Suzuki reaction,[150] in both the copper containing and copper free versions of the Sonogashira reaction. These bulky phosphines, such as the highly air sensitive, pyrophoric $P(Bu^t)_3$, have enjoyed extensive success in activating aryl iodides and bromides,[191,192] while the combination of $[PdCl(\eta^3\text{-}C_3H_5)]_2$ and the tetraphosphine ligand *cis,cis,cis*-1,2,3,4-tetrakis(diphenylphosphinomethyl)cyclopentane has shown activity toward aryl chlorides in both copper containing and copper free protocols.[193] However, at present there is no general protocol for activating aryl chlorides in the Sonogashira reaction.[79] This has led to the development of other types of ligands, the most common being *N*-heterocyclic carbenes[194] such as **IXL**. Pincer type ligands [195] (**XL**), and heteroleptic ligands based upon *P,N*[196] (**XLI**), and *P,O*[197] (**XLII**) moieties have also been developed, achieving differing levels of success in the cross-coupling reaction. Currently there are no examples of *N,E* ligands being used in the Sonogashira reaction. Therefore, a major aim of this project is to utilise palladium(II) halide complexes containing *N,E* ligands in the Sonogashira reaction in order to develop a new and effective palladium catalyst for this reaction.

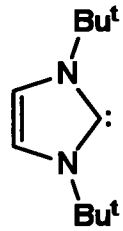

IXL

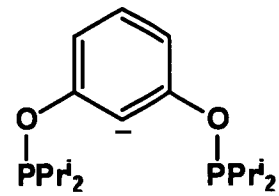

XL

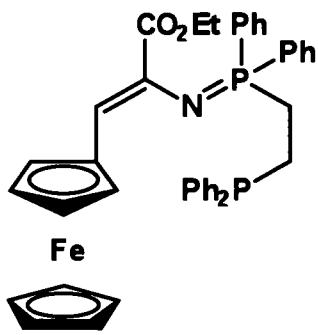

XLI

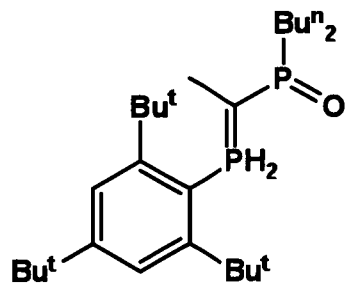

XLII

1.7 Scope of the Project

While heteroleptic ligands are increasingly displaying their versatility in both coordination and catalytic chemistry, this type of ligand is still little used in the development of palladium pre-catalysts for C–C bond formation processes. The aim of this project is to develop a series of palladium(II) pre-catalysts based upon the *N,E* motif, as generalised by **XVIII**, and utilise these compounds in Heck, Suzuki and Sonogashira C–C bond formation processes. This will be achieved in several ways:

1. Development of a general and versatile method of synthesis for ligands based upon **XVIII** to produce a wide variety of compounds with various functional groups on the pyridine and chalcogen, while also varying the chalcogen.
2. Synthesis of palladium(II) pre-catalysts containing a series of heteroleptic ligands.
3. Systematic testing of the new palladium(II) pre-catalysts in the Heck reaction in order to find which pre-catalyst contains the most ideal functionalities, thereby

optimising a pre-catalyst which will be highly versatile and efficient in the Heck reaction.

4. Utilisation of the optimised palladium(II) pre-catalyst in preliminary studies for the other C-C bond formation processes thereby testing the versatility of the newly developed *N,E* heteroleptic ligand containing catalytic system.
5. Development of a supported catalytic system based upon the optimised *N,E* motif attached to organic polymer supports. This will be achieved by designing a *N,E* reagent capable of attachment to solid supports such as Merrifield and Wang resins, and a newly developed support based upon a macroporous organic polymer (referred to as a monolith). It is hoped that these supported catalytic systems will offer significant advantages over homogeneous systems in catalytic reactions, such as higher catalytic stability and the possibility of catalyst recycling.
6. Development of a flow-through microreactor system utilising an *N,E* motif, This is anticipated to have advantages over conventional reaction systems, including better selectivity in reactions, and environmental and safety advantages resulting from use of small amounts of solvent. This work will be based upon a capillary filled with monolith and is to be explored as part of the development of new technology.[198-200] This will be the first microreactor based upon *N,E* ligands.

Aspects of aims 5 and 6 are introduced in more detail in **Chapter 5**.

1.8 References

1. Negishi, E.-I. *Handbook of Organopalladium Chemistry for Organic Synthesis Volume I*; Wiley, New York, **2002**.
2. Negishi, E.-I. *Handbook of Organopalladium Chemistry for Organic Synthesis Volume II*; Wiley, New York, **2002**.
3. Yin, L.; Liebscher J. *Chem. Rev.* **2007**, *107*, 133.
4. Nicolaou K. C.; Sorensen E. J. *Classics in Total Synthesis*; Wiley-VCH, New York, **1996**.

5. Yamamoto, A. *Organotransition metal chemistry: fundamental concepts and applications*; Wiley-VCH, New York, **1986**.
6. Ruelke, R. E.; Delis, J. G. P.; Groot, A. M.; Elsevier, C. J.; van Leeuwen, P. W. N. M.; Vrieze, K.; Goubitz, K.; Schenk, H. *J. Organomet. Chem.* **1996**, *508*, 109.
7. Kranenburg, M.; Delis, J. G. P.; Kamer, P. C. J.; van Leeuwen, P.W. N. M.; Vrieze, K.; Veldman, N.; Spek, A. L.; Goubitz, K.; Fraanje, J. *J. Chem. Soc., Dalton Trans.* **1997**, *11*, 1839.
8. Raper, E. S. *Coord. Chem. Rev.* **1996**, *153*, 199.
9. Raper, E. S. *Coord. Chem. Rev.* **1997**, *165*, 475.
10. Casey, M.; Lawless, J.; Shirran, C. *Polyhedron* **2000**, *19*, 517.
11. Dey, S.; Kumbhare, L. B.; Jain V. K.; Schurr, T.; Kaim, W.; Klein, A.; Belaj, F. *Eur. J. Inorg. Chem.* **2004**, 4510.
12. Vimal, K.; Jain, L. J. *Coord. Chem. Rev.* **2005**, *249*, 3075.
13. Dahlenburg, L. *Coord. Chem. Rev.* **2005**, *249*, 2962.
14. Li, Y.-M.; Kwong, F.-Y.; Yu W.-Y.; Chan, S. C. *Coord. Chem. Rev.* **2007**, *251*, 2119.
15. Canovese, L.; Chessa, G.; Visentin, F.; Uguagliati P. *Coord. Chem. Rev.* **2004**, *248*, 945.
16. Jones, R. C.; Madden, R. L.; Skelton, B. W.; Tolhurst, V.-A.; White, A. H.; Williams, A. M.; Yates, B. F. *Eur. J. Inorg. Chem.* **2005**, 1048.
17. Bader, A.; Lindner, E. *Coord. Chem. Rev.* **1991**, *108*, 27.
18. Braunstein, P.; Naud, F. *Angew. Chem. Int. Ed.* **2001**, *40*, 680.
19. Braunstein, P. *J. Organomet. Chem.* **2004**, 689, 3953.
20. Slone, C. S.; Weinberger, D. A.; Mirkin, C. A. *Prog. Inorg. Chem.* **1999**, *48*, 233.
21. Faller J.W.; Milheiro, S. C.; Parr, J. *J. Organomet. Chem.* **2008**, *693*, 1493.
22. Dey, S.; Jain, V. K.; Varghese, B.; Schurr, T.; Niemeyer, M.; Kaim, W.; Butcher, R. J. *Inorg. Chim. Acta* **2006**, *359*, 1449.
23. Cornils, B.; Herrmann, W. A. *Applied Homogeneous Catalysis with Organometallic Compounds*; Wiley-VCH, Weinheim, **2002**.
24. Rieger, B.; Baugh, L. S.; Kacker, S.; Striegler, S. *Late Transition Metal Polymerisation Catalysis*; Wiley-VCH, Weinheim, **2003**.
25. Jeffrey, J. C.; Rauchfuss, T. B. *Inorg. Chem.* **1979**, *18*, 2658.

26. Braunstein, P.; Matt, D.; Mathey, F.; Thavard, D. *J. Chem. Res. Synop.* **1978**, 232.
27. Braunstein, P.; Matt, D.; Mathey, F.; Thavard, D. *J. Chem. Res. Miniprint* **1978**, 3041.
28. Rauchfuss, T. B.; Patino, F. T.; Roundhill D. M. *Inorg. Chem.* **1975**, *14*, 652.
29. Knebel W. J.; Angelici, R. J. *Inorg. Chem.* **1974**, *13*, 623.
30. Bacci, M.; Midollini, S. *Inorg. Chim. Acta* **1971**, *5*, 220.
31. Espino, G.; Jalón, F. A.; Maestro, M.; Manzano, B. R.; Pérez-Manrique, M.; Bacigalupe, A. C. *Eur. J. Inorg. Chem.* **2004**, *12*, 2542.
32. Bertini, I.; Dapporto, P.; Fallani, G.; Sacconi, L. *Inorg.Chem.* **1971**, *10*, 1703.
33. Abel, E. W.; Kite K.; Perkins, P. S. *Polyhedron* **1987**, *6*, 549.
34. Werner H.; Stark, A.; Scholz M.; Wolf, J. *Organometallics*, **1992**, *11*, 1126.
35. Abel, E. W.; Orrell, K. G.; Osborne, A. G.; Sik, V. *J. Chem. Soc., Dalton Trans.* **1994**, 111.
36. Ecke, A.; Keim, W.; Bonnet, M. C.; Tkatchenko, I.; Dahan F. *Organometallics*, **1995**, *14*, 5302.
37. Jutzi, P.; Siemeling, U. *J. Organomet. Chem.* **1995**, *500*, 175.
38. Yang, H.; Alvarez, M.; Lugan, N.; Nathieu, R. *J. Chem. Soc., Chem. Commun.* **1995**, 1721.
39. Yang, H.; Alvarez-Gressier, M.; Lugan, N.; Mathieu, R. *Organometallics*, **1997**, *16*, 1401.
40. Esteruelas, M. A.; López, A. M.; Oro, L. A.; Pérez, A.; Schulz, M.; Werner, H. *Organometallics*, **1993**, *12*, 1823.
41. Bischoff, S.; Weigt, A.; Mieβner, H.; Lücke, B. *J. Mol. Catal.* **1996**, *107*, 339.
42. Lindner E., Bader, A.; Bräunling H.; Jira, R. *J. Mol. Catal.* **1990**, *57*, 291.
43. Abu-Gnim, C.; Amer, I. *J. Chem. Soc., Chem. Commun.* **1994**, 115.
44. Gladiali, S.; Pinna, L.; Arena C. G.; Rotondo, E.; Faraone, F. *J. Mol. Catal.* **1991**, *66*, 183.
45. Bressan, M.; Morvillo, A. *J. Chem. Soc. Chem. Commun.* **1988**, 650.
46. Burgess, K.; Ohlmeyer M. J.; Whitmire, K. H. *Organometallics*, **1992**, *11*, 3588.
47. Britovsek, G. J. P.; Keim, W.; Mecking, S.; Sainz, D.; Wagner, T. *J. Organomet. Chem.* **1985**, *279*, C1.
48. Britovsek, G. J. P.; Cavell, K. J.; Keim, W. *J. Mol. Catal.* **1996**, *110*, 77.

49. Krampe, O.; Song, C.-E.; Kläui, W. *Organometallics*, **1993**, *12*, 4949.
50. Dunbar, K. R.; Haefner S. C.; Quillevéré, A. *Polyhedron*, **1990**, *9*, 1695.
51. Mirkin, C. A.; Wrighton, M. S. *J. Am. Chem. Soc.* **1990**, *112*, 8596.
52. Singewald, E. T.; Slone, C. S.; Stern, C. L.; Mirkin, C. A.; Yap, G. P. A.; Liable-Sands, L. M.; Rheingold, A. L. *J. Am. Chem. Soc.* **1997**, *119*, 3048.
53. Shi, J. -C.;Wu. D. -X.; Weng, T. -B.; Hong, M. -C.; Liu, Q. -T.; Lu, B. -S. S. -J.; Wang, H. -Q. *J. Chem. Soc. Dalton Trans.* **1996**, 2911.
54. Dunbar, K. R.; Sun, J.-S.; Quillevéré, A. *Inorg. Chem.* **1994**, *33*, 3598.
55. Oberbeckmann-Winter, N.; Morise, X.; Braunstein, P.; Welter, R. *Inorg. Chem.* **2005**, *44*, 1391
56. Kloetzing, R. J.; Knochel, P. *Tetrahedron: Asymmetry*, **2006**, *17*, 116.
57. Cui, X.; Li, J.; Zhang, Z.-P.; Fu, Y.; Liu, L.; Guo, Q.-X. *J. Org. Chem.* **2007**, *72*, 9342.
58. Orrell K. G.; Osborne, A. G.; Sik, V.; Da Silva, M. W. *Polyhedron*, **1995**, *14*, 2797.
59. Heck R. F. *J. Am. Chem. Soc.* **1968**, *90*, 5531.
60. Heck R. F. *J. Am. Chem. Soc.* **1968**, *90*, 5535.
61. Heck R. F. *J. Am. Chem. Soc.* **1971**, *93*, 6896.
62. Mizoroki, T.; Mori, K.; Ozaki, A.; *Bull. Chem. Soc. Jpn.* **1971**, *44*, 581.
63. Heck R. F.; Nolley, J. P., *J. Org. Chem.* **1972**, *37*, 2320.
64. Dieck, H. A.; Heck, R. F. *J. Am. Chem. Soc.*, **1974**, *96*, 1133.
65. Ben-David, Y.; Portnoy, M.; Gozin, M.; Milstein, D. *Organometallics*, **1992**, *11*, 1995.
66. Jutland, A.; Mosleh, A. *Organometallics*, **1995**, *14*, 1810.
67. Fu, X.; Zhang, S.; Yin, J.; McAllister, T. L.; Jiang, S. A.; Tann, C. -H.; Thiruvengadam T. K.; Zhang, F. *Tetrahedron Lett.* **2002** *43*, 573.
68. Hansen A. L.; Skrydstrup, T. *Org. Lett.* **2005**, *7*, 5585.
69. Kikukawa, K.; Matsuda, T. *Chem. Lett.* **1977**, 159.
70. Jeffery, T. *J. Chem. Soc., Chem. Commun.* **1984**, 1287.
71. Sato, Y.; Sodeoka, M.; Shibasaki, M. *J. Org. Chem.* **1989**, *54*, 4738.
72. Sato, Y.; Sodeoka, M.; Shibasaki, M. *Chem. Lett.* **1990**, 1953.
73. Carpenter, N. E.; Kucera, D. J.; Overmann, L. E. *J. Org. Chem.* **1989**, *54*, 5846.

74. Du, X.; Suguro, M.; Hirabayashi K.; Mori, A. *Org. Lett.* **2001**, *3*, 3313.
75. Farina, V. *Adv. Synth. Catal.* **2004**, *346*, 1553.
76. Hartwig, J. F.; *Angew. Chem. Int. Ed.* **1998**, *37*, 2046.
77. Cardenas, D. J. *Angew. Chem. Int. Ed.* **2003**, *42*, 384.
78. Littke, A. F.; Fu, G. C. *J. Am. Chem. Soc.* **2001**, *123*, 6989.
79. Littke, A. F.; Fu, G. C. *Angew. Chem. Int. Ed.* **2002**, *41*, 4176.
80. Beller, M.; Zapf, A.; Maegerlain, W. *Chem. Eng. Technol.* **2001**, *24*, 575.
81. Tucker, C. E.; de Vries, J. G. *Top. Catal.* **2002**, *19*, 111.
82. de Vries J. G. *Can. J. Chem.* **2001**, *79*, 1086.
83. Masters, J.; Jung, D. K.; Bornmann, W.G.; Danishefsky S. J. *Tetrahedron Lett.*, **1993**, *34*, 7253.
84. Beletskaya, I. P.; Cheprakov, A. V. *Chem. Rev.* **2000**, *100*, 3009.
85. Bräse, S.; de Meijere A. *Palladium-catalysed Coupling of Organyl Halides to Alkenes – The Heck reaction,* Ed. F. Diederich, and P. J. Stang, Wiley-VCH, Germany, **1998**, 99.
86. Alonso, F.; Beletskaya, I. P.; Yus, M. *Tetrahedron*, **2005**, *61*, 11771.
87. de Meijere, A.; Meyer F. E. *Angew. Chem. Int. Ed.* **1995**, 33, 2379.
88. Shaw, B. L.; Perera, D.; Stanley, E. A. *Chem. Commun.* **1998**, 1361.
89. Ohff, M.; Ohff, A., van der Boom, M. E.; Milstein, D. *J. Am. Chem. Soc.* **1997**, *119*, 11687.
90. Beller, M.; Riermeier, T. H. *Eur. J. Inorg. Chem.* **1998**, 29.
91. Rosol, M.; Moyano, A. *J. Organomet. Chem.* **2005**, *690*, 2291.
92. Nilsson, P.; Wendt, O. F. *J. Organomet. Chem.* **2005**, *690*, 4197.
93. Böhm, V. P. W.; Herrmann, W. A. *Chem.-Eur. J.* **2001**, *7*, 4191.
94. d'Orlyé, F.; Jutand, A. *Tetrahedron*, **2005**, *61*, 9670.
95. Sundermann, A.; Uzan, O.; Martin, J. M. L. *Chem. Eur. J.* **2001**, *7*, 1703.
96. Cabri, W.; Candiani. I. *Acc. Chem. Res.* **1995**, *28*, 2.
97. Amatore, A.; Jutand, A. *Acc. Chem. Res.* **2000**, *33*, 314.
98. Amatore C.; Carré E.; Jutand, A.; M'Barki, M. A.; Meyer, G. *Organometallics,* **1995**, *14*, 5605.
99. Van Strijdonck, G. P. F.; Boele, M. D. K.; Kamer, P. C. J.; de Vries J. G.; Leewen, P. W. N. M. *Eur. J. Inorg. Chem.* **1999**, 1073.

100. Dyson, P. J.; Ellis, D. J.; Parker, D. G.; Welton, T *Chem. Commun.*, **1999**, 25.

101. Whitcombe, N. J.; Hii, K. K.; Gibson, S. E. , *Tetrahedron*, **2001**, *57*, 7449.

102. Grushin, V. V.; Alper, H. *Chem. Rev.*, **1994**, *94*, 1047.

103. Zapf, A.; Beller, M. *Top. Catal.* **2002**, *19*, 101.

104. Herrmann, W. A.; Brossmer, C.; Priermeier, T.; Öfele, K. *J. Organomet. Chem.* **1994**, *481*, 97.

105. Alonso, D. A.; Najera, C.; Pacheco, M. C. *Org. Lett.* **2000**, *2*, 1823.

106. Markies, B. A.; Wijkens, P.; Boersma, J.; Kooijman, H.; Veldman, N.; Spek, A. L.; van Koten, G. *Organometallics*, **1994**, *13*, 3244.

107. Wright, D. W.; Mok, H. J.; Dube, C. E.; Armstrong, W. H. *Inorg. Chem.* **1998**, *37*, 3714.

108. Rachel Madden, Honours Thesis, University of Tasmania, **2003**.

109. Chia, P. S. K.; Livingstone, S. E.; Lockyer, T. N. *Aust. J. Chem.* **1967**, *20*, 239.

110. Schaubroeck, J.; Goeminne, A. M. *Thermochim. Acta*, **1982**, *56*, 25.

111. Skelton, B. W.; Tolhurst, V.-A.; White, A. H.; Williams, A. M.; Wilson, A. J.; *J. Organomet. Chem.* **2003**, *674*, 38.

112. Canovese, L.; Visentin, F.; Chessa, G.; Uguagliati, P.; Dolmella, A. *J. Organomet. Chem.* **2000**, *601*, 1.

113. Canovese, L.; Visentin, F.; Chessa, G.; Santo, C.; Uguagliati, P.; Maini, L.; Polito, M.; *J. Chem. Soc., Dalton Trans.* **2002**, 3696.

114. Canovese, L.; Lucchini, V.; Santo, C.; Visentin, F.; Zambon, A. *J. Organomet. Chem.* **2002**, *642*, 58.

115. Canovese, L.; Visentin, F.; Chessa, G.; Uguagliati, P.; Bandoli, G. *Organometallics*, **2000**, *19*, 1461.

116. Canovese, L.; Visentin, F.; Chessa, G.; Santo, C.; Uguagliati, P.; Bandoli, G. *J. Organomet. Chem.* **2002**, *650*, 43.

117. Canovese, L.; Chessa, G.; Santo, C.; Visentin, F.; Uguagliati, P. *Inorg. Chim. Acta* **2003**, *346*, 158.

118. Canovese, L.; Visentin, F.; Chessa, G.; Uguagliati, P.; Santo, C.; Dolmella, A. *Organometallics*, **2005**, *24*, 3297.

119. Canovese, L.; Visentin, F.; Uguagliati, P.; Chessa, G.; Lucchini, V.; Bandoli, G. *Inorg. Chim. Acta* **1998**, *275-276*, 385.

120. Canovese, L.; Visentin, F.; Uguagliati, P.; Chessa, G.; Pesce, A. *J. Organomet. Chem.* **1998**, *566*, 61.

121. Canovese, L.; Visentin, F.; Santo, C.; Chessa, G.; Uguagliati, P. *Polyhedron*, **2001**, *20*, 3171.

122. Haviv, F.; DeNet, R. W.; Michaels, R. J.; Ratajczyk, J. D.; Carter, G. W.; Young, P. R. *J. Med. Chem.* **1983**, *26*, 218.

123. Chelucci, G.; Berta, D.; Saba A. *Tetrahedron*, **1997**, *53*, 3843.

124. Chelucci, G.; Berta, D.; Fabbri, D.; Pinna, G. A.; Saba, A.; Ulgheri, F. *Tetrahedron: Asymmetry*, **1998**, *9*, 1933.

125. Canovese, L.; Visentin, F.; Chessa, G.; Santo, C.; Levi, C.; Uguagliati, P. *Inorg. Chem. Commun.* **2006**, *9*, 388.

126. Canovese, L.; Visentin, F.; Chessa, G.; Uguagliati, P.; Santo, C.; Maini, L. *J. Organomet. Chem.* **2007**, *692*, 2342.

127. Canovese, L.; Visentin, F.; Santo, C. *J. Organomet. Chem.* **2007**, *692*, 4187.

128. Canovese, L.; Visentin, F.; Levi, C.; Santo, C. *J. Organomet. Chem.* **2008**, *693*, 3324.

129. Miyaura, N.; Suzuki, A. *Chem. Rev.* **1995**, *95*, 2457.

130. Suzuki, A. In *Metal-Catalyzed Cross-Coupling Reactions*; Diederich, F.; Stang, P. J., Eds.; Wiley-VCH: Weinheim, **1998**, 49.

131. Suzuki, A. *J. Organomet. Chem.* **1999**, *576*, 147.

132. Tamao, K.; Sumitani, K.; Kumada, M. *J. Am. Chem. Soc.* **1972**, *94*, 4374.

133. Tamao, K.; Kiso, Y.; Sumitani, K.; Kumada, M. *J. Am. Chem. Soc.* **1972**, *94*, 9268.

134. Corriu, R. J. P.; Masse, J. P. *J. Chem. Soc., Chem. Commun.* **1972**, 144.

135. Tamura, M.; Kochi, J. K. *J. Am. Chem. Soc.* **1971**, *93*, 1487.

136. Tamura, M.; Kochi, J. K. *Synthesis,* **1971**, 303.

137. Yamamura, M.; Moritani, I.; Murahashi, S. *J. Organomet. Chem.* **1975**, *91*, C39.

138. Negishi, E.; Baba, S. *J. Chem. Soc. Chem. Commun.* **1976**, 596.

139. Negishi, E.; King, A. O.; Okukado, N. *J. Org. Chem.* **1977**, *42*, 1821.

140. Negishi, E.; Van Horn, D. E. *J. Am. Chem. Soc.* **1977**, *99*, 3168.

141. Murahashi, S.; Yamamura, M.; Yanagisawa, K.; Mita, N.; Kondo, K. *J. Org. Chem.* **1979**, *44*, 2408.

142. Kosugi, M.; Simizu, Y.; Migita, T. *Chem. Lett.* **1977**, 1423.
143. Milstein, D.; Stille, J. K. *J. Am. Chem. Soc.* **1979**, *101*, 4992.
144. Hatanaka, Y.; Hiyama, T. *J. Org. Chem.* **1988**, *53*, 918.
145. Miyaura, N.; Yamada, K.; Suzuki, A. *Tetrahedron Lett.* **1979**, 3437.
146. Miyaura, N.; Suzuki, A. *J. Chem. Soc., Chem. Commun.* **1979**, 866.
147. Negishi, E. *J. Organomet. Chem.* **2002**, *653*, 34.
148. Negishi, E. *Aspects of Mechanism and Organometallic Chemistry*; Brewster, J. H. Eds.; Plenum Press: New York, **1978**, 285.
149. Negishi, E. *Acc. Chem. Res.* **1982**, *15*, 340.
150. Martin, R.; Buchwald, S. L. *Acc. Chem. Res.* **2008**, *41*, 1461.
151. Kertesz, M.; Choi, C. H.; Yang, S. *Chem. Rev.* **2005**, *105*, 3448.
152. Kaye, S.; Fox, J. M.; Hicks, F. A.; Buchwald, S. L. *Adv. Synth. Catal.* **2001**, *343*, 789.
153. Kotha, S.; Lahiri, K.; Kashinath, D. *Tetrahedron*, **2002**, *58*, 9633.
154. Hall, D. G. *Boronic Acids-Preparation, Applications in Organic Synthesis and Medicine*; Hall, D. G., Ed.; Wiley-VCH: Weinheim, Germany, **2005**, 1.
155. Lipton, M. F.; Mauragis, M. A.; Maloney, M. T.; Veley, M. F.; VanderBor, D. W.; Newby, J. J.; Appell, R. B.; Daugs, E. D. *Org. Process Res. Dev.* **2003**, *7*, 385.
156. Smith, G. B.; Dezeny, G. C.; Hughes, D. L.; King, A. O.; Verhoeven, T. R. *J. Org. Chem.* **1994**, *59*, 8151.
157. Ennis, D. S.; McManus, J.; Wood-Kaczmar, W.; Richardson, J.; Smith, G. E.; Carstairs, A. *Org. Process Res. Dev.* **1999**, *3*, 248.
158. Jacks, T. E.; Belmont, D. T.; Briggs, C. A.; Horne, N. M.; Kanter, G. D.; Karrick, G. L.; Krikke, J. J.; McCabe, R. J.; Mustakis, J. G.; Nanninga, T. N.; Risedorph, G. S.; Seamans, R. E.; Skeenan, R. E.; Winkle, D. D.; Zennie, T. M. *Org. Process Res. Dev.* **2004**, *8*, 201.
159. Suzuki, A. *Pure Appl. Chem.* **1994**, *66*, 213.
160. Miyaura, N. *Top. Curr. Chem.* **2002**, *219*, 11.
161. Bellina, F.; Carpita, A.; Rossi, R. *Synthesis*, **2004**, *15*, 2419.
162. Braga, A. A. C.; Morgon, N. H.; Ujaque, G.; Maseras, F. *J. Am. Chem. Soc.* **2005**, *127*, 9298.
163. Miyaura, N. *J. Organomet. Chem.* **2002**, *653*, 54.

164. Littke, A. F.; Dai, C.; Fu, G. C. *J. Am. Chem. Soc.* **2000**, *122*, 4020.

165. Harkal, S.; Rataboul, F.; Zapf, A.; Fuhrmann, C.; Riermeier, T.; Monsees, A.; Beller, M. *Adv. Synth. Catal.* **2004**, *346*, 1742.

166. Kantchev, E. A. B.; O'Brien, C. J.; Organ, M. G. *Angew. Chem., Int. Ed.* **2007**, *46*, 2768.

167. Dai, Q.; Gao, W.; Liu, D.; Kapes, L. M.; Zhang, X. *J. Org. Chem.* **2006**, *71*, 3928.

168. Punji, B.; Mague, J. T.; Balakrishna, M. S. *Inorg. Chem.* **2006**, *45*, 9454.

169. Safin, D. A.; Babashkina, M. G.; Klein, A. *Catal. Lett.* **2008**, Doi10.1007/s10562-008-9778-9

170. Kumar, A.; Agarwal, M.; Singh, A. K. *J. Organomet. Chem.* **2008**, *693*, 3533.

171. Chinchilla, R.; Nájera, C. *Chem. Rev.* **2007**, *107*, 874.

172. Diek, H. A.; Heck, F. R. *J. Organomet. Chem.* **1975**, *93*, 259.

173. Cassar, L. *J. Organomet. Chem.* **1975**, *93*, 253.

174. Sonogashira, K.; Tohda, Y.; Hagihara, N. *Tetrahedron Lett.* **1975**, *16*, 4467.

175. Stephens, R. D.; Castro, C. E. *J. Org. Chem.* **1963**, *28*, 2163.

176. Stephens, R. D.; Castro, C. E. *J. Org. Chem.* **1963**, *28*, 3313.

177. Eckhardt, M.; Fu, G. C. *J. Am. Chem. Soc.* **2003**, *125*, 13642.

178. Altenhoff, G.; Würtz, S.; Glorius, F. *Tetrahedron Lett.* **2006**, *47*, 2925.

179. Sumi, S.; Matsumoto, K.; Tokuyama, H.; Fukuyama, T. *Tetrahedron*, **2003**, *59*, 8571.

180. Lee, H.; Kim, H.; Yoon, T.; Kim, B.; Kim, S.; Kim, H.–D.; Kim, D. *J. Org. Chem.* **2005**, *70*, 8723.

181. Pahadi, N. K.; Camacho, D. H.; Nakamura, I.; Yamamoto, Y. *J. Org. Chem.* **2006**, *71*, 1152.

182. Li, Y.; Zhang, J.; Wang, W.; Miao, Q.; She, X.; Pan, X. *J. Org. Chem.* **2005**, *70*, 3285.

183. Sonogashira, K. *J. Organomet. Chem.* **2002**, 653, 46.

184. Brandsma, L. *Synthesis of Acetylenes, Allenes and Cumulenes: Methods and Techniques;* Elsevier: Oxford, **2004**, 293.

185. Posset, T.; Bümel, J. *J. Am. Chem. Soc.* **2006**, *128*, 8394.

186. Tougerti, A.; Negri, S.; Jutand, A. *Chem. Eur. J.* **2007**, *13*, 666.

187. Bertus, P.; Frécourt, F.; Bauder, C.; Pale, P. *New J. Chem.* **2004**, *28*, 12.

188. Létinois-Halbes, U.; Pale, P.; Berger, S. *J. Org. Chem.* **2005**, *70*, 9185.

189. Soheili, A.; Albaneze-Walker, J.; Murry, J. A.; Dormer, P. G.; Hughes, D. L. *Org. Lett.* **2003**, *5*, 4191.

190. Amatore, C.; Bensalen, S.; Ghalem, S.; Jutand, A. *J. Organomet. Chem.* **2004**, *689*, 4642.

191. Böhm, V. P.H.; Hermann, W. A. *Eur. J. Org. Chem.* **2000**, *6*, 3679.

192. Hundertmark, T.; Littke, A. F.; Buchwald, S. L.;Fu, G. C. *Org. Lett.* **2000**, *2*, 1729.

193. Feuerstein, M.; Doucet, H.; Santelli, M. *Tetrahedron Lett.* **2004**, *45*, 8443.

194. Caddick, S.; Cloke, F. G. N.; Clentsmith, G. K. B.; Hitchcock, P. B.; McKerrecher, D.; Titcomb, L. R.; Williams, M. R. V. *J. Organomet. Chem.* **2001**, *617-618*, 635.

195. Eberhard, M. R.; Wang, Z.; Jensen, C. M. *Chem. Commun.* **2002**, 818.

196. Arques, A.; Auñón, D.; Molina, P. *Tetrahedron Lett.* **2004**, *45*, 4337.

197. Nishide, K.; Liang, H.; Ito, S.; Yoshifuji, M. *J. Organomet. Chem.* **2005**, *690*, 4809.

198. Bolton, K. F.; Canty, A. J.; Deverell, J. A.; Guijt, R. M.; Hilder, E. F.; Rodemann, T.; Smith, J. A.; *Tetrahedron Lett.*, **2006**, *47*, 9321.

199. Canty, A. J.; Deverell, J. A.; Gömann, A.; Guijt, R. M.; Rodemann, T.; Smith, J. A.; *Aust. J. Chem.* **2008**, *61*, 630.

Chapter Two

Ligand Synthesis

2.1 Introduction

There are several known methods for preparing heteroleptic ligand systems such as **I**.

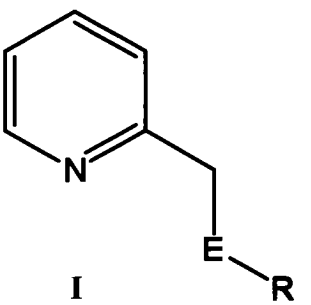

I

The most general method of preparation is via the synthesis of a chloro species such as 2-chloromethylpyridine and subsequent nucleophilic attack by thiolates, RS^-,[1-8] first reported by Michalski in 1957 for the synthesis of 2-(phenylthiomethyl)pyridine[9] (**Scheme 2.1**), and utilised by Canovese in the synthesis of palladium[1-5,10-12] and platinum[13] complexes. From this point forward, for 2-(phenylthiomethyl)pyridine the notation $pyCH_2SPh$ will be used, where py = 2-C_5H_4N. Similar compounds used or synthesised in this study will be abbreviated in a analogous fashion *i.e.*, for the compound 4-methyl-2-(phenylselenomethyl)pyridine the abbreviation 4-Me$pyCH_2SePh$ will be used.

$$pyCH_2Cl + NaSMe \longrightarrow pyCH_2SMe$$

Scheme 2.1 Synthesis of 2-(methylthiomethyl)pyridine developed by Michalski.

There has also been a report of a methylselenoether analogue obtained by the reaction of $pyCH_2Se^-Li^+$ with iodomethane, **Scheme 2.2**.[14]

$$pyCH_2Se^-\,Li^+ + MeI \longrightarrow pyCH_2SeMe$$

Scheme 2.2 Synthesis of 2-(methylselenomethyl)pyridine developed by Bhasin.

These methods of synthesis, although quite simple, tend to be specific for the individual target molecule, can be low yielding and the preparation of the desired 2-halomethyl pyridyl precursor is required. This protocol can be difficult and sometimes tedious for target molecules containing functionality on the pyridyl ring as inmost cases the 2-halomethyl pyridyl species is not commercially available. This often involves difficult and expensive synthetic procedures with several steps and extensive chromatography, as described for the synthesis of 6-methyl-2-(methylthiomethyl)pyridine[4] *via* the preparation of 6-MepyCH_2Cl,[15]**Scheme 2.3**. The overall yield for this particular reaction is only ~14%.Bhasin's method (**Scheme 2.2**), which does not use a halogenated reagent, involves selenium prepared by rigorous grinding followed by long stirring periods to get the highly insoluble selenium into solution.

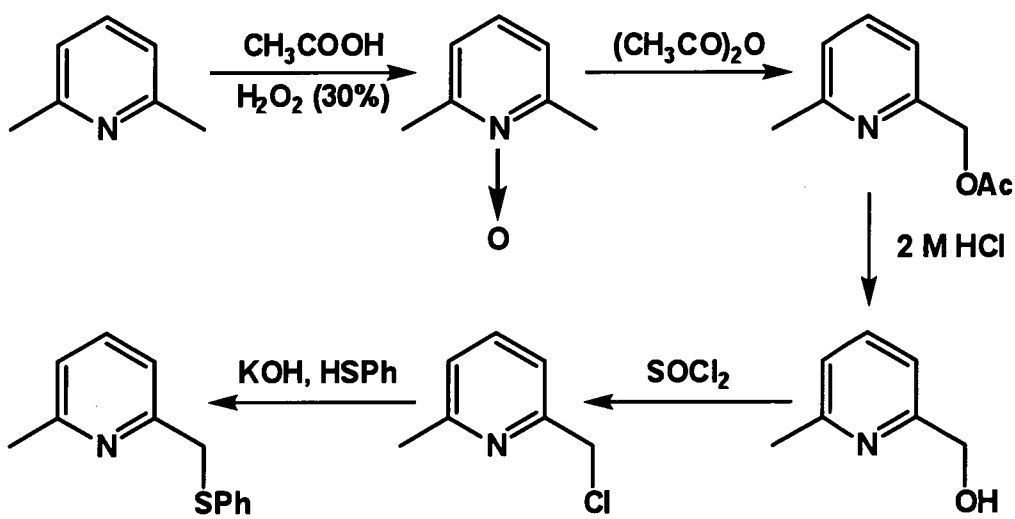

Scheme 2.3 Synthesis of 6-methyl-2-(phenylthiomethyl)pyridine.

One particular reported method of synthesis that appears more suitable is that based on the reaction of 2,3-lutidine with *n*-butyllithium and diphenyldisulfide to form 3-MepyCH_2SPh, **Scheme 2.4**.[16]

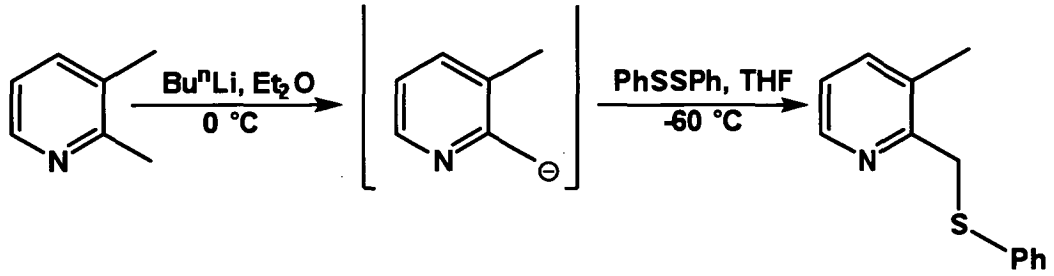

Scheme 2.4 Synthesis reported by Ghera and Ben-David.

This method, reported only by Ghera and Ben-David,[16] is a relatively simple 'one pot' synthesis and could be, unlike previous methodologies, potentially generalised to produce a wide variety of new heteroleptic ligands with various chalcogens, and various substitutions on both the chalcogen and pyridine ring. This freedom of choice is largely due to the extensive range of commercially available substituted pyridines and diorganyl dichalcogenides.

2.2 Results and Discussion

2.2.1 Synthesis

In Ghera and Ben-David's method, 2,3-lutidine is added to a cooled solution of *n*-butyllithium in dry diethyl ether.[16] However, when 2-picoline or 2,6-lutidine were used, large amounts of bis-substituted pyridyl thioether products were obtained, leading to low yields of the desired product. Consequently, the ligands for this study were prepared by a modification and optimisation of this method in which the alkyllithium solution was added drop-wise to a cooled solution of parent picoline (or lutidine) in cooled diethyl ether. The large excess of the picoline (or lutidine) present at all times prevented undesired secondary lithiation. Reaction with diorganyl dichalcogenide then gives the required product in good to high yield, **Scheme 2.5**.

All products are air and moisture stable oils having moderate sensitivity to temperature and light, and were consequently stored at 4°C to avoid discolouration. Discolouration has been found not to affect the yield or purity of complexes prepared from the ligands, but can easily be removed by silica chromatography or distillation.

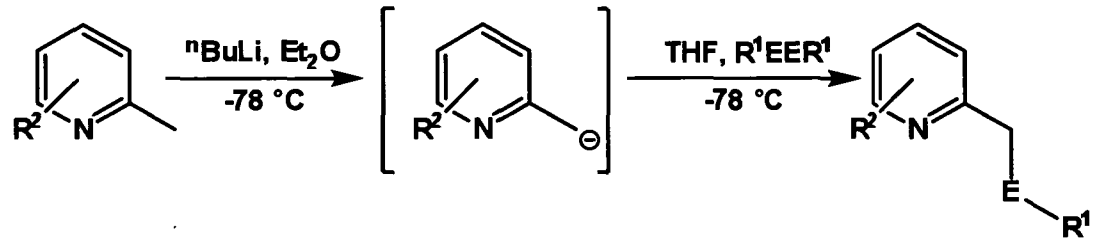

II III IV

Scheme 2.5 Method of ligand synthesis used in this study

R^2 = H, Me, Ph
R^1 = Me, Ph
E = S, Se

A wide range of new and known ligands were obtained, with varied substitutions on the pyridyl ring and organochalcogen group, **Figure 2.1**. This flexibility in synthesis is ideal, allowing access to a group of compounds tuned for electronic and steric factors.

While the synthetic method is superior to traditional nucleophilic attack by thiolates (**Scheme 2.1**) due to the large range of commercially available pyridyl reagents and, for selenium containing products, difficult to handle elemental selenium is not required.

Of the ligands shown in **Figure 2.1**, only 6-PhpyCH$_2$SMe, 6-PhpyCH$_2$SPh, and 6-PhpyCH$_2$SePh required more synthetic steps than that already described, owing to the limited (and costly) availability of 6-phenyl-2-picoline as a starting material from commercial sources such as Small Molecules Inc. This compound was prepared by a modification of the method reported by Zheng *et al.*[17] utilising the Suzuki reaction of 6-bromo-2-picoline and phenylboronic acid, **Scheme 2.6**. To enhance the yield, the procedure was modified by adding another 0.5 equivalents of the phenylboronic acid together with another 1 mol% of catalyst after six hours of reaction time, giving the desired compound in 98% yield. Micro-distillation was used to remove any slight discolouration of the product. 6-Phenyl-2-picoline was then reacted with *n*-butyllithium and the appropriate diorganyl dichalcogenide to afford 6-PhpyCH$_2$SMe, 6-PhpyCH$_2$SPh and 6-PhpyCH$_2$SePh in the manner described above.

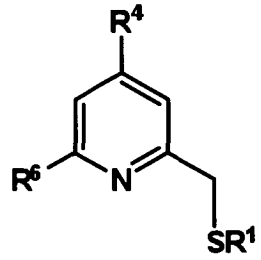

R^1	R^4	R^6	E	Compound	Previous Methods of Preparation	Yield (%)
Me	H	H	S	$pyCH_2SMe$	Scheme 2.1[1]	85 (82)
Me	Me	H	S	$4\text{-}MepyCH_2SMe$*		87
Me	H	Me	S	$6\text{-}MepyCH_2SMe$	Scheme 2.1[2]	68 (70)
Me	H	Ph	S	$6\text{-}PhpyCH_2SMe$*		94
Ph	H	H	S	$pyCH_2SPh$	Scheme 2.1[3,9]	47 (80)
Ph	Me	H	S	$4\text{-}MepyCH_2SPh$*		49
Ph	H	Me	S	$6\text{-}MepyCH_2SPh$	Scheme 2.3[4,15]	53 (96)
Ph	H	Ph	S	$6\text{-}PhpyCH_2SPh$*		76
Me	H	H	Se	$pyCH_2SeMe$	Scheme 2.2[14]	92 (85)
Ph	H	H	Se	$pyCH_2SePh$	Scheme 2.1[5]	70 (59)
Ph	Me	H	Se	$4\text{-}MepyCH_2SePh$*		77
Ph	H	Me	Se	$6\text{-}MepyCH_2SePh$	Scheme 2.1[5]	74 (87)
Ph	H	Ph	Se	$6\text{-}PhpyCH_2SePh$*		85

Figure 2.1 Ligands prepared by the new modified synthesis. * denotes new compounds synthesised in this study. Literature yields in brackets.

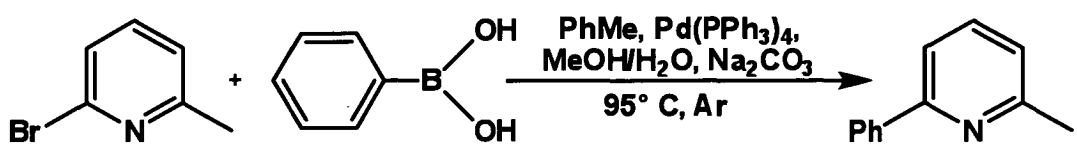

Scheme 2.6 Preparation of 6-phenyl-2-picoline.

2.2.2 Ligand Characterisation

The room temperature ^{1}H NMR and $^{13}C\{^{1}H\}$NMR spectra of all compounds are as expected and show no obvious trends upon substitution of the pyridyl ring, or when the chalcogen is altered from sulfur to selenium.

Representative ^{1}H NMR and $^{13}C\{^{1}H\}$NMR spectra for the2-(methylthiomethyl)pyridine compounds $pyCH_2SMe$, 4-$MepyCH_2SMe$, and 6-$MepyCH_2SMe$ are shown in **Figure 2.2** and **Figure 2.3**; 2-(phenylthiomethyl)- and2-(phenylselenomethyl)pyridine compounds $pyCH_2SPh$, 4-$MepyCH_2SPh$, 6-$MepyCH_2SPh$, $pyCH_2SePh$, 4-$MepyCH_2SePh$, and 6-$MepyCH_2SePh$ are shown in **Figure 2.4**and **Figure 2.5**; 6-phenyl-2-(phenylthiomethyl)- and 6-phenyl-2-(phenylselenomethyl)pyridine compounds 6-$PhpyCH_2SMe$,6-$PhpyCH_2SPh$, and6-$PhpyCH_2SePh$ are shown in **Figure 2.6**and **Figure 2.7**. In all cases, ranges marked on the spectra are ranges of the protons/carbons from that region for those compounds.

Electron ionisation (EI) Mass Spectra of all compounds exhibited ions corresponding to the molecular ion minus a proton. Elemental analysis conducted on all samples gave acceptable results.

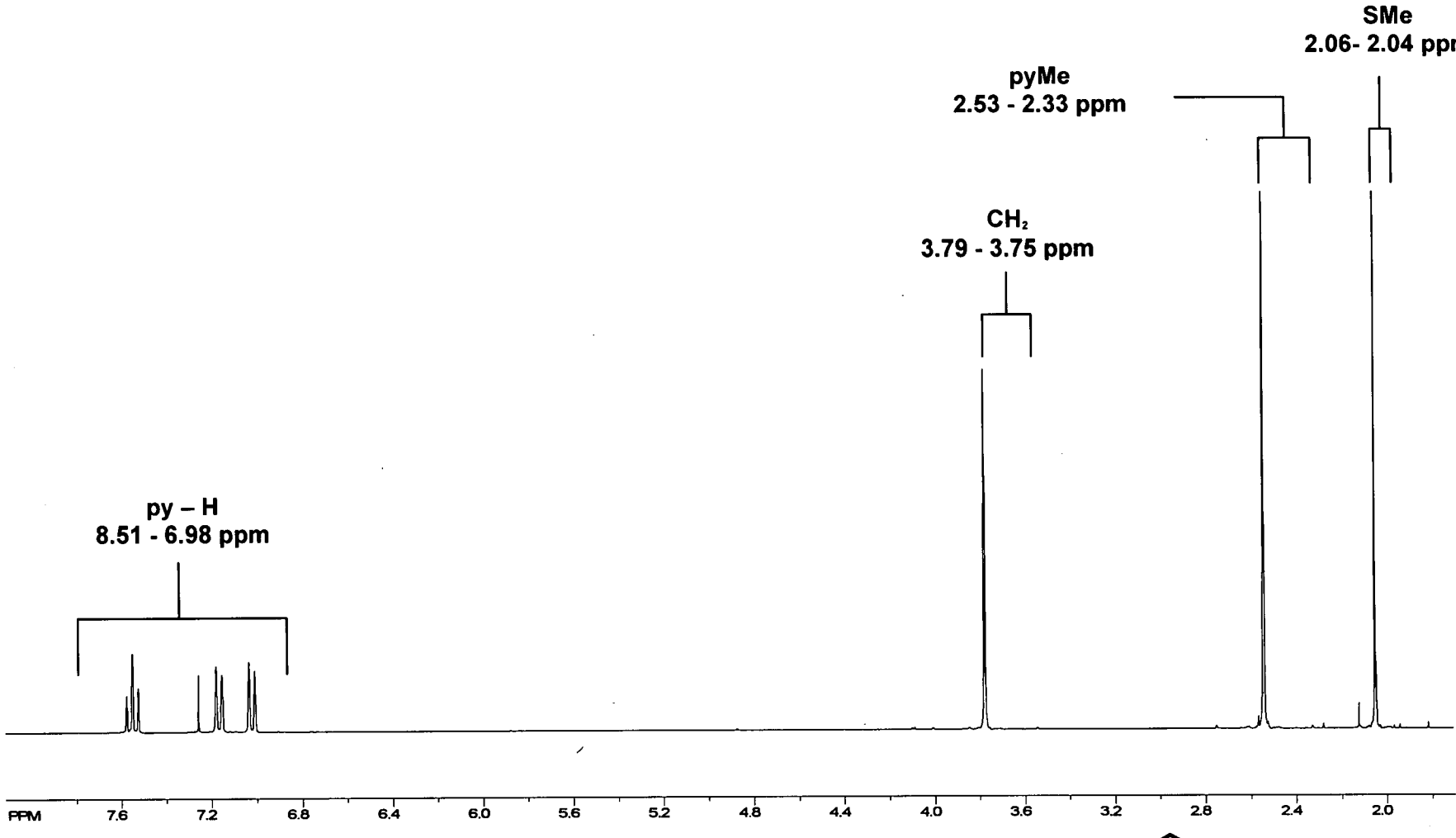

Figure 2.2 ^{1}H NMR spectrum of 6-MepyCH$_2$SMe; typical for all the 2-(methylthiomethyl)pyridine compounds with the formula R-pyCH$_2$SMe.

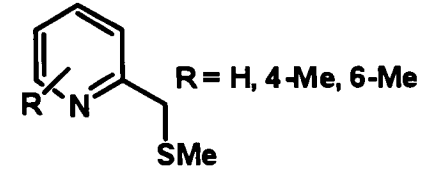

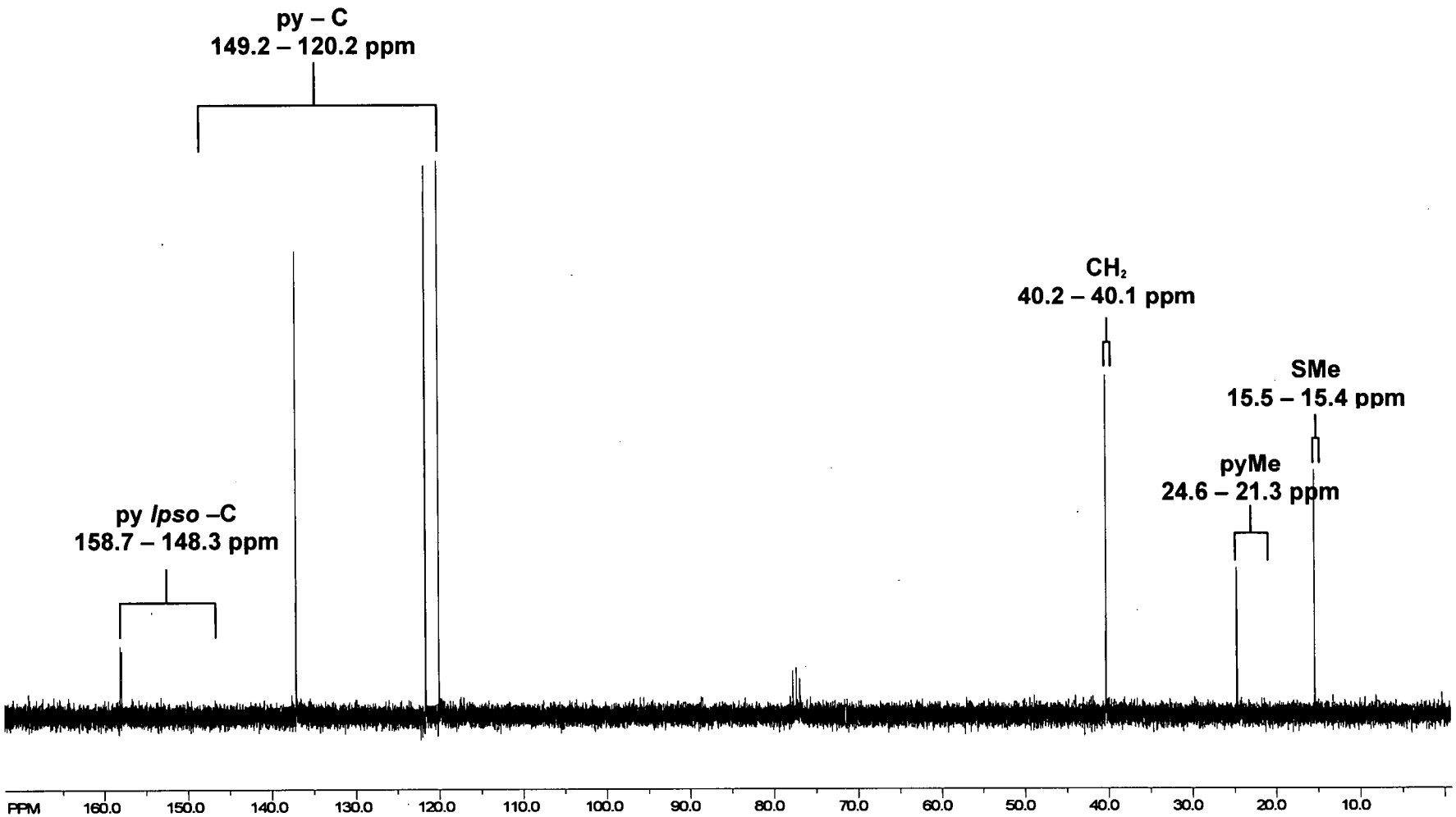

Figure 2.3 $^{13}C\{^{1}H\}$ NMR spectrum of 6-Me$pyCH_2SMe$; ranges marked are for the2-(methylthiomethyl)pyridine compounds with the formulaR-$pyCH_2SMe$.

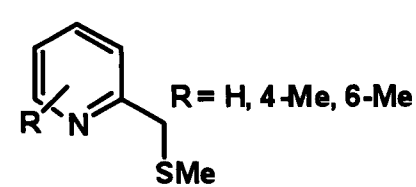

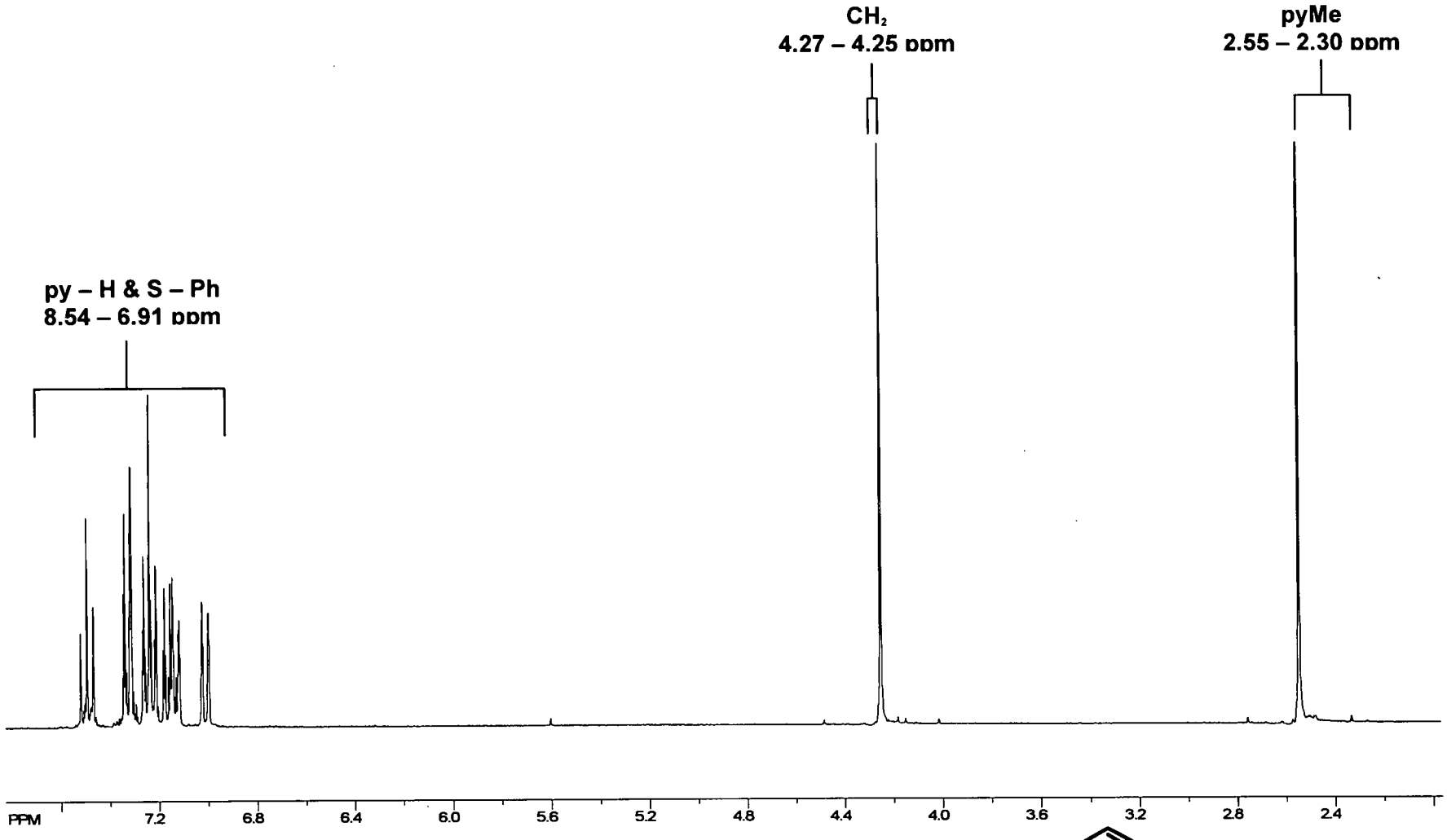

Figure 2.4 ^{1}H NMR spectrum of 6-MepyCH_2SPh; ranges marked are for the2-(methylchalcogenomethyl)pyridine compounds with the formula R-pyCH_2EPh.

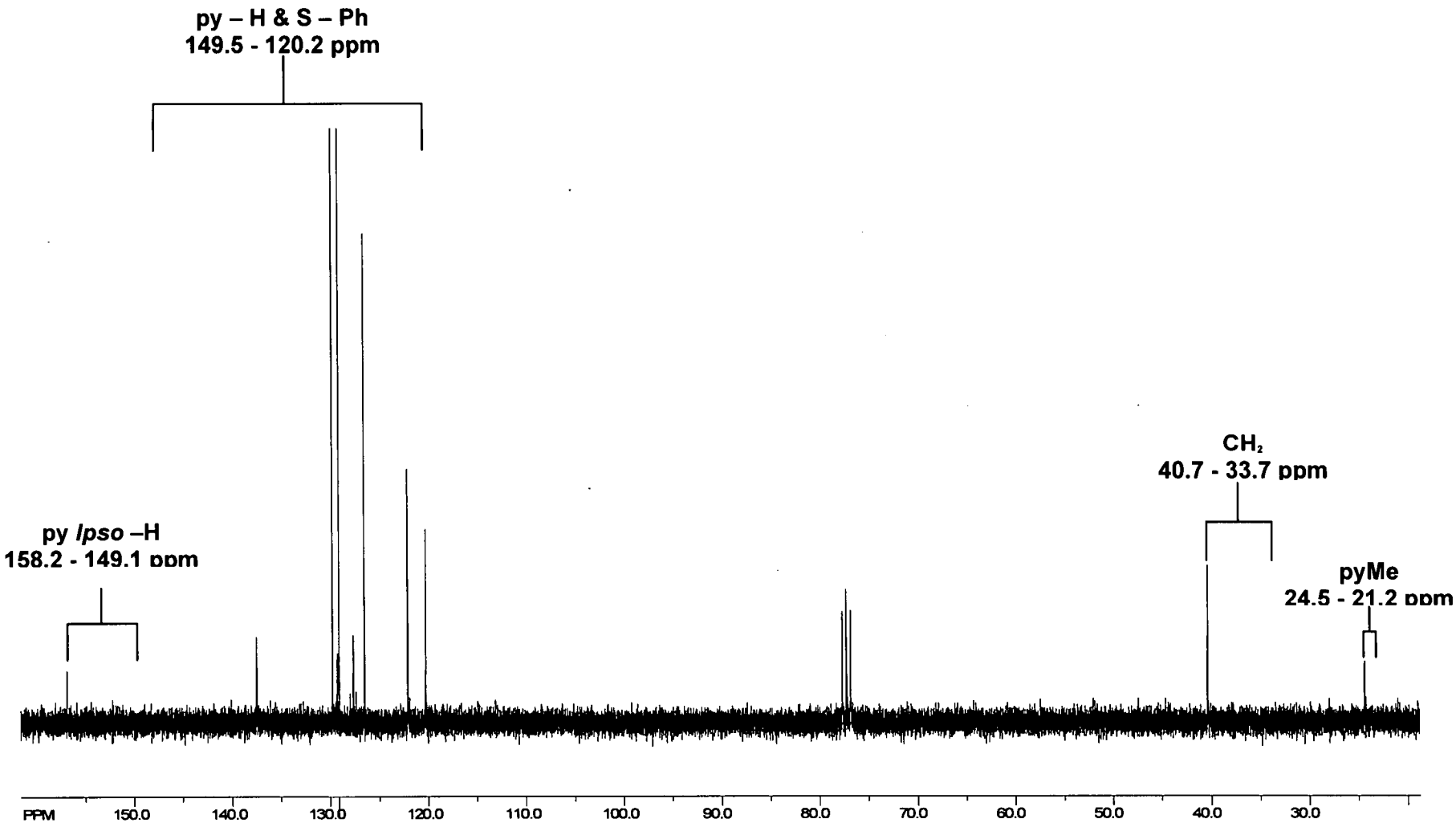

Figure 2.5 $^{13}C\{^1H\}$ NMR spectrum of 6-MepyCH_2SPh; ranges marked are for the2-(methylchalcogenomethyl)pyridinecompounds with the formula R-pyCH_2EPh.

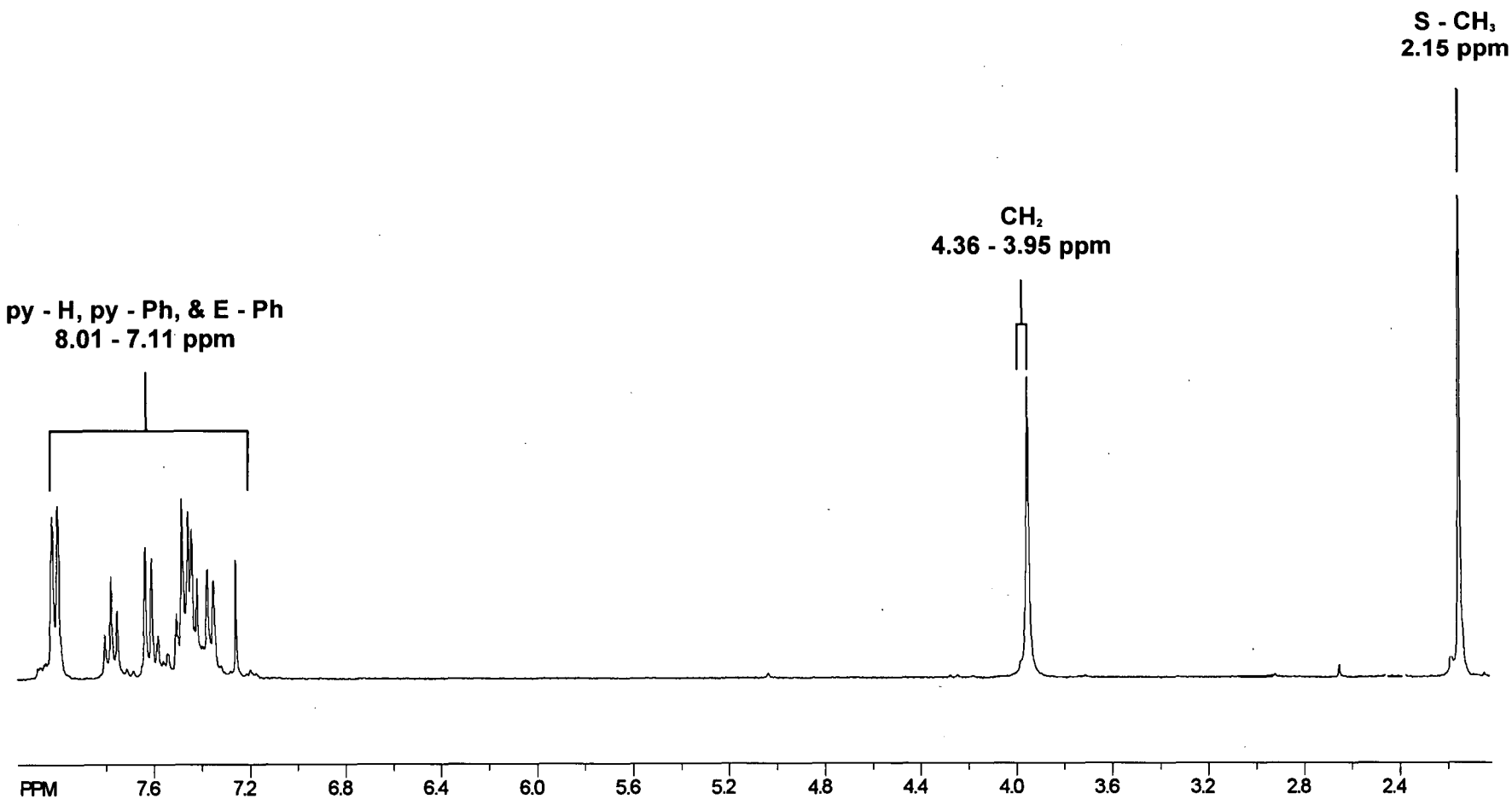

Figure 2.6 ^{1}H NMR spectrum of 6-PhpyCH$_2$SMe ranges marked are for the 6-phenyl-2-(methylchalcogenomethyl)pyridine compounds with the formula 6-PhpyCH$_2$ER.

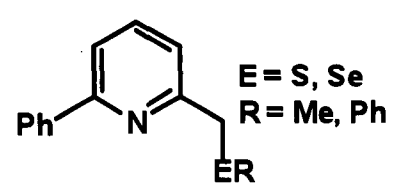

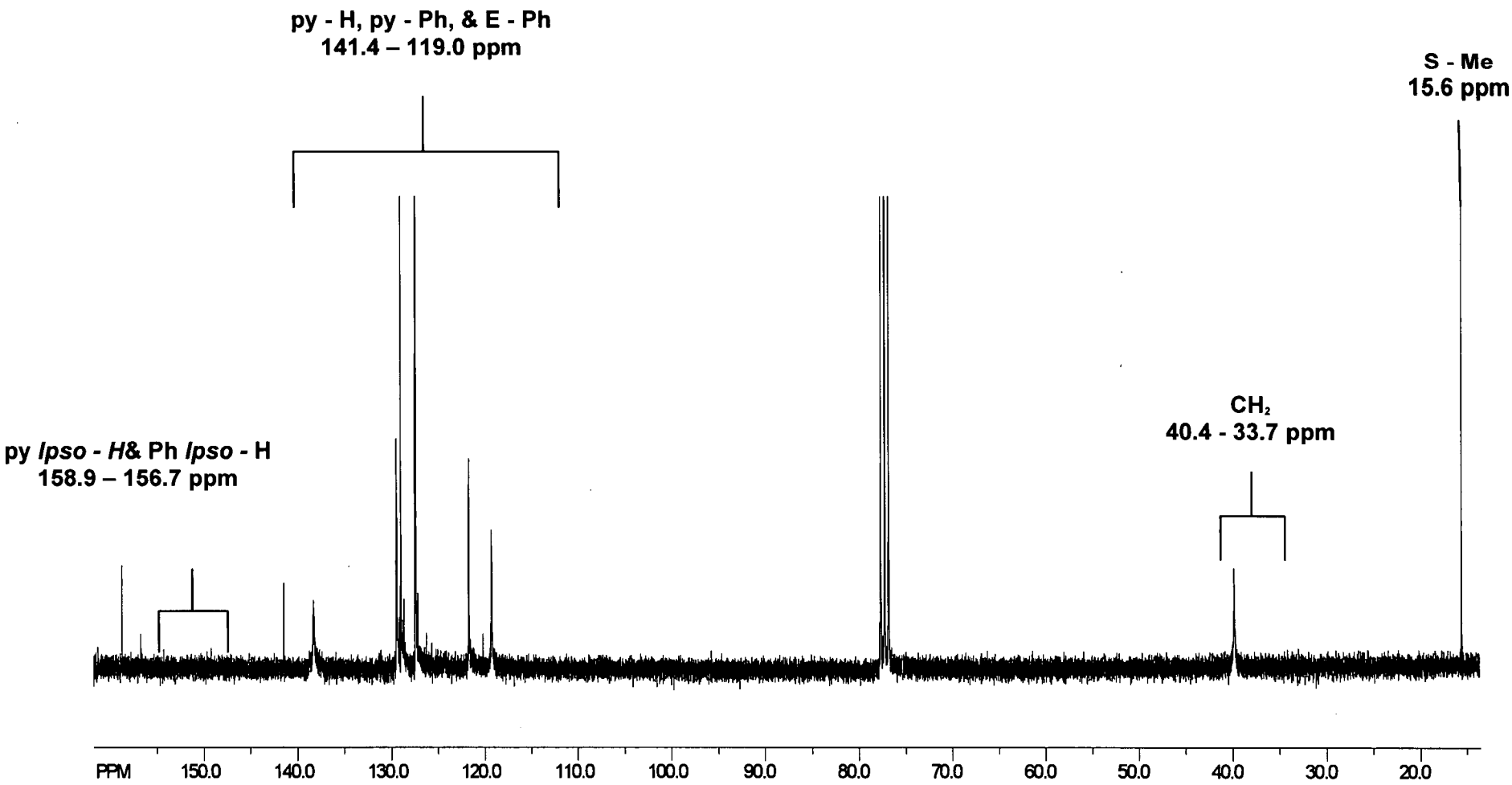

Figure 2.7 $^{13}C\{^{1}H\}$ NMR spectrum of 6-PhpyCH$_2$SMe; ranges marked are for the 6-phenyl-2-(methylchalcogenomethyl)pyridine compounds with the formula 6-PhpyCH$_2$ER.

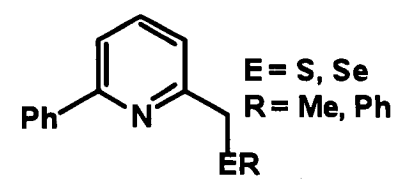

2.3 Conclusion

A new and simple 'one-pot' synthesis has been developed for the preparation of substituted 2-organothiomethyl- and 2-organoselenomethylpyridineligands, which is more widely applicable than previous routes. This allowed the synthesis of seven new ligands (4-MepyCH$_2$SMe, 6-PhpyCH$_2$SMe, 4-MepyCH$_2$SPh, 6-PhpyCH$_2$SPh, 4-MepyCH$_2$SePh, and 6-PhpyCH$_2$SePh) together with an improved and more direct route to the known compounds (pyCH$_2$SMe, 6-MepyCH$_2$SMe, pyCH$_2$SPh, 6-MepyCH$_2$SPh, pyCH$_2$SeMe, pyCH$_2$SePh, and 6-MepyCH$_2$SePh), thus achieving a major aim of this study. Future work in this area could include extension of this practical synthesis to compounds containing tellurium.

2.4 Experimental

2.4.1 General Experimental

All manipulations were carried out under argon using standard Schlenk techniques. Diethyl ether and THF were refluxed over Na/K alloy and sodium benzophenone, respectively, and then distilled under dinitrogen prior to use. All substituted pyridines were dried over 5Å molecular sieves, and distilled over anhydrous KOH and stored under argon. All other reagents used are commercially available from the Aldrich Chemical Co. and were used as received unless specified ^{n}BuLi was standardised[18] before use. Ultra high purity argon was purchased from BOC Gases.^{1}H NMR spectra were recorded on a Varian Mercury Plus 300 NMR Spectrometer at 299.9 MHz at ambient temperature using deuterated chloroform ($CDCl_3$), referenced to residual solvent (7.25 ppm $CHCl_3$). Chemical shifts (δ) are reported in ppm and all coupling constants are given in Hz. Peak multiplicity is denoted as singlet (s), doublet (d), triplet (t), multiplet (m), doublet of doublets (dd), triplet of doublets (td), doublet of doublet of doublets (ddd), or broad (br). For assignments where peak multiplicity is in quotation marks *e.g.*, "d", the multiplicity of the peak is considered a "pseudo" assignment *i.e.* only appears to have that multiplicity at current magnet strength and may not in higher magnetic fields. A diagram for NMR assignments is shown in **Figure 2.8**. All compounds (except for 6-phenyl-2-methylpyridine) were characterised by standard 2D NMR techniques; gradient COSY, gradient HMQC, and gradient HMBC. Microanalyses were performed by Dr. Graham Rowbottom of

the Central Science Laboratory (CSL), University of Tasmania using a ThermoFinnigan Flash EA 1112 Series Elemental Analyser. Mass spectrometry was conducted by Dr. Noel Davies and Dr. Marshall Hughes of the CSL. The EI (Electron Ionisation) were carried out using a Kratos ISQ mass spectrometer with a liquid matrix of nitrobenzyl alcohol using 10 kV Cs ions and a 5.3kV accelerating voltage.

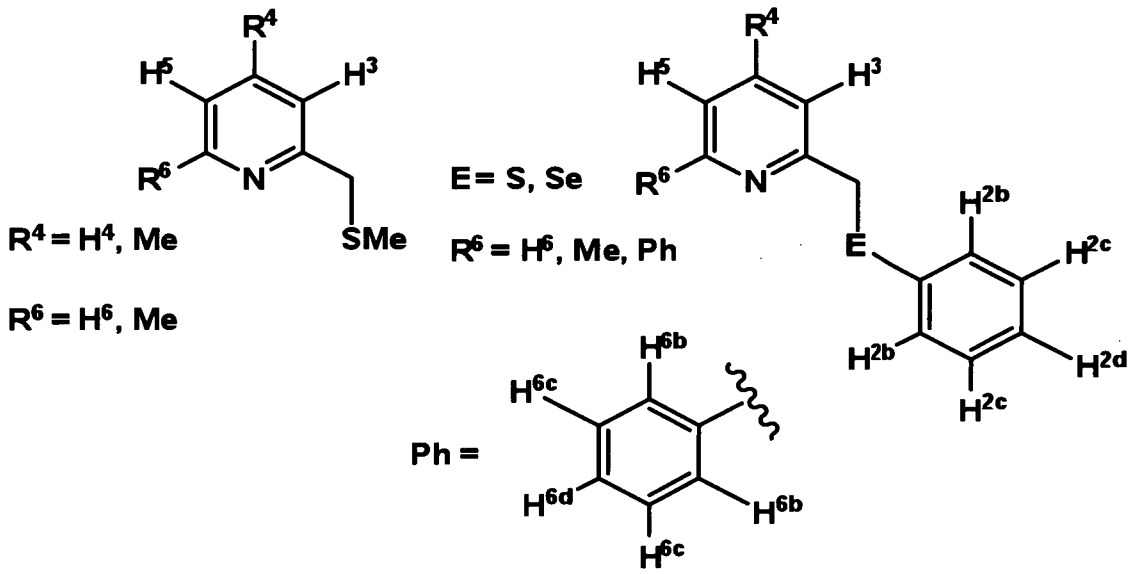

Figure 2.8 Diagram of NMR assignments for all compounds.

2.4.2Experimental Procedures

Synthesis of 2-(methylthiomethyl)pyridine, pyCH_2SMe

A solution of ^{n}BuLi (7.0 mL of a 1.6 M hexane solution, 1.1 eq.) was added dropwise to a stirred solution of 2-picoline (1.0 mL, 10.1 mmol) in Et_2O (25 mL) at –78 °C. The reaction was allowed to warm to ambient temperature, after which it was added dropwise to a stirred solution of dimethyl disulphide (1.00 mL, 11.1 mmol, 1.1 eq.) in THF (25 mL) at –78 °C. The solution was allowed to warm to room temperature and stirred for 3 h. Water was then added and the aqueous layer extracted with Et_2O (3 x 25 mL). The organic phases were combined and the solvent was removed *in vacuo* resulting in a pale yellow oil (1.20 g, 85%). The resultant oil did not require further purification (indicated by NMR) but was distilled under vacuum (28–31°C, 7.1 x 10^{-2} torr) to give a colourless oil for analysis (0.66 g, 46%).

^{1}H NMR (299.9 MHz, 20 °C, $CDCl_3$): δ 8.51 (dd, J = 7.8, 1.8 Hz, 1H, H^6), 7.66 ("dt", J = 7.8, 1.8 Hz, 1H, H^4), 7.35 (d, J = 7.8 Hz, 1H, H^3), 7.16 ("ddd", J = 7.8, 1.8, 0.9 Hz, 1H, H^5), 3.79 (s, 2H, CH_2), 2.04 (s, 3H, CH_3); **$^{13}C\{^1H\}$ NMR (75.4 MHz, 20 °C, $CDCl_3$):**δ 158.7 (C^2), 149.2 (C^6), 137.2 (C^4), 123.4 (C^3), 122.2 (C^5), 40.1 (CH_2), 15.4 (CH_3); ***Anal.* Calcd. for C_7H_9NS:** C, 60.39; H, 6.52; N, 10.06; S, 23.03%. Found: C, 60.35; H, 6.35; N, 10.18; S, 22.92%; **EI *m/z*** 138 $[M-H]^+$, $[^{12}C_7{}^1H_8{}^{14}N^{32}S$ 138].

Synthesis of 4-methyl-2-(methylthiomethyl)pyridine, 4-MepyCH$_2$SMe

This compound was prepared from 2,4-lutidine (1.00 mL, 8.65 mmol) and dimethyl disulfide (0.90 mL, 10.0 mmol, 1.1 equiv) using a similar procedure to that described for pyCH$_2$SMe (1.15 g, 87%).The resultant oil did not require further purification (indicated by NMR) but was distilled under vacuum (46-47°C, 6.9 x 10^{-2} torr) to give a colourless oil for analysis(0.58 g, 44%).

^{1}H NMR (299.9 MHz, 20 °C, $CDCl_3$): δ 8.36 (d, J = 5.1 Hz, 1H, H^6), 7.18 (s, 1H, H^3), 6.98 (d, J = 5.1 Hz, 1H, H^5), 3.75 (s, 2H, CH_2), 2.33 (s, 3H, C_4-CH_3), 2.04 (s, 3H, S-CH_3); **$^{13}C\{^1H\}$ NMR (75.4 MHz, 20 °C, $CDCl_3$):**δ 158.5 (C^2), 149.0 (C^6), 148.3 (C^4), 124.1 (C^3), 123.2 (C^5), 40.1 (CH_2), 21.3 (C^4-CH_3), 15.4 (S-CH_3); ***Anal.* Calcd. for $C_8H_{11}NS$:** C, 62.70; H, 7.24; N, 9.14; S, 20.92%;Found: C, 62.75; H, 7.24; N, 9.26; S, 20.68%.**EI *m/z*** 152 $[M-H]^+$, $[^{12}C_8{}^1H_{10}{}^{14}N^{32}S$ 152].

Synthesis of 6-methyl-2-(methylthiomethyl)pyridine, 6-MepyCH$_2$SMe

This compound was prepared from 2,6-lutidine (1.00 mL, 0.87 mmol) and dimethyl disulfide (0.90 mL, 0.10 mmol, 1.1 equiv) using a similar procedure to that described for pyCH$_2$SMe (0.90 g, 68%).The resultant oil did not require further purification (indicated by NMR) but was distilled under vacuum (45-46°C, 8.0 x 10^{-2} torr) to give a colourless oil for analysis (0.59 g, 45%).

^{1}H NMR (299.9 MHz, 20 °C, $CDCl_3$): δ 7.53 ("t", J = 7.8 Hz, 1H, H^4), 7.15 (d,J = 7.8, 1H, H^3), 7.01 (d, J = 7.8 Hz, 1H, H^5), 3.76 (s, 2H, CH_2), 2.53 (s, 3H, C_6-CH_3), 2.04 (s, 3H, S-CH_3); **$^{13}C\{^1H\}$ NMR (75.4 MHz, 20 °C, $CDCl_3$):**δ 158.0 (C^6), 157.9 (C^2), 137.3 (C^4), 121.8 (C^5), 120.2 (C^3), 40.2 (CH_2), 24.6 (C^6-CH_3), 15.5 (S-CH_3).

Anal.* Calcd. for $C_8H_{11}NS$:** C, 62.70; H, 7.24; N, 9.14; S, 20.92%;Found: C, 62.56; H, 7.38; N, 8.98; S, 20.61%; **EI *m/z 152 $[M-H]^+$, $[^{12}C_8{}^1H_{10}{}^{14}N^{32}S$ 152].

Synthesis 2-(phenylthiomethyl)pyridine, $pyCH_2SPh$

This compound was prepared from 2-picoline (1.00 mL, 10.1 mmol) and diphenyl disulfide (2.36 g, 10.8 mmol, 1.1 equiv) using a similar procedure to that described for $pyCH_2SMe$.The product was then purified by silica plug [5% diethyl ether in petroleum spirit (bp 40-60°C)] to remove contamination by diphenyl disulfide to give a yellow oil (0.96 g, 47%). The resultant oil did not require does not require further purification (indicated by NMR) but was distilled under vacuum (98-104°C, 6.6 x 10^{-2} torr) to give a pale yellow oil for analysis (0.42 g, 20%).

^{1}H NMR (299.9 MHz, 20 °C, $CDCl_3$): δ 8.54 (d, J = 4.8 Hz, 1H, H^6), 7.59 (m, 1H, H^4), 7.32 (m, 2H, H^3, H^{2b}), 7.24 (m, 1H, H^{2c}), 7.16 (m, 2H, H^5, H^{2d}), 4.27 (s, 2H, CH_2); **$^{13}C\{^1H\}$ NMR (75.4 MHz, 20 °C, $CDCl_3$):**δ 157.9 (C^2), 149.5 (C^6), 137.0 (C^4), 136.0 (C^{2a}), 129.9 (C^{2b}), 127.7 (C^{2c}), 126.6 (C^{2d}), 123.2 (C^3), 122.3 (C^5), 40.7 (CH_2); ***Anal.* Calcd. for $C_{12}H_{11}NS$:** C, 71.60; H, 5.51; N, 6.96; S, 15.93%. Found: C, 71.86; H, 5.64; N, 6.85; S, 15.79%.**EI*m/z*** 200 $[M-H]^+$, $[^{12}C_{12}{}^1H_{10}{}^{14}N^{32}S$ 200].

Synthesis of 4-methyl-2-(phenylthiomethyl)pyridine, 4-$MepyCH_2SPh$

This compound was prepared from 2,4-lutidine (1.00 mL, 8.65 mmol) and diphenyl disulfide (2.06 g, 9.42 mmol, 1.1 equiv) using a similar procedure to that described for $pyCH_2SMe$.The product was then purified by silica plug [5% diethyl ether in petroleum spirit (bp 40-60°C)] to remove contamination by diphenyl disulfide to give a yellow oil (0.91 g, 49%).The resultant oil does not require does not require further purification (indicated by NMR) but was distilled under vacuum (112-122 °C, 4.2 x 10^{-2} torr) to give a pale yellow oil for analysis (0.46 g, 25%).

^{1}H NMR (299.9 MHz, 20 °C, $CDCl_3$): δ 8.39 (d, J = 5.1 Hz, 1H, H^6), 7.33 ("dd", J = 8.4, 1.5 Hz, 2H, H^{2b}), 7.24 (m, 2H,H^{2c}), 7.17 (m, 2H, H^3, H^{2d}), 7.00 (d, J = 5.1 Hz, 1H, H^5), 4.25 (s, 2H, CH_2), 2.30 (s, 3H, C^4-CH_3); **$^{13}C\{^1H\}$ NMR (75.4 MHz, 20 °C, $CDCl_3$):** δ 157.3 (C^2), 153.8 (C^4), 148.6 (C^6), 132.7 (C^{2a}), 129.8 (C^{2b}), 129.1 (C^{2c}), 126.6 (C^{2d}), 124.3 (C^3), 123.5 (C^5), 40.2 (CH_2), 21.3 (C^4-CH_3); ***Anal.* Calcd. for**

$C_{13}H_{13}NS$: C, 72.52; H, 6.09; N, 6.51; S, 14.89%. Found: C, 72.68; H, 6.15; N, 6.43; S, 14.64%. **EI** ***m/z*** 214 $[M-H]^+$ $[^{12}C_{13}{}^{1}H_{12}{}^{14}N^{32}S$ 214].

Synthesis of 6-methyl-2-(phenylthiomethyl)pyridine, 6-MepyCH$_2$SPh

This compound was prepared from 2,6-lutidine (1.00 mL, 8.65 mmol) and diphenyl disulfide (2.08 g, 9.55 mmol, 1.1 equiv) using a similar procedure to that described for pyCH$_2$SMe.The product was then purified by silica plug [5% diethyl ether in petroleum spirit (bp 40-60°C)] to remove contamination by diphenyl disulfide to give a yellow oil (0.99 g, 53%).The resultant oil does not require did not require further purification (indicated by NMR) but was distilled under vacuum (104-110°C, 4.2 x 10^{-2} torr) to give a pale yellow oil for analysis (0.61 g, 32%).

^{1}H NMR (299.9 MHz, 20 °C, $CDCl_3$): δ 7.49 ("t", J = 7.5 Hz, 1H, H^4), 7.33 ("dd", J = 6.9, 1.2 Hz, 2H, H^{2b}), 7.24 (m, 2H, H^{2c}), 7.18 (m, 2H, H^3, H^{2d}), 7.01 (d, J = 7.5 Hz, 2H, H^5), 4.25 (s, 2H, CH_2), 2.55 (s, 3H, C^6-CH_3); **^{13}C{H} NMR (75.4 MHz, 20 °C, $CDCl_3$):**δ 158.2 (C^2), 156.9 (C^6), 137.3 (C^4), 136.3 (C^{2a}), 129.7 (C^{2b}), 129.1 (C^{2c}), 126.5 (C^{2d}), 122.0 (C^5), 120.2 (C^3), 40.5 (CH_2), 24.5 (C^6-CH_3); ***Anal.*** **Calcd. for $C_{13}H_{13}NS$:** C, 72.52; H, 6.09; N, 6.51; S, 14.89%. Found: C, 72.72; H, 6.12; N, 6.40; S, 14.61%. **EI** ***m/z*** 214 $[M-H]^+$ $[^{12}C_{13}{}^{1}H_{12}{}^{14}N^{32}S$ 214].

Synthesis of 2-(methylselenomethyl)pyridine, pyCH$_2$SeMe

This compound was prepared from 2-picoline (1.00 mL, 10.1 mmol) and dimethyl diselenide (1.05mL, 11.1 mmol, 1.1 equiv) using a similar procedure to that described for pyCH$_2$SMe.The product was then purified by silica plug [5% diethyl ether in petroleum spirit (bp 40-60°C)] to remove contamination by dimethyl diselenide to give a dark yellow oil (1.73 g, 92%).

^{1}H NMR (299.9 MHz, 20 °C, $CDCl_3$): δ 8.51 (d, J = 7.8 Hz, 1H, H^6), 7.64 ("dt", J = 7.8, 1.5 Hz, 1H, H^4), 7.29 (d, J = 7.8 Hz, 1H, H^3), 7.14 ("dt", J = 7.8, 1.5 Hz, 1H, H^5), 3.86 (s, 2H, CH_2), 1.99 (s, 3H, CH_3); **^{13}C{^{1}H} NMR (75.4 MHz, 20 °C, $CDCl_3$):** δ 159.8 (C^2), 149.0 (C^6), 137.3 (C^4), 123.4 (C^3), 121.9 (C^5), 29.8 (CH_2), 4.8 (CH_3); ***Anal.*** **Calcd. for C_7H_9NSe:** C, 45.17; H, 4.87; N, 7.53%. Found: C, 45.38; H, 4.79; N, 7.60%. **EI** ***m/z*** 186 $[M-H]^+$, $[^{12}C_7{}^{1}H_8{}^{14}N^{80}Se$ 186].

Synthesis of 2-(phenylselenomethyl)pyridine, $pyCH_2SePh$

This compound was prepared from 2-picoline (1.00 mL, 10.1 mmol) and diphenyl diselenide (3.35 g, 10.7 mmol, 1.1 equiv) using a similar procedure to that described for $pyCH_2SMe$.The product was then purified by silica plug [5% diethyl ether in petroleum spirit (bp 40-60°C)] to remove contamination by diphenyl diselenide to give a dark yellow oil (1.76 g, 70%). The resultant oil did not require further purification (indicated by NMR) but was distilled under vacuum (108-112°C, 4.0 x 10^{-2} torr) to give a yellow oil for analysis (1.35 g, 54%).

^{1}H NMR (299.9 MHz, 20 °C, $CDCl_3$): δ 8.50 (d, J = 4.8 Hz, 1H, H^6), 7.54 ("dt", J = 7.5, 1.8 Hz, 1H, H^4), 7.47 (m, 2H, H^{2b}), 7.24 (m, 3H, H^{2c}, H^{2d}), 7.10 (m, 2H, H_3, H^5), 4.23 (s, 2H, CH_2); **^{13}C{^{1}H} NMR (75.4 MHz, 20 °C, $CDCl_3$):**δ 158.8 (C^2), 149.3 (C^6), 137.0 (C^4), 133.9 (C^{2b}), 130.1 (C^{2a}), 129.3 (C^{2c}), 127.7 (C^{2d}), 123.4 (C^3), 122.0 (C^5), 33.8 (CH_2); ***Anal.* Calcd. for $C_{12}H_{11}NSe$:** C, 58.07; H, 4.47; N, 5.64%. Found: C, 57.89; H, 4.58; N, 5.41%. **EI *m/z*** 247 $[M]^+$, $[^{12}C_{12}{}^1H_{10}{}^{14}N^{80}Se$ 247].

Synthesis 4-methyl-2-(phenylselenomethyl)pyridine, 4-$MepyCH_2SePh$

This compound was prepared from 2,4-lutidine (1.00 mL, 8.65 mmol) and diphenyl diselenide (3.02 g, 9.67 mmol, 1.1 equiv) using a similar procedure to that described for$pyCH_2SMe$.The product was then purified by silica plug [5% diethyl ether in petroleum spirit (bp 40-60°C)] to remove contamination by diphenyl diselenide to give a dark yellow oil (1.74 g, 77%). The resultant oil did not require further purification (indicated by NMR) but was distilled under vacuum (118-122°C, 3.1 x 10^{-2} torr) to give a yellow oil for analysis (1.16 g, 51%).

^{1}H NMR (299.9 MHz, 20 °C, $CDCl_3$): δ 8.38 (d, J = 5.1 Hz, 1H, H^6), 7.46 (m, 2H, H^{2b}), 7.23 (m, 3H, H^{2c}, H^{2d}), 6.91 (m, 2H, H^3, H^5), 4.19 (s, 2H, CH_2), 2.24 (s, 3H, C_4-CH_3) ppm; **^{13}C{^{1}H} NMR (75.4 MHz, 20 °C, $CDCl_3$):**δ 158.4 (C^2), 149.1 (C^6), 148.1 (C^4), 133.8 (C^{2b}), 130.1 (C^{2a}), 129.2 (C^{2c}), 127.6 (C^{2d}), 124.3 (C^3), 123.1 (C^5), 33.8 (CH_2), 21.2 (C^4-CH_3) ppm; ***Anal.* Calcd. for $C_{13}H_{13}NSe$:** C, 59.55; H, 5.00; N, 5.34%. Found: C, 59.52; H, 4.89; N, 5.44%. **EI *m/z*** 261 $[M-H]^+$, $[^{12}C_{13}{}^1H_{12}{}^{14}N^{80}Se$ 261].

Synthesis 6-methyl-2-(phenylselenomethyl)pyridine, 6-MepyCH$_2$SePh

This compound was prepared from 2,6-lutidine (1.00 mL, 8.65 mmol) and diphenyl diselenide (2.93 g, 9.39 mmol, 1.1 equiv) using a similar procedure to that described for pyCH$_2$SMe. The product was then purified by silica plug [5% diethyl ether in petroleum spirit (bp 40-60°C)] to remove contamination by diphenyl diselenide to give a dark yellow oil (1.69 g, 74%). The resultant oil did not require further purification for complexation (indicated by NMR) but was distilled under vacuum (114-118°C, 2.8 x 10^{-2} torr) to give a yellow oil for analysis (1.22 g, 54%).

^{1}H NMR (299.9 MHz, 20 °C, CDCl$_3$): δ 7.47 (m, 3H, H^4, H^{2b}), 7.24 (m, 3H, H^{2c}, H^{2d}), 6.98 (d, *J* = 7.8 Hz, 1H, H^5), 6.91 (d, *J* = 7.8 Hz, 1H, H^3), 4.22 (s, 2H, CH$_2$), 2.53 (s, 3H, C^6-CH$_3$) ppm; **^{13}C{^{1}H} NMR (75.4 MHz, 20 °C, CDCl$_3$):** δ 158.0 (C^6), 157.9 (C^2), 137.4 (C^4), 134.0 (C^{2b}), 130.2 (C^{2a}), 129.2 (C^{2c}), 127.7 (C^{2d}), 121.8 (C^5), 120.4 (C^3), 33.7 (CH$_2$), 24.4 (C^6-CH$_3$), ppm; ***Anal.* Calcd. for C$_{13}$H$_{13}$NSe:** C, 59.55; H, 5.00; N, 5.34%. Found: C, 59.44; H, 5.17; N, 5.18%. **EI *m/z*** 261 [M-H]$^+$, [^{12}C$_{13}$^{1}H$_{12}$^{14}N^{80}Se 261].

Synthesis of 2-methyl-6-phenylpyridine, 6-PhpyMe

A solution of 2-bromo-6-methylpyridine (0.66 ml, 5.81 mmol) and Pd(PPh$_3$)$_4$ (0.34 g, 5 mol%) in toluene (26.0 mL) was treated with a degassed solution of Na$_2$CO$_3$ (1.39 g, 13.11 mmol, 2.2 equiv.) in H$_2$O (12.0 mL), followed by a solution of phenylboronic acid (1.06 g, 8.72 mmol, 1.5 equiv.) in MeOH (8.0 mL). The resulting mixture was then stirred at 95°C for 12 h under Ar. After 6 h another 0.5 eq. of phenylboronic acid and a further 1 mol% of catalyst was added to the solution. After 12 h the solution was cooled to room temperature and treated with a saturated solution of Na$_2$CO$_3$. The product was extracted with CH$_2$Cl$_2$ (3 x 25 mL), the combined organic layers were washed with saturated sodium chloride solution, dried over Na$_2$SO$_4$ and the solvent removed *in vacuo* resulting in a pale yellow oil (0.91 g, 98%). Although not required the product can bedistilled under vacuum (76 – 79°C, 2.9 x 10^{-2} torr) to give a colourlessoil (0.64 g, 69%).

^{1}H NMR (299.9 MHz, 20 °C, CDCl$_3$): δ 7.99 (dd, *J* = 8.4, 1.2 Hz, 2H), 7.69 (t, *J* = 7.7 Hz, 1H), 7.48 (m, 4H), 7.13 (d, *J* = 7.6 Hz, 1H), 2.69 (s, 3H, CH$_3$) ppm; **^{13}C{^{1}H}**

NMR (75.4 MHz, 20 °C, $CDCl_3$): δ 158.4 (Ar-C), 156.9 (Ar-C), 137.9 (Ar-C), 129.3 (Ar-C), 128.9 (Ar-C), 127.5 (Ar-C), 127.4 (Ar-C), 122.2 (Ar-C), 118.4 (Ar-C), 24.5 (CH_3), ppm.

Synthesis of 6-phenyl-2-(methylthiomethyl)pyridine, 6-PhpyCH$_2$SMe

This compound was prepared from 6-phenyl-2-methylpyridine (0.10 g, 0.59 mmol) and dimethyl disulfide (0.06mL, 0.65 mmol, 1.1 equiv) using a similar procedure to that described for pyCH$_2$SMe (0.12 g, 94%).

^{1}H NMR (299.9 MHz, 20 °C, $CDCl_3$): δ 8.01 (dd, J = 7.8, 1.2 Hz, 2H, H^{6b}), 7.78 ("t",1H, J = 7.8 Hz, 1H, H^4), 7.62 (d, J = 8.1 Hz, 1H, H^5), 7.46 (m, 3H, H^{2c}, H^{2d}), 7.36 (d, J = 7.5 Hz, 1H, H^3), 3.95 (s, 2H, CH_2), 2.15 (s, 3H, S-CH_3) ppm; **^{13}C{^{1}H} NMR (75.4 MHz, 20 °C, $CDCl_3$):** δ 158.8 (C^2), 156.7 (C^6), 141.4 (C^{6a}), 138.3 (C^4), 129.5 (C^{6d}), 129.0 (C^{6c}), 127.4 (C^{6b}), 121.7 (C^3), 119.3 (C^5),39.8 (CH_2) 15.6 (S-CH_3), ppm; ***Anal.* Calcd. for $C_{13}H_{13}NS$:** C, 72.52; H, 6.09; N, 6.51; S, 14.89%. Found: C, 72.48; H, 5.99; N, 6.52; S, 15.01%. **EI** ***m/z*** 214 $[M-H]^+$, $[^{12}C_{13}{}^1H_{12}{}^{14}N^{32}S$ 214].

Synthesis of 6-phenyl-2-(phenylthiomethyl)pyridine, 6-PhpyCH$_2$SPh

This compound was prepared from 6-phenyl-2-methylpyridine (0.10g, 0.59 mmol) and diphenyl disulfide (0.14 g, 0.65 mmol, 1.1 equiv) using a similar procedure to that described for pyCH$_2$SMe. The product was then purified by silica plug [10%toluene in hexanes] to remove contamination by diphenyl disulfide to give a pale yellow oil (0.12 g, 76%).

^{1}H NMR (299.9 MHz, 20 °C, $CDCl_3$): δ 7.95 (dd,J = 6.9, 0.9 Hz,2H, H^{6b}), 7.68 ("t",J = 7.5 Hz,1H, H^4), 7.57 (d, J = 8.1 Hz, 1H, H^5), 7.42 (m, 5H, H^{2a}, H^{6b}, H^{6c}), 7.26 (m, 4H, H^3, H^{2c}, H^{2d}), 4.35 (s, 2H, CH_2), ppm; **^{13}C{^{1}H} NMR (75.4 MHz, 20 °C, $CDCl_3$):** δ 157.8 (C^2), 156.9(C^6), 138.0 (C^4), 135.9 (C^{2a}), 132.8 (C^{2b}), 129.8 (C^{2c}), 129.4 (C^{6d}), 129.1 (C^{6c}), 128.0 (C^{2d}), 127.4 (C^{6b}), 121.6 (C^3), 119.3 (C^5), 40.4 (CH_2) ppm; ***Anal.* Calcd. for $C_{18}H_{15}NS$:** C, 77.94; H, 5.45; N, 5.05; S, 11.56%. Found: C, 78.00; H, 5.49; N, 5.02; S, 11.49%. **EI** ***m/z*** 276 $[M-H]^+$, $[^{12}C_{18}{}^1H_{14}{}^{14}N^{32}S$ 276].

Synthesis of 6-phenyl-2-(phenylselenomethyl)pyridine, 6-PhpyCH$_2$SePh

This compound was prepared from 6-phenyl-2-methylpyridine (0.10g, 0.59 mmol) and diphenyl diselenide (0.20 g, 0.65 mmol, 1.1 equiv) using a similar procedure to that described for pyCH$_2$SMe. The product was then purified by silica plug [5% toluene in hexanes] to remove contamination by diphenyl diselenide to give a pale yellow oil (0.16 g, 85%).

^{1}H NMR (299.9 MHz, 20 °C, $CDCl_3$): δ 7.94 ("dd", J = 7.8, 1.2 Hz, 2H, H^{6b}), 7.65("t", J = 7.5 Hz,1H,H^4), 7.56 (m, 3H,H^5,H^{2b}), 7.45 (m, 3H, H^{6c},H^{6d}), 7.26 (m, 3H, H^{2c},H^{2d}),7.11 (d, J = 7.8 Hz, 1H, H^3), 4.36 (s, 2H, CH_2) ppm; **^{13}C{^{1}H} NMR (75.4 MHz, 20 °C, $CDCl_3$):** δ 158.9 (C^2), 156.9 (C^6), 137.7 (C^4),133.8 (C^{2b}), 130.3 (C^{2a}) 129.5 (C^{6d}),129.3 (C^{2c}), 128.9 (C^{6c}), 127.6 (C^{2d}), 127.4 (C^{6b}), 121.7 (C^3), 119.0 (C^5), 33.7 (CH_2) ppm; ***Anal.* Calcd. for $C_{18}H_{15}NSe$:** C, 66.67; H, 4.66; N, 4.32%. Found: C, 66.58; H, 4.60; N, 4.28%. **EI *m/z*** 323 $[M-H]^+$, $[^{12}C_{18}{}^1H_{14}{}^{14}N^{80}Se323]$.

2.5 References

1. Canovese, L.; Visentin, F.; Chessa, G.; Uguagliati, P.; Dolmella, A. *J. Organomet. Chem.* **2000**, *601*, 1.
2. Canovese, L.; Chessa, G.; Santo, C.; Visentin, F.; Uguagliati, P. *Inorg. Chim. Acta***2003**, *346*, 158.
3. Canovese, L.; Visentin, F.; Uguagliati, P.; Chessa, G.; Lucchini, V.; Bandoli, G. *Inorg. Chim. Acta***1998**, *275-276*, 385.
4. Canovese, L.; Visentin, F.; Uguagliati, P.; Chessa, G.; Pesce, A. *J. Organomet. Chem.***1998**, *566*, 61.
5. Canovese, L.; Visentin, F.; Santo, C.; Chessa, G.; Uguagliati, P. *Polyhedron*, **2001**, 3171.
6. Haviv, F.; DeNet, R. W.; Michaels, R. J.; Ratajczyk, J. D.; Carter, G. W.; Young, P. R. *J. Med. Chem.***1983**, *26*, 218.
7. Bauer, L.; Gardella, L. A. *J. Org. Chem.* **1963**, *28*, 1323.
8. Trost, B. M.; Braslau, R. *J. Org. Chem.***1988**, *53*, 532.
9. Michalski, J.; Maruszewska-Wieczorkowska, E. *Roczniki Chemii*,**1957**,*31*, 543.

10. Canovese, L.; Visentin, F.; Chessa, G.; Uguagliati, P.; Bandoli, G. *Organometallics*, **2000**, *19*, 1461.
11. Canovese, L.; Visentin, F.; Chessa, G.; Santo, C.; Uguagliati, P.; Bandoli, G. *J. Organomet. Chem.***2002**, *650*, 43.
12. Canovese, L.; Visentin, F.; Chessa, G.; Uguagliati, P.; Santo, C.; Dolmella, A. *Organometallics*, **2005**, *24*, 3297.
13. Canovese, L.; Visentin, F.; Chessa, G.; Santo, C.; Uguagliati, P.; Maini, L.; Polito, M.; *J. Chem. Soc., Dalton Trans.***2002**, 3696.
14. Bhasin, K. K.; Singh, J.; Singh, K. N. *Phosphorus, Sulfur and Silicon*, **2002**, *177*, 587.
15. Baker, W.; Buggle, K. M.; McOmie, J. F. W.; Watkins, D. A. M. *J.Chem. Soc.***1958**, 3594.
16. Ghera, E.; Ben-David, Y.; Rapoport, H.*J. Org. Chem.***1983**, *48*, 774.
17. Huang, H; Chen, H.; Hu, X.; Bai, C.; Zheng Z.; *Tetrahedron: Asymmetry*, **2003**, *14*, 297.
18. Furnis, B.; Hannaford, A.; Rogers, V.; Smith, P.; Tatchell, A. *Vogel's Textbook of Practical Organic Chemistry 4th Ed.*: New York, **1987**.

Chapter Three
Synthesis and X-Ray Diffraction Studies of Metal(II) Complexes Containing *N,E* Heteroleptic Ligands

3.1 Introduction

Palladium(II) complexes containing bidentate heteroleptic ligands based upon pyridine and chalcogenoether groups have been synthesised containing allyl,[1-4] olefin,[1,5-7] and alkyl[8] groups and have been the subject of mechanistic studies.[1-11] However, although dihalogenopalladium(II) complexes containing this class of heteroleptic ligand are known,[12] there has not been an extensive and systematic study into their structure and catalytic properties. Palladium, and its congener platinum form dihalogeno complexes containing heteroleptic ligands of varying stability and hence are often employed as pre-catalysts in catalytic systems.[13-15]

Preliminary results showed that dihalogenopalladium(II) complexes of *N,E*-bidentate ligands are excellent pre-catalysts for the Heck reaction.[12] An extensive single crystal X-ray crystallographic study was undertaken of palladium(II) complexes synthesised for catalytic studies reported in Chapter 4, in an attempt to search for relationships between structure and activity. Initial results indicated the presence of complexes that are isomorphous with published platinum(II) analogues,[16] leading to an expansion of the crystallographic study to include additional platinum complexes to allow a comprehensive analysis of isomorphous relationships.

3.2 Results and Discussion

3.2.1 Synthesis

Synthesis of dihalogenometal(II) complexes containing neutral ligands is typically achieved *via* direct reaction of the ligand with the metal dihalide; displacement reactions of more labile ligands such as dimethylsulfide, acetonitrile, 1,5-

cyclooctadiene and tetramethylethylenediamine; or reaction of metallates such as $[PdCl_4]^{2-}$ with the ligand.

In this study dihalogenometal(II) complexes were prepared *via* either stoichiometric reaction of the metal dihalide or $MX_2(NCMe)_2$ with the ligand, **Scheme 3.1**.

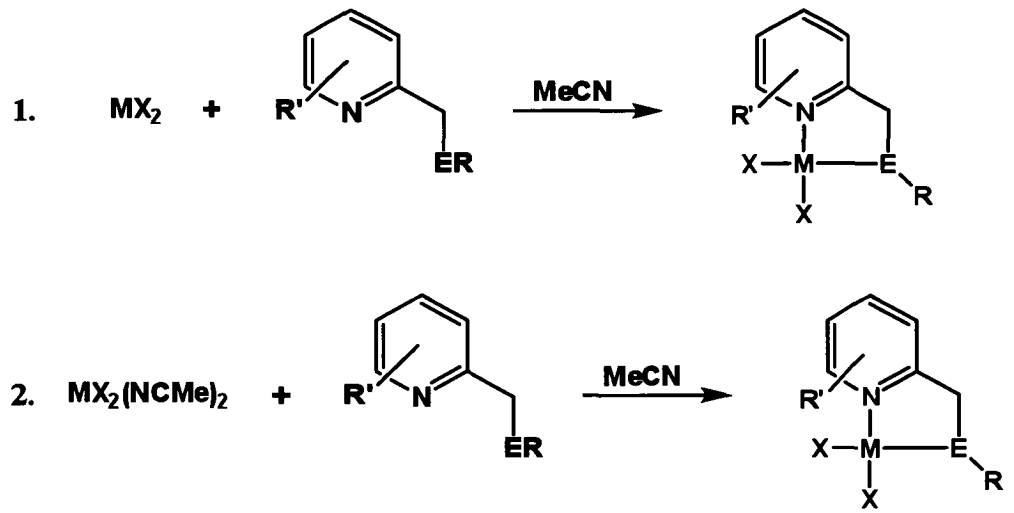

Scheme 3.1 Methods of synthesis for dihalogenometal(II) complexes containing heteroleptic *N,E* ligands.

For the preparation of the dichloropalladium(II) complexes, both methods were utilised. The use of $PdCl_2$ led to inconsistent results mainly due to low solubility and the presence of insoluble impurities in the starting material. Preparations utilising $PdCl_2(NCMe)_2$ as a starting material consistently resulted in high yields of the desired complexes, making it the method of choice. The complexes $PtCl_2(N,E)$ and $PdI_2(N,E)$ were obtained on reaction of the metal dihalide with ligands, also giving high yields of products. Dihalogenometal(II) complexes were formed in 78 – 95% yield. They are air and moisture stable, and are insoluble in most solvents with limited solubility in acetonitrile, dimethylsulfoxide and nitromethane. All complexes were examined by NMR, MS, elemental analysis and, some, by X-ray diffraction, **Table 3.1**.

Of special note are the palladium complexes prepared containing the palladated 6-phenylpyridyl substituted ligands $[6\text{-}C_6H_4pyCH_2SMe]^-$, $[6\text{-}C_6H_4pyCH_2SPh]^-$ and $[6\text{-}C_6H_4pyCH_2SePh]^-$. Instead of producing the expected dihalogenopalladium(II) complexes, the ligands 6-PhpyCH$_2$ER gave cyclopalladated species, **Scheme 3.2**.

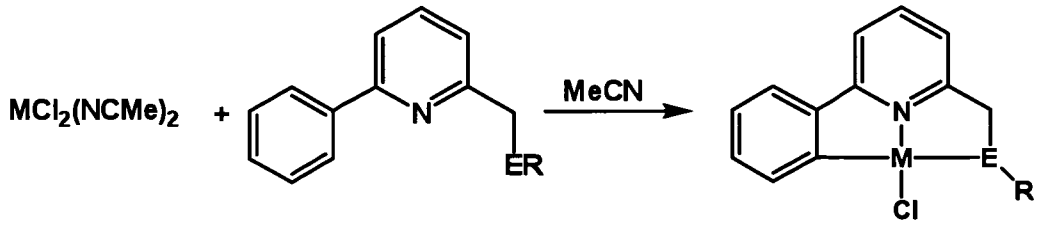

Scheme 3.2 Synthesis for complexes of the general formula PdCl(6-$C_6H_4pyCH_2ER$), where ER = SMe, SPh, and SePh.

R^1	R^4	R^6	E	X	M	Compound Number	Complex
Me	H	H	S	Cl	Pd	**3a**	$PdCl_2(pyCH_2SMe)$[#]
Me	Me	H	S	Cl	Pd	**3b**	$PdCl_2$(4-MepyCH_2SMe)
Me	H	Me	S	Cl	Pd	**3c**	$PdCl_2$(6-MepyCH_2SMe)
Me	H	Ph	S	Cl	Pd	**3d**	PdCl(6-$C_6H_4pyCH_2$SMe)*
Ph	H	H	S	Cl	Pd	**3e**	$PdCl_2(pyCH_2SPh)$[#]
Ph	Me	H	S	Cl	Pd	**3f**	$PdCl_2$(4-MepyCH_2SPh)
Ph	H	Me	S	Cl	Pd	**3g**	$[PdCl_2$(6-MepyCH_2SPh)$]_3$[†]
Ph	H	Ph	S	Cl	Pd	**3h**	PdCl(6-$C_6H_4pyCH_2$SPh)*
Ph	H	Ph	Se	Cl	Pd	**3i**	$PdCl_2(pyCH_2SePh)$
Me	H	H	Se	Cl	Pd	**3j**	$PdCl_2$(4-MepyCH_2SePh)
Ph	H	H	Se	Cl	Pd	**3k**	$[PdCl_2$(6-MepyCH_2SePh)$]_2$[†]
Ph	Me	H	Se	Cl	Pd	**3l**	PdCl(6-$C_6H_4pyCH_2$SePh)*
Ph	H	Me	S	I	Pd	**3m**	PdI_2(6-MepyCH_2SPh)$_2$[†]
Ph	H	H	Se	I	Pd	**3n**	$PdI_2(pyCH_2SePh)$
Me	Me	H	S	Cl	Pt	**3o**	$PtCl_2$(4-MepyCH_2SMe)
Me	H	Me	S	Cl	Pt	**3p**	$PtCl_2$(6-MepyCH_2SMe)
Ph	H	Me	S	Cl	Pt	**3q**	$PtCl_2$(6-MepyCH_2SPh)
Ph	H	H	Se	Cl	Pt	**3r**	$PtCl_2(pyCH_2SePh)$
Ph	Me	H	Se	Cl	Pt	**3s**	$PtCl_2$(4-MepyCH_2SePh)

Table 3.1 Complexes of heteroleptic *N,E* ligands. # denotes a previously reported complex,[12] * denotes unexpected cyclometallated complex, and † denotes unexpected solid state structure of the complex.

3.2.2 Characterisation Studies

Solid state structural analysis (X-ray diffraction, microanalysis) is presented followed by an assessment of solution state data (NMR, Liquid-Secondary Ionisation Mass Spectrometry (LSIMS)). The complexes are classified into three groups related to the substituent in the 6-position of the pyridyl ring as this was found to have a significant effect on the structure of the dihalogenometal(II) complexes (methyl substituent), or on reactivity of the ligands (phenyl substituent) resulting in cyclopalladation.

3.2.2.1 Solid State Characterisation of the Complexes

Microanalysis of all the complexes synthesised in this study gave empirical formulae corresponding to complexes containing one ligand and two halogen moieties bound to a palladium or platinum metal centre, *i.e.*, $MX_2(N,E)$, except for one complex of stoichiometry "Pd:2I:2(6-MepyCH$_2$SPh)" which was identified as PdI_2(6-MepyCH$_2$SPh)$_2$ by X-ray crystallography, and all 6-Ph substituted complexes. The latter complexes displayed microanalysis data corresponding to a "Pd:Cl:ligand–H" ratio of 1:1:1, and the complex containing 6-PhpyCH$_2$SePh was identified by X-ray crystallography as a cyclopalladated complex.

Crystals of complexes were grown by vapour diffusion of Et_2O into $MeNO_2$ (**3b, i, l, n-r**), MeCN (**3j, s**) or hot $MeNO_2$ (**3k, m**). Diffraction data was collected by the author at the School of Chemistry (**3b, i, j, l-s**) and the Australian Synchrotron (**3k**), or by Prof. Allan White at the School of Biomedical, Biomolecular and Chemical Science (**3g**), University of Western Australia. All structures except for **3g** were solved and refined by the author. For all complexes in this study bond distances and angles, and full molecular representations are displayed, except where noted, in crystallographic information files (cif) in **Appendix B** on CD at the back of this thesis.

MX_2(pyCH$_2$EPh) (M = Pd, X = Cl, E = S; X = I, E = Se; M = Pt, X = Cl, Br, E = S), MCl_2(4-MepyCH$_2$SePh) (M = Pd, Pt), and MX_2(4-MepyCH$_2$SMe) (M = Pd, X = Cl; M = Pt, X = Cl, Br)

Representative molecular structures are shown in **Figure 3.1**, bond distances and angles in all complexes are presented in **Tables 3.2 (i)** and **(ii)** for $MX_2(pyCH_2EPh)$, **Tables 3.3** $MCl_2(4\text{-}MepyCH_2SePh)$, and **Tables 3.4** for $MX_2(4\text{-}MepyCH_2SMe)$. Isomorphous structures are represented in *italics*. Simplified representations are shown below.

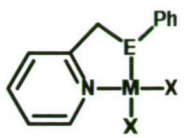

(3i,n,r)

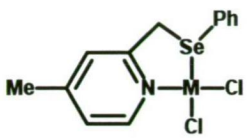

(3j,s)

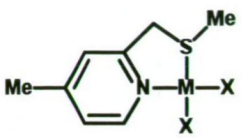

(3b,o)

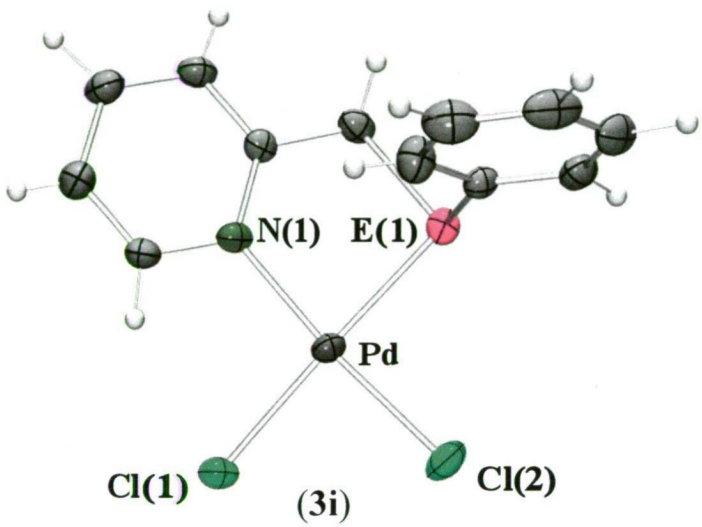

(3i)

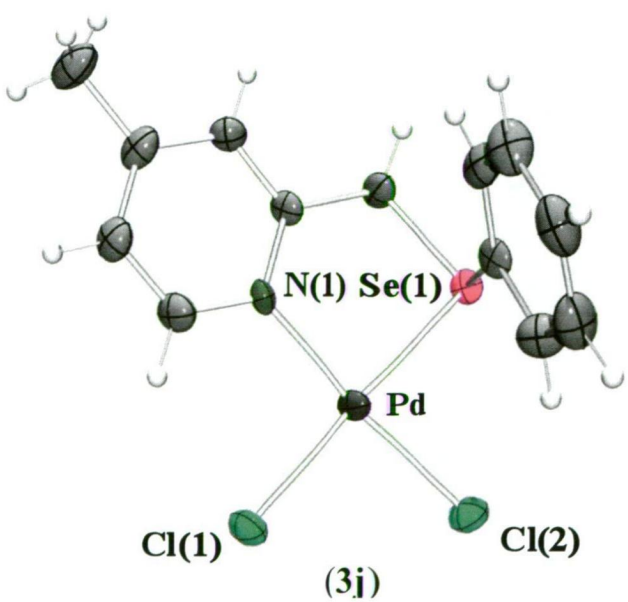

(3j)

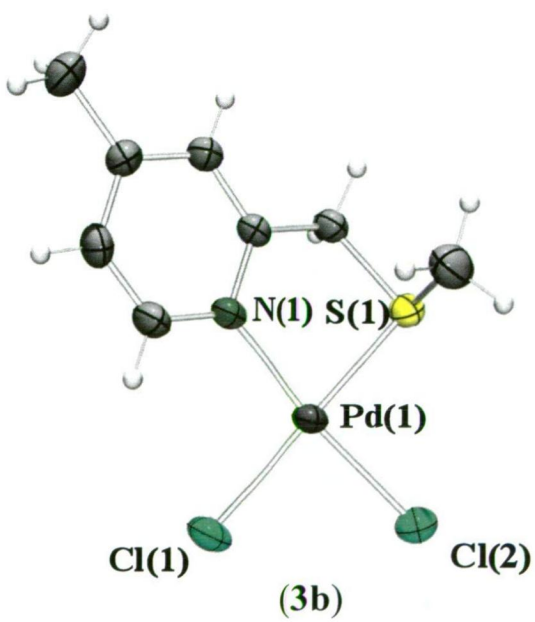

(3b)

Figure 3.1 Rendered ORTEPs of the molecular structures of $PdCl_2(pyCH_2SePh)$ (**3i**), $PdCl_2(4\text{-}MepyCH_2SePh)$ (**3j**), and $PdCl_2(4\text{-}MepyCH_2SMe)$ (**3b**). Displacement ellipsoids are drawn at the 50% probability level and H atoms are represented by circles of arbitrary size. In the case of **3b** only one molecule from the asymmetric unit is shown.

(i) Isomorphous $pyCH_2EPh$ complexes ($P2_1/n$)

Bond Distances (Å)	*M=Pd, X=Cl E=S (A)*[13]	*M=Pt, X=Cl E=S (B)*[13]	*M=Pt, X=Br E=S (C)*[17]	*M=Pd, X=Cl E=Se (3i)*	*M=Pt, X=Cl E=Se (3r)*
M-N(1)	*2.045(1)*	*2.034(3)*	*2.058(4)*	*2.043(3)*	*2.036(6)*
M-E(1)	*2.2540(5)*	*2.235(1)*	*2.2423(11)*	*2.3537(7)*	*2.3491(11)*
M-X	*2.3162(5)$_S$*	*2.316(1)$_S$*	*2.4512(9)$_S$*	*2.3257(11)$_{Se}$*	*2.3270(19)$_{Se}$*
	2.2887(6)$_N$	*2.296(1)$_N$*	*2.4243(1)$_N$*	*2.2844(11)$_N$*	*2.292(2)$_N$*
Bond Angles (°)					
N(1)–M–E(1)	*86.32(3)*	*86.6(1)*	*86.7(1)*	*86.81(9)*	*87.18(16)*
N(1)–M–X(1)	*94.50(3)*	*94.2(1)*	*94.9(1)*	*94.88(9)*	*94.35(16)*
N(1)–M–X(2)	*172.95(3)*	*174.73(9)*	*173.7(1)*	*172.70(9)*	*175.06(16)*
E(1)–M–X(1)	*174.40(1)*	*175.15(3)*	*174.20(3)*	*173.52(3)*	*174.38(4)*
E(1)–M–X(2)	*88.74(1)*	*89.70(4)*	*88.73(3)*	*88.14(4)*	*89.36(7)*
X(1)–M–X(2)	*90.90(2)*	*89.79(4)*	*90.06(2)*	*90.71(4)*	*89.43(8)*
N(1)–M–E(1)–C(22)	*93.12(6)*	*92.5(2)*	*94.8(2)*	*88.48(13)*	*87.8(3)*
N(1)–M–E(1)–C(21)	-	-	*-13.9(2)*	*-14.85(14)*	*-15.9(3)*
N(1)-C(2)-C(21)-E(21)	*-16.9(2)*	*-18.0(5)*	*-16.6(5)*	*-16.4(4)*	*-18.3(8)*
M-N(1)-C(2)-C(21)	*2.72(2)*	*3.1(5)*	*3.2(5)*	*1.1(4)*	*2.0(8)*
M-E(1)-C(21)-C(2)	*20.1(1)*	*21.4(3)*	*19.4(3)*	*20.0(3)*	*21.8(5)*

(ii) Three crystallographically independent molecules of 3n ($P\square$)

Bond Distances (Å)	M=Pd, X=I, E=Se (3n)		
M-N(1)	2.126(5)	2.115(5)	2.134(5)
M-E(1)	2.3978(12)	2.3982(9)	2.3897(12)
M-X	2.6171(12)$_{Se}$	2.6084 (8)$_{Se}$	2.6210(12)$_{Se}$
	2.5964(10)$_N$	2.5914(10)$_N$	2.6012(11)$_N$
Bond Angles (°)			
N(1)–M–E(1)	85.83(13)	84.41(4)	86.25(13)
N(1)–M–X(1)	96.59(13)	96.43(14)	96.66(13)
N(1)–M–X(2)	169.42(14)	172.38(14)	173.21(13)
E(1)–M–X(1)	173.64(3)	179.07(3)	176.92(3)
E(1)–M–X(2)	88.61(4)	88.84(3)	86.99(4)
X(1)–M–X(2)	89.89(4)	90.30(3)	90.11(3)
N(1)–M–E(1)–C(22)	-79.7(2)	-70.0(2)	86.9(2)
N(1)–M–E(1)–C(21)	21.4(2)	27.4(2)	-15.0(3)
N(1)-C(2)-C(21)-E(21)	36.7(7)	36.6(7)	-12.2(8)
M-N(1)-C(2)-C(21)	-15.0(7)	-8.1(7)	-3.9(8)
M-E(1)-C(21)-C(2)	-35.2(4)	-40.6(4)	18.6(5)

Table 3.2 (i) and **(ii)** Selected bond distances (Å), and angles (°), for complexes of $pyCH_2EPh$, data for isomorphous complexes shown in *italics*.

Bond Distances (Å)	*M=Pd (3j)*	*M=Pt (3s)*
M–N(1)	*2.055(5)*	*2.037(10)*
M–Se(1)	*2.3541(8)*	*2.3548(15)*
M–Cl	*2.3269(18)$_{Se}$*	*2.323(3)$_{Se}$*
	2.2870(19)$_{N}$	*2.294(4)$_{N}$*
Bond Angles (°)		
N(1)–M–Se(1)	*86.66(15)*	*87.7(3)*
N(1)–M–Cl(1)	*94.62(16)*	*93.3(3)*
N(1)–M–Cl(2)	*174.51(16)*	*176.6(3)*
Se(1)–M–Cl(1)	*178.33(6)*	*178.90(9)*
Se(1)–M–Cl(2)	*87.85(5)*	*89.02(10)*
Cl(1)–M–Cl(2)	*90.87(7)*	*89.97(13)*
N(1)–M–Se(1)–C(22)	*85.0(3)*	*84.2(5)*
N(1)–M–Se(1)–C(21)	*-17.8(3)*	*-20.3(5)*
N(1)-C(2)-C(21)-Se(1)	*-21.0(8)*	*-26.3(15)*
M-N(1)-C(2)-C(21)	*2.6(8)*	*5.7(15)*
M-Se(1)-C(21)-C(2)	*24.8(5)*	*29.0(10)*

Table 3.3 Selected bond distances (Å), and angles (°), for complexes of MCl_2(4-MepyCH$_2$SePh), data for isomorphous complexes shown in *italics*.

Bond Distances (Å)	M=Pd, X=Cl (3b)	M=Pt, X=Cl (3o)	M=Pt, X=Br (D)[17]
M–N(1)	2.042(4), 2.048(5)	2.003(14)	2.033(6)
M–S(1)	2.2563(14), 2.2520(18)	2.250(5)	2.238(2)
M–X	2.3270(15)$_{S}$	2.320(5)$_{S}$	2.4597(8)$_{S}$
	2.2891(15)$_{N}$,	2.285(5)$_{N}$	2.4322(9)$_{N}$
	2.3208(18)$_{S}$		
	2.275(2)$_{N}$		
Bond Angles (°)			
N(1)–M–S(1)	85.40(12), 85.39(14)	85.7(4)	85.5(2)
N(1)–M–X(1)	94.27(12), 93.99(14)	94.0(4)	95.1(2)
N(1)–M–X(2)	173.50(12), 173.85 (15)	175.7(4)	173.2(2)
S(1)–M–X(1)	177.98(6), 178.80(8)	178.3(2)	179.10(5)
S(1)–M–X(2)	89.03(5), 88.91(7)	90.4(2)	88.81(5)
X(1)–M–X(2)	91.42(6), 91.75(8)	90.0(2)	90.70(3)
N(1)–M–S(1)–C(22)	-81.2(3), 80.0(3)	84.9(9)	82.6(4)
N(1)–M–S(1)–C(21)	21.9(2), -23.7(3)	-16.3(7)	-20.6(3)
N(1)-C(2)-C(21)-S(1)	30.6(6), -29.3(7)	-23.7(19)	-31.1(8)
M-N(1)-C(2)-C(21)	-9.5(6), 5.8(7)	8.0(19)	11.6(9)
M-S(1)-C(21)-C(2)	-32.7(4), 34.0(5)	25.0(13)	32.1(5)

Table 3.4 Selected bond distances (Å), and angles (°), for metal(II) complexes of 4-MepyCH$_2$SMe.

The complex $PdCl_2(pyCH_2SePh)$, **3i** (**Figure 3.1**), and the analogous dichloroplatinum(II) complex $PtCl_2(pyCH_2SePh)$, **3r**, both crystallise as block shaped crystals in the monoclinc space group $P2_1/n$ with a single molecule in the asymmetric unit and are isomorphous with previously reported complexes $PdCl_2(pyCH_2SPh)$,[12] (**A**), $PtCl_2(pyCH_2SPh)$,[12] (**B**), and $PtBr_2(pyCH_2SPh)$[16] (**C**). The diiodopalladium(II) analogue, **3n**, crystallises as block shaped crystals in the triclinic space group $P\square$ with the asymmetric unit containing three crystallographically distinct monomeric complexes. The complex $PdCl_2(4\text{-}MepyCH_2SePh)$, **3j** (**Figure 3.1**), and the isomorphous dichloroplatinum(II) complex $PtCl_2(4\text{-}MepyCH_2SePh)$, **3s**, crystallise in the monoclinic space group $P2_1/c$, with the asymmetric unit of both complexes comprised of one monomeric complex and one MeCN solvent molecule.

The complex $PdCl_2(4\text{-}MepyCH_2SMe)$, **3b** (**Figure 3.1**), crystallises in the triclinic space group $P\square$ with the asymmetric unit comprised of two crystallographically distinct monomeric complexes and one disordered $MeNO_2$ solvent molecule. The analogous dichloroplatinum(II) complex $PtCl_2(4\text{-}MepyCH_2SMe)$, **3o**, crystallises as rod shaped crystals in the monoclinic space group $C2/c$ with the asymmetric unit consisting of one monomeric complex. The complexes **3b** and **3o** are structural analogues to the reported dibromoplatinum(II) complex containing the same ligand, $PtBr_2(4\text{-}MepyCH_2SMe)$,[16] (**D**).

The $pyCH_2EPh$, $4\text{-}MepyCH_2SePh$, and $4\text{-}MepyCH_2SMe$ ligated complexes have almost identical configurations of the ligand and the relationship of the ligand to the mean metal coordination plane as defined by M, X(1), X(2), N(1), E(1). The pyridyl ring forms dihedral angles of 13.5_6 (**A**), 13.6_7 (**B**), 15.6_0 (**C**), 15.5(2) (**3i**), 15.6(3) (**3r**), and 23.2(1) (**3n**) ($pyCH_2EPh$); 12.2(3) (**3j**), 14.9(5) (**3s**) ($4\text{-}MepyCH_2SePh$); and 15.9(3) (**3b**), 11.0(3) (**3o**), 15.1_0 ° (**D**) ($4\text{-}MepyCH_2SMe$), with the mean coordination plane. The phenyl and methyl chalcogen substituents are almost perpendicular to the coordination plane due to the stereochemistry enforced by the lone pairs on the chalcogen. The chelate rings are puckered, with the chalcogen atom lying out of the mean M, N(1), C(2), C(21) plane by 0.415(2) (**A**), 0.434(5) (**B**), 0.48_9 (**C**), 0.475(5) (**3i**), 0.513(8) (**3r**), 0.73(6) Å (**3n**) ($pyCH_2EPh$); 0.58(1) (**3j**), 0.65(2) Å (**3s**) ($4\text{-}MepyCH_2SePh$); 0.641(6) (**3b**), 0.49(2) (**3o**), and 0.60_5 Å (**D**) ($4\text{-}MepyCH_2SMe$).

PtX_2(6-$MepyCH_2SR$) (R = Me, Ph, X = Br, Cl)

The platinum complex $PtCl_2$(6-$MepyCH_2SMe$), **3p** (**Figure 3.2**), crystallises as block shaped crystals in the monoclinic space group $P2_1/n$. An isomorphous partner of $PtBr_2$(6-$MepyCH_2SMe$),[16] the asymmetric unit of **3p** consists of a single monomeric molecule. $PtCl_2$(6-$MepyCH_2SPh$), **3q** (**Figure 3.2**), crystallises as block shaped crystals in the triclinic space group P-1, containing two crystallographically distinct molecules in the asymmetric unit. Selected bond distances and angles are listed in **Table 3.5** and a simplified representation is shown below.

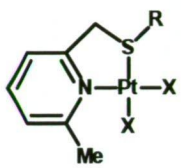

(3p,q)

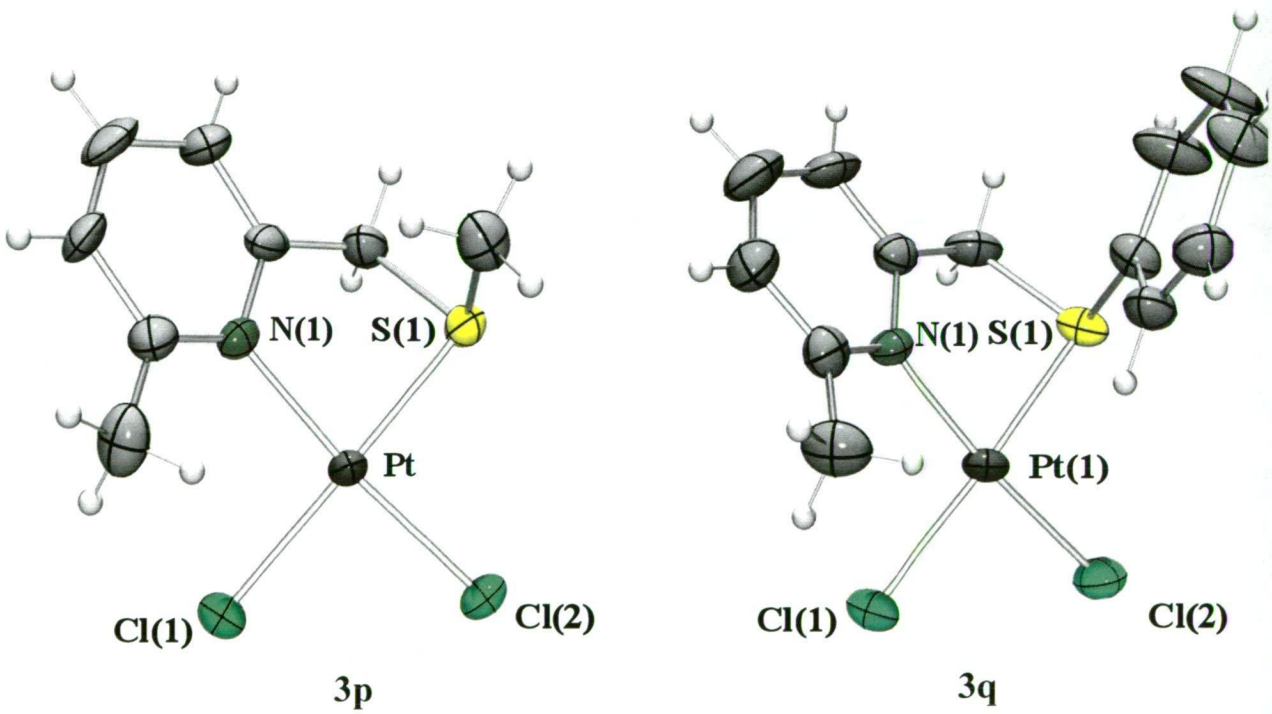

Figure 3.2 Rendered ORTEPs of the molecular structures of $PtCl_2$(6-$MepyCH_2SMe$) (**3p**) and $PtCl_2$(6-$MepyCH_2SPh$) (**3q**). Displacement ellipsoids are drawn at the 50% probability level and H atoms are represented by circles of arbitrary size. In the case of **3q** only one molecule from the asymmetric unit is shown for clarity.

Bond Distances (Å)	*X=Cl, SMe (3p)*	X=Cl, SPh (3q)	*X=Br, SMe (E)*[17]
Pt-N(1)	*2.054(13)*	2.055(6), 2.067(6)	*2.055(7)*
Pt-S(1)	*2.250(4)*	2.239(2), 2.245(2)	*2.248(2)*
Pt-X	*2.336(3)* *2.296(4)$_N$*	2.331(2) 2.312(2) 2.293(2)$_N$, 2.296(2)$_N$,	*2.4630(9)* *2.4220(9)$_N$*
Bond Angles (°)			
N(1)–Pt–S(1)	*84.2(4)*	83.33(17), 83.72(18)	*83.7(2)*
N(1)–Pt–X(1)	*96.8(4)*	96.19(17), 96.49(18)	*96.7(2)*
N(1)–Pt–X(2)	*173.6(3)*	174.05(17), 172.57(18)	*173.5(2)*
S(1)–Pt–X(1)	*167.91(12)*	170.90(7), 172.29(8)	*166.91(6)*
S(1)–Pt–X(2)	*89.80(15)*	90.74(8), 90.21(8)	*89.95(6)*
X(1)–Pt–X(2)	*89.53(14)*	89.58(8), 88.95(8)	*89.77(3)*
N(1)–Pt–S(1)–C(22)	*63.7(6)*	66.5(3), 67.0(3)	*62.0(5)*
N(1)–Pt–S(1)–C(21)	*-37.3(5)*	-37.5(3), -36.7(3)	*-37.9(4)*
N(1)-C(2)-C(21)-S(21)	*-34.7(15)*	-28.3(8), -28.4(9)	*-33.9(10)*
Pt-N(1)-C(2)-C(21)	*-2.5(15)*	-8.3(8), -7.8(9)	*-3.1(10)*
Pt-S(1)-C(21)-C(2)	*47.7(9)*	44.7(5), 44.2(6)	*47.5(6)*

Table 3.5 Selected bond distances (Å), for Pt(II) complexes of 6-MepyCH$_2$SMe and 6-MepyCH$_2$SPh, isomorphous complexes are shown in *italics*.

The presence of a methyl group in the 6-position of the pyridyl ring has a significant influence on the overall geometry of platinum(II) complexes. This effect is most clearly observed in changes in the torsion angles within the chelate ring and a twist in the PtCl$_2$NE plane relative to the pyridyl plane (**Table 3.4**). In the case of PtCl$_2$(pyCH$_2$SPh) (**B**), the pyridyl ring is relatively close to coplanar with the Pt coordination plane (13.7$_2$ °). However, for **3p**, **3q**, and PtBr$_2$(6-MepyCH$_2$SMe)[16] (**E**), the dihedral angle is significantly larger 37.5(3), 35.8(8), 38.0(9), and 39.4$_8$ °, respectively. Increased puckering in the chelate ring places the sulfur atom 1.01(1) Å (**3p**), 0.993(9), 1.003(8) Å (**3q**), out of the chelate plane (defined by Pt(1), N(1), C(2), and C(21), rms = 0.012, 0.032, and 0.034 Å, respectively), considerably larger than the 0.442$_4$ Å observed for PtCl$_2$(pyCH$_2$SPh) (**B**) but only slightly less than the 1.304$_4$ Å observed for PtBr$_2$(6-MepyCH$_2$SMe) (**E**) (rms = 0.012 and 0.013 Å, respectively), **Figure 3.3**. These effects parallel previous observations in counterpart *t*-butylthiomethyl substituted chloromethylpalladium(II) complexes,[8] and methylthiomethyl substituted dibromoplatinum(II) complexes.[16]

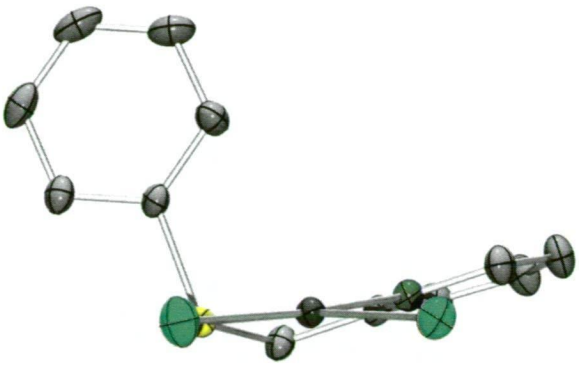

$PtCl_2(pyCH_2SPh)$, (**B**)

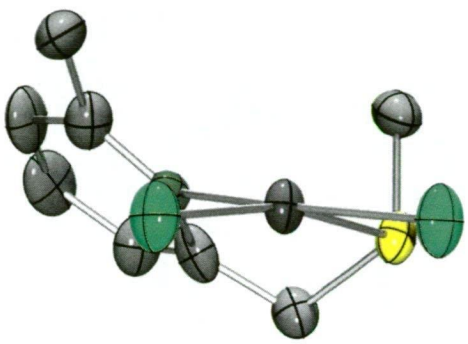

$PtCl_2(6\text{-}MepyCH_2SMe)$, **3p**

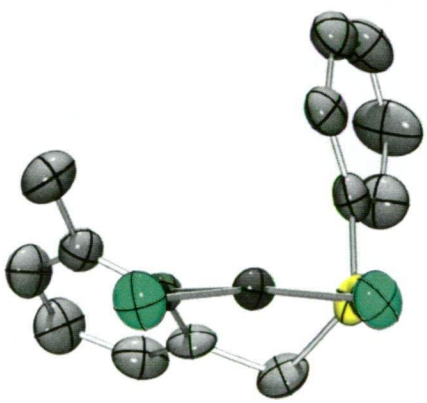

$PtCl_2(6\text{-}MepyCH_2SPh)$, **3q**

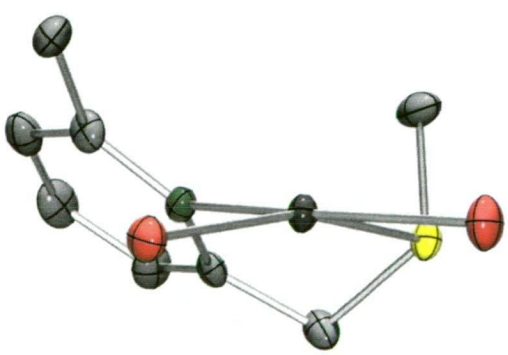

$PtBr_2(6\text{-}MepyCH_2SMe)$, (**E**)

Figure 3.3 Rendered ORTEPs of the molecular structures of **3p**, **3q**, $PtCl_2(pyCH_2SPh)$, and $PtBr_2(6\text{-}MepyCH_2SMe)$. Complexes are viewed down the X–M–X angle bisector. Displacement ellipsoids are drawn at the 50% probability level and H atoms have been omitted for clarity.

Comparison of Bond Lengths of Palladium(II) and Platinum(II) Centres for Complexes $MX_2(N,E)$

Difficulties in comparing bond lengths of complexes include variations in accuracy of bond length determinations resulting from crystal quality, and differences in intermolecular interactions within crystals of different crystal packing. Observed trends are of particular value when detected in an isomorphous series of complexes as crystal packing effects are similar. This is illustrated in an examination of the bond lengths observed in **3n**, **Table 3.2 (ii)**. The Pd–donor atom lengths for this complex vary widely, e.g. Pd–Se distances vary up to 3 standard deviations between the three different molecules of the asymmetric unit, giving a clear illustration of crystal packing effects on molecule bond distances.

The significant variation in ligand configuration for the 6-methyl substituted platinum(II) complexes indicates that these complexes should be assessed separately, except for the anticipated simple variation of M–X bond length with change of halogen. Palladium(II) complexes containing 6-methyl substituted ligands are also treated separately, as they have structures different from platinum(II) complexes.

For complexes with a hydrogen at the 6-position, clear and expected trends are observed as the halogen is varied, *i.e.*, Pd–Cl 2.276(2) – 2.3376(10) Å, (**A**, **3i**, **j**, **b**) < Pd–I 2.5914(10) – 2.6210(12) Å (**3n**); Pt–Cl 2.285(5) – 2.3270(19) Å, (**B**, **3r**, **s**, **o**) < Pt–Br 2.4243(1) – 2.4597(8) Å, (**C**[16]); and similarly for isomorphous PtX_2(6-MepyCH_2SMe) (X = Cl (**3p**) 2.336(3), 2.296(4) Å; X = Br (**E**) 2.4630(9), 2.4220(9) Å).

Other comparisons are listed in **Table 3.6** where, arbitrarily, in an attempt to estimate the influence of differences in intermolecular interactions mentioned above, ">" indicates values differing by at least 3 standard deviations, "≥" indicates values differing by ~3 standard deviations, and "~" indicates values differing by less than ~2 standard deviations.

Motif	Trend No.	Trends and Values
MCl_2NSR	1	*Pd–N 2.045(1) (A) ≥ Pt–N 2.034(3) (B)*
	2	Pd–N 2.042(4), 2.048(5) (**3b**) > Pt–N 2.003(14) (**3o**)
	3	*Pd–S 2.2540(5) (A) > Pt–S 2.235(1) (B)*
	4	Pd–S 2.2563(14), 2.2520(18) (**3b**) ~ Pt–S 2.250(5) (**3o**)
	5	*Pd–Cl_N 2.2887(6) (A) < Pt–Cl_N 2.296(1) (B)*
	6	Pd–Cl_N 2.275(2), 2.2891(15) (**3b**) ~ Pt–Cl_N 2.285(5) (**3o**)
	7	*Pd–Cl_S 2.3162(5) (A) ~ Pt–Cl_S 2.316(1) (B)*
	8	Pd–Cl_S 2.3270(15), 2.3208(18) (**3b**) ~ Pt–Cl_S 2.320(5) (**3o**)
MCl_2NSeR	9	*Pd–N 2.043(3) (3i) ~ Pt–N 2.036(6) (3r)*
	10	*Pd–N 2.055(5) (3j) ~ Pt–N 2.037(10) (3s)*
	11	*Pd–Se 2.3537(7) (3i) ≥ Pt–Se 2.3491(11) (3r)*
	12	*Pd–Se 2.3541(8) (3j) ~ Pt–Se 2.3548(15) (3s)*
	13	*Pd–Cl_N 2.2844(11) (3i) ~ Pt–Cl_N 2.292(2) (3r)*
	14	*Pd–Cl_N 2.2870(19) (3j) ~ Pt–Cl_N 2.294(4) (3s)*
	15	*Pd–Cl_{Se} 2.3257(11) (3i) ~ Pt–Cl_{Se} 2.3270(19) (3r)*
	16	*Pd–Cl_{Se} 2.3269(18) (3j) ~ Pt–Cl_{Se} 2.323(3) (3s)*
MCl_2NEPh	17	*Pd–Cl_{SPh} 2.3162(5) (A) < Pd–Cl_{SePh} 2.3257(10) (3i)*
	18	*Pt–Cl_{SPh} 2.316(1) (B) < Pt–Cl_{SePh} 2.3270(19) (3r)*

Table 3.6 Trends in bond lengths (Å) for various $MX_2(N,E)$ motifs where the ligand has a hydrogen at the 6-position. Subscripts for Cl_N, Cl_S, Cl_{SPh}, Cl_{SePh} indicate the donor atom *trans* to chloride.

M-N Distances

For the MCl_2NS motif a definite trend Pd–N ≥ Pt–N is reflected in values for both isomorphous and non-isomorphous pairs (trend numbers 1, 2). The same trend is

followed for MCl_2NSe, with less certainty (9, 10). The general trend is consistent with literature reports of other isomorphous pairs, for both M(II) and M(IV) oxidation states in organometallic complexes, [MMe_3(tris(pyrazol-1-yl)methane)]I (Pd–N 2.191(8), 2.207(7), 2.225(7), Pt–N 2.156(6), 2.156(5), 2.189(5) Å)[17] and MCl(C,N,S) ([C,N,S]$^-$ is the orthometallated 2-(methylthio)azobenzene fragment [4-$MeC_6H_3N_2C_6H_4SMe$]$^-$) (Pd–N 1.979(2), Pt–N 1.946(8) Å).[18]

A definite trend is observed for M–N distances with N *trans* to different halogens; $Pd–N_{Cl}$ (**3i**) < $Pd–N_I$ (**3n**) and $Pt–N_{Cl}$ (**3p**) < $Pt–N_{Br}$ (**E**), reflecting the anticipated *trans* influence of the halogens.

M-E Distances

The trend Pd–E > Pt–E is observed for both sulfur and selenium in two isomorphous pairs (3, 11). This is consistent with reported M–S bonds in the isomorphous organometallic compounds MCl(C,N,S) (Pd–S 2.387(1), Pt–S 2.354(3) Å).[18] In contrast, the trend is not detetcted in non-isomorphous pairs (4, 12).

As was observed for the M–N distances, a definite trend is observed for the corresponding M–E distances with E *trans* to different halogens; $Pd–E_{Cl}$ (**3i**) < $Pd–E_I$ (**3n**) and $Pt–E_{Cl}$ (**3p**) < $Pt–E_{Br}$ (**E**).

M-Cl Distances

For the chloro ligand *trans* to the nitrogen donor, $Pd–Cl_N$ < $Pt–Cl_N$ (5, 6, 13, and 14), but the bond distances are within 2σ (6, 14, and isomorphous pair 13), and only > 3σ for isomorphous pair 5. In contrast, $Pd–Cl_N$ > $Pt–Cl_N$ is isomorphous MCl(C,N,S) (2.303(1), 2.293(3) Å) although within 3σ.[18]

For the chloro ligand *trans* to a chalcogen, $Pd–Cl_S$ ~ $Pt–Cl_S$ (7, 8) and $Pd–Cl_{Se}$ ~ $Pt–Cl_{Se}$ for two isomorphous pairs (15, 16). In isomorphous pairs, both Pd–Cl and Pt–Cl *trans* to a phenylthioether donor are shorter than for a phenylselenoether donor (17, 18).

Solid State Structures of $[PdCl_2(6\text{-}MepyCH_2SPh)]_3$ (3g), $PdI_2(6\text{-}MepyCH_2SPh)_2$ (3m), and $[PdCl_2(6\text{-}MepyCH_2SePh)]_2$ (3k).

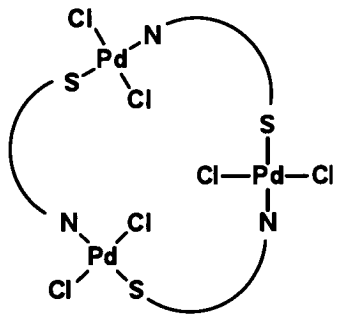

3g

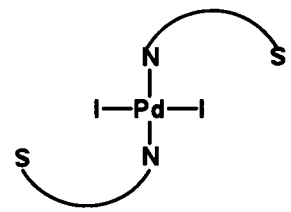

3m

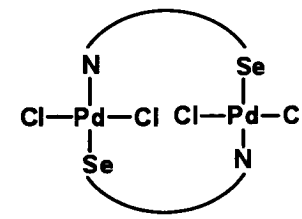

3k

For complexes **3g**, **m**, and **k** the substitution of a 6-methyl group results in significant structural differences relative to their corresponding unsubstituted analogues. The inclusion of a 6-methyl group on the pyridyl ring may result in a significant Me···X steric interaction, **Figure 3.4**. This contact can be relieved in several ways; an increased or large dihedral angle between pyridyl and metal coordination planes but retention of *cis* chelated distorted square planar geometry as observed in the *cis*-$PtCl_2(N,S)$ complexes **3p** and **3q** with very puckered chelate rings. Or by the loss of ligand chelation and formation of, either, a *trans* bridged $PdX_2(N,S)_2$ trimeric/dimeric compound as observed in **3g** and **3k**, or alternatively a *trans* monomeric PdX_2N_2, 2:1 metal ligand complex as displayed in **3m**. In the case of **3g**, **3m**, and **3k**, these are the first reported structures of their type involving *N,E* heteroleptic ligands. When the bond lengths of the Pd–donor atoms of the 6-methyl containing complexes **3g**, **3m**, and **3k** are compared to that of their respective unsubstituted analogues differences are observed, which, although not forming any specific trend, may be attributable to the *trans* influence of different donor atoms in the complexes.

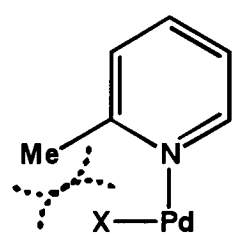

Figure 3.4 An illustration of the significant Me···X steric interaction caused by the introduction of a 6-methyl group on the pyridyl ring.

$[PdCl_2(6\text{-}MepyCH_2SPh)]_3$

The complex $PdCl_2(6\text{-}MepyCH_2SPh)$, **3g** (**Figure 3.5**), crystallises as block shaped crystals in the orthorhombic space group $Pca2_1$ containing one trimeric molecule and one $MeNO_2$ solvent molecule in the asymmetric unit. Molecules have three crystallographically distinct *trans*-dichloropalladium(II) moieties with bridging 6-$MepyCH_2SPh$ ligands. The structure contains a disorder which is restricted to the Pd, Cl, and S atoms of one palladium centre, refined anisotropically with refined complementary occupancies of major and minor disorder components of 82(14) and 18(14)%. This disorder model allowed a suitable refinement of the molecule giving an R_1 of 6.2%. The metal centres have square planar geometry with Cl–Pd–Cl angles of 177.7(2), 178.4(2) and 176.3(3) ° (167.0(2) ° minor disorder component). The trimer exists in a head-to-tail arrangement of the ligands, giving the '$PdCl_2NS$' configuration at each palladium atom with N–Pd–S angles of 176.4(5), 176.3(5) and 173.5(6) ° (175.8(14) ° minor disorder component). The fifteen membered ring containing the three palladium atoms is not planar, as illustrated in **Figure 3.5**.

A general comparison of bond lengths of **3g** with the *cis* chelated unsubstituted analogue $PdCl_2(pyCH_2SPh)$ (**A**) reveals that the Pd–N (2.052(3), 2.053(17), 2.054(19) Å, and Pd–E (2.280(7), 2.282(5), 2.277(5) Å **3g**, are within 3σ of the unsubstituted complex Pd–N 2.045; Pd–E 2.2540(5) Å (**A**): In the case of the Pd–Cl bond distances a good comparison cannot be made as the Pd–Cl distances in **3g** vary greatly due to crystal packing effects (2.269(7)–2.340(8) Å).

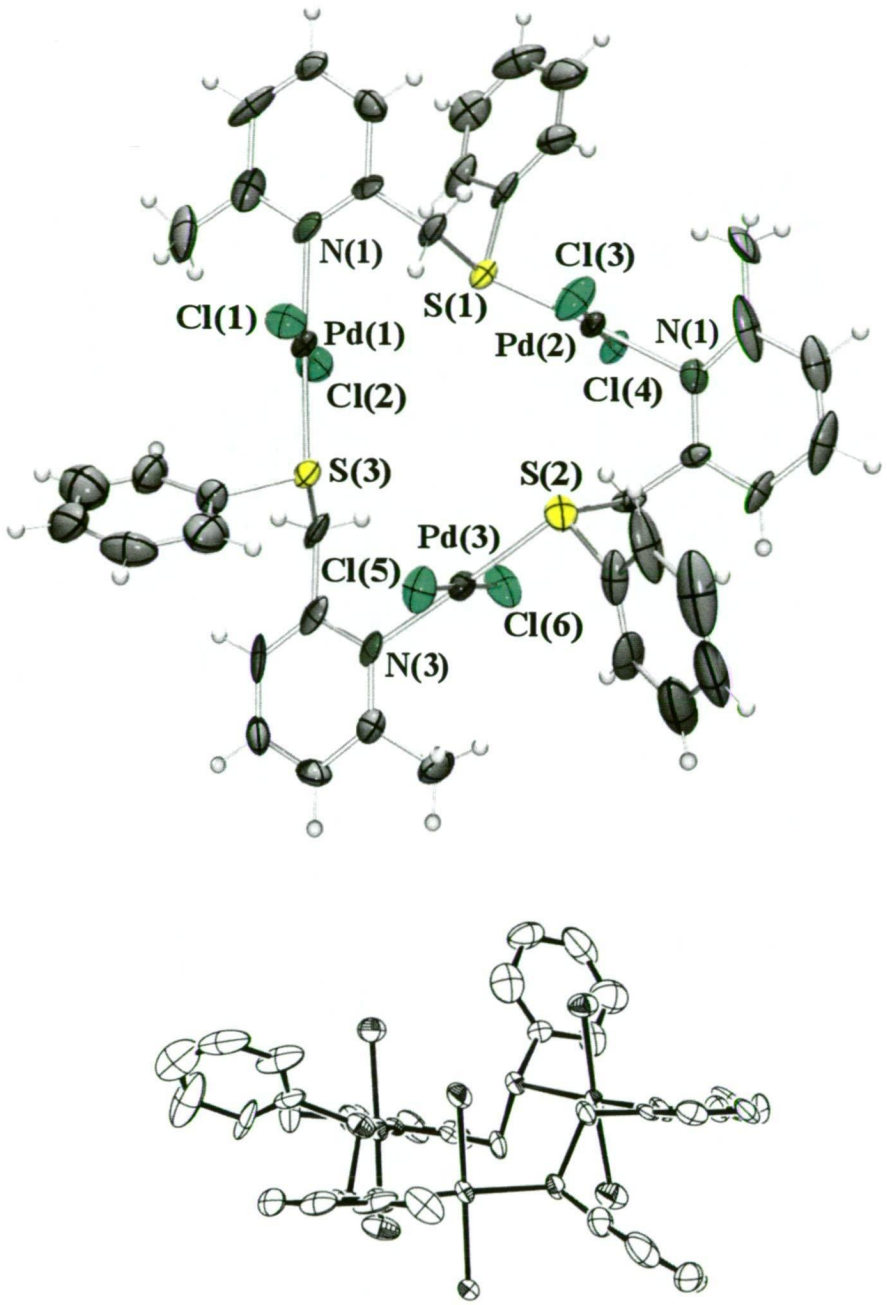

Figure 3.5 (I) Rendered ORTEP of the molecular structure of $[PdCl_2(6\text{-}CH_3pyCH_2SPh)]_3$ (**3g**). **(II)** ORTEP diagram with projection in the plane of the pyridyl rings of **3g**, illustrating the non-planar nature of the complex. Displacement ellipsoids are drawn at the 50% probability level, where displayed H atoms are represented by circles of arbitrary size. Disorder and the solvent molecule have been omitted for clarity, but can be examined in **Appendix B**.

PdI_2(6-MepyCH_2SPh)$_2$

The complex PdI_2(6-MepyCH_2SPh)$_2$, **3m** (**Figure 3.6**), crystallises as rod shaped crystals in the monoclinic space group *C*2/*c*, containing one half of the monomeric complex and one $MeNO_2$ solvent molecule in the asymmetric unit. The other half of the molecule of **3m** is generated by an inversion centre at (½, 0, ½). The molecule contains one *trans*-diiodopalladium(II) centre with two 6-MepyCH_2SPh ligands bound through the *N*-donor atoms giving the complex the general formula $PdI_2(N,S)_2$. The metal centre has square planar geometry with I–Pd–I and N–Pd–N angles of 180.0 °, indicating no distortion in the metal coordination sphere.

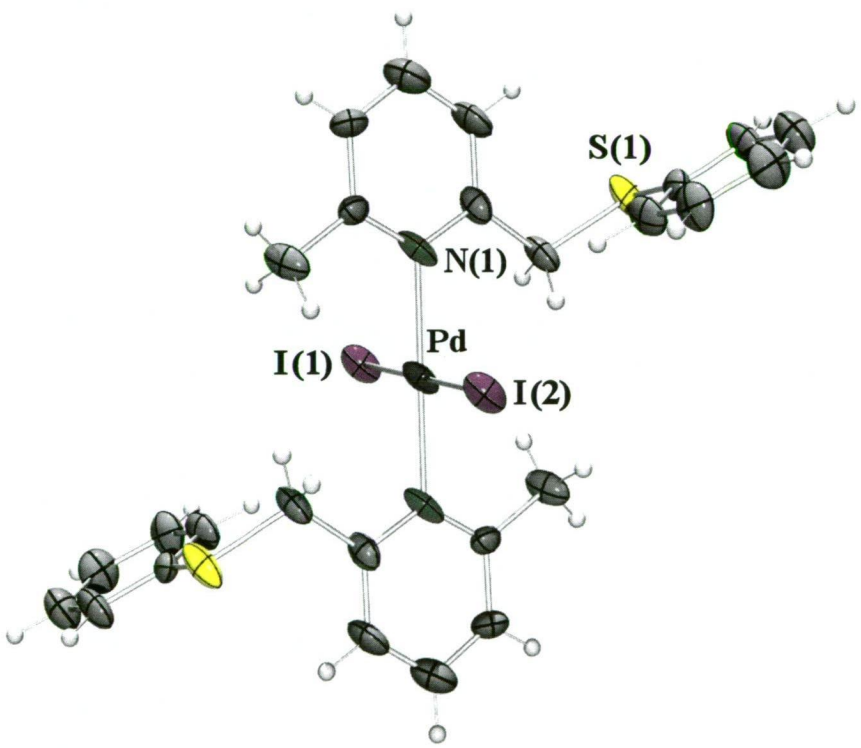

Figure 3.6 A rendered ORTEP of the molecular structure of PdI_2(6-MepyCH_2SPh)$_2$ (**3m**). Displacement ellipsoids are drawn at the 50% probability level and H atoms are represented by circles of arbitrary size. The solvent molecule has been omitted for clarity, but can be examined in **Appendix B**.

In a general comparison of the Pd–N bond distances of **3m** and the 6-unsubstituted chelated complex $PdI_2(pyCH_2SePh)$ (**3n**) indicates those of **3m** (2.080(11) Å) are slightly shorter than that observed in **3n** (2.126(5), 2.115(5), 2.134(5) Å) with values corresponding within ~3σ. The Pd–I bond distances of **3m** (2.6191(6) Å) however are much longer than that of the unsubstituted complex with values of **3m** >3σ than those observed in the **3n** ($2.6171(12)_{Se}$, $2.5964(10)_{N}$, $2.6084(8)_{Se}$, $2.5914(10)_{N}$, $2.6210(12)_{Se}$, $2.6012(11)_{N}$, Å).

$[PdCl_2(6\text{-}MepyCH_2SePh)]_2$

The complex $[PdCl_2(6\text{-}MepyCH_2SePh)]_2$, **3k** (**Figure 3.7 (I)**), crystallises as rod shaped crystals in the monoclinic space group $P2_1/n$ containing one half of the dimeric molecule in the asymmetric unit. The other half of the complex is generated by an inversion centre at (0, ½, ½), midway between the metal centres. The complex contains two square planar palladium(II) centres with *trans* orientated chlorine moieties and bridging $6\text{-}MepyCH_2SePh$ ligands. The dimer has a head-to-tail arrangement of the ligands, with N–Pd–Se and Cl–Pd–Cl angles of 174.58(3) and 176.81(9) ° respectively. The ten-membered ring containing the palladium metal centres is not planar, as illustrated in **Figure 3.7 (II)**.

A comparison of the Pd–N and Pd–Se bond lengths of **3k** with the unsubstituted chelated complex $PdCl_2(pyCH_2SePh)$ (**3i**) reveals that the Pd–N bond lengths of **3k** (2.053 (3) Å) are slightly longer than the unsubstituted complex (2.043(3) Å) with values corresponding to with 3σ. The Pd–Se bond lengths of **3k** (2.4057(6) Å) are, however, increased to >3σ than that observed for **3i** (2.3537(7) Å). For the Pd–Cl bond distances those of **3k** (2.3082(10), 2.3198(10) Å) are greater than the observed $Pd–Cl_N$ distance (2.2844(11) Å) >3σ but are much shorter than the corresponding $Pd–Cl_{Se}$ distance (2.3257(11) Å) <3σ observed for **3i**.

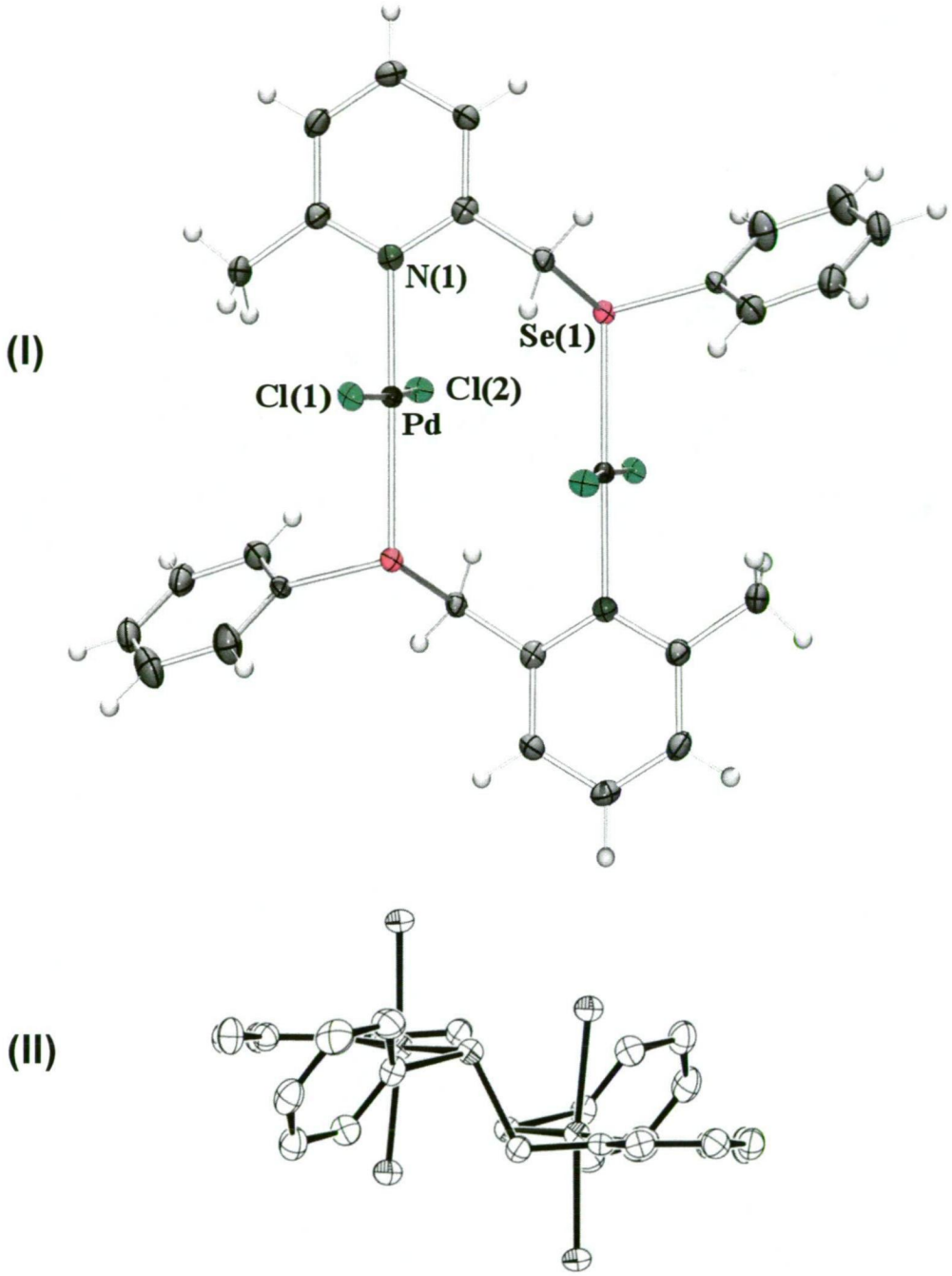

Figure 3.7 (I) A rendered ORTEP of the molecular structure of $[PdCl_2(6\text{-}MepyCH_2SPh)]_2$ (**3k**). Displacement ellipsoids are drawn at the 50% probability level and H atoms are represented by circles of arbitrary size. **(II)** An ORTEP of **3k** in the plane of the pyridyl rings H atoms have been omitted for clairty.

Cyclopalladation Involving Reactions With 6-PhpyCH$_2$SePh. Solid State Structure of PdCl(6-C$_6$H$_4$pyCH$_2$SePh).

The complex PdCl(6-C$_6$H$_4$pyCH$_2$SePh), **3l** (**Figure 3.8**), crystallises as block shaped crystals in the monoclinic space group *Cc* with four crystallographically distinct molecules in the asymmetric unit. The *ortho*-metallated ligand is present as a tridentate donor in the general formula PdCl(*C,N,Se*). The metal centre has a square planar geometry with C–Pd–Se (165.12(16), 163.43(16), 165.54(17) and 166.42(16)°) and N–Pd–Cl angles equal to (176.56(14), 177.01(15), 177.06(14) and 178.53(14) °).

A comparison of the Pd–N and Pd–Se bond lengths of **3l** with the unsubstituted complex PdCl$_2$(pyCH$_2$SePh) (**3i**) reveals that the Pd–N bond lengths of **3l** (2.010(5), 2.014(5), 2.005(5) and 2.006(5) Å) are shorter than the unsubstituted complex (2.043(3) Å) with values greater than 3σ. The Pd–Se bond lengths of **3l** (2.5201(10), 2.5434(11), 2.5081(10) and 2.5033(13) Å) are very much longer, >3σ, than that observed for **3i** (2.3537(7) Å). For the Pd–Cl bond distances, those of **3l** (2.3117(18), 2.3109(16), 2.3228(17) and 2.3024(18) Å) are greater than the observed Pd–Cl$_N$ distance (2.2844(11) Å) ~3σ observed for **3i**.

For complex **3l**, like the analogous 6-methyl substituted complexes, the substitution of a 6-phenyl group results in significant structural differences relative to their corresponding unsubstituted analogues. The inclusion of a 6-phenyl group on the pyridyl ring has resulted in the formation of a cyclopalladated species with a tridentate coordinating ligand. When the bond lengths of the Pd–donor atoms of the 6-phenyl containing complex, **3l**, are compared to that of the respective unsubstituted analogue PdCl$_2$(pyCH$_2$SePh), most notably the Pd–Se bond length is increased well beyond that expected by *trans*-ligand effects. This may be due to the planarity of the C–N chelate ring forcing strain in the N–Se chelate ring and thereby weakening the Pd–Se bond.

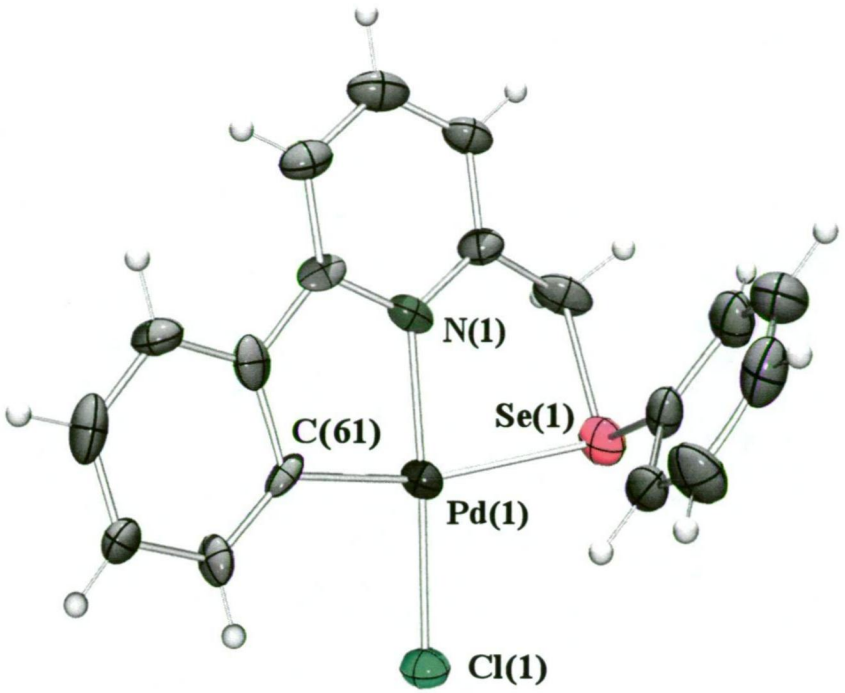

Figure 3.8 Rendered ORTEP of the molecular structure of PdCl(6-C_6H_4pyCH_2SePh) (**3l**). Displacement ellipsoids are drawn at the 50% probability level and H atoms are represented by circles of arbitrary size. Only one molecule from the asymmetric unit is displayed for clarity, however all four molecules are shown in **Appendix B**.

3.2.2.2 Solution State Characterisation of the Complexes

Liquid Secondary Ionisation Mass Spectroscopy (LSIMS) Analysis

LSIMS analysis of all complexes containing a 6-H or a 6-Ph substituent exhibited ions corresponding to the calculated molecular ion of the complex with the loss of one halogen atom, i.e. $[MX(N,E)–X]^+$ and $[M(C,N,E)–Cl]^+$, respectively. For complexes containing a 6-Me substituent on the pyridyl ring, LSIMS data could only be obtained for $PtCl_2$(6-MepyCH$_2$SMe) and $[PdCl_2$(6-MepyCH$_2$SePh)$]_2$, corresponding to the molecular ions $[PtCl$(6-MepyCH$_2$SMe)$]^+$ and $[PdCl$(6-MepyCH$_2$SePh)$]^+$. Low solubility of other 6-Me substituted complexes precluded detection of ions.

NMR Analysis

Solution state characterisation of the complexes synthesised in this study is classified into three groups related to the substituent in the 6-position of the pyridyl ring.

All complexes display low solubility in most common organic solvents except for partial solubility in dimethylsulfoxide (DMSO). Consequently, $^{13}C\{^{1}H\}$ NMR and detailed structural assignments by 2D NMR techniques were not undertaken for any complex in this study.

The previously reported complexes $MCl_2(pyCH_2SMe)$ and $MCl_2(pyCH_2SPh)$ (M = Pd, Pt) exhibit aromatic resonances between 9.13–6.63 ppm, and a AB spin system for the methylene protons in the 2-position of the pyridyl ring.[12] This AB spin system results from the formation of a stereogenic centre at the chalcogen centre upon coordination to the metal centre, leading to diastereotopic CH_aH_b resonances, typical of complexes containing this type of heteroleptic ligand.[1-12, 16]

On warming, the AB spin systems begin to coalesce to form two broad singlets at temperatures >90 °C for the Pd and >160 °C for the Pt containing complexes.[12] Three possible fluxional processes were identified that could account for these observations and are illustrated in **Figure 3.9**, reproduced from earlier work.[12]

Density Functional Theory (DFT) at the B3LYP level with a LANL2 augmented:6-311+G(2d,p) basis set was used to calculate the structures shown in **Figure 3.9**.[12] Process (a) (**I** ↔ **II**) shows the conformational change of the chelate ring, *i.e.*, ring flip, where the transition state contains a nearly flat five-membered ring which is quasi-coplanar with the coordination plane of the metal. Process (b) illustrates pyramidal inversion at the chalcogen for structure **I**, where the transition state has a planar five-membered ring. Process (c) illustrates dissociation of the chalcogen donor from structure **I** to give **IV**. Further to this, the opposite enantiomer of **I** (labelled **I***) may also undergo the processes described above to form **II**, **III**, and **IV**. The processes shown in **Figure 3.9** illustrate the possible presence of four isomers: **I/I***, **II**, **III**, and **IV**.

DFT calculations for processes illustrated in **Figure 3.9** reveal that a low activation energy (2.7 kJ mol^{-1}) is present for the ring flip process suggesting that it occurs readily at room temperature and may explain the presence of only one AB spin system rather than two, as would be expected for two possible conformers given that each species has similar energies.[12] Thus the formation of AB spin system is most likely caused by an pyramidal inversion of the chalcogen, a chalcogen dissociation process, or a combination of the two. Attempts to use DFT studies to identify which was the dominant process produced inconclusive results revealing very similar energy barriers for both processes in most cases, except for the complexes $PdCl_2(pyCH_2SMe)$ and $PtCl_2(pyCH_2SMe)$ where calculations indicated that the AB spin system most likely resulted from the pyramidal inversion of the sulfur (10-40 kJ mol^{-1} lower in energy than the corresponding sulfur dissociation process).[12]

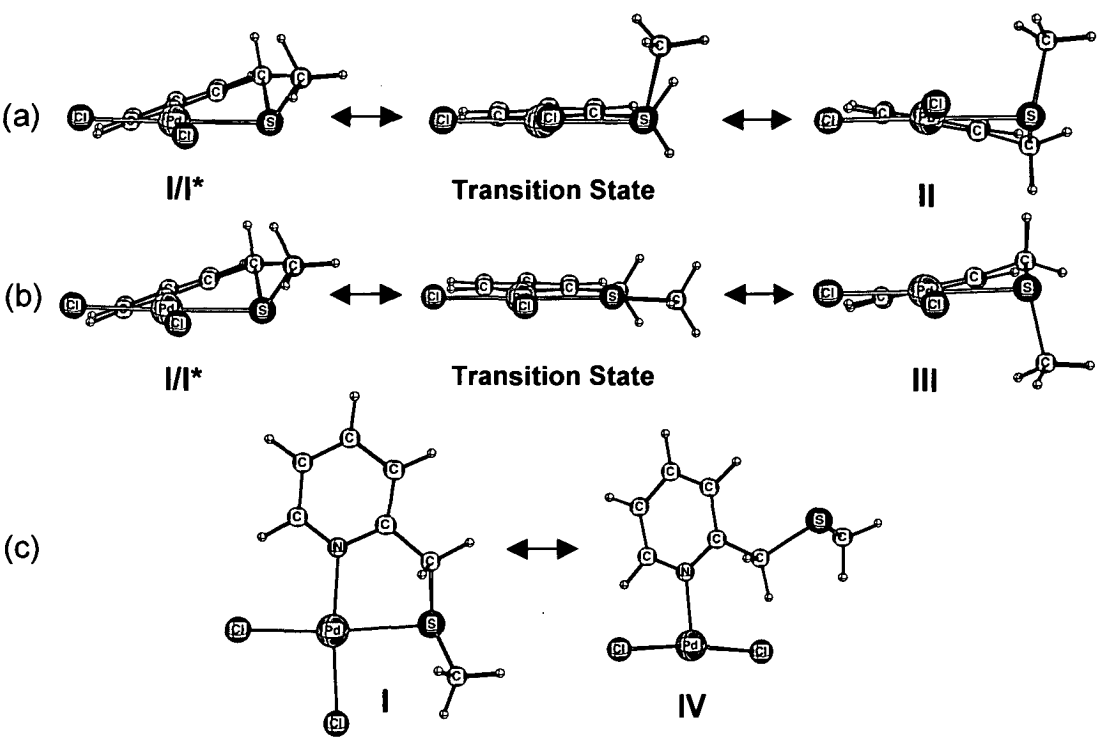

Figure 3.9 B3LYP LANL2 augmented:6-311+G(2d,p) calculated structures of conformers and transition states for (a) ring flip, (b) pyramidal chalcogen inversion, and (c) chalcogen dissociation for $PdCl_2(pyCH_2SMe)$.[12]

Complexes with a 6-H Substituent on the Pyridyl Ring

Room temperature ^1H NMR spectra of the complexes in d^6-DMSO may be interpreted as above, despite poor spectra owing to low solubility. All complexes

displayed a downfield shift in aromatic and SMe resonances with respect to that of the free ligands (~0.6 ppm Pd; ~0.8 ppm Pt), with no clear trend on altering the chalcogen from sulfur to selenium. The complexes exhibit resonances between 9.46–7.33 ppm assigned as aromatic protons of the pyridyl and phenyl rings. 4-Methyl resonances were observed as singlets between 2.48–2.31 ppm while all complexes containing a thiomethyl group displayed singlets for this group between 2.53–2.32 ppm. A single AB spin system is observed for the methylene protons of the 2-carbon for all complexes between 5.31–4.41 ppm, (except for $PdI_2(pyCH_2SePh)$ which displays a broad doublet at 5.05 ppm). Thus, spectra are consistent with that previously reported for complexes $MCl_2(pyCH_2SeR)$ (M = Pd, Pt; R = Me, Ph)[12] and with the solid state structures obtained in this study, established as monomeric $MCl_2(N,E)$.

Complexes with a 6-Me Substituent on the Pyridyl Ring

Room temperature ^{1}H NMR spectra of dilute solutions of the complexes in d^6-DMSO display similar downfield shift in resonances with respect to that of the free ligands (~0.5 ppm), with no apparent change on altering the chalcogen from sulfur to selenium. In most cases, broad signals and low signal to noise ratios are observed reflecting the very low solubility of the complexes.

The complex $PtCl_2(6\text{-}MepyCH_2SMe)$ has a monomeric structure in the solid state, similar to all complexes with a 6-H substituent on the pyridyl ring, and is discussed first. The room temperature ^{1}H NMR spectrum displays multiple resonances corresponding to one major and minor species in solution (~50:50 ratio). All major peaks have a twin in an upfield position (~0.07 ppm in the case of the aromatic signals). The spectra for the major and minor species, respectively, display two AB spin systems (4.81, 4.66, and 4.45, 4.24 ppm) corresponding to the methylene protons, and sharp singlets corresponding to methyl substituents (3.32 and 3.18 ppm, 6-Me; 2.52 and 2.41 ppm, SMe). A ^{1}H NMR spectrum recorded at 85 °C indicated coalescence of each set of signals had occurred to form broad lumps, and two broad resonances were observed in place of the AB spin systems. The multiple signals in the spectra and their coalescence at high temperature are most readily interpreted as indicating the presence of two different structural conformations of the one compound in equilibrium. The presence of the 6-Me group causes significant

disruption to the coordination environment of the complexes (see **Section 3.2.2.1**) owing to the Me···Cl interaction. A higher barrier for the ring flip process is expected, resulting in slow equilibrium between conformers and observation of both species in NMR spectra as previously discussed in **Figure 3.9**. Thus, the spectra obtained, is consistent with the solid state structure obtained for $PtCl_2$(6-$MepyCH_2SMe$) as the monomeric form $MCl_2(N,E)$.

The diiodopalladium(II) complex PdI_2(6-$MepyCH_2SPh)_2$, displays broad aromatic resonances between 7.86–7.17 ppm, and broad resonances corresponding to the methylene and 6-methyl protons at 5.02 and 3.05 ppm, respectively, where the downfield shifts of ~0.4 ppm for all resonances is less than for the above complexes where ligands are present as chelating bidentates in the solid state. Thus, the NMR spectrum is supportive of the structure determined for the solid state, *i.e.*, $PdI_2(N)_2$.

For the complexes $[PdCl_2$(6-$MepyCH_2SPh)]_3$ and $[PdCl_2$(6-$MepyCH_2SePh)]_2$, all signals are broad and difficult to interpret. In the methylene region, the spectra exhibit two broad resonances, one shifted downfield by ~0.8 ppm in a similar manner to complexes above where the ligands are bidentate $PdCl_2(N,E)$, together with a resonance shifted downfield by only ~0.01 ppm from the free ligand value. For both complexes, these broad resonances are in the ratio ~60:40 and ~70:30, respectively. Solutions of $[PdCl_2$(6-$MepyCH_2SPh)]_3$ and $[PdCl_2$(6-$MepyCH_2SePh)]_2$ were heated to 85 °C with spectra recorded in 5 °C increments. A reduction in the intensity of the minor methylene signal and a broadening of the major methylene signal was detected, with no indication of coalescence. This behaviour indicates a process(es) other than the simple fluxional exchange process observed for monomeric complexes $MX_2(N,E)$ is occurring in solution. In the solid state $[PdCl_2$(6-$MepyCH_2SPh)]_3$ and $[PdCl_2$(6-$MepyCH_2SePh)]_2$ have different structures but show similar NMR behaviour that differs from that of monomeric complexes $MX_2(N,E)$ and $MI_2(N)_2$. Due to the high insolubility of both complexes determination of solution state structure is difficult. Similarly, typical physical methods such as molecular weight determination also require solubility. A possible explanation for the complex NMR spectra is that both complexes in solution may undergo an equilibrium between various forms of oligomeric structures, **Figure 3.10**, which in turn may undergo further processes than those indicated for the monomeric complexes $MX_2(N,E)$, (**Figure 3.9**), *e.g.*, hemilabile behaviour with solvent coordination.

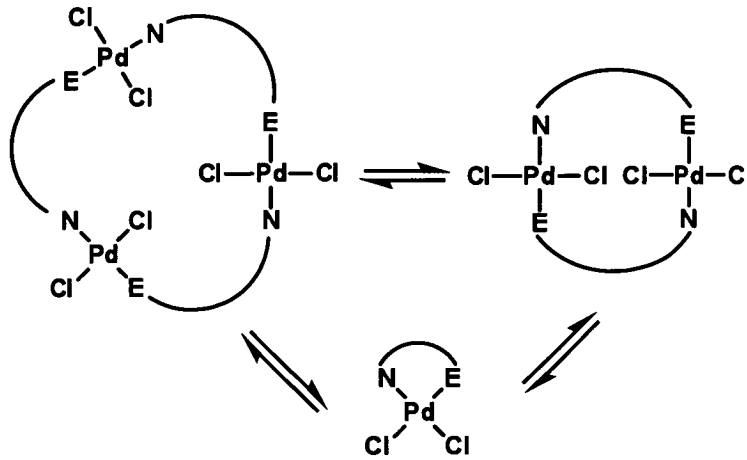

Figure 3.10 Examples of possible equilibrium processes between various oligomeric structures of $[PdCl_2(6\text{-}MepyCH_2SPh)]_3$ and $[PdCl_2(6\text{-}MepyCH_2SePh)]_2$.

In the case of $PdCl_2(6\text{-}MepyCH_2SMe)$, for which a crystal structure is unavailable, all resonances are broad and shifted ~0.5 ppm downfield from free ligand values, with resonances between 7.92–7.43 ppm assigned to aromatic protons of the pyridyl ring and resonances at 3.06 and 2.26 ppm assigned to the 6-Me and SMe functionalities, respectively. In the case of the methylene protons a broad resonance is observed at 4.72 ppm. Like the other 6-Me substituted dichloropalladium(II) complexes discussed above, NMR spectra provides little information and are thus difficult to fully interpret.

Complexes with a 6-Ph Substituent on the Pyridyl Ring

The solid state structure of $PdCl(6\text{-}C_6H_4pyCH_2SePh)$ has been determined, **Figure 3.7**, and, as this complex and $PdCl(6\text{-}C_6H_4pyCH_2SR)$ (R = Me, Ph) exhibit similar NMR spectra, they are discussed together. The ^1H NMR spectra are complex, with broad signals in the aromatic region between 8.03–7.09 ppm assigned to aromatic pyridyl and *o*-phenylene and phenyl protons. Two broad resonances in 1:1 ratio are observed for the methylene protons, one shifted downfield by ~1 ppm and one shifted downfield by ~0.03 ppm from the free ligands.

In the case of $PdCl(6\text{-}C_6H_4pyCH_2SMe)$, an SMe signal was not observed, as it appears to reside under a broad solvent peak (2.56–2.49 ppm). On warming to 85 °C

with spectra recorded in 5 °C increments, a broadening of the downfield methylene signal and a reduction in the more upfield methylene signal (near free ligand value) was detected, changing the ratio to ~65:35 for all three complexes. In the case of PdCl(6-C_6H_4pyCH_2SMe) the aromatic resonances simplified from the broad signals observed at room temperature to sharp signals with an upfield twin shifted by ~0.06 ppm in ~65:35 ratio. In addition, two sharp singlets for the SMe protons in ~65:35 ratio were observed, shifted ~0.4 ppm and ~0.05 ppm downfield respectively from the free ligand. Thus, it is possible that two conformers of the one complex are present, and processes such as chalcogen dissociation may occur leading to a solvent coordinated adduct or *cis/trans* chloride bridged dimers of the form [PdCl(6-C_6H_4pyCH_2ER)]$_2$, **Figure 3.11**. It is of note that the possibility of Pd–Se fluxionality should be suspected given the very long Pd–Se distance observed in **3l** with respect to the unsubtituted complex PdI_2(pyCH_2SePh) **3n**, (**Section 3.2.2.1**).

Similar observations were made for PdCl(6-C_6H_4pyCH_2SPh) and PdCl(6-C_6H_4pyCH_2SePh), but the complexity of the resonances from the three aromatic rings made positive identification of species difficult.

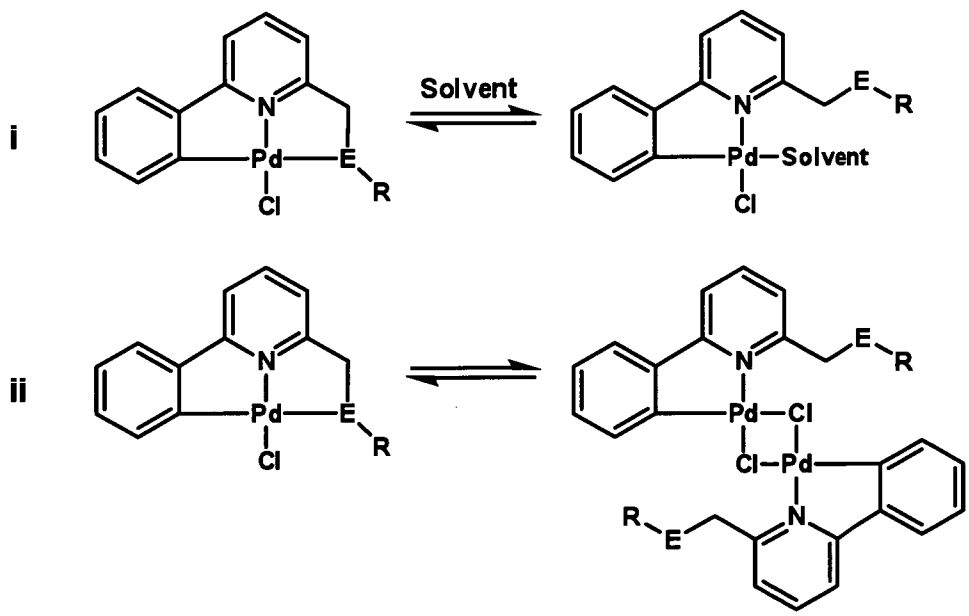

Figure 3.11 Possible equilibrium processes that may occur in solution for the 6-*o*-C_6H_4 substituted compounds; **i** formation of a solvent adduct complex, **ii** formation of a chloro- bridged dimer.

3.3 Conclusion

A simple synthesis has been developed for the preparation of dihalogenopalladium(II) complexes containing substituted 2-(organothiomethyl)-pyridines and 2-(organoselenomethyl)pyridines, in preparation for catalysis studies. X-ray structure determinations were carried out on a selection of complexes, revealing that some are isomorphous with preliminary reported Pd(II) and Pt(II) complexes. This discovery encouraged the synthesis of analogous platinum(II) complexes, allowing a comprehensive study of substituent effects on the coordination sphere of the metal centres. Placing a substituent in the 4-position of the pyridyl ring or varying the chalcogen or substituent on the chalcogen had little effect on the overall geometry of the complexes. The bond length trends Pd–N > Pt–N and Pd–E > Pt–E match earlier reports of isomorphous organometallic complexes of palladium and platinum, but the trend $Pd–Cl_N < Pt–Cl_N$ is opposite to a literature report for an organometallic complex.

Substitution of a 6-methyl group on the pyridyl ring results in a significant Me···X steric interaction which can be relieved by increasing the dihedral angle between the pyridyl ring and the coordination plane with retention of a very puckered chelate arrangement by the ligand, or loss of ligand chelation. In the complexes examined here, loss of chelation occurred only for palladium complexes, resulting in *trans*-$PdCl_2$ configurations in either trimeric species with *N,S* bridging (**3g**), dimeric species with *N,Se* bridging (**3k**) or a monomeric 2:1 ligand:metal species with *N*-coordination in *trans*-$PdI_2(N,S)_2$ (**3m**). Complexes **3g**, **3k**, and **3m** are the first reported structures of this type involving *N,E* heteroleptic ligands. If the substituent on the 6-position of the pyridyl ring is a phenyl group, *ortho*-metallation of the ligand occurs producing complexes in which a tridentate heteroleptic ligand $[C,N,S]^-$ is present, the first reported cyclometallated structure containing heteroleptic ligands of this type.

Microanalysis of complexes gave empirical formulae consistent with results of X-ray structural studies.

Room temperature ^1H NMR spectra of complexes containing a 6-H substituent on the pyridyl ring are consistent with solid state structures, $MX_2(N,E)$. For complexes

containing a 6-Me and 6-Ph substituent on the pyridyl ring, ^{1}H NMR spectra were not interpreted except in general terms. Multiple species are present for some complexes, and these are believed to undergo equilibrium processes, but appear to be consistent with the presence of the structures determined in the solid state.

3.3 Experimental

3.4.1 General

All manipulations were carried out under argon using standard Schlenk techniques. All reagents, except ligands described in **Chapter 2**, are commercially available from the Aldrich Chemical Co. and were used as received unless specified. Ultra high purity argon was purchased from BOC Gases. ^{1}H NMR spectra were recorded on a Varian Mercury Plus 300 NMR Spectrometer at 299.9 MHz at ambient temperature using deuterated dimethylsufoxide ($(CD_3)_2SO$), referenced to residual solvent (2.50 ppm). Chemical shifts (δ) are reported in ppm relative to TMS and all coupling constants are given in Hz. Peak multiplicity is denoted as singlet (s), doublet (d), triplet (t), multiplet (m), doublet of doublets (dd), triplet of doublets (td), doublet of doublet of doublets (ddd), or broad (br). Microanalyses were performed by Dr. Graham Rowbottom and Dr. Thomas Rodemann of the Central Science Laboratory (CSL), University of Tasmania using a ThermoFinnigan Flash EA 1112 Series Elemental Analyser. Mass spectrometry was conducted by Dr. Noel Davies and Dr. Marshall Hughes of the CSL. LSIMS (Liquid Secondary Ionisation Mass Spectrometry) analysis was carried out using a Kratos ISQ mass spectrometer with a liquid matrix of nitrobenzyl alcohol using 10 kV Cs ions and a 5.3 kV accelerating voltage.

3.4.2 Collection and Treatment of X-ray Crystallographic Data

Cell determinations and data acquisitions were carried out, usually at -80°C, using an Enraf-Nonius CAD4 diffractometer with a graphite single crystal monochromated molybdenum radiation source, with λ assumed to be 0.71073 Å (K_α). Unit cell calibration was carried out using 25 reflections well separated in reciprocal space.
The data set was collected within a preset 2θ limit (usually $2\theta = 50°$) using conventional scans. Three, approximately orthogonal, standard reflections were

measured every one hour of exposure time, and were used to scale the data and correct for any variation in instrumental fluctuation or deterioration of the crystal. The same three standard reflections were measured every 100 reflections as a check for reorientation.

The reflection intensities were corrected for Lorentz and polarisation effects. Extinction effects were not significant and were not applied. Neutral atom scattering factors[19] were corrected for anomalous dispersion (Δf' and Δf''),[20] employing mass absorption coefficients.[20] Absorption corrections were applied where required using psi-scans or analytical correction methods.

Direct method routines were used for structure solution, which located the position of most of the non-hydrogen atoms. After initial phasing of Fourier maps, successive use of three dimensional Fourier maps were used to locate all of the remaining light, non-hydrogen atoms in the structure refinement. Full matrix refinement of the structures was carried out. All non-hydrogen atoms were refined with anisotropic temperature factors of the form, exp ($-2\pi^2$ [$h^2(a^*)^2U_{11} + k^2(b^*)^2U_{22} + l^2(c^*)^2U_{33} + 2hka^*b^*U_{12} + 2hla^*c^*U_{13} + 2klb^*c^*U_{23}$])

Refinements were against F^2, $\Sigma w \left| |F_o| - |F_c| \right|^2$, which was minimised using full least-squares methods using the weighting scheme given below. All parameter shifts were less than 0.001 σ at convergence. Residuals quoted are,

$$R_1 = \Sigma \left| |F_o| - |F_c| \right| / \Sigma |F_o|$$

$$wR_2 = [\Sigma w \left| |F_o|^2 - |F_c|^2 \right|^2 / \Sigma w |F_o^2|^2]^{1/2}$$

$$w = 1 / [\sigma^2(F_o)^2 + (aP)^2 + bP], \text{ where } P = [F_c^2 + \text{Max}(F_o^2, 0)]/3$$

$$s = [\Sigma \left| |F_o|^2 - |F_c|^2 \right| / (n-p)]^{1/2}$$

Computation for data collection, semi-empirical absorption correction, cell refinement, data reduction, structure solution and refinement was carried out using CAD4 Express,[21] WinGX,[22] XCAD4,[23] PsiScans,[24] SHELXS97,[25] and SHELXL97[25] program systems implemented on a PC running Windows 2000.

The cif files of all complexes including diagrams can be found in **Appendix B**. The number in parentheses is the least squares estimated standard deviation of the last digit.

X-SEED[26] and ORTEP3 for Windows[27] computer packages were used for the molecular structure and unit cell diagrams.

3.4.3 Experimental Procedures

Synthesis of $PdCl_2(pyCH_2SMe)$

$PdCl_2(NCMe)_2$ (0.10 g, 0.39 mmol) was added to a stirred solution of $pyCH_2SMe$ (64.4 mg, 0.46 mmol, 1.2 equiv.) in dry acetonitrile (25 mL), the yellow coloured suspension was stirred for 12 h at room temperature. The solvent was then reduced *in vacuo* to *ca.* 5 mL and Et_2O was added precipitating the title complex as yellow solid which was filtered and washed with Et_2O (0.11 g, 90%).

^{1}H NMR (299.9 MHz, 20 °C, $(CD_3)_2SO$): δ 9.10 (d, J = 6 Hz, 1H, py-H), 8.09 ("t", J = 7.8 Hz, 1H, py-H), 7.74 (d, J = 6 Hz, 1H, py-H), 7.56 ("t", J = 7.8 Hz, 1H, py-H), 4.80, 4.48 (AB spin system, J = 16.2 Hz, 2H, CH_2), 2.53 (s, 3H, S-CH_3); ***Anal.* Calcd. for $PdC_7H_9NSCl_2$:** C, 26.56; H, 2.87; N, 4.42; S, 10.13%. Found: C, 26.34; H, 2.76; N, 4.41; S, 10.22%. **LSIMS** ***m/z*** 281 $[M\text{-}Cl]^+$, $[^{12}C_7{}^1H_9{}^{35}Cl^{14}N^{32}S^{106}Pd$ 281]. **M.S. High res. Calcd for** "$[C_7H_9ClNSPd]^+$" = 279.91791 amu: **Found** M^+ = 279.91765 amu by LSIMS.

Synthesis of $PdCl_2(4\text{-}MepyCH_2SMe)$

This compound was prepared from $PdCl_2(NCMe)_2$ (0.10 g, 0.39 mmol) and 4-$MepyCH_2SMe$ (70.9 mg, 0.46 mmol, 1.2 equiv.) using a similar procedure to that described for $PdCl_2(pyCH_2SMe)$. The title complex was obtained as a yellow solid (0.11 g, 87%).

^{1}H NMR (299.9 MHz, 20 °C, $(CD_3)_2SO$): δ 8.92 (d, J = 6 Hz, 1H, py-H), 7.58 (s, py-H), 7.39 (d, J = 6, py-H), 4.74, 4.41 (AB spin system, J = 16.5 Hz, 2H, CH_2), 2.48 (s, 3H, C_4-CH_3), 2.37 (s, 3H, S-CH_3); ***Anal.* Calcd. for $PdC_8H_{11}NSCl_2$:** C, 29.07; H, 3.35; N, 4.24; S, 9.70%. Found: C, 29.25; H, 3.42; N, 4.29; S, 9.61%. **LSIMS** ***m/z*** 295 $[M\text{-}Cl]^+$, $[^{12}C_8{}^1H_{11}{}^{35}Cl^{14}N^{32}S^{106}Pd$ 295]. **M.S. High res. Calcd for** "$[PdC_8H_{11}NSCl]^+$" = 293.93356 amu: **Found** M^+ = 293.93378 amu by LSIMS.

Synthesis of $PdCl_2$(6-MepyCH_2SMe)

The compound was prepared from $PdCl_2(NCMe)_2$ (0.10 g, 0.39 mmol) and 6-MepyCH_2SMe (70.9 mg, 0.46 mmol, 1.2 equiv.) using a similar procedure to that described for $PdCl_2$(pyCH_2SMe). The title complex was obtained as a yellow solid (0.12 g, 95%).

^{1}H NMR (299.9 MHz, 20 °C, $(CD_3)_2SO$): δ 7.92 (br m, 1H, py-H), 7.57 (br m, 1H, py-H), 7.43 (br m, 1H, py-H), 4.72 (br s, 2H, CH_2), 3.06 (br s, 3H, C_6-CH_3), 2.26 (br s, 3H, S-CH_3) ppm; ***Anal.* Calcd. for $PdC_8H_{11}NSCl_2$:** C, 29.07; H, 3.35; N, 4.24; S, 9.70%. Found: C, 29.18; H, 3.38; N, 4.38; S, 9.45%.

Synthesis of PdCl(6-C_6H_4pyCH_2SMe)

The compound was prepared from $PdCl_2(NCMe)_2$ (0.10 g, 0.39 mmol) and 6-PhpyCH_2SMe (99.6 mg, 0.46 mmol, 1.2 equiv.) using a similar procedure to that described for $PdCl_2$(pyCH_2SMe). The title complex was obtained as a dark yellow solid (0.13 g, 94%).

^{1}H NMR (299.9 MHz, 20 °C, $(CD_3)_2SO$): δ 8.03 – 7.83 (m, 6H, Ar-H, both species), 7.61 – 7.58 (m, 2H, Ar-H, both species), 7.50 – 7.35 (br m, 6H, Ar-H, both species), 7.09 – 7.06 (m, 2H, Ar-H, both species), 4.58 (s, 2H, CH_2, major species), 3.83 (s, 2H, CH_2, minor species); ***Anal.* Calcd. for $PdC_{13}H_{12}NSCl$:** C, 43.84; H, 3.40; N, 3.93; S, 9.00%. Found: C, 43.75; H, 3.32; N, 3.86; S, 9.25%. **LSIMS *m/z*** 321 $[M\text{-}Cl]^+$, $[^{12}C_{13}{}^1H_{12}{}^{14}N^{32}S^{106}Pd$ 321]. **M.S. High res. Calcd for** "$[PdC_{13}H_{12}NS]^+$" = 319.97253 amu: **Found** M^+ = 319.97265 amu by LSIMS.

Synthesis of $PdCl_2$(pyCH_2SPh)

The compound was prepared from $PdCl_2(NCMe)_2$ (0.10 g, 0.39 mmol) and pyCH_2SPh (93.1 mg, 0.46 mmol, 1.2 equiv.) using a similar procedure to that described for $PdCl_2$(pyCH_2SMe). The title complex was obtained as a yellow solid (0.11 g, 78%).

^{1}H NMR (299.9 MHz, 20 °C, $(CD_3)_2SO$): δ 9.09 (br s, 1H, py-H), 8.09 (br s, py-H), 7.79 (br s, 2H, Ph-H), 7.52 (m, 4H, py-H, Ph-H), 5.35, 4.81 (AB spin system, J = 16.2 Hz, 2H, CH_2); ***Anal.* Calcd. for $PdC_{12}H_{11}NSeCl_2$:** C, 38.07; H, 2.93; N, 3.70%. Found: C, 37.95; H, 2.84; N, 3.65%. **LSIMS *m/z*** 343 $[M\text{-}Cl]^+$, $[^{12}C_{12}{}^1H_{11}{}^{35}Cl^{14}N^{32}S^{106}Pd$ 343]. **M.S. High res. Calcd for** "$[PdC_{12}H_{11}NSCl]^+$" = 341.93356 amu: **Found** M^+ = 341.93348 amu by LSIMS.

Synthesis of $PdCl_2$(4-MepyCH_2SPh)

The compound was prepared from $PdCl_2(NCMe)_2$ (0.10 g, 0.39 mmol) and 4-MepyCH_2SPh (99.6 mg, 0.46 mmol, 1.2 equiv.) using a similar procedure to that described for $PdCl_2$(pyCH_2SMe). The title complex was obtained as a yellow solid (0.15 g, 96%).

^{1}H NMR (299.9 MHz, 20 °C, $(CD_3)_2SO$): δ 8.91 (d, J = 6 Hz, 1H, py-H), 7.80 (d, J = 7.8 Hz, 2H, Ph-H), 7.58 (s, 1H, py-H), 7.47 (m, 3H, Ph-H), 7.38 (d, J = 6 Hz, 1H, py-H), 5.29, 4.69 (AB spin system, J = 17.4 Hz, 2H, CH_2) 2.35 (s, 3H, C_4-CH_3); ***Anal.* Calcd. for $PdC_{13}H_{13}NSCl_2$:** C, 39.77; H, 3.34; N, 3.57; S, 8.17%. Found: C, 39.90; H, 3.42; N, 3.63; S, 8.22%. **LSIMS *m/z*** 357 $[M\text{-}Cl]^+$, $[^{12}C_{13}{}^1H_{13}{}^{35}Cl^{14}N^{32}S^{106}Pd$ 357]. **M.S. High res. Calcd for** "$[PdC_{13}H_{13}NSCl]^+$" = 355.94921 amu: **Found** M^+ = 355.94932 amu by LSIMS.

Synthesis of $[PdCl_2$(6-MepyCH_2SPh)$]_3$

The compound was prepared from $PdCl_2(NCMe)_2$ (0.10 g, 0.39 mmol) and 4-MepyCH_2SPh (99.6 mg, 0.46 mmol, 1.2 equiv.) using a similar procedure to that described for $PdCl_2$(pyCH_2SMe). The title complex was obtained as a yellow solid (0.12 g, 81%).

^{1}H NMR (299.9 MHz, 20 °C, $(CD_3)_2SO$): δ 7.87 – 7.84 (m, 2H, py-H, both species), 7.59 – 7.53 (m, 2H, py-H, both species), 7.45 – 7.42 (m, 2H, py-H, both species), 7.35 – 7.15 (m, 10H, Ph-H, both species), 5.22 (br s, 1H, CH_2, major species), 4.26 (br s, 1H, CH_2, minor species), 3.23 (s, 6H, C_6-CH_3, both species);

***Anal.* Calcd. for $PdC_{13}H_{13}NSCl_2$:** C, 39.77; H, 3.34; N, 3.57; S, 8.17%. Found: C, 39.84; H, 3.38; N, 3.62; S, 8.28%.

Synthesis of PdCl(6-C_6H_4pyCH$_2$SPh)

The compound was prepared from $PdCl_2(NCMe)_2$ (0.10 g, 0.39 mmol) and 6-PhpyCH$_2$SPh (0.13 g, 0.46 mmol, 1.2 equiv.) using a similar procedure to that described for $PdCl_2$(pyCH$_2$SMe). The title complex was obtained as a dark yellow solid (0.15 g, 92%).

^{1}H NMR (299.9 MHz, 20 °C, $(CD_3)_2SO$): δ 8.02 – 7.93 (m, 4H, Ar-H, both species), 7.82 – 7.80 (m, 2H, Ar-H, both species), 7.74 (d, J = 7.2 Hz, 2H, Ar-H, both species), 7.61 – 7.59 (m, 2H, Ar-H, both species), 7.53 – 7.25 (br m, 12H, Ar-H, both species), 7.16 – 7.07 (m, 4H, Ar-H, both species), 5.05 (s, 2H, CH_2, major species), 4.39 (s, 1H, CH_2, minor species); ***Anal.* Calcd. for $PdC_{18}H_{14}NSCl$:** C, 51.69; H, 3.37; N, 3.35; S, 7.67%. Found: C, 51.58; H, 3.32; N, 3.30; S, 7.92%. **LSIMS *m/z*** 383 $[M\text{-}Cl]^+$, $[^{12}C_{18}{}^1H_{14}{}^{14}N^{32}S^{106}Pd$ 383]. **M.S. High res. Calcd for** "$[PdC_{18}H_{14}NS]^+$" = 381.98818 amu: **Found** M^+ = 381.98825 amu by LSIMS.

Synthesis of $PdCl_2$(pyCH$_2$SePh)

The compound was prepared from $PdCl_2(NCMe)_2$ (0.10 g, 0.39 mmol) and pyCH$_2$SePh (0.11 g, 0.46 mmol, 1.2 equiv.) using a similar procedure to that described for $PdCl_2$(pyCH$_2$SMe). The title complex was obtained as a dark yellow solid (0.14 g, 87%).

^{1}H NMR (299.9 MHz, 20 °C, $(CD_3)_2SO$): δ 9.17 (d, J = 5.4 Hz, 1H, py-H), 9.02 ("t", J = 7.8 Hz, py-H), 7.84 (d, J = 6.3 Hz, 2H, Ph-H), 7.66 (d, J = 5.4 Hz,1H, py-H), 7.46 (m, 4H, py-H, Ph-H), 5.22, 4.66 (AB spin system, J = 15.9 Hz, 2H, CH_2); ***Anal.* Calcd. for $PdC_{12}H_{11}NSeCl_2$:** C, 33.87; H, 2.61; N, 3.29%. Found: C, 33.67; H, 2.54; N, 3.18%. **LSIMS *m/z*** 390 $[M\text{-}Cl]^+$, $[^{12}C_{12}{}^1H_{11}{}^{35}Cl^{14}N^{79}Se^{106}Pd$ 390]. **M.S. High res. Calcd for** "$[PdC_{12}H_{11}NSeCl]^+$" = 389.87801 amu: **Found** M^+ = 389.87825 amu by LSIMS.

Synthesis of $PdCl_2$(4-MepyCH_2SePh)

The compound was prepared from $PdCl_2(NCMe)_2$ (0.10 g, 0.39 mmol) and 4-MepyCH_2SePh (0.12 g, 0.46 mmol, 1.2 equiv.) using a similar procedure to that described for $PdCl_2$(pyCH_2SMe). The title complex was obtained as a dark yellow solid (0.16 g, 92%).

^{1}H NMR (299.9 MHz, 20 °C, $(CD_3)_2SO$): δ 9.00 (d, J = 6 Hz, 1H, py-H), 7.85 ("t", J = 8.1 Hz, 2H, Ph-H), 7.50 (s, 1H, py-H), 7.44 (m, 3H, py-H, Ph-H), 7.33 (d, J = 6 Hz, 1H, py-H), 5.17, 4.57 (AB spin system, J = 15.9 Hz, 2H, CH_2), 2.31 (s, 3H, C_4-CH_3); ***Anal.* Calcd. for $PdC_{13}H_{13}NSeCl_2$:** C, 35.52; H, 2.98; N, 3.19%. Found: C, 35.38; H, 2.92; N, 3.12%. **LSIMS *m/z*** 404 $[M\text{-}Cl]^+$, $[^{12}C_{13}{}^1H_{13}{}^{35}Cl^{14}N^{79}Se^{106}Pd$ 404]. **M.S. High res. Calcd for** "$[PdC_{13}H_{13}NSeCl]^+$" = 403.89366 amu: **Found** M^+ = 403.89354 amu by LSIMS.

Synthesis of $[PdCl_2$(6-MepyCH_2SePh)$]_2$

The compound was prepared from $PdCl_2(NCMe)_2$ (0.10 g, 0.39 mmol) and 6-MepyCH_2SePh (0.12 g, 0.46 mmol, 1.2 equiv.) using a similar procedure to that described for $PdCl_2$(pyCH_2SMe). The title complex was obtained as a dark yellow solid (0.14 g, 80%).

^{1}H NMR (299.9 MHz, 20 °C, $(CD_3)_2SO$): δ 7.79 (br s, 2H, py-H, both species), 7.64 – 7.56 (br m, 6H, py-H, Ph-H, both species), 7.37 – 7.21 (br m, 8H, py-H, Ph-H, both species), 5.14 (br s, 2H, CH_2, major species), 4.27 (br s, 1H, CH_2, minor species), 3.19 (br s, 6H, C_6-CH_3, both species); ***Anal.* Calcd. for $PdC_{13}H_{13}NSeCl_2$:** C, 35.52; H, 2.98; N, 3.19%. Found: C, 35.59; H, 3.05; N, 3.24%. **LSIMS *m/z*** 404 $[M\text{-}Cl]^+$, $[^{12}C_{13}{}^1H_{13}{}^{35}Cl^{14}N^{79}Se^{106}Pd$ 404]. **M.S. High res. Calcd for** "$[PdC_{13}H_{13}NSeCl]^+$" = 403.89366 amu: **Found** M^+ = 403.89374 amu by LSIMS.

Synthesis of PdCl(6-C_6H_4pyCH_2SePh)

The compound was prepared from $PdCl_2(NCMe)_2$ (0.10 g, 0.39 mmol) and 6-PhpyCH$_2$SePh (0.15 g, 0.46 mmol, 1.2 equiv.) using a similar procedure to that

described for $PdCl_2(pyCH_2SMe)$. The title complex was obtained as an orange solid (0.17 g, 96%).

^{1}H NMR (299.9 MHz, 20 °C, $(CD_3)_2SO$): δ 7.97 – 7.95 (m, 2H, Ar-H, both species), 7.83 – 7.76 (m, 4H, Ar-H, both species), 7.54 – 7.52 (m, 4H, Ar-H, both species), 7.45 – 7.25 (br m, 12H, Ar-H), 7.10 – 7.08 (m, 2H, Ar-H, both species) 4.90 (s, 2H, CH_2, major species), 4.41 (s, 2H, CH_2, minor species); ***Anal.* Calcd. for $PdC_{18}H_{14}NSeCl$:** C, 46.48; H, 3.03; N, 3.01%. Found: C, 46.58; H, 3.10; N, 3.09%. **LSIMS *m/z*** 430 $[M\text{-}Cl]^+$, $[^{12}C_{18}{}^1H_{14}{}^{14}N^{79}Se^{106}Pd$ 430]. **M.S. High res. Calcd for** "$[PdC_{18}H_{14}NSe]^+$" = 429.93263 amu: **Found** M^+ = 429.93275 amu by LSIMS.

Synthesis of $PdI_2(6\text{-}MepyCH_2SPh)_2$

PdI_2 (0.10 g, 0.28 mmol) was added to a stirred solution of 6-$MepyCH_2SPh$ (71.7 mg, 0.33 mmol, 1.2 equiv.) in dry acetonitrile (25 mL), the dark coloured suspension was stirred for 12 h at room temperature. The solvent was then reduced *in vacuo* to *ca.* 5 mL and Et_2O was added precipitating the title complex as purple solid which was filtered and washed with Et_2O (0.19 g, 85%). Single crystals suitable for elemental analysis were grown from hot nitromethane.

^{1}H NMR (299.9 MHz, 20 °C, $(CD_3)_2SO$): δ 7.83 (m, 2H, py-H), 7.56 (m, 2H, py-H), 7.40 (m, 6H, Ar-H), 7.28 (m, 4H, Ar-H), 7.17 (m, 2H, py-H), 5.03 (br s, 4H, CH_2) 3.05 (s, 6H, C_6-CH_3); ***Anal.* Calcd. for $PdC_{26}H_{26}N_2S_2I_2$:** C, 39.49; H, 3.31; N, 3.54; S, 8.11%. Found: C, 39.58; H, 3.37; N, 3.62; S, 8.24%.

Synthesis of $PdI_2(pyCH_2SePh)$

The compound was prepared from PdI_2 (0.10 g, 0.28 mmol) and $pyCH_2SePh$ (82.6 mg, 0.33 mmol, 1.2 equiv.) using a similar procedure to that described for $PdCl_2(pyCH_2SMe)$. The title complex was obtained as an orange solid (0.16 g, 92%).

^{1}H NMR (299.9 MHz, 20 °C, $(CD_3)_2SO$): δ 9.57 (d, J = 7.2 Hz, 1H, py-H), 7.99 (t, J = 7.2 Hz, py-H), 7.77 (m, 3H, py-H, Ar-H), 7.42 (m, 5H, py-H, Ar-H), 5.05 (br d, 2H, CH_2); ***Anal.* Calcd. for $PdC_{12}H_{11}NSeI_2$:** C, 23.69; H, 1.82; N, 2.30%. Found: C, 23.42; H, 1.67; N, 2.22%. **LSIMS *m/z*** 481 $[M\text{-}I]^+$, $[^{12}C_{12}{}^1H_{11}{}^{126}I^{14}N^{79}Se^{106}Pd$

481]. **M.S. High res. Calcd for** "$[PdC_{12}H_{11}NSeI]^+$" = 481.81362 amu: **Found** M^+ = 481.81312 amu by LSIMS.

Synthesis of $PtCl_2$(4-MepyCH_2SMe)

$PtCl_2$ (0.10 g, 0.38 mmol) was added to a stirred solution of 4-MepyCH_2SMe (69.1 mg, 0.45 mmol, 1.2 equiv.) in dry acetonitrile (30 mL), the yellow coloured suspension was stirred for 12 h at room temperature. The solvent was then reduced *in vacuo* to *ca.* 5 mL and Et_2O was added precipitating the title complex as yellow solid which was filtered and washed with Et_2O (0.23 g, 87%).

^{1}H NMR (299.9 MHz, 20 °C, $(CD_3)_2SO$): δ 9.21 (d, J = 6 Hz, 1H, py-H), 7.67 (s, 1H, py-H), 7.38 (d, J = 6 Hz, 1H, py-H), 4.70, 4.40 (AB spin system, J = 16.8 Hz, 2H, CH_2), 2.45 (s, 3H, C_4-CH_3), 2.32 (s, 3H, S-CH_3); ***Anal.* Calcd. for $PtC_8H_{11}NSCl_2$:** C, 22.92; H, 2.64; N, 3.34; S, 7.65%. Found: C, 22.81; H, 2.59; N, 3.44; S, 7.81%. **LSIMS *m/z*** 384 $[M\text{-}Cl]^+$, $[^{12}C_8{}^1H_{11}{}^{35}Cl^{14}N^{32}S^{195}Pt$ 384]. **M.S. High res. Calcd for** "$[PtC_8H_{11}NSCl]^+$" = 382.99485 amu: **Found** M^+ = 382.99474 amu by LSIMS.

Synthesis of $PtCl_2$(6-MepyCH_2SMe)

The compound was prepared from $PtCl_2$ (0.10 g, 0.38 mmol) and 6-MepyCH_2SMe (69.1 mg, 0.45 mmol, 1.2 equiv.) using a similar procedure to that described for $PtCl_2$(4-MepyCH_2SMe). The title complex was obtained as a pale yellow solid (0.12 g, 78%).

^{1}H NMR (299.9 MHz, 20 °C, $(CD_3)_2SO$): δ 7.71 ("t", J = 7.5 Hz, 1H, py-H), 7.29 (d, J = 6 Hz, 1H, py-H), 7.15 (d, J = 6 Hz, 1H, py-H), 4.81, 4.65 (AB spin system, J = 14.7 Hz, 2H, CH_2), 3.18 (s, 3H, C_6-CH_3), 2.52 (s, 3H, S-CH_3); ***Anal.* Calcd. for $PtC_8H_{11}NSCl_2$:** C, 22.92; H, 2.64; N, 3.34; S, 7.65%. Found: C, 22.81; H, 2.59; N, 3.44; S, 7.81%. **LSIMS *m/z*** 384 $[M\text{-}Cl]^+$, $[^{12}C_8{}^1H_{11}{}^{35}Cl^{14}N^{32}S^{195}Pt$ 384]. **M.S. High res. Calcd for** "$[PtC_8H_{11}NSCl]^+$" = 382.99485 amu: **Found** M^+ = 382.99474 amu by LSIMS.

Synthesis of $PtCl_2$(6-MepyCH_2SPh)

The compound was prepared from $PtCl_2$ (0.10 g, 0.38 mmol) and 6-PhpyCH_2SPh (0.13 g, 0.45 mmol, 1.2 equiv.) using a similar procedure to that described for $PtCl_2$(4-MepyCH_2SMe). The title complex was obtained as a pale yellow solid (0.17 g, 82%).

^{1}H NMR (299.9 MHz, 20 °C, $(CD_3)_2SO$): δ 7.87–7.28 (br m, 8H, py-H, Ar-H), 5.20 (br s, 2H, CH_2), 3.20 (s, 3H, C_6-CH_3); ***Anal.* Calcd. for $PtC_{18}H_{15}NSCl_2$:** C, 32.44; H, 2.72; N, 2.91; S, 6.66%. Found: C, 32.48; H, 2.79; N, 2.98; S, 6.74%. **LSIMS *m/z*** 446 $[M\text{-}Cl]^+$, $[^{12}C_{13}{}^1H_{13}{}^{35}Cl^{14}N^{32}S^{195}Pt$ 446]. **M.S. High res. Calcd for** "$[PtC_{18}H_{15}NSCl]^+$" = 445.01050 amu: **Found** M^+ = 445.01054 amu by LSIMS.

Synthesis of $PtCl_2$(pyCH_2SePh)

The compound was prepared from $PtCl_2$ (0.10 g, 0.38 mmol) and 4-MepyCH_2SePh (0.11 g, 0.45 mmol, 1.2 equiv.) using a similar procedure to that described for $PtCl_2$(4-MepyCH_2SMe). The title complex was obtained as a yellow solid (0.18 g, 91%).

^{1}H NMR (299.9 MHz, 20 °C, $(CD_3)_2SO$): δ 9.46 (d, J = 6 Hz, 1H, py-H), 8.06 ("t", J = 6 Hz, py-H), 7.75 (m, 3H, py-H, Ar-H), 7.40 (m, 4H, py-H, Ar-H), 5.05, 4.65 (AB spin system, J = 15.3 Hz, 2H, CH_2); ***Anal.* Calcd. for $PtC_{12}H_{11}NSeCl_2$:** C, 28.03; H, 2.16; N, 2.72%. Found: C, 27.95; H, 2.09; N, 2.65%. **LSIMS *m/z*** 479 $[M\text{-}Cl]^+$, $[^{12}C_{12}{}^1H_{11}{}^{35}Cl^{14}N^{79}Se^{195}Pt$ 479]. **M.S. High res. Calcd for** "$[PtC_{12}H_{11}NSeCl]^+$" = 478.93930 amu: **Found** M^+ = 478.93921 amu by LSIMS.

Synthesis of $PtCl_2$(4-MepyCH_2SePh)

The compound was prepared from $PtCl_2$ (0.10 g, 0.38 mmol) and 4-MepyCH_2SePh (0.12 g, 0.45 mmol, 1.2 equiv.) using a similar procedure to that described for $PtCl_2$(4-MepyCH_2SMe). The title complex was obtained as a yellow solid (0.16 g, 82%).

^{1}H NMR (299.9 MHz, 20 °C, $(CD_3)_2SO$): δ 9.28 (d, J = 6 Hz, 1H, py-H), 7.78 (m, 2H, Ph-H), 7.55 (br s, 1H, py-H), 7.41 (m, 3H, Ph-H), 7.31 (d, J = 6 Hz, 1H, py-H),

5.01, 4.56 (AB spin system, J = 15.6 Hz, 2H, CH_2), 2.06 (s, 3H, C_4-CH_3); ***Anal.* Calcd. for $PtC_{13}H_{13}NSeCl_2$:** C, 29.56; H, 2.48; N, 2.65%. Found: C, 29.64; H, 2.57; N, 2.61%. **LSIMS** ***m/z*** 493 $[M\text{-}Cl]^+$, $[^{12}C_{13}{}^{1}H_{13}{}^{35}Cl^{14}N^{79}Se^{195}Pt$ 493]. **M.S. High res. Calcd for** "$[PtC_{13}H_{13}NSeCl]^+$" = 492.95495 amu: **Found** M^+ = 492.95457 amu by LSIMS.

3.4 References

1. Canovese, L.; Chessa, G.; Vistentin, F.; Uguagliati P. *Coord. Chem. Rev.* **2004**, *248*, 945.
2. Canovese, L.; Visentin, F.; Uguagliati, P.; Chessa, G.; Lucchini, V.; Bandoli, G. *Inorg. Chim. Acta* **1998**, *275-276*, 385.
3. Canovese, L.; Visentin, F.; Uguagliati, P.; Chessa, G.; Pesce, A. *J. Organomet. Chem.* **1998**, *566*, 61.
4. Canovese, L.; Visentin, F.; Santo, C.; Chessa, G.; Uguagliati, P. *Polyhedron*, **2001**, *20*, 3171.
5. Canovese, L.; Visentin, F.; Chessa, G.; Uguagliati, P.; Dolmella, A. *J. Organomet. Chem.* **2000**, *601*, 1.
6. Canovese, L.; Visentin, F.; Chessa, G.; Santo, C.; Uguagliati, P.; Maini, L.; Polito, M. *Dalton Trans.* **2002**, 3696.
7. Canovese, L.; Lucchini, V.; Santo, C.; Visentin, F.; Zambon, A. *J. Organomet. Chem.* **2002**, *642*, 58.
8. Canovese, L.; Visentin, F.; Chessa, G.; Uguagliati, P.; Bandoli, G. *Organometallics*, **2000**, *19*, 1461.
9. Canovese, L.; Visentin, F.; Chessa, G.; Santo, C.; Uguagliati, P.; Bandoli, G. *J. Organomet. Chem.* **2002**, *650*, 43.
10. Canovese, L.; Chessa, G.; Santo, C.; Visentin, F.; Uguagliati, P. *Inorg. Chim. Acta* **2003**, *346*, 158.
11. Canovese, L.; Visentin, F.; Chessa, G.; Uguagliati, P.; Santo, C.; Dolmella, A. *Organometallics*, **2005**, *24*, 3297.
12. Jones, R. C.; Madden, R. L.; Skelton, B. W.; Tolhurst, V.-A.; White, A. H.; Williams, A. M.; Yates, B. F. *Eur. J. Inorg. Chem.* **2005**, 1048.
13. Oberbeckmann-Winter, N.; Morise, X.; Braunstein, P.; Welter, R. *Inorg. Chem.* **2005**, *44*, 1391.

14. Kloetzing, R. J.; Knochel, P. *Tetrahedron: Asymmetry* **2006**, *17*, 116.
15. Bader, A.; Linder, E, *Coord. Chem. Rev.* **1991**, *108*, 27.
16. Jones, R. C.; Skelton, B. W.; Tolhurst, V.-A.; White, A. H.; Wilson, A. J.; Canty, A. J. *Polyhedron*, **2007**, *26*, 708.
17. Canty, A. J.; Dedieu, A.; jin, H.; Milet, A.; Skelton, B. W.; Trofimenko, S.; White, A. H. *Inorg. Chim. Acta* **1999**, *287*, 27.
18. Chattopadhyay, S.; Sinha, C.; Basu, P.; Chakravorty, A. *Organometallics*, **1991**, *10*, 1135.
19. *International Tables for Crystallography*, Hahn, Ed., Kluwer Academic Publishers, Dordrecht, The Netherlands, **1995**.
20. Cromer, D. T.; Liberman, D. *J. Chem. Phys.*, **1970**, *53*, 1891.
21. *CAD4 Express Software*, **1994**, Enraf-Nonius, Delft, The Netherlands.
22. Farrugia, L. J. *J. Appl. Crystallogr.* **1999**, *32*, 837.
23. Harms K.; Wocadlo, S. *XCAD4, CAD4 Data Reduction*, University of Marburg, **1995**.
24. North, A. C. T.; Phillips, D. C. Mathews, F. S. *Acta. Crystallogr. Sect A* **1968**, *24*, 351.
25. Sheldrick G.M., *Shelx97, Programs for Crystal Structure Analysis,* University of Göttingen, **1997**.
26. Barbour, L. J. *X-Seed - A Software Tool for Supramolecular Crystallography, J. Supramol. Chem.* **2001**, *1*, 189.
27. Farrugia, L. J. *J. Appl. Crystallogr.* **1997**, *30*, 565.

Chapter Four

Complexes of *N,E*-Heteroleptic Ligands as Precatalysts in Heck and Suzuki Reactions

4.1 Introduction

The catalytic activity of palladium(II) complexes containing heteroleptic ligands synthesised in this study was assessed for Heck (**Scheme 4.1**) and Suzuki (**Scheme 4.2**) coupling reactions.

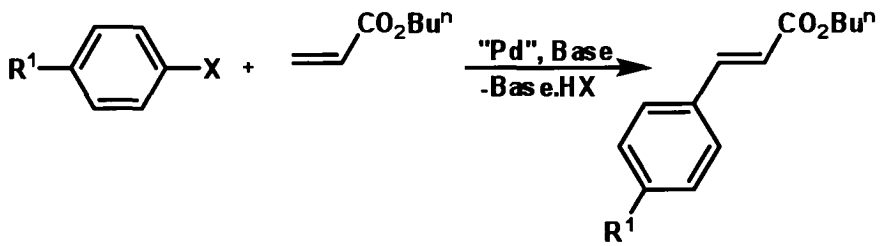

Scheme 4.1 The Heck coupling reaction.

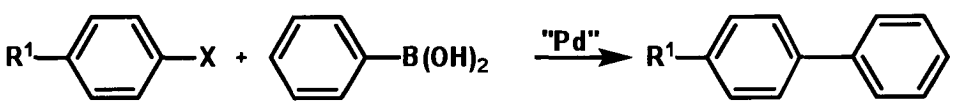

Scheme 4.2 The Suzuki coupling reaction.

Preliminary testing of $PdCl_2(pyCH_2SPh)$ as a precatalyst in the Heck reaction of aryl bromides and *n*-butyl acrylate provided an indication of possible high yields and TONs for this class of complex, with a >99% yield and 1,000,000 TON achieved for 4-bromoacetophenone, and a 94% yield and 94 TON achieved for 4-bromotoluene.[1]

In the present study, the aryl halide 4-bromotoluene was chosen as a substrate for testing as it is a deactivated aryl bromide and does not readily react in coupling protocols, making it a suitable for comparisons of catalytic activity. Similarly, *n*-butyl acrylate was chosen as a non-activated alkene. A more comprehensive

discussion of the effects of aryl halide and alkene on reactivity of the Heck reaction is provided in **Chapter 1, Section 1.5.3**.

A comparison of Heck reaction catalytic activity of all dichloropalladium(II) and cyclopalladated complexes described in Chapter 3 is reported here. The complex achieving the highest yield of product at the lowest catalyst loading is assumed to be the best precatalyst. This "optimised" catalyst was then tested in further Heck and Suzuki reactions using various aryl halides.

4.2 Results and Discussion

4.2.1 The Heck Reaction

Conditions that are typically used in the Heck reaction focus on four key elements: the addition of a phase transfer reagent, the choice of base, a reducing agent and temperature.

Phase transfer reagent

The rates of some steps in the catalytic cycle of the Heck reaction can be increased by the addition of additives. Halides, acetate anions and other negatively charged species have been found to increase the rate of the oxidative addition step in some systems by increasing the electron density on the palladium atom *via* the formation of an electron rich anionic zerovalent palladium species.[2] In particular, tetraalkylammonium salts have been highly successful in enhancing the reactivity and selectivity of inter- and intramolecular Heck-type reactions.[3-5]

The tetraalkylammonium salts Bu^n_4NBr and Bu^n_4NCl have been extensively used in the Heck reaction[6-8] and, in addition to providing anions, may act as a phase transfer agent between the solid salts (base, reducing agent) and the solvent.[9] The use of tetraalkylammonium salts in the Heck reaction was extensively developed by Jeffery, leading to widespread adoption of "Jeffery's conditions".[5,7,10-12] Jeffery showed that tetraalkylammonium salts can have a high accelerating effect on the Heck reaction, particularly in combination with alkali metal carbonate or acetate bases, but strictly anhydrous conditions in a highly polar solvent are required for achieving the best

yields.[7] Subsequently, Jeffery found that the effect of tetraalkylammonium salts is mainly dependent upon the quaternary ammonium cation rather than the corresponding anionic component.[7] However, Bräse and de Meijere have shown that Bu^n_4NCl gives the best conversion out of three different ammonium salts tested (Bu^n_4NCl, Bu^n_4NBr and $Bu^n_4NHSO_4$), particularly in phosphine-free conditions where the chloride anion may also act as a supporting ligand for the Pd(0) catalyst.[13]

Solvent

The choice of solvent can be system dependent; however most systems require a highly polar solvent for a successful Heck reaction to occur. Typical solvents or solvent systems reported in the literature are dimethylformamide (DMF), *N,N*-dimethylacetamide (DMA), or 1,4-dioxane; with DMF and DMA being most common. DMA was used successfully as a solvent for preliminary studies of $PdCl_2(pyCH_2SPh)$ as a precatalyst for the Heck reaction[1] and was also adopted for the present investigation without further optimisation.

Base

There are many different choices of base available for use in the Heck reaction, with amines and metal carbonates or acetates being most common.[9] The choice of base can be crucial in increasing stereoselectivity of the products (if required) with results mainly dependent on the catalytic system being used, particularly if used in combination with a tetraalkylammonium salt. Previous research in our group has shown that the addition of Na_2CO_3 to a Heck reaction involving the $pyCH_2SPh$ ligand increases the level of conversion of the aryl halide to product, while NaOAc was found to increase the level of stereoselectivity of the products.[1] Thus, Na_2CO_3 is the base of choice for the present study as reactions where stereoselectivity may be important were not examined.

Reducing agent

Induction periods in the Heck reaction may be prolonged unless a reducing agent is added.[14] The reducing agent is assumed to reduce the Pd(II) precatalyst to the active Pd(0) species. Typical reducing reagents used in the Heck reaction include sodium

formate[14,15] and hydrazine.[15] For simplicity and technical feasibility, solid sodium formate was used in this study.

Temperature

The choice of temperature is system dependent with some catalysts requiring high temperatures (>140 °C) for complete conversion, particularly in the case of deactivated aryl bromides and chlorides.[9,16] In previous studies of the catalytic properties of $PdCl_2(pyCH_2SPh)$ in the Heck reaction, good conversion of an activated aryl bromide (4-bromoacetophenone) was achieved at 100 °C and for a deactivated aryl bromide (4-bromotoluene) at 120 °C.[1] Thus, 120 °C was chosen as the minimum temperature likely to yield useful comparisons of precatalysts.

In summary, the conditions used in this study for the Heck reaction were as follows: NaO_2CH, Bu^n_4NCl, Na_2CO_3, in anhydrous DMAc under argon at 120 °C for 48 h.

4.2.2 Determination of the Best Precatalyst for the Heck Reaction

Before any catalytic testing was conducted, blank experiments were undertaken in which the respective substrates in both coupling reactions were tested without the presence of palladium. No reactivity was observed, **Scheme 4.3**.

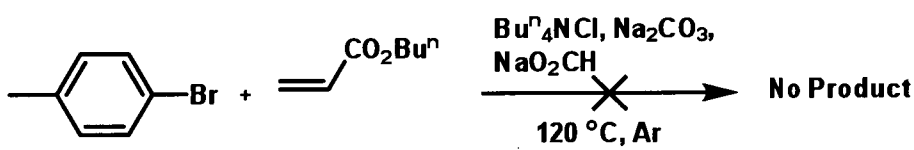

Scheme 4.3 Heck reaction blank testing.

The results of the catalytic testing of the palladium(II) complexes at 1 mol% catalyst loading in the reaction of 4-bromotoluene and *n*-butyl acrylate are shown in **Table 4.1**.

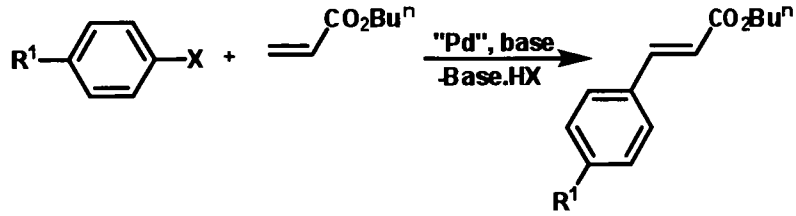

The thiomethyl and thiophenyl containing complexes (entries 1 – 6) and cyclometallated complexes (11 and 12) display high yield, unlike the selenophenyl substituted compounds (entries 8 – 10 and 13) which show little to no activity in the coupling reaction.

Entry	X	R^1	R^2	Precatalyst Used	Yield[a]	TON
1	Br	Me	H	$PdCl_2(pyCH_2SMe)$	100	100
2	Br	Me	H	$PdCl_2(4\text{-}MepyCH_2SMe)$	100	100
3	Br	Me	H	$PdCl_2(6\text{-}MepyCH_2SMe)$	97	97
4	Br	Me	H	$PdCl_2(pyCH_2SPh)$	90	90
5	Br	Me	H	$PdCl_2(4\text{-}MepyCH_2SPh)$	83	83
6	Br	Me	H	$PdCl_2(6\text{-}MepyCH_2SPh)$	79	79
8	Br	Me	H	$PdCl_2(pyCH_2SePh)$	~0.5	~0.5
9	Br	Me	H	$PdCl_2(4\text{-}MepyCH_2SePh)$	1	1
10	Br	Me	H	$PdCl_2(6\text{-}MepyCH_2SePh)$	0	0
11	Br	Me	H	$PdCl(6\text{-}C_6H_4pyCH_2SMe)$	100	100
12	Br	Me	H	$PdCl(6\text{-}C_6H_4pyCH_2SPh)$	100	100
13	Br	Me	H	$PdCl(6\text{-}C_6H_4pyCH_2SePh)$	32	32

All reactions were carried out with 1.5 mmol of aryl halide, 4.0 mmol of alkene, 3.0 mmol of Na_2CO_3, 2.25 mmol of Bu^n_4NCl, 1.65 mmol of NaO_2CH, in 5 mL of DMAc at 120 °C for 48 h. **[a]** determined by GC (diphenyl ether standard).

Table 4.1 Results of catalytic testing in the Heck reaction with a 1.0 mol% catalyst loading for all complexes.

In order to confirm the trend in activity 1 – 3 > 4 – 6 in **Table 4.1**, and to detect any differences in activity between 1 – 3, 11, 12, catalysis was examined at a lower mol% precatalyst loading (0.1) followed by 0.01 mol% for $pyCH_2SMe$ and 4-$MepyCH_2SMe$ as ligands, **Table 4.2**.

(a) 0.1 mol% precatalyst

Entry	X	R^1	R^2	Precatalyst Used	Yield[a]	TON
1	Br	Me	H	$PdCl_2(pyCH_2SMe)$	100	1,000
2	Br	Me	H	$PdCl_2(4\text{-}MepyCH_2SMe)$	100	1,000
3	Br	Me	H	$PdCl_2(6\text{-}MepyCH_2SMe)$	78	780
4	Br	Me	H	$PdCl_2(pyCH_2SPh)$	74	740
5	Br	Me	H	$PdCl_2(4\text{-}MepyCH_2SPh)$	65	650
6	Br	Me	H	$PdCl_2(6\text{-}MepyCH_2SPh)$	11	110
7	Br	Me	H	$PdCl(6\text{-}C_6H_4pyCH_2SMe)$	67	670
8	Br	Me	H	$PdCl(6\text{-}C_6H_4pyCH_2SPh)$	85	854

(b) 0.01 mol% precatalyst

Entry	X	R^1	R^2	Precatalyst Used	Yield[a]	TON
10	Br	Me	H	$PdCl_2(pyCH_2SMe)$	100	10,000
11	Br	Me	H	$PdCl_2(4\text{-}MepyCH_2SMe)$	92	9,200

All reactions were carried out with 1.5 mmol of aryl halide, 4.0 mmol of alkene, 3.0 mmol of Na_2CO_3, 2.25 mmol of Bu^n_4NCl, 1.65 mmol of NaO_2CH, in 5 mL of DMAc at 120 °C for 48 h. **[a]** determined by GC (diphenyl ether standard).

Table 4.2 Results of catalytic testing in the Heck reaction of all thioether and cyclometallated compounds with loadings of 0.1 mol% (**a**) and 0.01 mol% (**b**).

Entries 3 – 6 in **Table 4.2** confirm the trend noted for these entries in **Table 4.1**. Substitution by a methyl group at the 6-position (with different precatalyst structure, **Section 3.2.3.4**) results in a reduction in activity (1 > 3; 4 > 6), replacement of –SMe by –SPh results in a reduction in activity (1 > 4; 2 > 5; 3 > 6), and cyclometallation also leads to lower activity (7, 8).

The results indicate that the unsubstituted thiomethyl containing precatalyst $PdCl_2(pyCH_2SMe)$ (entries 1, 10 in **Table 4.2**) has the highest catalytic activity.

4.2.3 Catalytic Testing of $PdCl_2(pyCH_2SMe)$ in the Heck Reaction Using a Range of Aryl Halides and Alkenes

The precatalyst $PdCl_2(pyCH_2SMe)$ was highly effective in the Heck reaction of both activated and deactivated aryl iodides and bromides, **Table 4.3**. High yields of cinnamate products (>97%) were achieved using aryl iodides and the activated aryl bromide 4-bromoacetophenone (entries 1 – 5), with each coupling product being formed with TONs equal or close to 1,000,000 in each case. These values compare well with results obtained by Tu utilising bis-(benzimidazolylidene) pincer complexes (TONs ranging from 270,000 – 938,000 for similar substrates such as bromobenzene, 4-iodoanisole, iodobenzene, and 4-iodoacetophenone),[17] but are nearly an order of magnitude less than that obtained by Herrmann using mixed phosphine carbene complexes (TONs of 6,200,000 for 4-bromoacetophenone).[18] Good TONs were obtained for bromobenzene and 4-bromotoluene (6 and 7), matching, or bettering values obtained by Cui using hemilabile quinoline-8-carboxylate ligated complexes under similar conditions (TONs of 45,500 for bromobenzene and 44,000 for 4-bromotoluene).[19] In the case of 4-bromoanisole (8) the TON obtained is less than that obtained by Cui (36,500)[19] but an order of magnitude greater than those obtained by Herrmann (520 – 860 using mixed phosphorus carbene complexes).[18] In the case of aryl chlorides (9 and 10), however the complex showed little to no activity, giving low yields for the activated aryl chloride 4-chloroacetophenone (9).

Yields of the tri-substituted alkene product utilising iodo- and bromobenzene in the Heck reaction with *n*-butylcinnamate are good, with a regioselectivity of >99% (11 and 12), indicating the possibility of achieving high TONs for sterically hindered internal alkenes.

The TONs obtained for all aryl iodides and bromides in this study are much lower than observed for the best phosphine-free Pd catalysts currently available (*e.g.*, Pd pincers and Pd NHC complexes),[20-23] by a factor of 30 in the case of 4-bromoanisole, but are sufficient for synthesis. Both activated and deactivated aryl bromides could efficiently be converted to the desired products in high yields using $PdCl_2(pyCH_2SMe)$ as a precatalyst, with TONs in most cases being in the order of or greater than 10^4. The results indicate that $PdCl_2(pyCH_2SMe)$ can be considered as a

simple, yet efficient, phosphine-free precatalyst for many Heck-type reactions of both activated and deactivated aryl iodides and, more importantly, aryl bromides.

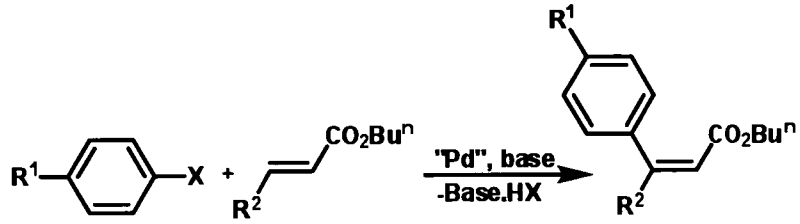

Entry	X	R^1	R^2	Yield[a]	TON	Precatalyst Loading (mol %)
1	I	COMe	H	100	1,000,000	0.0001
2	I	H	H	100	1,000,000	0.0001
3	I	Me	H	99	987,000	0.0001
4	I	OMe	H	97	978,000	0.0001
5	Br	COMe	H	100	1,000,000	0.0001
6	Br	H	H	36	365,000	0.0001
7	Br	Me	H	43	44,000	0.001
8	Br	OMe	H	58	6,000	0.01
9	Cl	COMe	H	13	13	1
10	Cl	H	H	<1	<1	1
11	I	H	Ph	93	93,000	0.001
12	Br	H	Ph	47	47,000	0.001

All reactions were carried out with 1.5 mmol of aryl halide, 4.0 mmol of alkene, 3.0 mmol of Na_2CO_3, 2.25 mmol of $^nBu_4NCl$, 1.65 mmol of NaO_2CH, in 5 mL of DMAc at 120 °C for 48 h. [a] determined by GC (diphenyl ether standard).

Table 4.3 Results of catalytic testing in the Heck reaction of $PdCl_2(pyCH_2SMe)$ with various aryl halides and alkenes, and mol% precatalyst.

4.2.4 Catalytic Testing of $PdCl_2(pyCH_2SMe)$ in the Heck Reaction Using Bu^n_4NCl as a Solvent

The use of non-aqueous ionic liquids (NAILs) has been a relatively recent development in Heck chemistry, including aryl chloride coupling.[24] The application of molten salts was first reported by Kaufmann in the vinylation of aryl halides using

$Pd(OAc)_2$ and other simple precatalysts.[25] Herrmann significantly developed their use in the Heck reaction.[26] NAILs are defined as liquid electrolytes composed entirely of ions,[24] most contain an organic cation and an inorganic anion. The most commonly used cations are alkylammonium, alkylphosphonium, *N,N'*-dialkylimidazolium, and *N*-alkylpyridinium species, while inorganic anions are typically halides.[24]

NAILs can allow an enhanced stability of organometallic reagents and catalytic species, they possess excellent chemical and thermal stability, and are typically non-flammable.[27] Furthermore, the volatile components of the reaction can be removed by distillation. Thus the entire catalyst containing melt can be recycled,[9] reducing environmental issues associated with metal leaching.[14] However, other products remain, in particular halide ions and cations.

Herrmann has reported the successful coupling of bromo- and chloroarenes with styrene utilising Bu^n_4NBr as a solvent and phosphapalladacycles as precatalysts,[26] and most of the results obtained in an ionic solution of Bu^n_4NBr were considerably better than those obtained with the same reaction under similar conditions using solvents such as DMF and DMA.[28] Herrmann documented the first coupling of chlorobenzene and styrene, in 86% yield, in only two hours in the presence of 2 mol% of $Pd_2(dba)_3/2P(Bu^t)_3$ (where dba = dibenzylideneacetone) in an ionic solution of Bu^n_4NBr; DMF as the solvent resulted in a 56% yield in two hours.[28] The mechanism of the Heck reaction in NAILs remains unclear.[27]

The activity of $PdCl_2(pyCH_2SMe)$ in the Heck reaction of both activated and deactivated aryl chlorides with *n*-butyl acrylate using the NAIL solvent Bu^n_4NCl was investigated, **Table 4.4**.

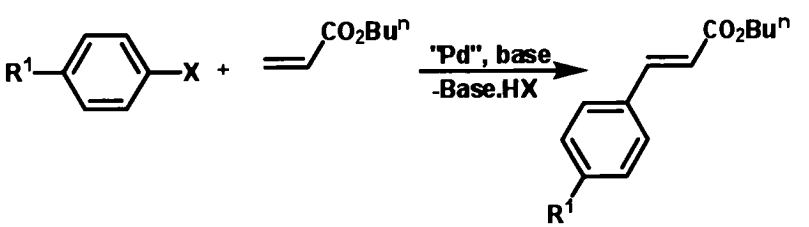

Entry	X	R^1	Yield[a]	TON
1	Cl	COMe	100	100
2	Cl	H	87	87
3	Cl	Me	9	9

All reactions were carried out with 1.5 mmol of aryl halide, 4.0 mmol of alkene, 3.0 mmol of Na_2CO_3, 1.65 mmol of NaOC(O)H, in 2.48 g of Bu^n_4NCl under Ar at 120 °C for 48 h. [a] determined by GC (diphenyl ether standard).

Table 4.4 Results of catalytic testing of $PdCl_2(pyCH_2SMe)$ (1 mol%) in the Heck reaction of various aryl chlorides in the non-aqueous ionic liquid Bu^n_4NCl.

The complex $PdCl_2(pyCH_2SMe)$ was found to facilitate the reaction between 4-chloroacetophenone and chlorobenzene (entries 1 and 2) with *n*-butyl acrylate in high yield, with results obtained for both reactions in Bu^n_4NCl higher than that obtained under the same conditions using *N,N*-dimethylacetamide. This is an excellent result, with turnover numbers greater than that achieved by Wang using a $Pd(OAc)_2$ precatalyst in a poly(ethylene glycol)imidazolium chloride melt (TONs of 16 for 4-chloroacetophenone, and 5 for chlorobenzene in the Heck reaction with *n*-ethyl acrylate)[29] but are less than those obtained by Herrmann using phosphapalladacycles as catalysts in Bu^n_4NBr (TONs of 990 for 4-chloroacetophenone and 390 for chlorobenzene), although these reactions were studied at 150 °C using styrene as the alkene.[26] The reaction of 4-chlorotoluene with *n*-butyl acrylate (3) resulted in a 9% yield of product. Although this is a poor conversion, 4-chlorotoluene is a deactivated aryl chloride and difficult to facilitate in Heck reactions. However, Zapf and Beller have achieved a 65% conversion of 4-chlorotoluene in the reaction with styrene in a Bu^n_4NBr melt.[30]

4.2.5 Discussion of Heck Catalysis Results

The nature of the active catalyst in the Heck reactions in this study is not fully understood, *e.g.*, the reaction may follow a "molecular" mechanism as described in **Chapter 1**,[31] or it may involve palladium nanoparticles, for example, depending upon the nature of the precatalyst and conditions. Recently, the formation of nanoparticles has been often suggested to occur at temperatures >120 °C in the Heck reaction, irrespective of the nature of the precatalyst used.[32] The nature of the "true"

active catalyst was not comprehensively investigated in this study due to the difficulty in the experimental detection of palladium nanoparticles. Tests used for their identification, such as the addition of mercury, often give inconclusive results.[33] The presence of nanoparticles can be achieved by transmission electron microscope (TEM) imaging of a completed reaction solution, but equipment required for this type of investigation was not available.

In the case of the 6-phenyl substituted ligands, leading to cyclopalladated complexes used as precatalysts, formation of nanoparticles is likely, with many reports in the literature observing that such species act as reservoirs of palladium metal present as nanoparticles during catalysis.[34-39]

6-Methyl substitution of the pyridyl ring gave chelated monomers, dimeric and trimeric dichloropalladium(II) complexes and thus their catalytic activity is addressed separately.

If a "molecular" mechanism is followed for the complexes of ligands that are known to afford monomeric, chelated precatalysts, with the additional possibility of hemilability as a component of the mechanism (*i.e.*, according to **Scheme 1.11** and **Scheme 1.12 (a)** in **Chapter 1**), then possible interpretations of the catalytic results can be considered in relation to the factors observed to have major effects on activity. Also, when nanoparticles are involved, it is likely that individual Pd atoms are involved in cycles such as **Schemes 1.11** and **1.12 (a)** in most cases, possibly via oxidation of surface atoms by the aryl halide substrate.[32]

For the purposes of this discussion the term "molecular" means coordination (e.g. monodentate, bidentate, or both) by the *N,E* ligand during the catalytic cycle, to distinguish this from complexes which have no involvement of ligands except for the organic reactants, solvent, and inorganic ligands such as halides during reaction steps. In the case of the 6-substituted complexes reduction of precatalysts to Pd(0) means that the dimeric, trimeric, and palladacycle structures are not highly relevant to the reaction mechanism. However, the solid state structures have illustrated that a substituent at the 6-position of the pyridyl ring, illustrated clearly in the case of a 6-Me substituent, has steric effects on the coordination geometry of the Pd(II) species. This may have an effect on mechanism involving Pd(0) and Pd(II) intermediates, in

particular for Pd(0) and aryl bromide and chloride substrates if Pd(0) atoms are released from nanoparticles prior to oxidation as the oxidative addition step of the catalytic cycle is highly likely to be the rate determining step.

Consideration of a "molecular" mechanism for complexes without a 6-methyl or 6-phenyl substituent

Substitution in the 4-position of the pyridyl ring has little effect on catalytic activity, but changing the chalcogen atom from sulfur to selenium resulted in a reduction of catalytic activity, in particular for the precatalyst pairs $PdCl_2(pyCH_2EPh)$ and $PdCl_2(4\text{-}MepyCH_2EPh)$, which have bidentate *N,E* coordination. This trend could be regarded as consistent with the ligand retaining a bidentate configuration in a rate determining step as sulfur and selenium have different donor characteristics. The trend would also be consistent with pyridyl or chalcogen dissociation. It is of interest that $PdCl_2(MeSCH_2CH_2SMe)$ and $PdCl_2(bipy)$ achieved TONs of 90 and 64 respectively in the reaction of 4-bromoacetophenone with alkyl *trans*-cinnamates,[1] indicating that the homoleptic *N,N* or *S,S* donor systems are not as active as the heteroleptic *N,E* containing complexes tested here. Changing the substituent on the chalcogen from Me to Ph resulted in a reduction in catalytic activity for the complexes, again consistent with either bidentate coordination or unidentate coordination in a rate determining step. Alteration of methyl for phenyl may have both electronic and steric effects.

Consideration of a "molecular" mechanism for complexes containing a 6-methyl substituent

Complexes containing a methyl substituent in the 6-position of the pyridyl ring displayed lower catalytic activities than their unsubstituted analogues.

The presence of a 6-methyl substituent results in a significant Me···Cl steric interaction which is relieved through loss of ligand chelation resulting in *trans*-$PdCl_2$ configurations in the solid state as either a trimeric species with monodentate *N,S* bridging ligands, $[PdCl_2(6\text{-}MepyCH_2SPh)]_3$, or a dimeric species with monodentate *N,Se* bridging ligands, $[PdCl_2(6\text{-}MepyCH_2SePh)]_2$, **Section 3.2.2.1**, **Chapter 3**. A structural determination of the other 6-methyl substituted complex studied, $PdCl_2(6\text{-}$

MepyCH$_2$SMe), has not been possible. However, bidentate coordination "PdCl$_2$(*N,E*)" is feasible for the 6-methyl substituted ligands in view of the occurrence of this configuration for PdClMe(6-MepyCH$_2$SBu^t).[40] In this case, the 6-Me···Cl interaction results in conformational changes for the ligand that are similar to the dichloroplatinum(II) complex of 6-MepyCH$_2$SPh described in **Chapter 3**.

Interpretation of the catalysis results is thus more speculative for the 6-methyl substituted precatalysts. If a common structure for all of the active catalysts is formed, reactions that occur to form this structure will differ for the different precatalysts. If the active species in the Heck reaction is assumed to have a monomeric bidentate structure, as observed in the solid state for PdClMe(6-MepyCH$_2$SBu^t)[40] and for complexes of ligands without a 6-methyl substituent, the following interpretation of the catalytic results is feasible.

With this assumption, lower catalytic activity in the presence of the 6-methyl group would appear to be more consistent with either retention of bidentate coordination or chalcogen dissociation in a rate determining step rather than dissociation of the pyridyl donor. Pyridyl dissociation can be ruled out as the donor properties of the chalcogen and flexibility in the coordination environment at palladium are expected to be identical for pyCH$_2$SMe, 4-MepyCH$_2$SMe, and 6-MepyCH$_2$SMe bound only through the S, and thus similar yields and TONs would be expected. Pyridyl ring coordination, with or without chalcogen dissociation, may have an effect on yield and TON as the 6-substitution is varied, owing to altered flexibility in orientation of the pyridyl ring.

Nanoparticles

The presence of nanoparticles acting as catalysts cannot be discounted. If nanoparticles are the active catalyst, *i.e.*, act as a reservoir of active Pd(0) species, or Pd(II) species if the aryl halide oxidises surface palladium atoms, which undergo the Heck reaction in a homogeneous fashion. Although the results may be interpreted as involving a "molecular" mechanism with ligand coordination, it is also feasible that different yields and TONs using different ligands may be obtained, because the nature, stability, and activity of the nanoparticles may be influenced by differing surface interactions with different ligands.

4.2.6 The Suzuki Reaction

Initial studies into reaction protocols for successful coupling were conducted. A 3:1 ratio of DMF:H_2O was trialled as a solvent combination, a common solvent combination for the Suzuki reaction,[41] but early results indicated that the presence of water led to the formation of palladium black and little to no product formation. With anhydrous *N*,*N*-dimethylacetamide as a solvent (a solvent which is also typically used in the Suzuki reaction), little decomposition was observed and product yields increased. Testing was initially conducted without the presence of the phase transfer reagent Bu^n_4NCl, leading to decreased yield. With the change of solvent and addition of the Bu^n_4NCl, leading to increased yields, the temperature and reaction time were set at 80 °C and 24 h. These values were chosen as it was ascertained from the literature[41-43] that these are the upper limits for reaction temperature and duration for most catalytic studies.

From these observations, the reaction conditions adopted for the Suzuki chemistry in this study involved minor modifications from that used in the Heck reactions: Bu^n_4NCl, Na_2CO_3, in anhydrous DMA, under argon at 80 °C for 24 h.

Blank experiments were undertaken in which 4-bromotoluene and phenylboronic acid were tested in the Suzuki reaction without the presence of palladium. No reactivity was observed, **Scheme 4.4**.

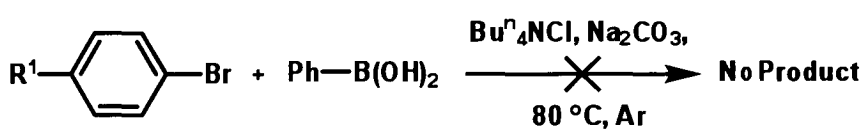

Scheme 4.4 Suzuki reaction blank testing.

Suzuki reactions of both activated and deactivated aryl iodides and bromides were successfully facilitated in the Suzuki reaction using $PdCl_2(pyCH_2SMe)$ as a precatalyst (**Table 4.5**). Excellent yields (> 96%) and TONs (~10^5) were obtained for aryl iodides (entries 1 – 3) while low to moderate yields were obtained for aryl bromides (4 – 6), and little to no activity for aryl chlorides. Yields and TONs are much less than that obtained by Cui using quinoline-8-carboxylate ligands (TONs of 46500 was achieved using 4-bromoanisole)[19] or that typically obtained using bulky

electron rich phosphine containing catalysts as illustrated by Martin and Buchwald.[44] These preliminary results offer the prospect of improvement in catalysis *via* modification of the conditions or the testing of related complexes as precatalysts.

Entry	X	R^1	Yield[a]	TON	Precatalyst Loading (mol %)
1	I	H	97	97,000	0.001
2	I	COMe	99	98,700	0.001
3	I	Me	97	96,500	0.001
4	Br	COMe	48	48,000	0.001
5	Br	Me	33	3,000	0.01
6	Br	OMe	15	150	0.1
7	Cl	COMe	3	3	1
8	Cl	Ph	<1	<1	1

All reactions were carried out with 1.5 mmol of aryl halide, 4.0 mmol of phenylboronic acid, 3.0 mmol of Na_2CO_3, 2.25 mmol of Bu^n_4NCl in 5 mL of DMAc at 80 °C for 24 h. [a] determined by GC (diphenyl ether standard).

Table 4.5 Results of catalytic testing of $PdCl_2(pyCH_2SMe)$ in the Suzuki reaction of various aryl halides and phenylboronic acid.

4.3 Conclusion

The structurally simple and chemically stable precatalyst $PdCl_2(pyCH_2SMe)$ gave the highest yields in the Heck reaction, achieving TONs up to 10^6 for aryl iodides and bromides. Closely related selenium containing ligands, or ligands with a 6-methyl substituent on the pyridyl ring, are much less active. Activation of aryl chlorides using $PdCl_2(pyCH_2SMe)$ was also achieved using $^nBu_4NCl$ as a solvent, giving higher yields for both 4-chloroacetophenone and chlorobenzene than that obtained under the same conditions using DMA as a solvent.

Preliminary results employing the precatalyst $PdCl_2(pyCH_2SMe)$ in the Suzuki reaction gave promising results, with high yields obtained for aryl iodides and bromides including the deactivated species 4-bromoanisole.

Although the active catalytic species is not known, $PdCl_2(pyCH_2SMe)$ can be considered as a simple phosphine-free precatalyst for many Suzuki and Heck-type reactions of both activated and deactivated aryl iodides and, more importantly, aryl bromides in moderate to high yields and TONs.

4.4 Experimental

4.4.1 General Experimental

The palladium precatalysts were prepared according to the procedure outlined in Chapter 3. All other reagents used are commercially available from the Aldrich Chemical Co. and were used as received. Ultra high purity argon was purchased from BOC Gases. Gas Chromatography-Flame Ionisation Detection (GC-FID) measurements were performed by the author on a Shimadzu GC-2014AFsc gas chromatograph equipped with a 25 m length (ID 0.32 mm) ID-BPX5 SGE capillary column. Standards were purchased or synthesised using conventional techniques and mixtures with different concentration ratios were used for calibration.

Calibration of Gas Chromatography Instrument

Five solutions of aryl halide or product (1, 2, 3, 4, and 5 mmol) were prepared in CH_2Cl_2 (25 mL). Diphenyl ether (DPE, 0.170 g, 1.0 mmol) was added to each solution and samples from each solution (2 x 1 μL) were analysed by GC. A graph of the ratio (area aryl halide/area standard (DPE)) versus aryl halide or product formed (mmol) was plotted and the line of best fit was obtained. This process was used for all coupling reactions used in this study.

4.4.2 Experimental Procedures

General procedure for cross-coupling reactions:

The Heck reaction

The precatalyst was added to a solution of aryl halide (1.5 mmol), *n*-butyl acrylate (0.60 mL, 4.0 mmol), Na_2CO_3 (0.32 g, 3.0 mmol, 2 equiv.), Bu^n_4NCl (0.63 g, 2.3 mmol, 1.5 equiv.), and NaO_2CH (0.11 g, 1.7 mmol 1.1 equiv.) in DMA (5 mL) under

argon. The resulting mixture was then stirred at 120 °C for 48 h under Ar. Once cooled to room temperature, diphenyl ether was added (0.170 g, 1.00 mmol) and an aliquot (1.50 mL) was taken and diluted with CH_2Cl_2, then washed with an aqueous solution saturated with NaCl (3 x 1.5 mL). The organic layer was extracted, dried over $MgSO_4$ and filtered. For NAIL catalysis, Bu^n_4NCl (2.48g) was used and DMA was omitted. Yields were determined by GC-FID.

The Suzuki reaction

The precatalyst was added to a solution of aryl halide (1.5 mmol), phenylboronic acid (0.27 g, 2.3 mmol, 1.5 equiv.), Na_2CO_3 (0.32 g, 3.0 mmol, 2 equiv.), and Bu^n_4NCl (0.63 g, 2.3 mmol, 1.5 equiv.) in DMA (5 mL) under argon. The resulting mixture was then stirred at 80 °C for 24 h under Ar. Once cooled to room temperature, diphenyl ether was added (0.170 g, 1.0 mmol) and an aliquot (1.50 mL) was taken and diluted with CH_2Cl_2 then washed with an aqueous solution saturated with NaCl (3 x 1.5 mL). The organic layer was extracted, dried over $MgSO_4$ and filtered. Yields were determined by GC-FID.

4.5 References

1. Jones, R. C.; Madden, R. L.; Skelton, B. W.; Tolhurst, V.-A.; White, A. H.; Williams, A. M.; Yates, B. F. *Eur. J. Inorg. Chem.* **2005**, 1048.
2. Crisp, G. T. *Chem. Soc. Rev.* **1998**, *27*, 427.
3. de Meijere, A.; Meyer, F. E. *Angew. Chem., Int. Ed. Engl.* **1994**, *33*, 2379.
4. Grigg, R. *J. Heterocycl. Chem.* **1994**, *31*, 631.
5. Jeffery, T. *Tetrahedron*, **1996**, *52*, 10113.
6. Rigby, J. H.; Hughes, R. C.; Heeg, M. J. *J. Am. Chem. Soc.* **1995**, *117*, 7834.
7. Jeffery, T. *J. Chem. Soc., Chem. Commun.* **1984**, 1287.
8. Larock, R. C.; Tu, C. *Tetrahedron*, **1995**, *51*, 6635.
9. Beletskaya, I. P.; Cheprakov, A. V. *Chem. Rev.* **2000**, *100*, 3009.
10. Jeffery, T. *Synthesis*, **1987**, 70.
11. Jeffery, T. *Synth. Commun.* **1988**, *18*, 77.
12. Jeffery, T. *Tetrahedron Lett.* **1990**, *31*, 6641.

13. Bräse, S.; de Meijere A. *Palladium-Catalysed Coupling of Organoanyl Halides to Alkenes – The Heck Reaction*, Ed. Diedrerich, F.; Stang, P. J., Wiley-VCH, Germany, **1998**.
14. Whitcombe, N. J.; Hii, K. K.; Gibson, S. E. *Tetrahedron*, **2001**, *57*, 7449.
15. Shaw, B. *New J. Chem.* **1998**, 77.
16. Littke, A. F.; Fu, G. C. *Angew. Chem. Int. Ed.* **2002**, *41*, 4176.
17. Tu, T.; Malineni, J.; Dötz, K. H. *Adv. Synth. Catal.* **2008**, *350*, 1791.
18. Schneider, S. K.; Roembke, P.; Julius, G. R.; Raubenheimer, H. G.; Herrmann, W. A. *Adv. Synth. Catal.* **2006**, *348*, 1862.
19. Cui, X.; Li, J.; Zhang, Z.-P.; Fu, Y.; Liu, L.; Guo, Q.-X. *J. Org. Chem.* **2007**, *72*, 9342.
20. Weck, M.; Jones, C. W. *Inorg. Chem.* **2007**, *46*, 1865.
21. Yai, Q.; Zabawa, M.; Woo, J.; Zheng, C. *J. Am. Chem. Soc.* **2007**, *129*, 3088.
22. Dupont, J.; Consorti, C. S.; Spencer, J. *J. Chem. Rev.* **2005**, *105*, 2527.
23. Buckley, B. R.; Neary, S. P. *Adv. Synth. Catal.* **2009**, *351*, 71.
24. Alonso, F.; Beletskaya, I. P.; Yus, M. *Tetrahedron*, **2005**, *61*, 11771.
25. Kaufmann, D. E.; Nouroozian, M.; Henze, H. *Synlett.* **1996**, 1091.
26. Herrmann, W. A.; Böhm, V. P. W. *J. Organomet. Chem.* **1999**, *572*, 141.
27. Dupont, J.; de Souza, R. F.; Suarez, P. A. Z. *Chem. Rev.* **2002**, *102*, 3667.
28. Herrmann, W. A.; Böhm, V. P. W. *Chem. Eur. J.* **2000**, *6*, 1017.
29. Wang, L.; Zhang, Y.; Xie, C.; Wang, Y *Synlett.* **2005**, 1861.
30. Selvakumar, K.; Zapf, A.; Beller, M. *Org. Lett.* **2002**, *4*, 3031.
31. Cabri, W.; Candiani. I. *Acc. Chem. Res.* **1995**, *28*, 2.
32. de Vries, J. G. *Dalton Trans.* **2006**, 421.
33. Widegren, J. A.; Finke, R. G. *J. Mol. Catal. A: Chem.* **2003**, *198*, 317.
34. Beller, M.; Riermeier, T. H. *Eur. J. Inorg. Chem.* **1998**, 29.
35. Rosol, M.; Moyano, A. *J. Organomet. Chem.* **2005**, *690*, 2291.
36. Nilsson, P.; Wendt, O. F. *J. Organomet. Chem.* **2005**, *690*, 4197.
37. Böhm, V. P. W.; Herrmann, W. A. *Chem. Eur. J.* **2001**, *7*, 4191.
38. d'Orlyé, F.; Jutand, A. *Tetrahedron* **2005**, *61*, 9670.
39. Sundermann, A.; Uzan, O.; Martin, J. M. L. *Chem. Eur. J.* **2001**, *7*, 1703.
40. Canovese, L.; Visentin, F.; Chessa, G.; Uguagliati, P.; Bandoli, G. *Orgnaometallics*, **2000**, *19*, 1461.
41. Bellina, F.; Carpita, A.; Rossi, R. *Synthesis*, **2004**, *15*, 2419.
42. Miyaura, N. *Top. Curr. Chem.* **2002**, *219*, 11.

43. Suzuki, A. *Pure Appl. Chem.* **1994**, *66*, 213.

44. Martin, R.; Buchwald, S. L. *Acc. Chem. Res.* **2008**, *41*, 1461.

Chapter Five

Organic Polymers as Support Materials for Catalytic Sites Involving *N,S* Heteroleptic Ligands

5.1 Introduction

Homogeneous palladium mediated catalysis is an important tool in synthetic chemistry due to the ability to produce a wide variety of compounds, with a wide range of functional groups utilising a range of reaction classes.[1-3] Homogeneous and heterogeneous catalysis have particular advantages and disadvantages and, for homogeneous catalysis, the principle disadvantage relates to catalyst recycling.[4] This leads to the loss of expensive metal and ligands as impurities in the products, which then require purification steps in order to remove them as waste or for reuse.[4,5] Reducing or eliminating this requirement would significantly improve the application of palladium mediated homogeneous coupling reactions in industry,[6-12] particularly in the synthesis of pharmaceuticals where low levels of impurities are required.[13] This is also true for combinatorial chemistry which requires high throughput with little purification and waste to produce large molecule libraries.[14]

Heterogeneous catalysts present several advantages such as easy handling and separation of the palladium metal from the reaction mixture, allowing catalyst recycling.[11,15,16] However, heterogeneous catalysts are generally less selective in product distributions, lacking the high level of catalytic site design possible with homogeneous systems.[17] The anchoring of homogeneous catalysts onto the surface of insoluble solid supports offers a possible solution to these problems. Although often requiring more forcing reaction conditions (*e.g.*, higher temperatures) than their homogeneous counterparts, supported palladium catalysts are generally quite stable.[3,18,19] This stability allows higher reaction temperatures to be used, allowing for compensation of lower activities and often permits reactions to be run under less rigorous conditions, *i.e.*, without the exclusion of air.[20] In some cases supported palladium catalysts show higher activities than their homogeneous counterparts.[21]

Heterogeneous catalysts include palladium metal deposited directly onto a surface such as activated carbon, zeolites,[16] porous glass,[22] clays,[23] or organic polymers.[16] Palladium can also be attached to a solid support as a complex, *i.e.*, the palladium is attached to ligands which are covalently bound to the solid support and thus may act as centres for "homogeneous catalysis". A wide range of supports have been investigated, including organic polymers due to their high surface area and ease of attachment of organic ligands.[11]

There are several types of organic support materials available. Most of these are based upon a polystyrene bead with a functional group usually containing a benzylic halide which can then react with a ligand. One such resin is (4-chloromethyl)polystyrene, **I**, a type of Merrifield resin. Originally used in peptide and oligosaccharide synthesis,[24] it can be synthesised by suspension polymerisation of 4-chloromethyl styrene (as the functionalised monomer) and divinylbenzene (as a cross-linker) in the presence of a radical initiator such as azobisisobutyronitrile (AIBN) (**Scheme 5.1**).[25] This type of solid support is popular for catalysis due to its commercial availability and high stability to a wide range of conditions.[26] It can easily be filtered away from the reaction media, while the resin itself can be easily modified depending upon requirements. Compounds containing phenol,[27] phosphine,[17] carbene,[28] and amine[29] functional groups have been attached successfully to Merrifield resins.

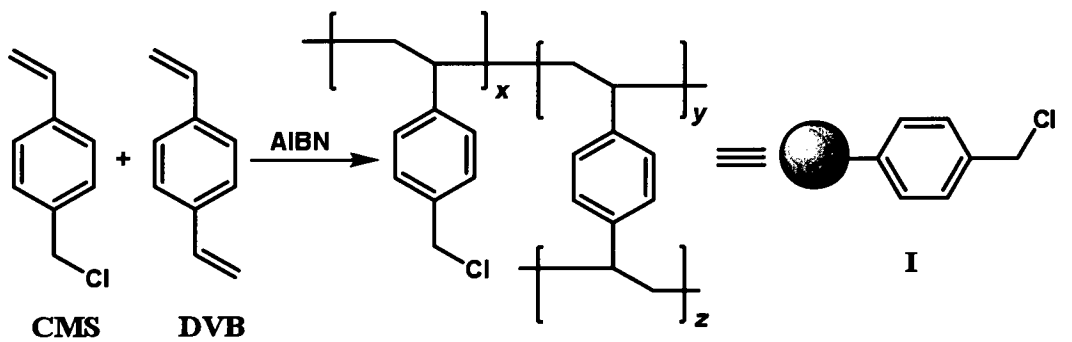

Scheme 5.1 Synthesis of (4-chloromethyl)polystyrene, a type of Merrifield resin, from 4-chloromethylstyrene (CMS) and divinylbenzene (DVB) as cross-linker (typically 1-2%).

One type of solid support currently in the early stages of investigation in supported catalysis are monoliths. Monoliths are typically formulated as exemplified in

Scheme 5.1, but with a monomer:crosslinker ratio of ~ 60:40 and formed in the presence of porogens.[30] The unique quality of these compounds is their fairly uniform architecture and porosity. They have a three dimensional porous sponge-like structure containing a series of macropores (a series of continuous channels) and microglobules (small lobes protruding into the macropores) that house a series of micropores (nanometer in size) giving the monolith a very high surface area.[31] Monoliths can be synthesised using different monomers, cross-linkers and porogens. Monoliths can be designed to suit the application required and, in some cases, replicate or replace polystyrene beads such as the Merrifield resin in analytical separation applications.[32] One such monolith based upon co-polymerisation of a functionalised monomer, 4-chloromethyl styrene (CMS), and a cross-linker, divinylbenzene (DVB), **Scheme 5.1**,[30,31,33] has a formulation closely related to that of poly(4-chloromethyl)styrene.[30]

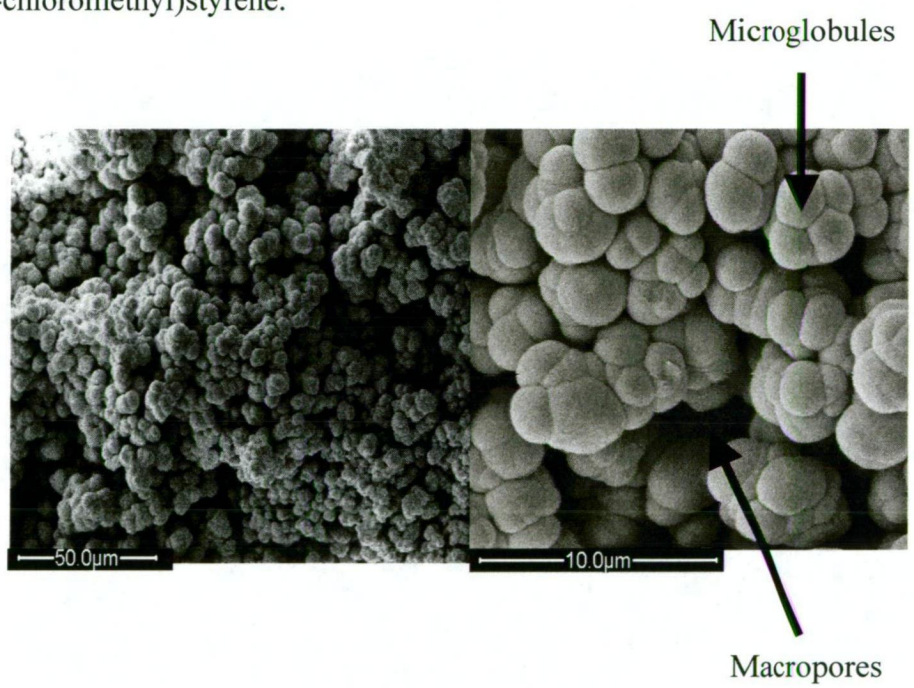

Figure 5.1 Scanning electron micrographs of a poly(glycidylmethacrylate-*co*-ethylenedimethacrylate) monolith.[34]

To date, monoliths have been used extensively in analytical chemistry as separation media for liquid chromatography,[35] capillary electrophoresis,[36] and solid phase extraction,[37] but limited to a few recent reports as catalyst supports.[38-42] At the current early stages of development of monoliths as supports for catalysis sites, there appear to be significant advantages over classical supports. These include ease of fabrication and a highly configurable surface chemistry. This latter feature is very

important and allows, the size of the characteristic macropores and micropores to be modified by changes in the composition of monomers, crosslinkers and porogenic solvents.[30,31] Furthermore, due to their very high surface area and porous nature, reaction mixtures flow through the monolith rather than around beads resulting in an increased contact area of the reaction solution with the support surface and, consequently, the attached catalyst.[43] For a polystyrene bead the reaction solution contacts principally the functionalised surface.[43]

Flow-through microreactors, such as that shown in **Figure 5.2**, offer advantages over batch systems, *e.g.*, high reactivity, high throughput, minimal workup, high ratio of surface to volume and continuous operation.[44-47] In addition, reactions can be carried out under isothermal conditions with well-defined residence times, so that undesirable side reactions and fragmentations are limited. The small dimensions of microreactors allow the use of minimal amounts of reagents and solvents under precisely controlled conditions, making the process more environmentally benign than standard batch systems.[47-53] Consequently, there have been attempts to develop catalysis in microreactors, including the use of conventional polystyrene beads packed into capillaries to form microreactors. These systems, however, tend to have significant limitations, such as swelling which leads to the beads becoming soft and compressible resulting in preferred solvent paths. There are also significant technical challenges in packing and confining the beads within the capillary.[43] Reaction mixtures prefer to flow around the beads and into interstitial voids rather than through them, such that only catalyst sites on the surface tend to be accessed by the reaction mixture. Monoliths, on the other hand, are essentially an incompressible solid with macro and microchannels that permit rapid heat and mass transfer, and thus suggest the possibility for excellent performance over both bulk beads and bead type microreactors.[54-56]

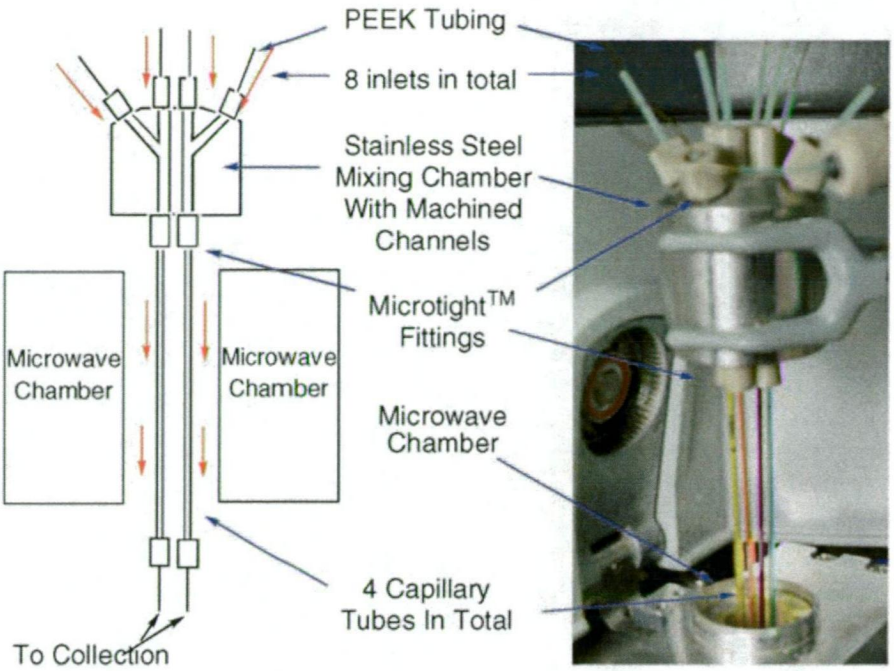

Figure 5.2 A continuous flow, microwave-assisted, open channel parallel-capillary microreactor used for homogeneous Suzuki catalysis.[57] This system allows the preparation of four different products simultaneously via four different mixing chambers. Also, a constant flow of one reagent can be maintained while the other can be varied *in situ* to produce a large range of products.

The majority of examples in the literature of monolith-supported catalysts are based upon phosphine ligands. Currently, there are no examples in the literature of a catalyst based upon a heteroleptic ligand with a pyridine and a chalcogenoether group, such as the class of ligand described in **Chapter 2**. A major aim of this work was to extend previous catalytic studies on *N,E* heteroleptic ligand systems by synthesising a heteroleptic ligand suitable for attachment to different types of solid supports, such as polymeric resins and polymer monoliths, and test their viability and versatility in supported catalysis. Simultaneously, a comparison can be made between the supported catalysts and their model homogeneous analogues, while also participating in the early development of flow through microreactors incorporating monoliths. Attachment of catalysis sites to solid supports is usually achieved by either synthesising a complex containing a functional group suitable for reaction with the support, or anchoring a ligand followed by reaction of the supported ligand with a metal salt. The latter approach was adopted here as the heteroleptic *N,S* motif is

expected to be unreactive toward the benzylic chloride group of the polystyrene beads and CMS/DVB monolith.

5.2 Results and Discussion

5.2.1 Synthesis of Ligands

A phenol moiety was selected as a potential functional group to attach the ligand to the solid support as such groups are known to easily displace halide functionalities by base assisted nucleophilic attack. To assess the feasibility of this approach, the trial reaction shown in **Scheme 5.2** was studied using solvents and bases considered appropriate for attachment based on recent reports of anchoring of ligands to organic monoliths.[58] In all occasions complete conversion to the product was achieved, **Table 5.1**.

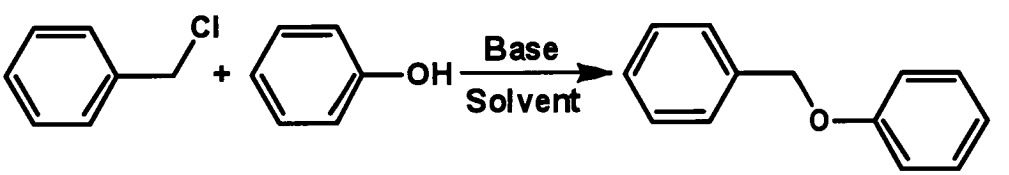

Scheme 5.2 Trial attachment reaction using a simulated ligand (phenol) and a simulated Merrifield resin (benzyl chloride).

Solvent/base system	Conversion (%)
Acetonitrile/triethylamine	100
Acetonitrile/Hünig's base	100
Ethanol/triethylamine	100
Ethanol/Hünig's base	100

Table 5.1 Results of attachment trials.

A ligand synthesis was sought in which the desired molecule would contain a pyridine, 2-(methylthiomethyl)pyridine (which can bind the palladium to the ligand), and a phenolic group which would be used to anchor the molecule to the solid support. Once attached to the solid support the phenolic derived ether functionality

would also result in extended distance of the metal coordination site from the surface of the solid support. Thus more closely simulating catalysis under homogeneous conditions, **Scheme 5.3**.

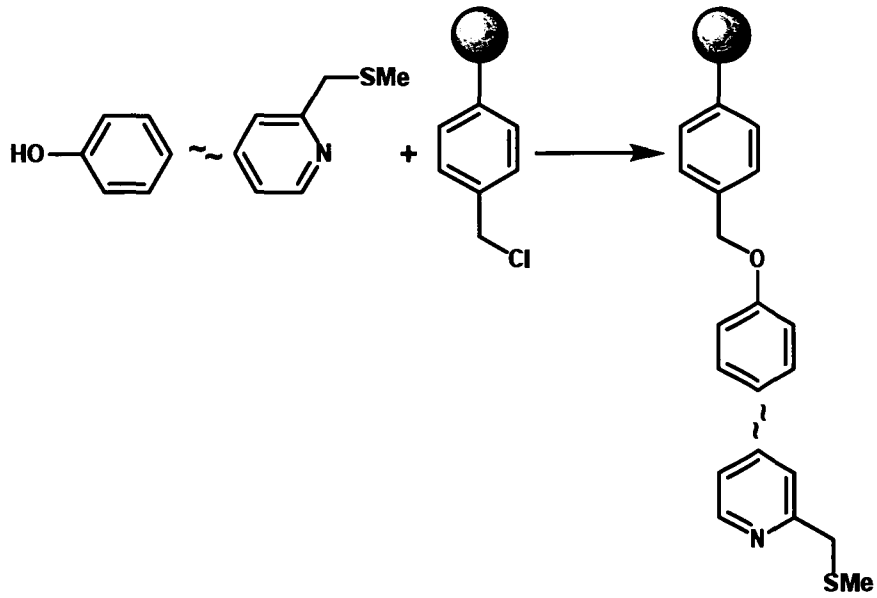

Scheme 5.3 Proposal for organic polymer support containing an *N,S* heteroleptic ligand.

Studies of the effect of functional groups at the 6- and 4-positions of the pyridine ring on catalytic efficiency are documented in **Chapter 4**. These results showed that substituents present at the 4-position had little effect on overall catalysis. The 4-position on the pyridyl ring is also further removed from the *N,E* coordination site than the 6-position, ensuring an absence of steric influence at the metal centre. Thus, the 4-position was chosen as suitable for incorporation of a hydroxyphenyl group to anchor the heteroleptic ligand to an organic polymer. One of the established protocols for synthesis of the thiomethyl functionality (developed by Ghera and David,[59] a modification of which is described in **Chapter 2**) appeared suitable for use in synthesising the desired compound, providing the hydroxyl group is protected, **Scheme 5.4**.

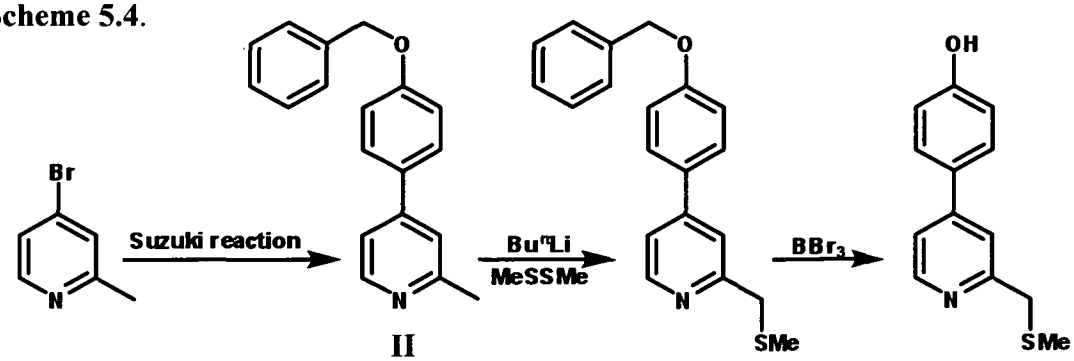

Scheme 5.4 Initial ligand synthesis proposal.

The Suzuki protocol was chosen as a possible effective method of attaching a protected phenol to the picoline ring. However, for this reaction to occur a halide moiety is required on the 4- position of the picoline. Bromine was selected as the halide of choice due to synthetic practicalities for both bromo substitution on the ring and its susceptibility to undergo the intended Suzuki reaction. However, there are no reports of direct bromination of 2-picoline in the 4- position by conventional electrophilic means, although the desired bromination via either a nitro or an amine intermediate has been reported.[60] Following this approach, 4-nitro-2-picoline[60] was reacted with acetyl bromide at reflux in a series of solvents affording very little of the final product, as shown in **Table 5.2**.

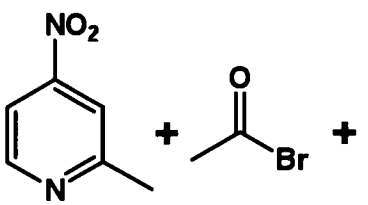

Solvent	Product Yield (%)
$CH_3C(O)Br$[60]	20
CH_2Cl_2	22
$CHCl_3$	32
CH_2ClCH_2Cl	28
EtOAc	38

Table 5.2 Solvents trialled in the synthesis of 4-bromo-2-picoline.

Due to these disappointing results, a better yield of 4-bromo-2-picoline was sought via bromination of 4-amino-2-picoline where, due to cost consideration, 4-amino-2-picoline was synthesised directly from 4-nitro-2-picoline. Two different methods were trialled, direct hydrogenation of 4-nitro-2-picoline with Pd/C (43% yield), and reduction of the nitro group *via* Ti(0) ($TiCl_4$ reduced *in situ* with $LiAlH_4$),[61] or Ti(II) ($TiCl_4$ reduced *in situ* with anhydrous $SnCl_2$),[62] giving 55 and 48% yield, respectively. In all cases disappointing results were achieved, and in the case of the titanium reagents emulsions formed making isolation difficult. As a result, this synthetic pathway was abandoned.

It has been shown that picoline *N*-oxides undergo nucleophilic substitution far more readily than picoline itself, as the *N*-oxide group can act as either an electron donor (**A**) or an electron acceptor (**B**). This unique ability to enhance the reactivity of the ring arises from conjugation of the oxygen atom of the *N*-oxide group with the aromatic system, as exemplified in resonance structures of pyridine *N*-oxide, **Figure 5.3**.[63]

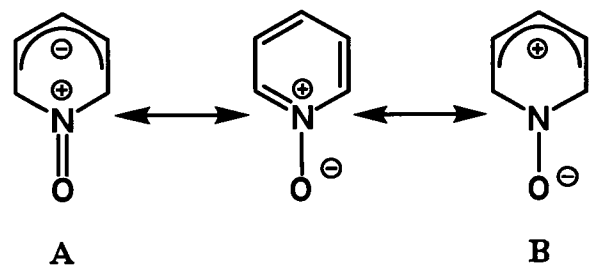

Figure 5.3 Resonance structures of pyridine *N*-oxide.

With this in mind a modification of a protocol developed by Maerker[64] was utilised to produce the desired picoline. In Maerker's case, 4,4′-dinitro-2,2′-bipyridine-1,l′-dioxide was reacted with excess acetyl bromide in glacial acetic acid by reflux for 2 h to produce 4,4′-dibromo-2,2′-bipyridine-1,l′-dioxide in 88% yield. Following this procedure, the desired 4-bromo-2-picoline *N*-oxide was obtained in 78% yield. The lower yield in this case may result from lower reactivity of 4-nitro-2-picoline *N*-oxide to bromination. Consequently, the reagents were refluxed in a solution of glacial acetic acid and an excess of acetyl bromide at 120 °C for 3 h affording 4-bromo-2-picoline *N*-oxide in 92% yield.

Deoxygenation of the picoline was then achieved by the reaction of 4-bromo-2-picoline *N*-oxide with PCl_3 in $CHCl_3$[61] giving the desired 4-bromo-2-picoline in 98% yield, which smoothly underwent a Suzuki reaction with 4-(benzyloxyphenyl)boronic acid to give the desired 4-(4-benzyloxyphenyl)-2-picoline, **Scheme 5.4 (II)**. However, when the synthetic method described in **Chapter 2** was utilised to form the chalcogenoether function (**Section 2.2.1**), secondary lithiation occurred at the benzylic CH_2 protons producing bis- and tris- substituted by-products, **Figure 5.4**. After many attempts using various reaction conditions (including different solvents for lithiation, *e.g.*, diethyl ether, tetrahydrofuran and a 1:1 mixture of them, while concurrently trialling different lithiating agents, *e.g.*, *n*-

butyllithium and lithium di-*i*-propylamide) very little of the desired product was formed. Thus, this synthetic pathway was abandoned.

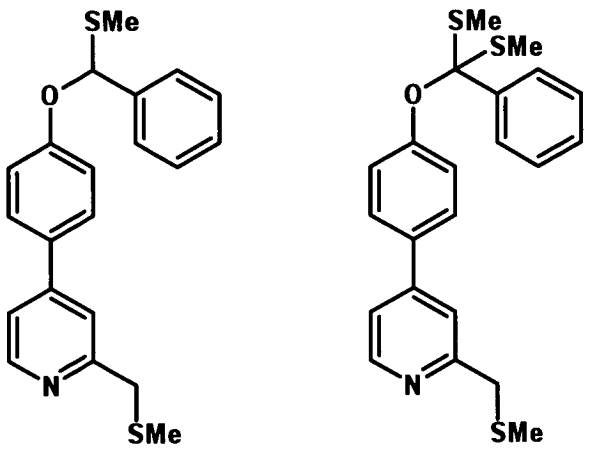

Figure 5.4 Examples of the unwanted by-products produced in the lithiation of 4-(4-benzyloxyphenyl)-2-picoline.

Adopting a new approach, the synthesis of two heteroleptic ligands was developed as shown in **Scheme 5.5**. A protocol developed by van den Heuvel[65] was utilised in which 5-bromo-2-picoline *N*-oxide was refluxed in neat trifluoroacetic anhydride for 30 min followed by stirring in a basic aqueous solution (pH 8) to produce (5-bromo-2-pyridinyl)methanol in 81% yield. The desired (4-bromo-2-pyridinyl)methanol, **V**, was synthesised in 55% yield using this method. Subsequently, a modification was made in which the desired product **V** was produced in 62% yield by refluxing 4-bromo-2-picoline *N*-oxide in a solution of trifluoroacetic anhydride in CH_2Cl_2 overnight, followed by overnight stirring of the ester intermediate in a basic biphasic mixture of water and CH_2Cl_2.

Next, 4-bromo-2-(bromomethyl)pyridinium bromide, **VI**, was synthesised in 87% yield by refluxing **V** in a solution of PBr_3 and $CHCl_3$, and addition of HBr to isolate the product in Et_2O. The pyridinium salt was then reacted with an ethanolic solution of KOH and NaSMe by modification of the procedure developed by Canovese,[66] giving 4-bromo-2-(methylthiomethyl)pyridine, **VII**, in 72% yield. In Canovese's case 6-chloro-2-(chloromethyl)pyridine was reacted directly with NaSMe in basic dimethylsulfoxide solution. However, in this instance a large amount of the unwanted bis-substituted pyridine thiol compound, 4-thiomethyl-2-

(methylthiomethyl)pyridine was produced forcing a modification employing very slow addition of an ethanolic solution of NaSMe to a stirred basic ethanolic solution of **VI**.

The target compound, **VIII**, was obtained in 90% yield *via* Suzuki coupling of 4-bromo-2-(methylthiomethyl)pyridine, **VII**, and 4-hydroxyphenylboronic. The analogous benzyloxyphenyl ligand, **IX**, was obtained in 82% yield. The overall yield of **IX** from 4-nitro-2-picoline *N*-oxide is 32%, over six steps.

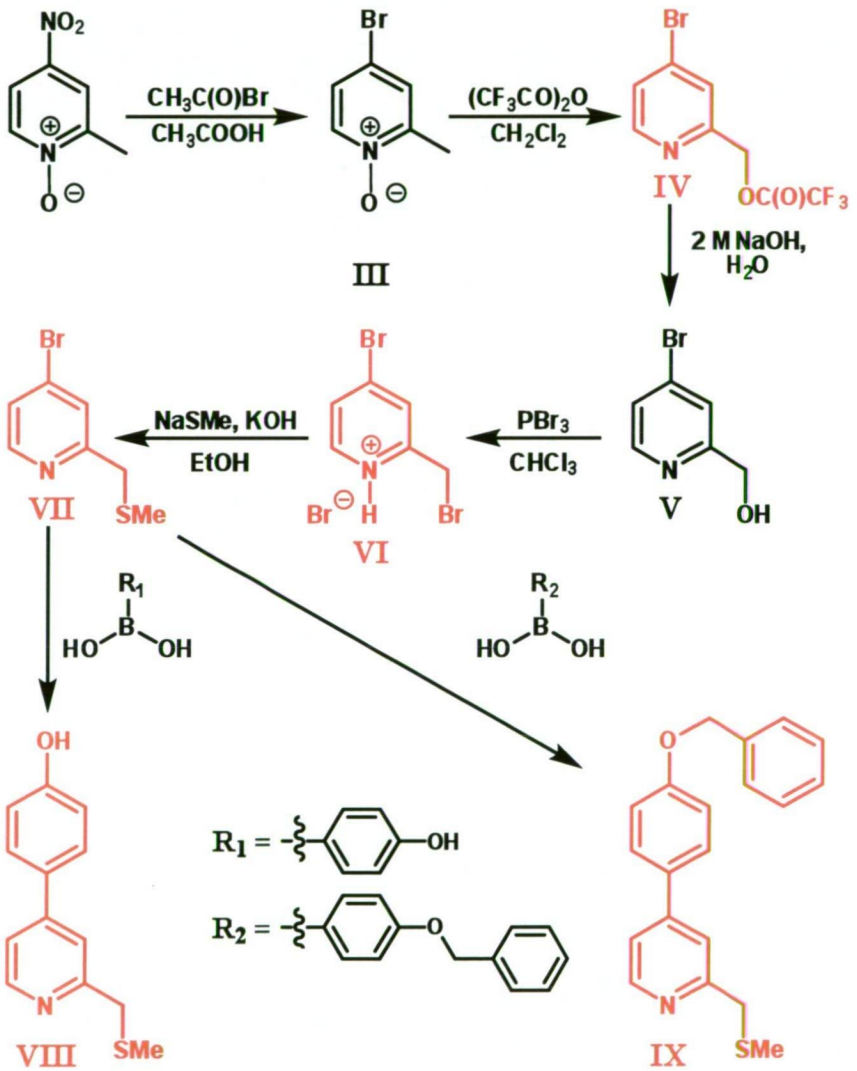

Compounds marked in red are new compounds.

Scheme 5.5 Synthesis of 4-(4-hydroxyphenyl)-2-methylthiomethylpyridine, **VIII**, and 4-(4-benzyloxyphenyl)-2-methylthiomethylpyridine, **IX**. X-ray structures of **VI** and **VIII** have been obtained see **Section 5.2.4**.

5.2.2 Heteroleptic Ligand NMR Studies

NMR spectra of the new heteroleptic ligands and their precursors exhibited resonances for the pyridyl and thiomethyl group in accordance with the ranges shown in **Figures 2.2 – 2.6 (Chapter 2)** for related compounds. The spectrum of 4-(4-hydroxyphenyl)-2-methylthiomethylpyridine, **VIII**, displays one additional feature of note. The molecule undergoes a deuterium exchange process in wet deuterated methanol at room temperature, exhibited as a decrease of the CH_2 resonance from an expected integration of 2 to ~ 0.5. In order to elucidate a potential mechanism for this process, NMR spectra in two different dry deuterated solvents, methanol and acetone were studied. In these solvents there was no evidence of deuterium exchange, thereby indicating that the process involves water. To test this, a known quantity of the compound was dissolved in deuterated acetone and ~1 equiv. of D_2O was added in progressive 0.1 equiv. amounts. Upon addition of the heavy water there was a decrease of the CH_2 resonance from 2 to ~0.2 in area and a complete disappearance of the OH resonance. When a solution of **VIII** in wet deuterated methanol was analysed by high resolution atmospheric pressure chemical ionisation quadrupole mass spectrometry (APCI-MS), the spectrum showed one major species with the incorporation of 4 deuterium atoms present in the *N*-deuterated cation, **Figure 5.5**, corresponding to d^4-**X**.

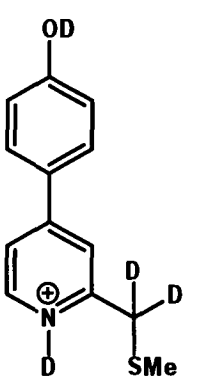

Figure 5.5 Major product of deuterium exchange as shown by APCI-MS.

As 4-(4-hydroxyphenyl)-2-methylthiomethylpyridine, **VIII**, contains both phenoxide and pyridine functionality, it is anticipated to exist in the tautomeric forms **VIII** and **XI/XII (Scheme 5.6)**,[67] similar to that of 4-hydroxypyridine, together with the protonation equilibrium involving **X**. When the benzyloxy analogue **IX** was

dissolved in wet CD_3OD no deuterium exchange was observed, inferring that the phenoxy functionality along with wet CD_3OD are required for the deuterium exchange to occur.

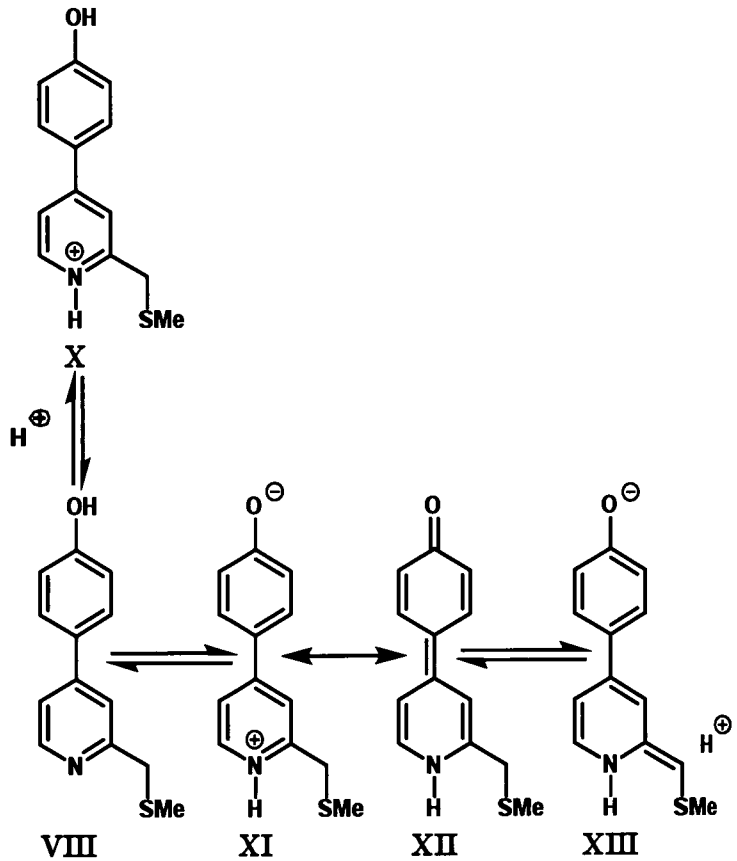

Scheme 5.6 Tautomeric (**VIII**, **XI/XII**, **XIII**) and mesomeric (**XI**, **XII**) forms of 4-(4-hydroxyphenyl)-2-methylthiomethylpyridine, by analogy with the behaviour of 4-hydroxypyridine, together with protonation equilibrium to form **X**.

Thus, deuterium exchange at the methylene protons may result from their increased acidity caused the presence of the thiomethyl functionality in addition to the presence of the phenoxide moiety and wet CD_3OD, *via* a step-wise mechanism through the tautomeric species **XIII**.

5.2.3 Synthesis and NMR Studies of Model Palladium(II) Complexes

Anchoring of **VIII** to (4-chloromethyl)polystyrene (Merrifield resin), 4-(bromomethyl)phenoxymethyl styrene (Wang resin) and CMS/DVB monolith is

described in **Section 5.2.5**. Complexes of **VIII** and **IX** were also synthesised, as models for dichloropalladium(II) anchored to the polymeric supports. The palladium(II) complexes were synthesised according to the procedure developed in **Chapter 3**, *i.e.*, the stoichiometric reaction of $PdCl_2(NCMe)_2$ with the appropriate ligand in acetonitrile. The resulting air and moisture stable palladium(II) complexes formed as yellow powders in high yield.

NMR spectra of the complexes exhibited resonances for the pyridyl and thiomethyl group in accordance with the ranges decribed in **Section 3.2.2, Chapter 3** for related compounds. Thus, room temperature ^1H NMR spectra of both complexes in d^6-DMSO exhibit resonances between 9.02 – 6.91 ppm ascribed to the aromatic protons on the pyridine, phenylene and phenyl rings of the ligands. Second order AB spin systems displaying germinal coupling is observed for the methylene protons of the α-carbons upon coordination to the metal centre for both complexes, due to the formation of a new stereogenic centre at the chalcogen upon coordination. The protons corresponding to the benzylic methylene protons and thiomethyl groups exhibit resonances at 2.55 and 5.20 ppm, respectively, while the OH moiety exhibits a resonance at 10.18 ppm.

Room temperature $^{13}C\{^1H\}$ NMR spectra of both palladium(II) complexes in d^6-DMSO exhibit aromatic resonances between 163.9 – 116.4 ppm, ascribed to the aromatic protons of pyridine, phenylene and phenyl rings. For the complex formed by **IX**, the benzylic methylene carbon and methylene carbon attached to the pyridyl ring exhibit resonances at 70.1 and 45.3 ppm, respectively, while the resonances of the carbons corresponding to the thiomethyl and hydroxy groups occur at 22.9 and 160.9 ppm, respectively.

5.2.4 Solid State Structures of ligand precursors VI and VIII and model dichloropalladium complexes.

Crystals of 4-Br$pyCH_2Br$.HBr (**5a**), 4-(4-HOC_6H_4)$pyCH_2SMe$ (**5b**), $PdCl_2${4-(4-HOC_6H_4)$pyCH_2SMe$} (**5c**), and $PdCl_2${4-(4-$BnOC_6H_4$)$pyCH_2SMe$} (**5d**) suitable for X-ray crystallographic studies were grown from vapour diffusion of $MeNO_2/Et_2O$, a hot EtOH solution, vapour diffusion of $MeNO_2/Et_2O$ and hot $MeNO_2$, respectively. Diffraction data for **5a-c** were collected by the author at the School of Chemistry and

for **5d** by the author at the Australian Synchrotron. Selected bond distances and angles for all compounds are shown in **Table 5.6**, while crystallographic information files of all compounds can be found in **Appendix B**. All non-hydrogen atoms were refined anistropically; *N*-bound and *O*-bound hydrogen atoms were positionally refined freely but constrained in U_{iso}, and all other hydrogen atoms were placed in calculated positions and refined using a riding model with fixed C–H distances of 0.95 (sp^2C–H), 0.99 Å (methylene H), 0.98 Å (methyl H), and $U_{iso}(H) = 1.2U_{eq}(C)$ except for methyl H atoms where $U_{iso}(H) = 1.5U_{eq}(C)$.

The hydrobromide salt **5a** (**Figure 5.6**) crystallises in the monoclinic space group $P2_1/n$ and contains one cation/anion pair in the asymmetric unit. The overall geometry is consistent with related salts such as 2,6-bis(bromomethyl)pyridinium bromide[68] and 2-(chloromethyl)pyridinium chloride.[69] The molecular structure shows that C(21) lies in the plane of the pyridine ring, while Br(1) sits above this plane (0.01(1) Å) with a torsion angle of 75.4(8) ° (N(1), C(2), C(21), and Br(1)). The Br(1)–C(21) bond (1.948(8) Å) is longer than Br(2)–C(4) (1.869(8) Å), as expected for the aryl carbon C(4).

The compound displays hydrogen bonding N(1)–H(1)···Br(3^i) with a N(1) to Br(3^i) distance of 3.139(7) Å (**Table 5.3**), comparable to that in 2,6-bis(bromomethyl)pyridinium bromide[68] which displays a N···Br distance of 3.242(2) Å. Hydrogen atom contacts of the form C–H···*X* are observed, but are long (uncorrected H···*X* > 2.9 Å) and/or markedly non-linear. Upon close examination of molecular packing within the crystal lattice (**Figure 5.7**), no π stacking is apparent, with hydrogen bonding limited to discrete N–H···Br interactions.

	N(1)–H(1)	H···*Br(3^i)*	*N(1)*···*Br(3^i)*	*N(1)*–H(1)···*Br(3^i)*
N(1)–H(1)···Br(3^i)	0.90(1)	2.26(10)	3.139(7)	164(8)

Symmetry code: (i) $-x-1/2, y+1/2, -z+1/2$.

Table 5.3 Hydrogen bond geometry (Å, °) in 4-BrpyCH$_2$Br.HBr.

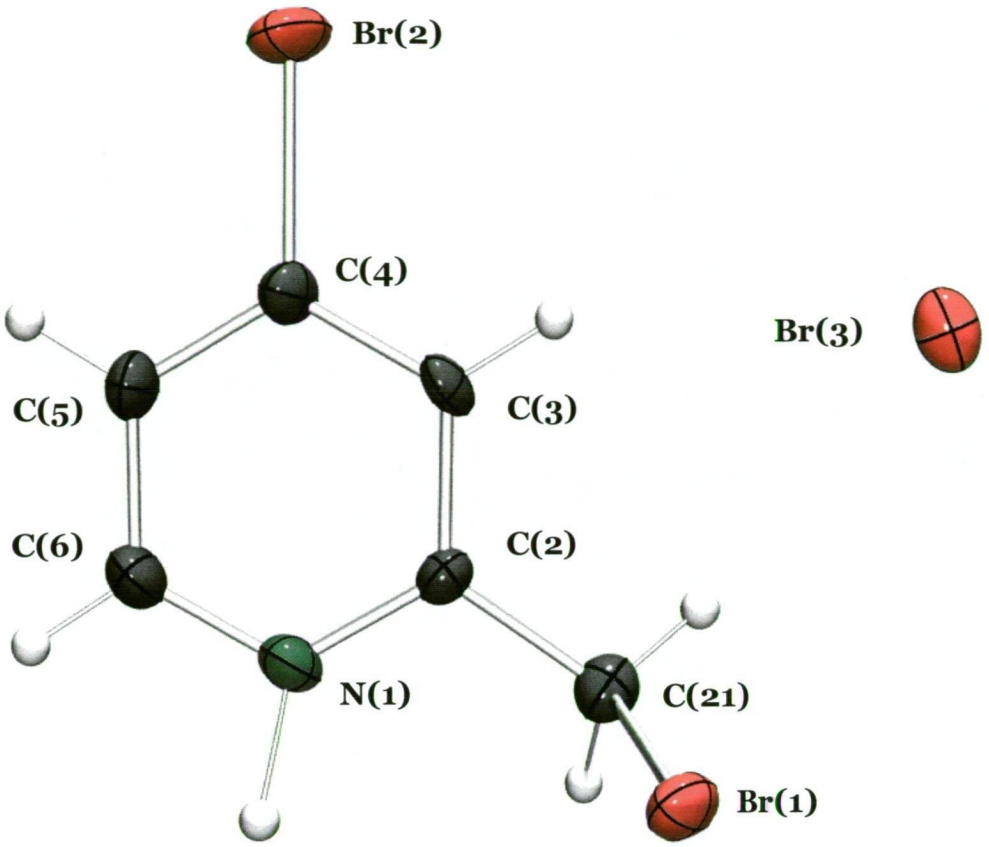

Figure 5.6 A rendered ORTEP of the structure of **5a**, showing the atom labelling scheme. Displacement ellipsoids are drawn at the 50% probability level and H atoms are represented by circles of arbitrary size.

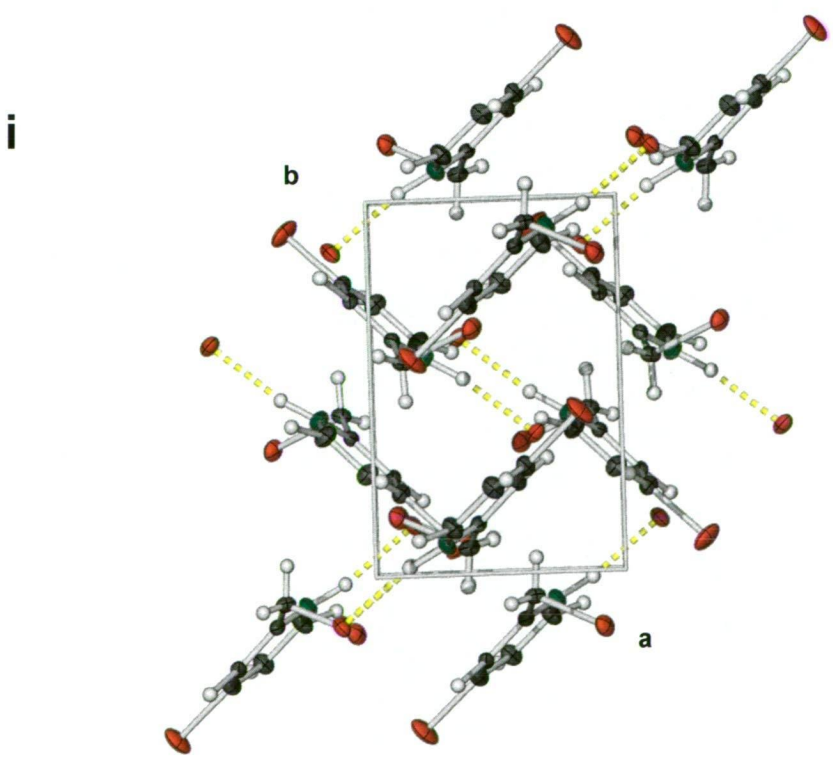

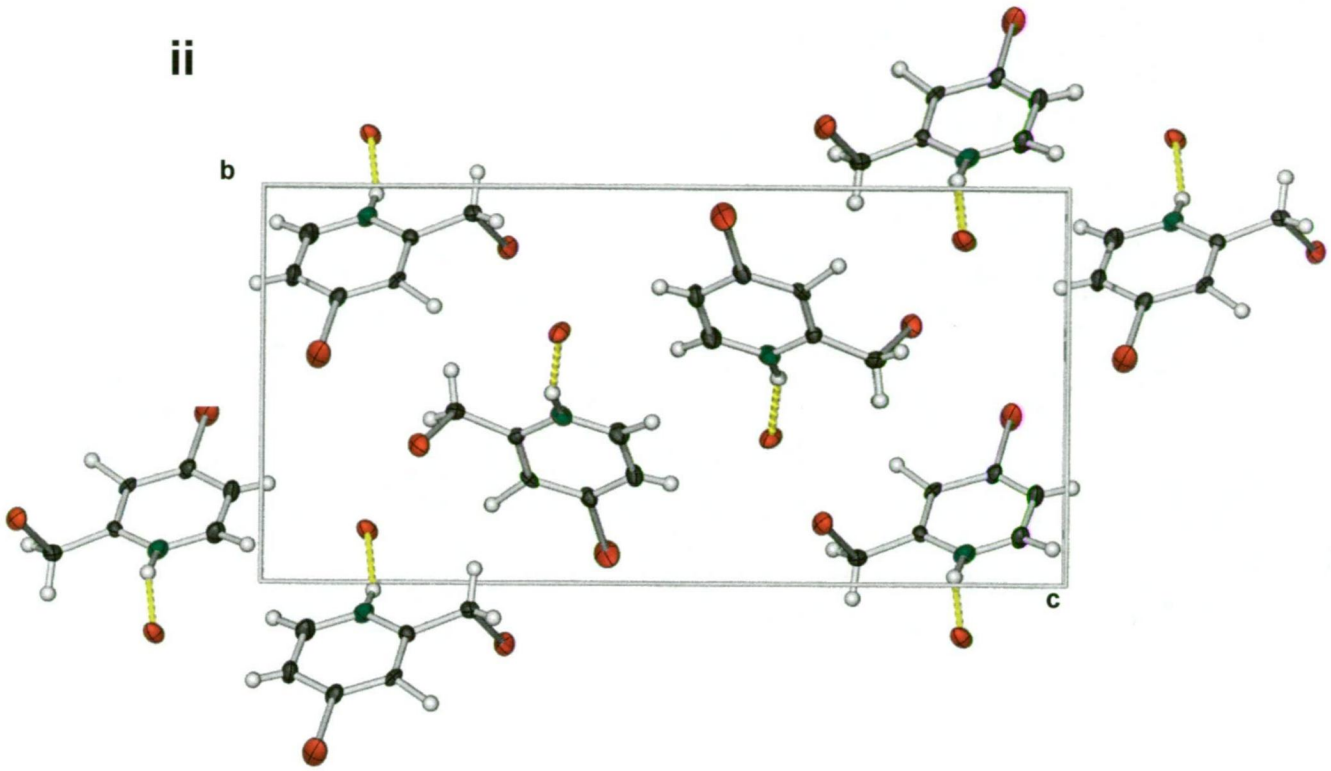

Figure 5.7 Unit cell contents of 4-BrpyCH$_2$Br.HBr (**5a**), down the *c* axis (**i**) and down the *a* axis (**ii**), respectively. Both diagrams indicate the presence of discrete hydrogen bonding N(1)–H(1)···Br(3^{i}). Displacement ellipsoids are drawn at the 50% probability level and H atoms are represented by circles of arbitrary size.

Compound **5b** (**Figure 5.8**) was refined in the monoclinic space group $P2_1/n$ and contains molecule in the asymmetric unit with no crystallographic symmetry. The compound is not planar, exhibiting an arene–arene dihedral twist of 29.9(1) °, a feature which is common to similar compounds such as 4-(3,5-dimethyl-pyridin-4-yl)-3,5-dimethyl phenol (84.2 °, the high dihedral twist in this case is due to the steric strain of the 4 methyl groups),[70] 1-methyl-2-[4-phenyl-6-(pyridinium-2-yl)pyridinium diperchlorate (30.6 °), and 2-[4-(methoxyphenyl)-2,2′-bipyridin-6-yl]-1-methylpyridinium iodide (30.7 °).[71]

The compound displays hydrogen bonding with a O(1)···N(1^{i}) distance of 2.700(3) Å (**Table 5.4**), comparable to that in 4-(3,5-dimethyl-pyridin-4-yl)-3,5-dimethyl phenol[70] which displays a O···N distance of 2.721(2) Å. Upon closer examination of this interaction, H(1) is closer to O(1) (0.61(3) Å) rather than N(1^{i}) (2.10(3) Å), indicating that the solid state structure of 4-HOC$_6$H$_4$pyCH$_2$SMe is consistent with the

tautomeric form **VIII**, rather than the quinone tautomer **XII** (**Scheme 5.6**). This interpretation is also supported by the (ring)C–C(ring) distance of 1.476(3) Å, which is similar to that of typical biaryls (~1.487 Å),[72] and the C(44)–O(1) bond length of 1.353(3) Å, both of which are both much longer than quinoidal structures, typically ~ 1.349 Å for (ring)C–C(ring) and ~1.222 Å for C=O.[72]

	O(1)–H(1)	H(1)···*N(1^{i})*	O(1)··· N(1^{i})	O(1)–H(1)···N(1^{i})
O(1)–H(1)···N(1^{i})	0.61(3)	2.10(3)	2.700(3)	167(4)

Symmetry code: (i) *x*+3/2, -*y*-1/2, *z*+1/2.

Table 5.4 Hydrogen bond geometry (Å, °) in 4-(4-HOC_6H_4)pyCH_2SMe (**5b**).

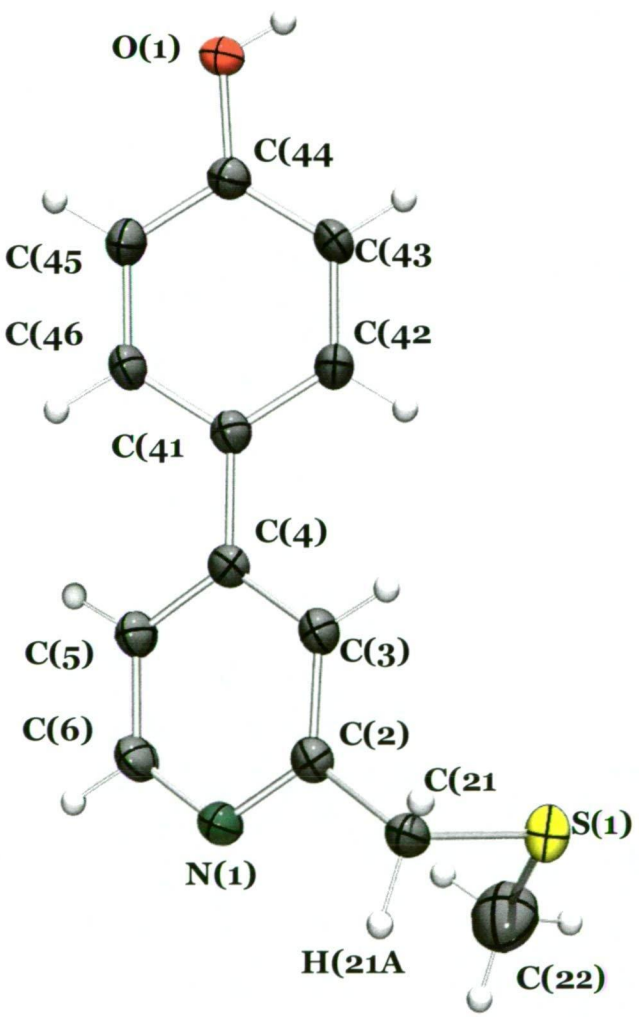

Figure 5.8 A rendered ORTEP of the molecular structure of 4-(4-HOC_6H_4)pyCH_2SMe (**5b**), showing the atom labelling scheme. Displacement ellipsoids are drawn at the 50% probability level and H atoms are represented by circles of arbitrary size.

Upon close examination of molecular packing within the crystal lattice of **5b** (**Figure 5.9**), it can be seen that the molecule is orientated into polymeric chains arranged into parallel running stacks displaying limited π-stacking between adjacent pyridyl and aryl rings. This leads to an intermolecular distance of 5.59_8 Å between the aromatic rings of vertical neighbours, **Figure 5.9** (**ii**), considerably longer than the sum of the van der Waals radii between planar co-facial π-electron systems (~3.50 Å).[73]

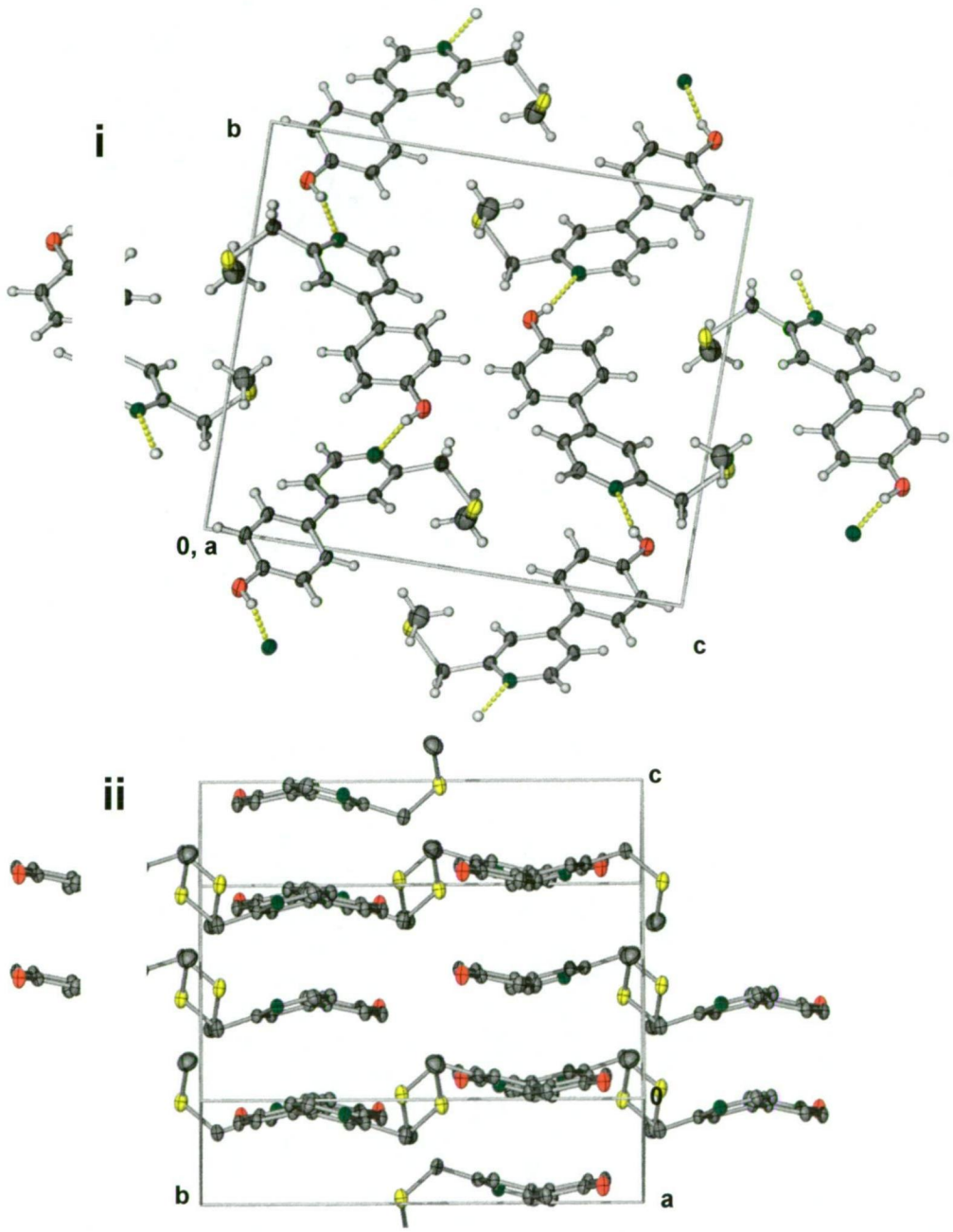

Figure 5.9 Unit cell contents of 4-(4-HOC_6H_4)pyCH_2SMe (**5b**), looking down *a*, **i** and along the polymeric strands, **ii**. Displacement ellipsoids are drawn at the 50% probability level and H atoms are represented by circles of arbitrary size. In **ii**, H atoms have been omitted for clarity.

The complex $PdCl_2$(4-(4-HOC_6H_4)pySMe) (**5c**) (**Figure 5.10**) crystallises in the monoclinic space group $P2_1/n$ and was refined as a mononuclear compound with one molecule in the asymmetric unit. It has a distorted square planar geometry characteristic of palladium(II) complexes, with the same overall structure as some palladium(II) precatalysts without 6-methyl or 6-phenyl substituents described earlier (**Chapter 3**). Upon coordination, the ligand has flattened, as indicated by a reduction in the arene–arene dihedral twist from 29.9(2) ° in the free ligand **5b** to 8.1(7) ° in the complex **5c**.

The O(1)···Cl(1^i) distance, 3.002(8) Å, **Table 5.5**, is shorter than similar "[ECE]" (E = N, S) pincer complexes MCl($C_6H_2(CH_2NMe_2)_2$-2,6-OH-4) (M = Pt[74], Pd[75]) and PdCl($C_6H_2(CH_2SPh)_2$-2,6-OH-4)[76] which display O–H···Cl distances in a range of 3.1040(18) – 3.127(8) Å for similar chain structures. Within the crystal lattice of **5c** (**Figure 5.11**), molecules are orientated into linear polymeric chains, linked by hydrogen bonding, **Table 5.5**. In contrast to **5b**, the polymeric strands of **5c** stack antiparallel into dimeric units involving offset face-face π-stacking that is aided by the near planar aryl-pyridyl moieties allowing an intermolecular of 3.43(2) Å. Palladium coordination planes between paired sets of chains are close to being directly aligned, but Pd···Pd contact of 3.711(3) Å indicates the absence of a metal-metal interaction (van der Waals radius 1.63 Å).[77] The (ring)C–C(ring) distances and the C(44)–O(1) bond length are within one standard deviation of values for the free ligand, indicating no evidence of a quinoidal type structure within the complex.

	O(1)–H	H···*Cl(1^i)*	*O(1)*···*Cl(1^i)*	*O(1)*–H(1)···*Cl(1^i)*
O(1)–H(1)···Cl(1^i)	0.72(14)	2.36(15)	3.002(8)	149(15)
O–H···Cl[74]	0.84(14)	2.32(13)	3.127(12)	162(15)
O–H···Cl[75]	0.72(3)	2.42(3)	3.119(2)	165(4)
O–H···Cl[76]	0.79(3)	2.31(3)	3.1040(18)	178(3)

Symmetry code: (i) $x, y+1, z$.

Table 5.5 Hydrogen bond geometry (Å, °) in $PdCl_2$(4-(4-HOC_6H_4)pyCH_2SMe) (**5c**).

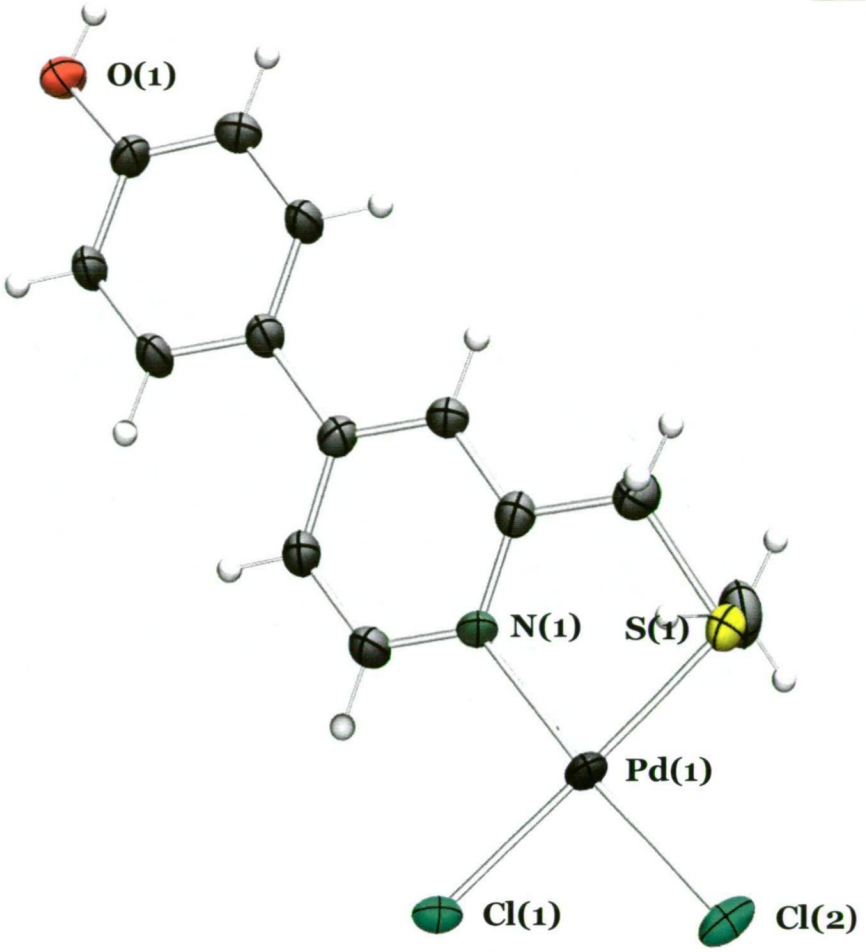

Figure 5.10 Rendered ORTEP of the molecular structure of $PdCl_2$(4-(4-HOC_6H_4)pyCH_2SMe) (**5c**), showing the partial atom labelling scheme. Displacement ellipsoids are drawn at the 50% probability level and H atoms are represented by circles of arbitrary size.

The complex $PdCl_2$(4-(4-$BnOC_6H_4$)pyCH_2SMe) (**5d**) (**Figure 5.12**) crystallises in the monoclinic space group $P2_1/c$ and was refined as a mononuclear compound with one molecule in the asymmetric unit. It has the same overall structure as the analogous complex **5c** with Pd–S, Pd–Cl_N and Pd–Cl_S distances of 2.2617(12), 2.2967(12) and 2.3305(12) Å, respectively, $\geq 3\sigma$ and an Pd–N distance of 2.037(3) Å within 1σ with those observed in **5c**. The complex is quite flat with only a small arene-arene dihedral twist of 19.8(1) ° between aromatic rings **R(I)** and **R(II)**. The arene-arene dihedral twist between **R(II)** and **R(III)** is larger at 26.6(1) °.

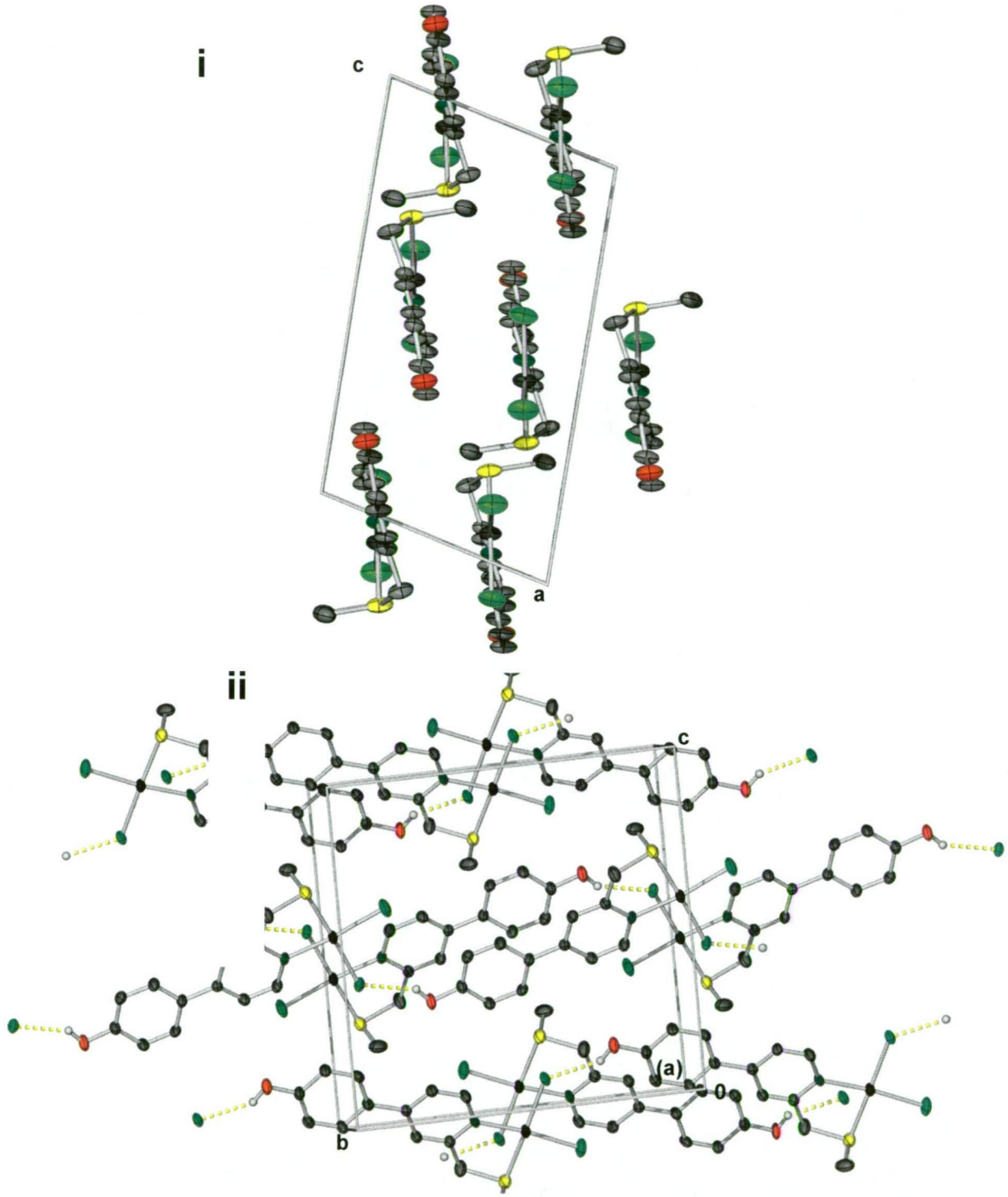

Figure 5.11 Unit cell contents of $PdCl_2(4\text{-}(4\text{-}HOC_6H_4)pyCH_2SMe)$ (**5c**), down *b*, **i** and through the polymeric strands, **ii**. Displacement ellipsoids are drawn at the 50% probability level, where shown H atoms are represented by circles of arbitrary size.

Within the crystal lattice of **5d** (**Figure 5.13**) the linear polymeric chains observed in **5b** and **5c** are absent, however the molecules retain a rough alignment of the now, quite extended polyaromatic ligand framework in the overall structure. π-Stacking between the molecules is limited to the central aryl rings (3.63_2 Å) that extends

indefinitely and may be caused by the influences of the greater torsion angle between the pyridyl and aryl rings and the incorporation of the saturated benzylic carbon centre. Coplanarity of metal coordination planes (3.63_2 Å) within these stacks is noted; however the metal centres are offset giving a metal-metal separation of 5.13_3 Å.

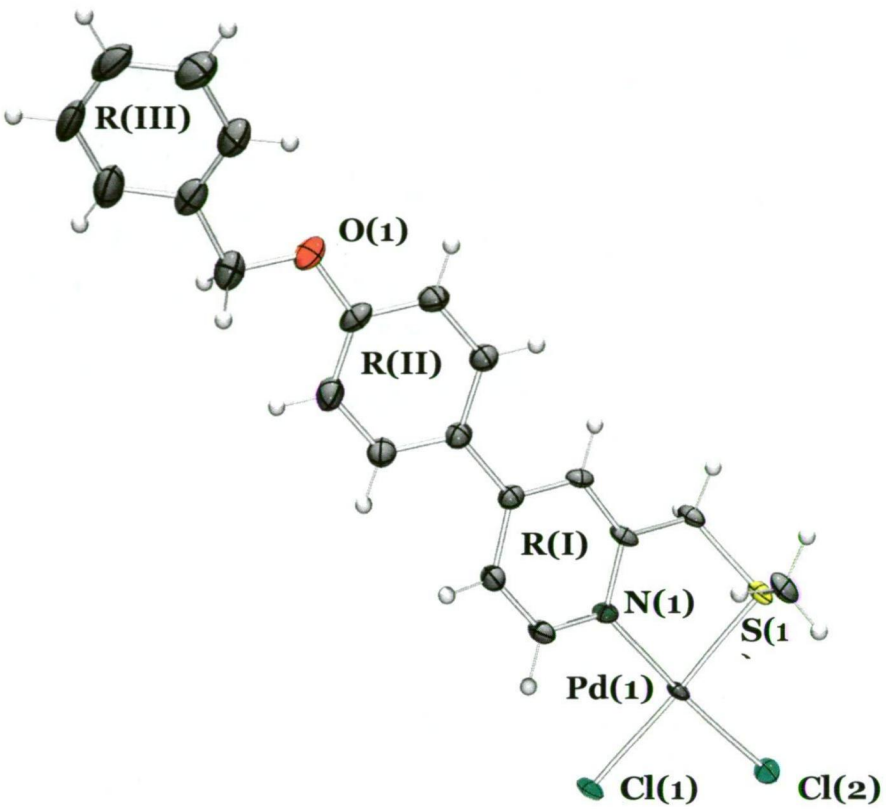

Figure 5.12 Rendered ORTEP of the molecular structure of $PdCl_2$(4-(4-$BnOC_6H_4$)pyCH_2SMe) (**5d**), showing the partial atom labelling scheme. Displacement ellipsoids are drawn at the 50% probability level and H atoms are represented by circles of arbitrary size.

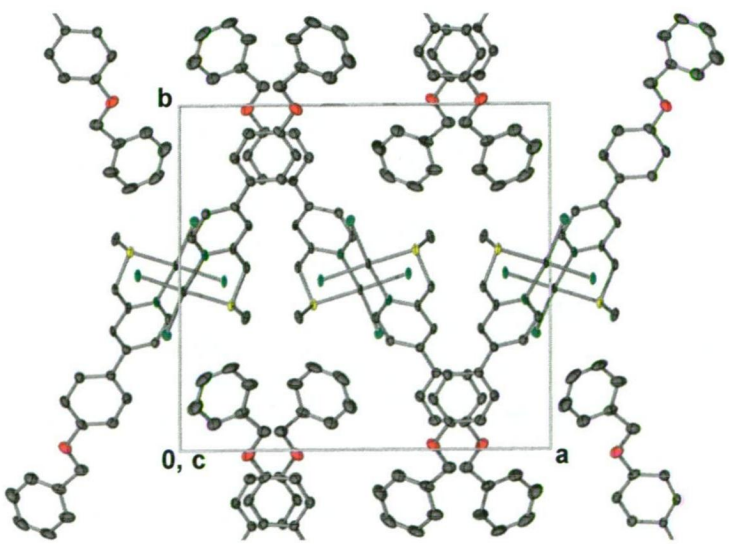

Figure 5.13 Unit cell contents of $PdCl_2$(4-(4-$BnOC_6H_4$)pyCH_2SMe) (**5d**) looking down *c*. Displacement ellipsoids are drawn at the 50% probability level and H atoms have been omitted for clarity.

	(5a)		(5b)		(5c)	(5d)
Bond distances (Å)		**Bond distances (Å)**		**Bond distances (Å)**		
N(1)–C(2)	1.331(10)	N(1)–C(2)	1.341(3)	Pd(1)–N(1)	2.039(8)	2.037(3)
C(21)–Br(1)	1.948(8)	C(21)–S(1)	1.809(3)	Pd(1)–S(1)	2.247(3)	2.2617(12)
C(2)–C(3)	1.386(11)	S(1)–C(22)	1.794(3)	Pd(1)–Cl(1)	2.321(3)	2.3305(12)
C(4)–Br(2)	1.869(8)	C(2)–C(3)	1.388(3)	Pd(1)–Cl(2)	2.299(3)	2.2967(12)
		O(1)–C(44)	1.353(3)			
				Bond angles (°)		
Bond angles (°)		**Bond angles (°)**		N(1)–Pd–S(1)	84.5(2)	84.58(8)
C(2)–N(1)–C(6)	124.1(7)	C(2)–N(1)–C(6)	117.0(19)	N(1)–Pd–Cl(1)	93.8(2)	93.31(8)
N(1)–C(2)–C(21)	119.1(7)	N(1)–C(2)–C(21)	116.6619)	N(1)–Pd–Cl(2)	174.3(2)	174.29(8)
N(1)–C(2)–C(21)–Br(1)	-75.4(8)	N(1)–C(2)–C(21)–S(1)	114.3(2)	S(1)–Pd–Cl(1)	178.29(10)	177.88(3)
				S(1)–Pd–Cl(2)	90.03(10)	90.40(4)
				N(1)–C(2)–C(21)–S(1)	26.2(14)	33.1(4)
				N(1)–Pd–S(1)–C(21)	22.1(5)	27.14(14)
				Pd–N(1)–C(2)–C(21)	-4.6(14)	-6.5(4)
				Pd–S(1)–C(21)–C(2)	-31.2(9)	-38.5(2)

Table 5.6 Selected bond distances (Å) and angles (°) of compounds **5a**, **5b**, **5c**, and **5d**.

5.2.5 Attachment of Ligand to Merrifield and Wang Resins

The commercial availability of polystyrene resins in a variety of cross-linked densities and particle sizes provides a large choice of resins for study. Two different commercially available resins were chosen for attachment to produce a supported catalyst. Merrifield resin, or (4-chloromethyl)polystyrene crosslinked with 1% divinylbenzene, and Wang resin, 4-(bromomethyl)phenoxymethyl styrene crosslinked with 1% divinylbenzene, are chosen due to their different functional groups and varying tether lengths from the polymer backbone.

The complex **5c** has low solubility in most common solvents, and therefore could not be added directly to the solid supports. Therefore, ligand is attached first, followed by addition of $PdCl_2(NCMe)_2$. Attachment of the ligand to the resins was achieved by base-assisted nucleophilic attack of the hydroxyl functionality of the ligand on the benzylic halide moiety of the resins, **Scheme 5.7**, following the success of the trial reactions described in **Section 5.2.1** (**Table 5.1**). Hünig's base (di-*i*-propylethylamine) was chosen as an appropriate base for attachment as it is a good base but a poor nucleophile, and thus considered ideal for facilitating the ligand attachment to the resin without possibly producing unwanted by products. Dimethylsulfoxide has been used recently as a solvent in anchoring ligands to organic monoliths,[41,42] but Hünig's base was found to be only partially soluble in dimethylsulfoxide. Furthermore, the quaternary ammonium salt formed upon addition of Hünig's base was completely insoluble in dimethylsulfoxide, thereby rendering the solvent unsuitable for the attachment procedure. Methanol has also been successfully utilised in attachment procedures,[58] but 4-(4-HOC_6H_4)pyCH_2SMe and the quaternary ammonium salt formed upon addition of Hünig's base have low solubility in methanol. Ethanol gave similar results, with temperatures >55 °C required for complete solubility. A second base, Bu^n_4NOH, was selected for testing in the attachment procedure with ethanol. This base was chosen as, like Hünig's base, it is a good non-nucleophilic base. Upon addition of Bu^n_4NOH the reagent 4-(4-HOC_6H_4)pyCH_2SMe was found to be completely soluble in an ethanol at room tempertaure.

The attachment reactions of 4-(4-HOC_6H_4)pyCH_2SMe to the resins were undertaken several times in ethanol at three temperatures with two concentrations of both

Hünig's base and Bu^n_4NOH. The functionalised resin was then reacted with a palladium source, and the palladium loading determinations were used to give an indication of the influence of temperature and concentration of base. To attach palladium to the system under similar conditions to those for synthesis of complex **5d**, the ligand functionalised resin was stirred in a solution of $PdCl_2(NCMe)_2$ in acetonitrile at room temperature overnight, after which time a sample was submitted for ICP-MS analysis, **Table 5.7** and **Table 5.8**. During each step of the attachment procedure great care was taken with vigorous washing of the resins to remove free ligand, base, or palladium.

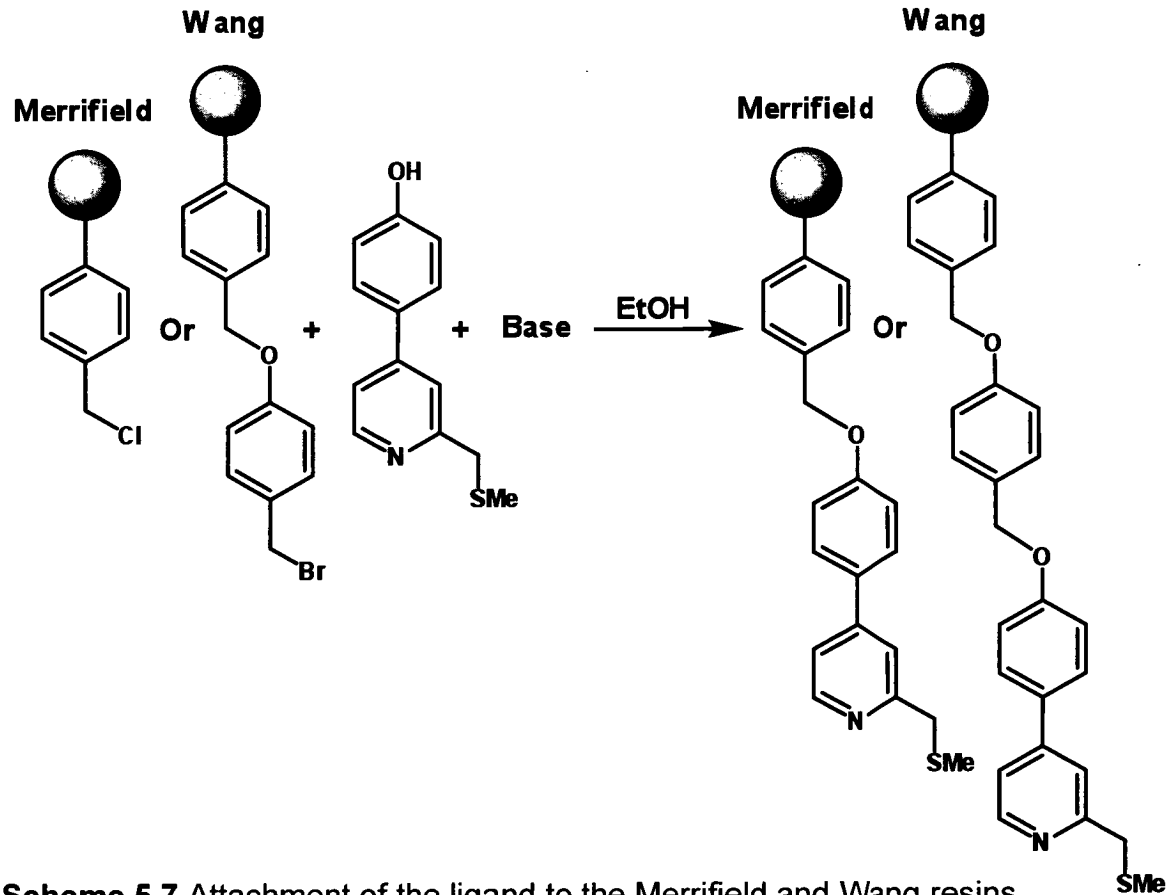

Scheme 5.7 Attachment of the ligand to the Merrifield and Wang resins

Resin	room temp 2 equiv. of base	room temp large excess of base	60 °C 2 equiv. of base	60 °C large excess of base	reflux 2 equiv. of base	reflux large excess of base
Merrifield	0.02	0.40	0.74	0.75	0.77	0.80
Wang	0.04	0.12	0.27	0.32	0.25	0.35

Table 5.7 Palladium loadings (wt%) of the resins, using Hünig's base in ethanol at different concentrations and temperatures during the attachment of 4-(4-HOC_6H_4)pyCH_2SMe.

Resin	60 °C large excess of base	reflux 2 equiv. of base	reflux large excess of base
Merrifield	0.72	0.45	0.79
Wang	0.35	0.10	0.42

Table 5.8 Palladium loadings (wt%) of the resins, using Bu^n_4NOH in ethanol at different concentrations and temperatures during the attachment of 4-(4-HOC_6H_4)pyCH_2SMe.

The ICP-MS results show that a large excess of base and heating at or close to reflux for the duration of the attachment procedure increases the palladium loading when using both bases. However, choice of base has essentially no effect on loading for the resins.

In order to determine whether the attachment procedure for the ligand had an effect on the morphology of the resins, scanning electron micrograph (SEM) images were taken of the resins before and after attachment. **Figure 5.14** show Merrifield and Wang resins before attachment, indicating spheres with no obvious structural peculiarities.

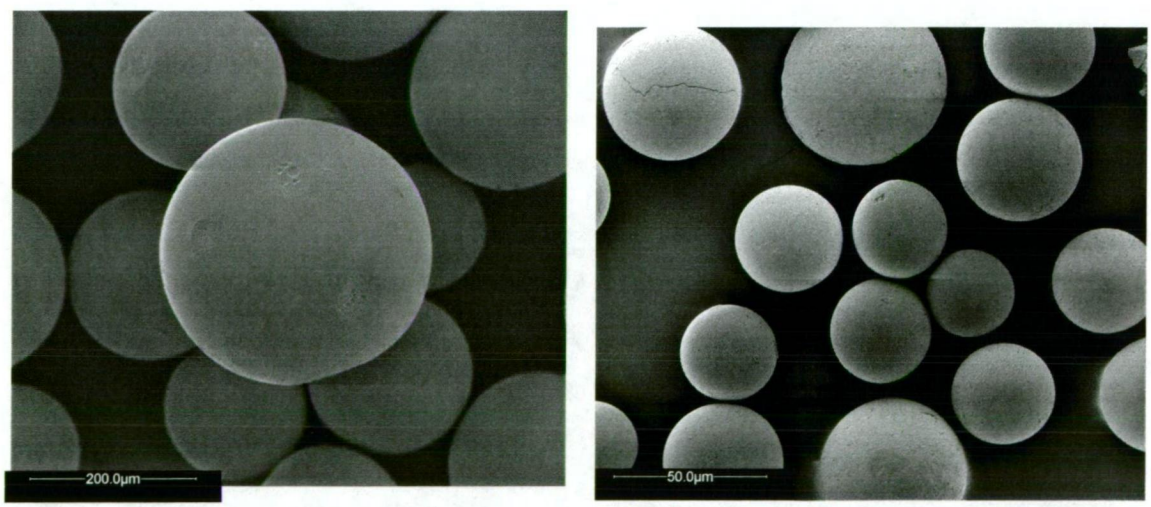

Figure 5.14 SEM images of the Merrifield (left) and Wang (right) resins before Pd loading. An accelerating voltage of 3.0 kV and working distances of 4.6 mm and 6.2 mm, for the Merrifield and Wang resins, respectively, were used for micrograph imaging.

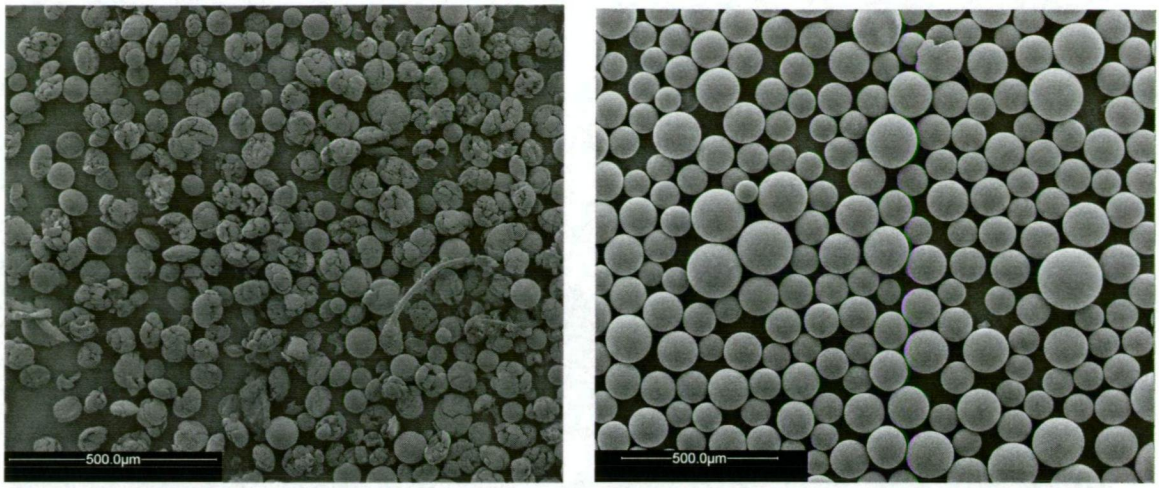

Figure 5.15 SEM images of the Merrifield and Wang resins after attachment of the ligand and palladium. An accelerating voltage of 3.0 kV and working distances of 5.6 mm and 6.1 mm for the Merrifield and Wang resins, respectively, were used for micrograph imaging.

Figure 5.15 shows that the mechanical action of vigorous stirring during the ligand attachment process has broken the spherical structure of the Merrifield resin while the Wang resin has remained unaffected. This "crushing" of the Merrifield resin, does not occur in the absence of stirring. Styring and co-workers state that mechanical failure of Merrifield resin supports is typical, and that heating while stirring is particularly detrimental to the bulk structure of the beads resulting, for some cases, in the formation of a fine powder.[78] Bead breakage may be one reason for the higher palladium loading on the Merrifield resin compared to that of the Wang resin, as breaking of the resin spheres may allow the ligand to access sites on a larger surface area.

5.2.6 Synthesis and Attachment of Ligand to Monolith

The synthesis of polymer monolith supports for chromatographic applications in analytical chemistry has been reported extensively in the literature, documenting multiple methods of preparation to give different properties to the support, *e.g.*, varying the monomers alters the surface chemistry, enabling different types of monolith to be synthesised,[79] while varying the porogen alters the pore sizes and surface area of the monolith.[30,79] There are two main methods of monolith synthesis, grafting and copolymerisation. Copolymerisation is the process where a functional

monomer, containing a particular desired functional group, is polymerised with a cross-linking monomer in the presence of a porogenic solvent. This method was chosen for the synthesis of the monolith used in this study as the reactive functional groups are directly incorporated in the polymer backbone,[80] very similar to that used in the synthesis of Merrifield resins.

For the development of monolith based microreactors, the monolith requires pores with a relatively low flow resistance in conjunction with a high surface area and reactive functional groups on the surface of the monolith for ligand attachment. A monolith fitting this description was developed by Fréchet,[30,31,33] formed by copolymerisation of CMS and DVB in a similar manner to (4-chloromethyl)polystyrene (**Scheme 5.1**, 1-2% crosslinker). The poly(chloromethylstyrene-*co*-divinylbenzene) (CMS/DVB) monolith formed has a pore size of ~1 μm in internal diameter and benzyl chloride functional groups suitable for ligand attachment. It has the necessary physical characteristics required for a microreactor, but is also directly structurally comparable to the Merrifield resin used in this study.

A bulk CMS/DVB monolith was prepared by the procedure outlined by Fréchet[30,31,33] and, when crushed to a fine powder with a mortar and pestle, the heteroleptic ligand 4-(4-HOC_6H_4)pyCH_2SMe and palladium were attached by the procedure used for the resins. Again, different solvent temperatures were used with two different bases and in two different concentrations to allow comparisons on loading, **Table 5.9**.

Base	room temp 2 equiv. of base	room temp large excess of base	60 °C 2 equiv. of base	60 °C large excess of base	reflux 2 equiv. of base	reflux large excess of base
Hünig's	0.06	0.20	0.28	0.57	0.38	0.82
Bu_4NOH	-	-	0.43	1.19	1.08	2.96

Table 5.9 Palladium loadings (wt%) of the monolith, using Hünig's base and Bu_4NOH in ethanol at different concentrations and different temperatures during the attachment of 4-(4-HOC_6H_4)pyCH_2SMe.

As was seen for the resin attachment experiments, heating at reflux for the duration of ligand attachment increases the palladium loading considerably for both bases. Unlike the resins, however, using a large excess of Bu^n_4NOH at high temperatures results in a much higher loading, by a factor of ~2 compared to that obtained using Hünig's base under the same conditions. As observed for the Wang resin, SEM images before and after palladium attachment showed no difference in overall appearance of the monolith. The SEM of the final palladium attached material shown in **Figure 5.14**.

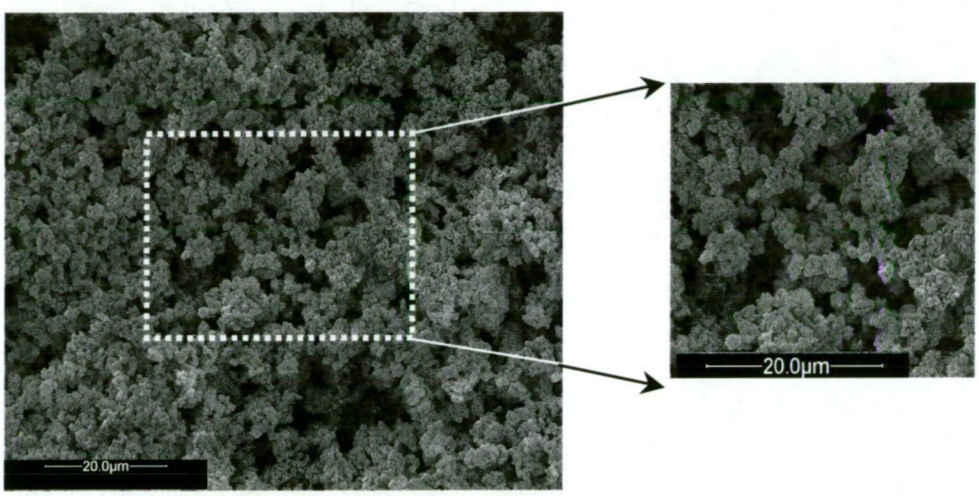

Figure 5.16 SEM of the bulk monolith after attachment of ligand and palladium (accelerating voltage of 3.0 kV, working distance of 4.5 mm, x 3000 magnification).

5.2.7 Catalysis Using Resins and Bulk Monolith

The catalytic activity of the functionalised resins and bulk monolith were tested in Heck (**Scheme 5.8**) and Suzuki (**Scheme 5.9**) reactions using various aryl halides as described in **Section 4.2.3** and **4.2.5**, with results compared against the model homogeneous palladium(II) precatalyst $PdCl_2(4\text{-}(4\text{-}BnOC_6H_4)pyCH_2SMe)$.

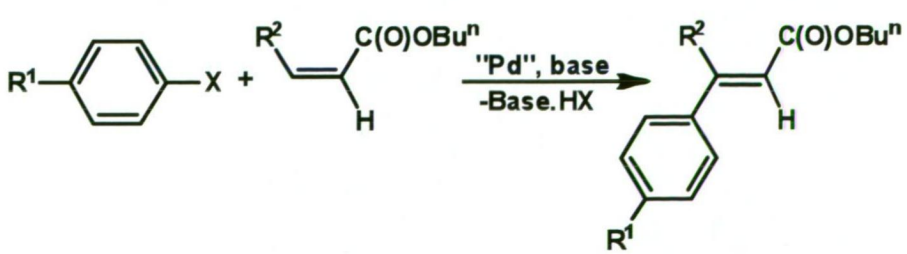

Scheme 5.8 The Heck coupling reaction.

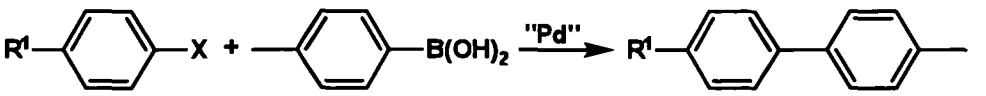

Scheme 5.9 The Suzuki coupling reaction.

Experiments were conducted to test for Heck catalytic activity of the support materials that had been treated in the manner described in **Section 5.2.5** for ligand attachment only and for palladium attachment only, **Figure 5.17**, **A** and **B**, respectively. In both cases, the materials (5 mg) were stirred with bromobenzene and *n*-butyl acrylate in DMA at 120 °C for 48 h.

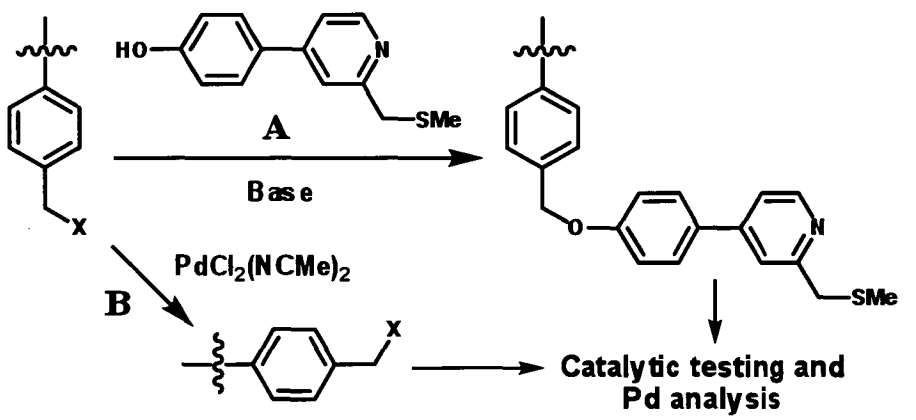

Figure 5.17 Catalytic and Pd loading experiments utilising partly modified polymeric supports.

No catalytic activity was displayed and ICP-MS analysis of the reaction eluent exhibited Pd loadings which were within one standard deviation of the instrument blank. Thus it can be assumed that any catalytic activity displayed by the materials (see below) are as a result of palladium anchored to ligand modified polymeric support materials. Modified bulk resins and monolith were tested in the Heck and Suzuki reactions using various aryl halides, **Tables 5.10** and **5.11**.

Entry	X	R^1	R^2	Merrifield Yield[a]	Wang Yield[a]	Monolith Yield[a]	TON[b]
1	I	H	H	100	100	100	8500, 20000, 5000
2	Br	H	H	95	86	93	8000, 17100, 5000
3	Br	Me	H	85	70	78	7200, 14000, 4000
4	Cl	4-COMe	H	12	<1	15	1000, <199, 804
5	Cl	H	H	<1	<1	1	<85, <199, 54
6[c]	I	H	Ph	100	100	100	8500, 20000, 5400
7[c]	Br	H	Ph	85	72	87	7200, 14000, 4700

All reactions were carried out with 5 mg of functionalised polymer, 3.0 mmol (0.3 M) of aryl halide, 4.5 mmol (0.45 M) of alkene, 6.0 mmol of Na_2CO_3, 4.5 mmol (0.45 M) of Bu^n_4NCl in 10 mL of DMA at 120 °C for 48 hr. **[a]** Determined by GC (diphenyl ether standard). **[b]** The TONs reported are for the functionalised Merrifield, Wang and Monolith with Pd loading based upon wt% of Pd (0.75 for Merrifield (0.012 mol%), 0.32 for Wang (0.005 mol%) and 1.19 for Monolith (0.019 mol%)). **[c]** For entries 6 and 7 > 99%, regioselectivity of the *trans* product was achieved.

Table 5.10 Results of catalytic testing in the Heck reaction using the three functionalised polymers.

Entry	X	R^1	Merrifield Yield[a]	Wang Yield[a]	Monolith Yield[a]	TON[b]
1	I	H	100	100	100	8500, 20000, 5400
2	Br	H	100	85	100	8500, 17000, 5400
3	Cl	4-COMe	8	<1	12	681, <199, 644

All reactions were carried out with 5 mg of functionalised polymer, 3.0 mmol (0.3 M) of aryl halide, 4.5 mmol (0.45 M) of boronic acid, 6.0 mmol of Na_2CO_3, 4.5 mmol (0.45 M) of Bu^n_4NCl in 10 ml of DMF:H_2O (3:1) mixture at 80 °C for 24 hr. [a] determined by GC (diphenyl ether standard). **[b]** The TONs reported are for the functionalised Merrifield, Wang and Monolith with Pd loading based upon wt% of Pd (0.75 for Merrifield (0.012 mol%), 0.32 for Wang (0.005 mol%) and 1.19 for Monolith (0.019 mol%)).

Table 5.11 Results of catalytic testing in the Suzuki reaction using the three functionalised polymers.

The resins and monolith were all effective in both Heck and Suzuki reactions achieving high TONs in both coupling reactions. In the Heck reaction high yields of cinnamate products were achieved using iodobenzene, bromobenzene, the deactivated aryl bromide 4-bromotoluene (entries 1 - 3) as substrates, furthermore

high yields of the tri-substituted alkene product utilising bromobenzene and *n*-butyl cinnamate with a regioselectivity of > 99% (entries 6 and 7) were achieved. For the Suzuki reaction all three supported catalytic systems displayed excellent activity with activation of both aryl iodides and aryl bromides in high yields. Moderate activation of 4-chloroacetophenone was achieved in both Heck (entry 4) and Suzuki (entry 3) reactions. These preliminary results provide an indication that with further catalyst design and development supported heteroleptic ligands involving *N,S* moieties such as those utilised here could be excellent catalysts in these catalytic systems.

The results for each polymeric support cannot be compared directly due to the differing Pd loadings of the materials, but a comparison of the catalytic activity of the functionalised support materials and the model palladium(II) complex $PdCl_2$(4-(4-$BnOC_6H_4$)pyCH_2SMe) is feasible. This was achieved by using the same Pd loading (mol%) of model complex as found for each of the polymeric support materials for both the Heck and the Suzuki reactions. Bromobenzene was chosen as the aryl halide in both reactions for comparison, **Table 5.12**.

Entry	0.012 mol% Pd Yield[a]	0.005 mol% Pd Yield[a]	0.019 mol% Pd Yield[a]	TON[b]
Heck	6	<1	11	511, <200, 590
Suzuki	57	6.4	64	4900, 1300, 3400

[a] determined by GC (diphenyl ether standard). [b] TONs are based upon Pd loadings described in table. The comparisons are based upon Merrifield resin 0.012 mol%, Wang resin 0.005 mol% and Monolith 0.019 mol%.

Table 5.12 Catalytic results of the model homogeneous precatalyst $PdCl_2$(4-(4-$BnOC_6H_4$)pyCH_2SMe) for Heck coupling of bromobenzene and *n*-butyl acrylate, and Suzuki coupling of bromobenzene and 4-tolylboronic acid.

The results show that the supported catalysts are superior to the model complex in both coupling reactions, giving further evidence that greater catalytic activities can be achieved by anchoring ligands to solid supports.

Palladium leaching studies were conducted on the functionalised resins and monolith for both the Heck (entry 2 for all supported catalysts) and the Suzuki (entry 2 for all

supported catalysts) reactions. After a catalytic reaction had taken place a 3 mL aliquot was then taken and once the volatiles were removed by evaporation, the residue was submitted for ICP-MS analysis. Due to the presence of Pd in most laboratory chemicals[81] a blank was conducted in which all the catalysis reagents except for the Pd source were placed into a flask and reacted in the usual manner for a Heck reaction. The results show that in all cases the leaching for the bulk resins and monolith were within one standard deviation of the blank, indicating that very little Pd was leached from any of the functionalised materials and that it may be possible for these materials to be recovered and utilised multiple times until catalyst deactivation.

5.2.8 Attachment of Ligand to Monolith in a Microreactor

A major challenge of flow-through supported catalysis systems is the utilisation of highly intensive surface properties as a factor in achieving higher conversion of substrates.[82] In order to fulfil this aim, the attachment of transition metal catalysts to monolith supports inside capillaries has been reported recently, with the ultimate aim of producing lab-on-a-chip devices.[41,42,58] These studies include synthesis of poly(glycidylmethacrylate-*co*-ethylene dimethacrylate) (GMA/EDMA) monoliths *in-situ* inside capillaries and attaching a phenanthroline-type ligands and palladium, thereby producing flow-through microreactors that could be tested in Suzuki catalysis.[41,42] An extension of this approach to CMS/DVB monoliths is in current development.[58] The attachment of a heteroleptic ligand/palladium described above continues the further development of this technology as well as further exploring the catalytic activity of the pyridine/chalcogen heteroleptic ligand system.

The CMS/DVB polymer monolith was prepared inside silica capillaries with an internal diameter of 250 μm after a modification of the surface of the inner wall following a procedure developed by Fréchet *et al.*[83] Surface modification places a silanol anchoring group on the capillary wall (**Figure 5.18**) which the monolith can grow from (thereby attaching it to the capillary walls), allowing complete filling of the capillary volume, prevention of monolith shrinkage and allowing application of high pressures without dislodging the monolith.

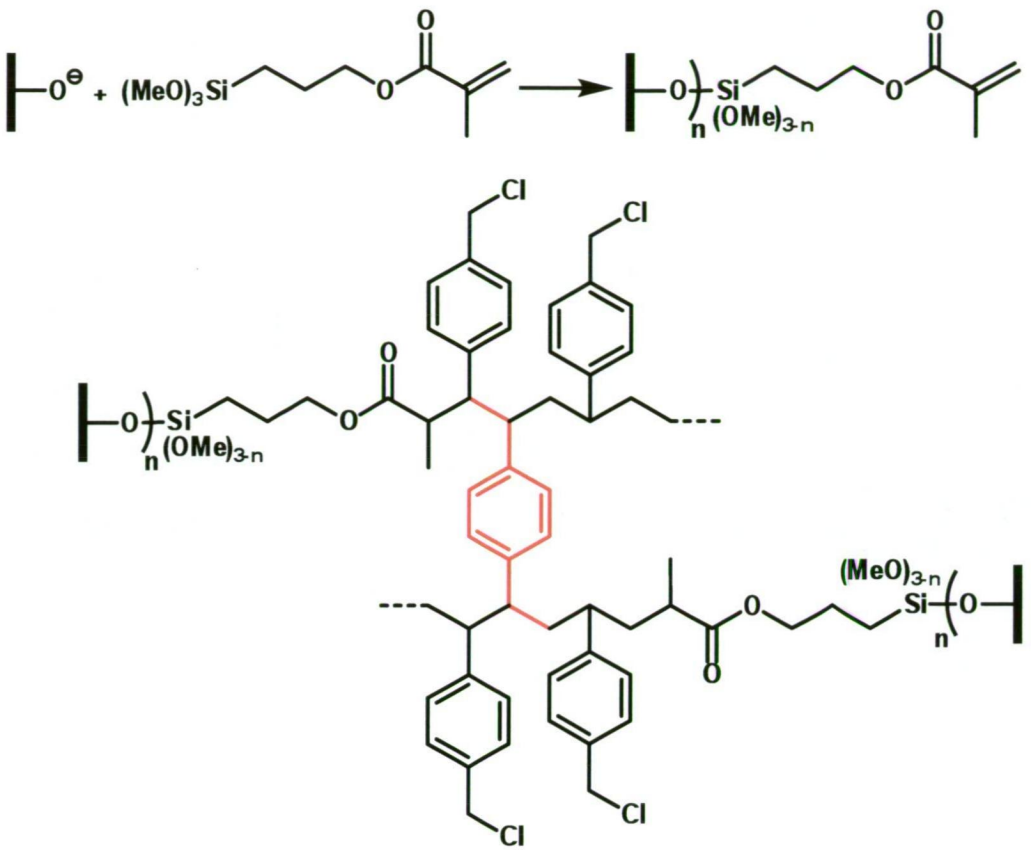

Figure 5.18 Surface modification of the capillary walls and consequent *in situ* monolith synthesis inside the capillary to form a microreactor. The schematic structure of the polymer is an alternative representation of the same structure illustrated in **Scheme 5.1**; cross-linker is shown in red.

A mixture containing 60% porogens (1-dodecanol and toluene), 24% CMS and 16% DVB were placed inside the capillaries according to a recommended reagent ratio.[30,31,33] This allows a suitable porosity and void volume of ~60% to be achieved, a level consistent with good flow-through and high surface area characteristics.[84] Once inside the capillaries, the mixture (containing radical initiator AIBN) was heated to 70 °C using a water bath to form the monolith inside the capillary with the surface modification successfully anchoring the monolith to the walls of the capillary.

The capillary filled monolith was functionalised with the heteroleptic ligand 4-(4-HOC_6H_4)pyCH_2SMe by flushing with the ligand in a solution of solvent and base as shown in **Figure 5.19**. It is particularly important that any solution being flushed

through the capillary is completely homogeneous as particulate matter will block the capillaries. Consequently, the base and solvent combination chosen was ethanol/Bu^n_4NOH, based upon the results of attachment trials (**Section 5.2.5** and **5.2.6**), which indicated 4-(4-HOC_6H_4)pyCH_2SMe was completely soluble in this solvent and base combination at room temperature, thereby removing the possibility of blockages during attachment.

The ethanolic Bu^n_4NOH and 4-(4-HOC_6H_4)pyCH_2SMe solution was filtered and flushed through the capillary at a relatively fast rate of 0.5 μL min^{-1} in one direction over 8 h, reversed and pumped in the other direction at the slower rate of 0.2 μL/min for 18 h in order to ensure maximum and uniform attachment of the ligand to the monolith filled capillary. The temperature for attachment was 60 °C, as this is the minimum temperature required to give good ligand attachment to the bulk monolith (**Table 5.10**). Once the ligand was attached, $PdCl_2(NCMe)_2$ was flushed through the capillary using the same flow rates as that for the ligand attachment, but at room temperature corresponding to bulk monolith treatment to produce the functioning flow-through microreactor.

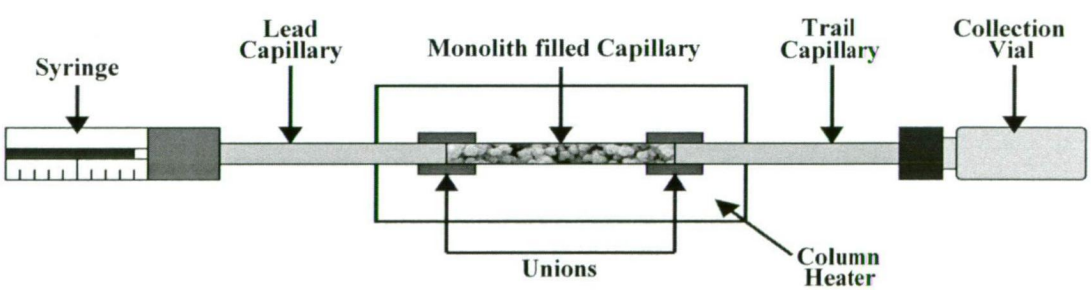

Figure 5.19 Syringe pump and column heater arrangement for experiments using capillaries.

SEM micrographs were taken of the capillary containing monolith before and after ligand/Pd attachment. As observed for the Wang resin and bulk monolith, the SEMs show no difference in the overall appearance of the blank and the ligand/palladium functionalised monolith. From the expanded picture, clear confirmation is given that the surface modification of the capillary walls successfully anchored to the formed monolith inside the capillary.

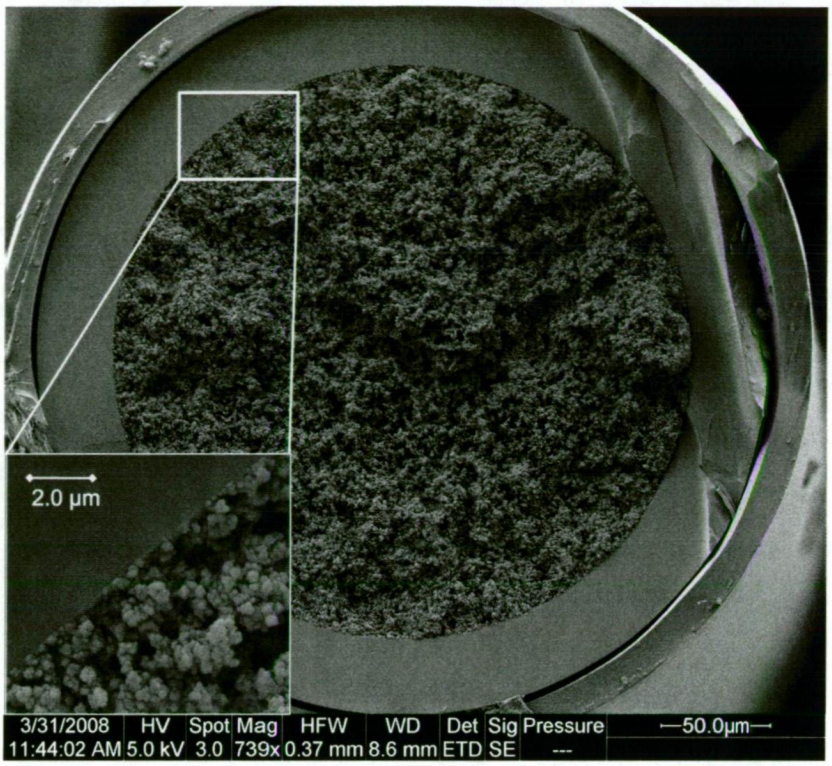

Figure 5.20 SEM of a cross section of a 250 µm capillary filled with CMS/DVB monolith, after ligand and palladium functionalisation.

5.2.9 Catalysis using the Microreactor

The catalytic activity of the microreactor was tested in Heck (**Scheme 5.8**) and Suzuki (**Scheme 5.9**) coupling reactions using various aryl halides as described for the bulk monolith.

Reactions undertaken using untreated monolith and ligand modified monolith (test **A**), **Figure 5.17**, yielded no catalytic activity. For test **B**, **Figure 5.17**, also giving no catalytic activity, $PdCl_2(NCMe)_2$ in MeCN was passed through the capillary at 0.5 µL min^{-1} for 8 h, followed by thorough flushing with MeCN. Heck reaction mixtures of bromobenzene, triethylamine, and *n*-butyl acrylate in DMA were passed through the capillary at 0.1 µL min^{-1} for 48 h at 120 °C, reaction tailings were analysed by GC.

Fully modified microreactors tested in the Heck and Suzuki reactions using various aryl halides gave the results shown in **Tables 5.13** and **5.14.**

Entry	X	R^1	R^2	Yield[a]
1	I	H	H	98
2	Br	H	H	45
3	Br	H	H	43[b]

The reactions were carried out with a 10 cm length of microreactor, 1.0 mmol (0.1 M) of aryl halide, 1.5 mmol (0.15 M) of alkene, 2.0 mmol (0.2 M) of NEt_3, in 10 mL of DMA at 120 °C for 24 hr. **[a]** Determined by GC (diphenyl ether standard). **[b]** A duplicate reaction run using the same capillary immediately after completion of the first reaction.

Table 5.13 The results of catalytic testing using a monolith filled microreactor for the Heck reaction.

Entry	X	R^1	Yield[a]
1	I	H	96
2	Br	H	65

The reactions were carried out with 10 cm length of microreactor, 1.0 mmol (0.1 M) of aryl halide, 1.5 mmol (0.15 M) of boronic acid, 2.0 mmol (0.2 M) of NEt_3, in 10 ml of DMF:H_2O (3:1) mixture at 80 °C for 24 hr. **[a]** Determined by GC (diphenyl ether standard).

Table 5.14 The results of catalytic testing using a monolith filled microreactor for the Suzuki reaction.

The preliminary results show that the microreactors are effective in both the Heck and Suzuki reactions with high product yields for aryl iodides and good to high yields for aryl bromides in the Suzuki reaction. The microreactor displayed little to no decrease in activity during repeat catalytic trials in the Heck reaction, as shown in entries 2 and 3 (**Table 5.13**). These are excellent preliminary results, indicating that microreactors based upon monolith filled capillaries functionalised with *N,S* heteroleptic ligands with further development could be very effective in catalytic C-C bond formation processes.

Palladium leach studies were conducted on the microreactor after both types of catalytic reaction, **Table 5.15**. As was observed for the bulk samples very little Pd leaching occurs during catalytic runs, with leaching decreasing by factor of 26 and 21 respectively in successive reactions. This effect, common in similar supported systems,[85] provides an indication that with further development, the microreactor

could be a viable means of synthesis without significant loss of palladium as an impurity in products.

Entry[a]	Pd Leached (wt%)
Heck	1.30
Heck[b]	0.05
Suzuki	0.84
Suzuki[b]	0.04

[a] In all cases the aryl halide used for the catalytic reaction was bromobenzene. Reaction tailings were filtered, evaporated to dryness and analysed by ICP-MS. [b] A repeat was conducted in the same capillary directly after the first reaction trial. The capillary was flushed between reactions using MeCN to avoid cross-contamination of Pd residue.

Table 5.15 Palladium leach data for the microreactor in both the Heck and Suzuki reactions.

5.3 Conclusion

Two new heteroleptic *N,S* ligand systems based upon a pyridine and thioether backbone, have been synthesised featuring hydroxyl (**VIII**) and benzylic (**IX**) functionalised aromatic rings in the 4- position of the pyridine ring. Dichloropalladium(II) complexes of these ligands were structurally characterised by single crystal diffraction, revealing interesting structural features.

A simple and direct method was developed for the synthesis of supported catalysts based upon Merrifield, Wang, and Monolith polymeric supports containing the 2-(methylthiomethyl)pyridine donor motif. These were successfully tested in Heck and Suzuki reactions and were shown to be highly active for aryl iodides and bromides, including tri-substituted alkene products with a >99% stereoselectivity in product formation. Activation of 4-chloroacetophenone was also achieved in both protocols indicating that, with further development, activation of deactivated aryl chlorides may be possible with this class of ligand. The catalytic activities of the heterogeneous catalysts were then compared to a closely related homogeneous palladium precatalyst which were all shown to be more active than the model palladium complex.

A fully functioning microreactor based upon a monolith filled capillary was developed and shown to be highly active for aryl iodides in both Heck and Suzuki reactions. Activation for aryl bromides was also achieved, and with further development of microreactor and catalytic conditions, high TONs for aryl bromides and chlorides may be possible.

5.4 Experimental

5.4.1 General Experimental

Dichloromethane was refluxed over calcium hydride and then distilled under dinitrogen prior to use. Chloroform was dried over 5 Å sieves and stored under argon. 4-Nitro-2-picoline *N*-oxide was purchased from the Oakwood. 4-Benzyloxyphenylboronic acid and 4-hydroxyphenylboronic acid were purchased from Boron Molecular Pty. Ltd.; 4-(bromomethyl)phenoxymethyl polystyrene (Wang Resin) was purchased from Novabiochem and stored between 2–8 °C; (4-chloromethyl)polystyrene (Merrifield Resin) was purchased from Fluka. Chloromethylstyrene (CMS) and divinylbenzene, purchased from Sigma-Aldrich Pty. Ltd., were distilled before use and stored at 2 °C under argon. 2,2′-Azobis-(2-isobutyronitrile) (AIBN) was purchased from MP Biomedicals Australasia Pty. Ltd. (Seven Hills, Australia) and recrystallised before use. All other reagents and solvents used were purchased from Aldrich and were used as received unless specified. Ultra high purity argon was purchased from BOC Gases. All manipulations were carried out under argon using standard Schlenk techniques unless specified.

^{1}H NMR spectra were recorded on a Varian Mercury Plus 300 NMR Spectrometer at 299.9 MHz at ambient temperature using deuterated chloroform ($CDCl_3$), referenced to residual solvent (7.25 ppm $CHCl_3$). Chemical shifts (δ) are reported in ppm and all coupling constants are given in Hz. Peak multiplicity is denoted as singlet (s), doublet (d), triplet (t), multiplet (m), doublet of doublets (dd), triplet of doublets (td), doublet of doublet of doublets (ddd), or broad (br). For assignments where peak multiplicity is in quotation marks *e.g.*, "d", the multiplicity of the peak is considered a "pseudo" assignment *i.e.* only appears to have that multiplicity at current magnet strength and may not in higher magnetic fields. A diagram for NMR assignments is

shown in **Figure 5.22**. All compounds were characterised by standard 2D NMR techniques.

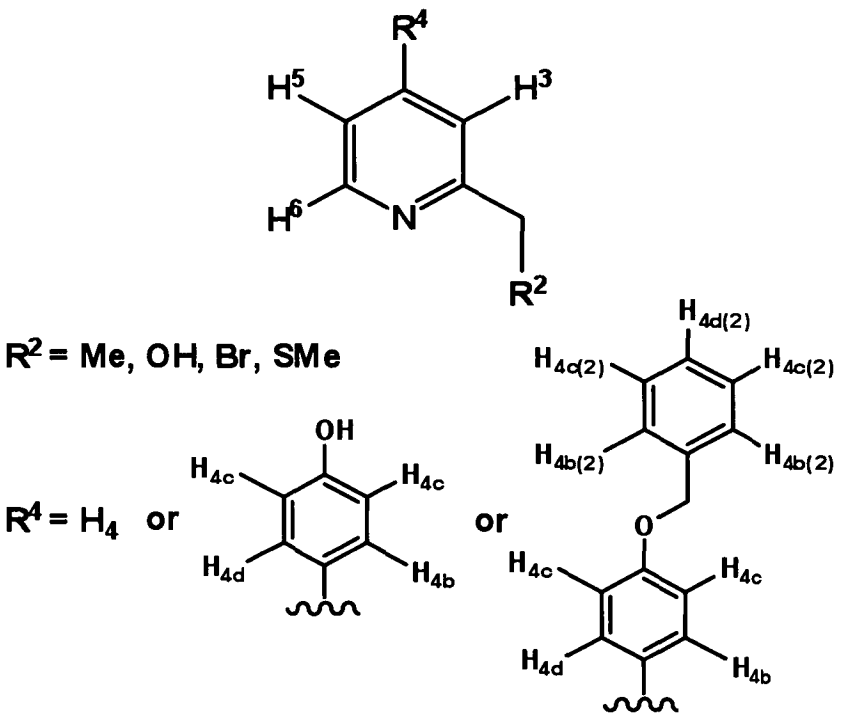

Figure 5.22 NMR assignment diagram

Microanalyses were performed by Dr. Thomas Rodemann of the Central Science Laboratory (CSL), University of Tasmania using a ThermoFinnigan Flash EA 1112 Series Elemental Analyser. Mass spectrometry was conducted by Dr. Noel Davies and Dr. Marshall Hughes of the CSL, University of Tasmania. The EI (Electron Ionisation) mass spectrometry was carried out using a Kratos ISQ mass spectrometer with a liquid matrix of nitrobenzyl alcohol using 10 kV Cs ions and a 5.3 kV accelerating voltage.

For the microreactor catalysis reactions, controlled solvent pumping was performed using a Harvard Apparatus model PHD 2000 (Holliston, Massachusetts, USA) twin syringe pump and 250 μL Hamilton (Reno, Nevada, USA) Gastight® glass syringes. All capillaries and syringes were connected using Upchurch Scientific (Oak Harbor, Washington, USA) capillary connections. Fused silica capillaries of internal diameter 250 μm with the outer surface coated with polyimide (Polymicro Technologies, Phoenix, Arizona) were heated using a Waters Millipore (Billerica, Massachusetts, USA) 112/WTC-120 temperature controlled column heater. Leading and trailing capillary sections were used to ensure that the whole microreactor was inside the

column heater. Polymerisations were performed using a temperature controlled water bath.

Scanning electron micrograph analysis of the resins and monolith were performed by the author in the Central Science Laboratory, University of Tasmania, using an FEI Quanta 600 MLA ESEM using an accelerating voltage and working distance recorded in the text.

The palladium content determinations of the resins and bulk monolith were performed by Dr. Ashley Townsend of the Central Science Laboratory (CSL), University of Tasmania using an Inductively Coupled Plasma Mass Spectrometer (ICP-MS). For preparation, samples (50-100 mg) were digested in freshly prepared *aqua regia* (4 mL) for 18 h with sonication, diluted to a final mass of 30 g, and indium (100 ppb) was added as an internal standard. The measurements were performed using an ELEMENT high resolution ICP-MS (Finnigan-MAT, Bremen, Germany) on the low resolution setting of 300 m/(Δm) at 10% valley definition; palladium was measured as a total of isotopes 105, 106 and 108.

GC-FID and GC-MS measurements on catalytic residue samples were performed by the author as described in **Section 4.4.1**, **Chapter 4**. GC-FID calibration was conducted as described in **Section 4.4.1**, **Chapter 4**.

Crystals of **5a**, **5b**, and **5c** were mounted on a glass fiber with the diffraction data collected at –80 °C by the author at the School of Chemistry, The University of Tasmania using an Enraf-Nonius CAD4 diffractometer as described in **Section 3.4.2**, **Chapter 3**. Crystals of **5d** were mounted on a Hampton Scientific cryoloop with diffraction data collected at –173 °C by the author at the PX1 beamline of the Australian Synchrotron.

5.4.2 Experimental Procedures

Synthesis of 4-bromo-2-methylpyridine *N*-oxide: 4-BrpyMe *N*-oxide (III)

Acetyl bromide (34.6 mL, 0.46 mol, 29 equiv.) was added portion-wise to a solution of 4-nitro-2-picoline *N*-oxide (2.47 g, 0.02 mol) in glacial acetic acid (35 mL) at 55

°C. The resulting solution was then heated to reflux with stirring for 2.5 h in air. After cooling to room temperature the solution was poured into crushed ice and made basic with K_2CO_3 and the product extracted with CH_2Cl_2 (4 x 30 mL). The combined organic phases were washed with brine and dried over Na_2SO_4. The solvent was removed *in vacuo* resulting in a pale orange oil which was used without further purification (2.75 g, 91%).

^{1}H NMR (299.9 MHz, 20 °C, $CDCl_3$): δ 8.11 (d, J = 6.9 Hz, 1H, H^6), 7.41 (d, J = 2.4 Hz, 1H, H^3), 7.27 (dd, J = 6.9, 2.4 Hz 1H, H^5), 2.48 (s, 3H, CH_3); **^{13}C(^{1}H) NMR (75.4 MHz, 20 °C, $CDCl_3$):** δ 150.6 (C^2), 140.2 (C^6), 129.6 (C^3), 127.0 (C^5), 119.4 (C^4), 17.9 (CH_3). **EI** ***m/z*** 187 $[M]^+$, $[^{12}C_6H_6{}^{79}Br^{14}N^{16}O$ 187]. **M.S. High res. Calcd for** "$[C_6H_6BrNO]^+$" = 186.96328 amu: **Found** M-H^+ = 186.96339 amu by EI.

Synthesis of 4-bromo-2-(hydroxymethyl)pyridine: 4-BrpyCH$_2$OH (V)

Under argon, trifluoroacetic acid anhydride (9.24 mL, 66.5 mmol, 5 equiv.) was added dropwise (with extreme caution) to a solution of 4-bromo-2-picoline *N*-oxide (2.50 g, 13.30 mmol) in dry CH_2Cl_2 (40 mL) at 0 °C. The resulting solution was then refluxed overnight with stirring. After cooling to room temperature the trifluoroacetic acid anhydride and CH_2Cl_2 were removed *in vacuo* resulting in a dark yellow oil; CH_2Cl_2 (40 mL) was added to the yellow oil, and with vigorous stirring, 2 M NaOH was added until the resulting biphasic mixture was basic (pH 12-14). Vigorous stirring was continued for 12 h under argon, and the mixture extracted with CH_2Cl_2 (3 x 30 mL). The combined organic phases were combined, washed with brine, and dried over Na_2SO_4. The solvent was removed *in vacuo*, resulting in a dark brown oil which was used without further purification (1.55 g, 62%).

^{1}H NMR (299.9 MHz, 20 °C, $CDCl_3$): δ 8.36 (d, J = 5.4 Hz, 1H, H^6), 7.52 (d, J= 1.8 Hz, 1H, H^3), 7.39 (dd, J = 5.4, 1.8 Hz 1H, H^5), 4.75 (s, 2H, CH_2), 4.16 (s, 1H, OH); **^{13}C(^{1}H) NMR (75.4 MHz, 20 °C, $CDCl_3$):** δ 161.1 (C^2), 149.2 (C^6), 134.1 (C^4), 126.0 (C^5), 124.3 (C^3), 63.9 (CH_2). **EI** ***m/z*** 187 $[M-H]^+$, $[^{12}C_6H_5{}^{79}Br^{14}N^{16}O$ 186]. **M.S. High res. Calcd for** "$[C_6H_5BrNO]^+$" = 185.95545 amu: **Found** M-H^+ = 185.95554 amu by EI.

Synthesis of 4-bromo-2-(bromomethyl)pyridine hydrobromide:

4-BrpyCH$_2$Br.HBr (VI)

PBr_3 (5.55 mL, 59.0 mmol, 6 equiv.) was added dropwise (with extreme caution) to a solution of 4-bromo-2-hydroxymethylpyridine (1.85 g, 9.84 mmol) in dry $CHCl_3$ (50 mL) at 0 °C; the resulting solution was then heated to reflux overnight with vigorous stirring. After cooling to room temperature the solution was poured into crushed ice and made basic (pH ~14) with K_2CO_3 and the product extracted with CH_2Cl_2 (4 x 50 mL). The combined organic phases were washed with brine, and dried over Na_2SO_4. The solvent was removed *in vacuo* resulting in a pale brown oil which was then dissolved in diethyl ether and, with vigorous stirring, HBr/AcOH solution was added drop-wise precipitating an off-white solid which was collected by filtration and washed thoroughly with diethyl ether (2.84 g, 87%). Single crystals for X-ray structure determination and elemental analysis were grown from vapour diffusion of diethyl ether into nitromethane.

^{1}H NMR (299.9 MHz, 20 °C, CD_3OD): δ 8.70 (d, J = 6.3 Hz, 1H, H^6), 8.42 (d, J = 2.1 Hz, 1H, H^3), 7.39 (dd, J = 6.3, 2.1 Hz 1H, H^5), 4.81 (s, 2H, CH_2); **^{13}C(^{1}H) NMR (75.4 MHz, 20 °C, CD_3OD):** δ 153.4 (C^2), 144.1 (C^4), 143.7 (C^6), 130.9 (C^5), 130.1 (C^3), 24.8 (CH_2); ***Anal.* Calcd. for $C_6H_6Br_3N$:** C, 21.72; H, 1.82; N, 4.22. **Found:** C, 22.12; H, 1.78; N, 4.20; **EI** ***m/z*** 251 $[M\text{-}HBr]^+$, $[^{12}C_6H_5{}^{79}Br_2{}^{14}N$ 251]. **M.S. High res. Calcd for** "$[C_6H_5Br_2N]^{+}$" = 248.87887 amu: **Found** $M\text{-}HBr^+$ = 248.87875 amu by EI.

Synthesis of 4-bromo-2-(methylthiomethyl)pyridine: 4-BrpyCH$_2$SMe (VII)

A stirred solution of sodium thiomethoxide (0.35 g, 4.97 mmol, 1.1 equiv.) in dry ethanol (50 mL) was added dropwise over 10 min to a stirred solution of 4-bromo-2-bromomethylpyridine hydrobromide (1.50 g, 4.52 mmol) and powdered KOH (0.76 g, 13.6 mmol, 3 equiv.) in dry ethanol (100 mL). Stirring was continued for 12 h after which the ethanol was removed *in vacuo*, resulting in a pale brown oil. Water (25 mL) was added and the product extracted with dichloromethane (3 x 25 mL). The combined organic phases were washed with brine and dried over Na_2SO_4. The solvent was removed *in vacuo*, resulting in a pale brown oil which was then purified

by column chromatography [40% ethyl acetate in hexanes] to give a pale yellow oil (0.75 g, 72%).

^{1}H NMR (299.9 MHz, 20 °C, $CDCl_3$): δ 8.34 (d, J = 5.4 Hz, 1H, H^6), 7.56 (d, J = 1.8 Hz, 1H, H^3), 7.34 (dd, J = 5.4, 1.8 Hz 1H, H^5), 3.76 (s, 2H, CH_2) 2.06 (s, 3H, S-CH_3) ; **^{13}C(^{1}H) NMR (75.4 MHz, 20 °C, CD_3OD):** δ 159.1 (C^2), 148.6 (C^6), 132.7 (C^4), 125.4 (C^3), 124.4 (C^5), 38.5 (CH_2) 14.2 (S–CH_3); **EI** ***m/z*** 218 $[M]^+$, [$^{12}C_7H_8{}^{79}Br^{14}N^{32}S$ 218]. **M.S. High res. Calcd for** "$[C_7H_8BrNS]^+$" = 216.95608 amu: **Found** M^+ = 216.95611 amu by EI.

Synthesis of 4-(4-hydroxyphenyl)-2-(methylthiomethyl)pyridine: 4-$HOC_6H_4pyCH_2SMe$ (VIII)

A solution of 4-bromo-2-(methylthiomethyl)pyridine (1.50 g, 6.88 mmol) and $Pd(PPh_3)_4$ (0.397 g, 5 mol%) in toluene (28 mL) was treated with a degassed solution of Na_2CO_3 (1.60 g, 13.1 mmol, 2.2 equiv.) in H_2O (14 mL), followed by a solution of 4-hydroxyphenylboronic acid (1.42 g, 10.3 mmol, 1.5 equiv.) in MeOH (10 mL). The resulting mixture was then stirred at 95 °C for 6 h under Ar. Another 0.5 equiv. (0.474 g) of 4-hydroxyphenylboronic acid and 1 mol% of catalyst (0.079 g) were added to the solution and refluxing continued for a further 6 h. The solution was then cooled to room temperature and treated with a saturated solution of Na_2CO_3. The product was extracted with CH_2Cl_2 (3 x 25 mL), the combined organic layers washed with saturated sodium chloride solution, dried over Na_2SO_4 and the solvent removed *in vacuo* to give in a dark oil. The oil was dissolved in dichloromethane (5 mL) and hexane added to precipitate a tan solid (1.56 g, 98%). The product was then recrystallised from hot ethanol to give a dark brown solid (1.43 g, 90%).

^{1}H NMR (299.9 MHz, 20 °C, $(CD_3)_2SO$): δ 8.43 (d, J = 5.1 Hz, 1H, H^6), 7.62 (m, 3H, H^3, H^{4b}), 7.47 (d, J = 4.2 Hz, 2H, H^5), 6.87 (d, J = 8.7 Hz, 2H, H^{4c}), 3.77 (s, 2H, CH_2), 2.49 (s, 3H, S–CH_3) ppm; **^{13}C(^{1}H) NMR (75.4 MHz, 20 °C, $(CD_3)_2SO$):** δ 159.7 (C^2), 159.5 (C-OH), 150.2 (C^6), 148.1 (C^4), 128.7 (C^{4b}), 128.2 (C^{4a}), 120.0 (C^3), 119.2 (C^5), 116.7 (C^{4c}), 15.4 (S–CH_3), ppm; ***Anal.*** **Calcd. for $C_{13}H_{13}NSO$:** C, 67.50; H, 5.66; N, 6.06%. Found: C, 67.54; H, 5.62; N, 6.11%. **APCI** ***m/z*** 232 $[M+H]^+$,

[$^{12}C_{13}H_{14}{}^{14}N^{16}O^{32}S$ 232]. **M.S. High res. Calcd for** "$[C_{13}H_{14}NOS]^+$" = 232.07961 amu: **Found** $M+H^+$ = 232.07941 amu by APCI.

Synthesis of 4-(4-benzyloxy)-2-(methylthiomethyl)pyridine: 4-(BnOC$_6$H$_4$)pyCH$_2$SMe (IX)

This compound was prepared from 4-bromo-2-(methylthiomethyl)pyridine (1.50 g, 6.88 mmol) and 4-benzyloxyphenylboronic acid (2.35 g, 10.3 mmol, 1.5 equiv.) using a similar procedure to that described for 4-(4-HOC$_6$H$_4$)pyCH$_2$SMe. The product was purified by column chromatography [40% ethyl acetate in hexanes] to remove contamination by benzylphenylether, giving a pale yellow oil (1.88 g, 85%).

^{1}H NMR (299.9 MHz, 20 °C, (CD$_3$)$_2$SO): δ 8.53 (d, *J* = 5.4 Hz, 1H, H^6), 7.76 (dd, *J* = 5.4, 1.8 Hz, 1H, H^5), 7.60 (d, *J* = 8.7 Hz, 2H, H^{4b}), 7.56 (d, *J* = 1.8 Hz, 1H, H^3) 7.46-7.34 (m, 5H, H$^{4b(2)}$, H$^{4c(2)}$, H$^{4d(2)}$), 7.07 (d, *J* = 8.7 Hz, 1H, H^{4c}), 5.12 (s, 2H, CH$_2$), 3.86 (s, 2H, S–CH$_2$), 2.10 (s, 3H, S–CH$_3$) ppm; **^{13}C(^{1}H) NMR (75.4 MHz, 20 °C, (CD$_3$)$_2$SO):** δ 160.1 (C^2), 158.9 (C^{4d}), 149.4 (C^6), 149.1 (C^4), 136.8 (C$^{4a(2)}$), 128.9 (C^{4b}), 128.6 (C$^{4c(2)}$), 128.4 (C$^{4d(2)}$), 127.7 (C$^{4b(2)}$), 120.7 (C^5), 119.8 (C^3), 115.7 (C^{4c}), 70.0 (CH$_2$), 40.0 (S–CH$_2$), 22.9 (S–CH$_3$), ppm; ***Anal.* Calcd. for C$_{13}$H$_{13}$NSO:** C, 74.73; H, 5.96; N, 4.36%. Found: C, 74.80; H, 5.90; N, 4.41%. **EI *m/z*** 321 $[M]^+$, [$^{12}C_{20}H_{19}{}^{14}N^{16}O^{32}S$ 321]. **M.S. High res. Calcd for** "$[C_{20}H_{19}NOS]^+$" = 321.11873 amu: **Found** M^+ = 321.11868 amu by EI.

Synthesis of Dichloro(4-(4-hydroxyphenyl)-2-(methylthiomethyl)pyridine)-palladium(II): PdCl$_2$(4-(4-HOC$_6$H$_4$)pyCH$_2$SMe)

PdCl$_2$(NCMe)$_2$ (0.15 g, 0.64 mmol) was added to a stirred suspension of 4-(4-hydroxyphenyl)-2-methylthiomethylpyridine (0.18 g, 0.77 mmol, 1.2 equiv.) in dry acetonitrile (30 mL). The brown suspension was stirred for 12 h at 50 °C. The solvent was then reduced in *vacuo* to *ca.* 5 mL and diethyl ether was added precipitating the title complex as yellow solid which was filtered and washed with diethyl ether (0.23 g, 87%). Single crystals suitable for X-ray structure determination and elemental analysis were grown from vapour diffusion of diethyl ether into nitromethane.

^{1}H NMR (299.9 MHz, 20 °C, $(CD_3)_2SO$): δ 10.18 (s, 1H, OH), 8.99 (d, J = 6.6 Hz, 1H, H^6), 8.04 (d, J = 1.8 Hz, 1H, H^3), 7.83 (dd, J = 6.6, 1.8 Hz, 2H, H^5), 7.78 (d, J = 8.7 Hz, 2H, H^{4b}), 6.91 (d, J = 8.7 Hz, 2H, H^{4c}), 4.76, 4.47 (AB spin system, J = 16.5 Hz, 2H, CH_2), 2.55 (s, 3H, S–CH_3) ppm; **$^{13}C(^1H)$ NMR (75.4 MHz, 20 °C, $(CD_3)_2SO$):** δ 163.8 (C^2), 160.9 (HO-C), 151.7 (C^6), 150.5 (C^4), 129.7 (C^{4b}), 125.7 (C^{4a}), 120.7 (C^5), 120.4 (C^3), 117.0 (C^{4c}), 45.3 (CH_2) 22.9 (S–CH_3), ppm; ***Anal.* Calcd. for $PdC_{13}H_{13}NSOCl_2$:** C, 38.21; H, 3.21; N, 3.43; S, 7.85%. Found: C, 38.30; H, 3.07; N, 3.67; S, 7.45%. **LSIMS** ***m/z*** 373 $[M\text{-}Cl]^+$, [$^{12}C_{13}H_{13}{}^{35}Cl^{14}N^{32}S^{16}O^{106}Pd$ 373]. **M.S. High res. Calcd for** "$[PdC_{13}H_{13}ClNSO]^+$" = 371.94412 amu: **Found** M^+ = 371.94521 amu by EI.

Synthesis of Dichloro(4-(4-benzyloxyphenyl)-2-(methylthiomethyl)pyridine)-palladium(II): $PdCl_2(4\text{-}(4\text{-}BnOC_6H_4)pyCH_2SMe)$

$PdCl_2(NCMe)_2$ (0.15 g, 0.64 mmol) was added to a stirred suspension of 4-(benzyloxyphenyl)-2-(methylthiomethyl)pyridine (0.25 g, 0.77 mmol, 1.2 equiv.) in dry acetonitrile (30 mL), instantly affording a bright yellow suspension which was stirred for 12 h at room temperature. The solvent was then reduced *in vacuo* to *ca.* 5 mL and diethyl ether was added. The title complex was collected by filtration as a bright yellow solid and washed with diethyl ether (0.27 g, 85%). Single crystals suitable for X-ray structure determination and elemental analysis were grown from vapour diffusion of diethyl ether into nitromethane.

^{1}H NMR (299.9 MHz, 20 °C, $(CD_3)_2SO$): δ 9.02 (d, J = 6.3 Hz, 1H, H^6), 8.10 (d, J = 1.8 Hz, 1H, H^3), 7.89 (m, 3H, H^5, H^{4b}), 7.39 (m, 5H, $H^{4b(2)}$, $H^{4c(2)}$, $H^{4d(2)}$), 7.19 (d, J = 8.7 Hz, 1H, H^6), 5.19 (s, 2H, CH_2), 4.77, 4.48 (AB spin system, J = 16.8 Hz, 2H, S–CH_2), 2.55 (s, 3H, S–CH_3) ppm; **$^{13}C(^1H)$ NMR (75.4 MHz, 20 °C, $(CD_3)_2SO$):** δ 163.9 (C^2), 161.3 (C^{4d}), 151.7 (C^6), 150.2 (C^4), 137.3 ($C^{4a(2)}$), 129.6 (C^{4b}), 129.2 ($C^{4c(2)}$), 128.7 ($C^{4d(2)}$), 128.5 ($C^{4b(2)}$), 127.6 (C^{4a}), 121.1 (C^5), 120.9 (C^3), 116.4 (C^{4c}), 70.1 (CH_2), 45.3 (S–CH_2), 22.9 (S–CH_3), ppm; ***Anal.* Calcd. for $PdC_{20}H_{19}NSOCl_2$:** C, 48.16; H, 3.84; N, 2.81%. Found: C, 47.89; H, 3.74; N, 2.72%. **LSIMS** ***m/z*** 463 $[M\text{-}Cl]^+$, [$^{12}C_{20}H_{19}{}^{35}Cl^{14}N^{32}S^{16}O^{106}Pd$ 463]. **M.S. High res. Calcd for** "$[PdC_{20}H_{19}ClNSO]^+$" = 461.99107 amu: **Found** M^+ = 461.99215 amu by EI.

General procedure for ligand attachment to resins

Resin (0.05 g) was added to a suspension of 4-(4-hydroxyphenyl)-2-methylthiomethylpyridine (0.08 g, 0.35 mmol) and base (1.75 mmol) in ethanol (5 mL). The mixture was stirred for 24 h at reflux after which the resin was filtered under vacuum, resuspended in ethanol, stirred vigorously for 30 min, and recovered again by filtration. The resin was washed twice more with ethanol, and dried *in vacuo*.

General procedure for synthesis of bulk monolith

The monolith was prepared by thoroughly mixing toluene (0.606 mL) and 1-dodecanol (1.53 mL), to which chloromethylstyrene (CMS, 0.48 g), divinylbenzene (DVB, 0.72 g) and 2,2-azobis-(2-isobutyronitrile) (AIBN, 12 mg) were added and the solution purged with nitrogen for 10 min prior to use. The monolith formed after heating at 70 °C for 24 h was broken up and washed with tetrahydrofuran in a Soxhlet apparatus for 14 h, and then dried *in vacuo*.

General procedure for ligand attachment to bulk monolith

Monolith (0.05 g) was finely ground in a mortar and pestle and added to a suspension of 4-(4-hydroxyphenyl)-2-methylthiomethylpyridine (0.08 g, 0.35 mmol) and base (1.75 mmol) in ethanol (5 mL). The mixture was stirred for 24 h at reflux after which the monolith was filtered under vacuum, resuspended in ethanol, stirred vigorously for 30 min, and recovered again by filtration. The monolith was washed twice more with ethanol, and dried *in vacuo*.

Palladium attachment to resins and bulk monolith

Modified resin or monolith (0.05 g) was added to a solution of $PdCl_2(NCMe)_2$ (0.70 g) in acetonitrile (5 mL) and the mixture was stirred for 24 h at room temperature. The monolith was then filtered under vacuum, resuspended in acetonitrile, stirred vigorously for 30 min, and recovered again by filtration. The monolith was washed twice more with acetonitrile, and dried *in vacuo*.

General procedure for cross-coupling reactions for resins and bulk monolith:

Heck

The aryl halide (3.0 mmol) was added to a solution of *n*-butylacrylate (0.65 mL, 4.5 mmol), Na_2CO_3 (2.0 equiv.), catalyst (5.0 mg) and Bu^n_4NCl (1.5 equiv.) in DMA under argon. The resulting mixture was then stirred at 120 °C for 48 h under Ar. Once cooled to room temperature, diphenyl ether was added (0.170 g, 1.0 mmol) and an aliquot (1.50 mL) was taken and diluted with CH_2Cl_2 then washed three times with an aqueous solution saturated with NaCl. The organic layer was extracted, dried over $MgSO_4$ and filtered. Yields were determined by GC-FID.

Suzuki

The aryl halide (3.0 mmol) was added to a solution of tolylboronic acid (0.612 g, 4.5 mmol), Na_2CO_3 (2.0 equiv.), and catalyst (5.0 mg) in a 3:1 mixture of DMF:H_2O (10 mL) under argon. The resulting mixture was then stirred at 80 °C for 24 h under Ar. Once cooled to room temperature, diphenylether was added (0.170 g, 1.0 mmol) and an aliquot (1.50 mL) was taken and diluted with CH_2Cl_2 then washed three times with an aqueous solution saturated with NaCl. The organic layer was extracted, dried over $MgSO_4$ and filtered. Yields were determined by GC-FID.

General procedure for surface modification of capillaries and synthesis of monolith

Prior to the monolith attachment the inner surface of capillaries were modified by briefly rinsing the capillary with acetone followed by 0.2 M NaOH (2.0 μL min^{-1}) for 2 h. The capillaries were washed with water, and rinsed with 0.2 M HCl (2.0 μL min^{-1}) for 2 h before being rinsed with water, followed by ethanol (2.0 μL min^{-1}) for 30 min and finally the surface modifying agent (solution of 20 wt.% of 3-(trimethoxysilyl)propyl methacrylate) in ethanol adjusted to pH 5, 0.25 μL min^{-1}) was passed through the capillaries for 1 h.[23] The capillaries were then washed with acetone and dried by passing air through the capillaries for 24 h. Toluene (0.606 mL) and 1-dodecanol (1.53 mL) were thoroughly mixed and, to this, chloromethylstyrene (CMS, 0.48 g), divinylbenzene (DVB, 0.72 g) and 2,2-azobis-(2-isobutyronitrile) (AIBN, 12 mg) were added and the solution purged with nitrogen

for 10 min prior to use. The capillaries were completely filled with the CMS/DVB pre-polymerisation mixture until no air bubbles were apparent, sealed at both ends and placed in a water bath at 70 °C for 20 h. The monolith filled capillary was then flushed with THF (2.0 μL min^{-1}, 1 h).

Ligand attachment to monolith in capillaries

The monolith filled capillary was flushed with ethanol for 30 min at 60 °C (2.0 μL min^{-1}). A filtered solution of 4-(4-hydroxyphenyl)-2-methylthiomethyl-pyridine (85 mg) and Bu^n_4NOH (1.5 mL) in ethanol (3.5 mL) was pumped through the capillary at 60 °C for 18 h (0.2 μL min^{-1}), then the capillary was reversed and the solution was pumped for a further 8 h (0.5 μL min^{-1}). The capillary was washed with ethanol for 1 h (2.0 μL min^{-1}) to remove unreacted ligand and base from the monolith.

Palladium attachment to monolith in capillaries

The monolith filled capillary was flushed with acetonitrile for 30 min at room temperature (2.0 μL min^{-1}). A filtered solution of $PdCl_2(NCMe)_2$ (10 mg) in acetonitrile (2 mL) was pumped through the capillary at room temperature for 8 h (0.5 μL min^{-1}), then the capillary was reversed and the solution was pumped for a further 18 h (0.2 μL min^{-1}). The capillary was flushed with acetonitrile for 1 h (2.0 μL min^{-1}).

General procedure for cross-coupling reactions in capillaries:

Heck

To equilibrate the microreactor prior to the reaction, the capillary (10 cm) was flushed with DMA (3:1) for 1 h at rt (2.0 μL min-1), then with solvent mixture containing 2 M of Et_3N for 2 h at 80 °C (2.0 μL min-1) with the microreactor placed in the preheated column heater. The reaction mixtures were passed once through the capillary at a flow rate of 0.1 μL min-1 for 24 h. The product was collected from the opposing end and analysed by GC-FID.

Suzuki

To equilibrate the microreactor prior to the reaction, the capillary (10 cm) was flushed with DMF/H_2O (3:1) for 1 h at rt (2.0 μL min-1), then with solvent mixture containing 2 M of Et_3N for 2 h at 80 °C (2.0 μL min-1) with the microreactor placed in the preheated column heater. The reaction mixtures were passed once through the capillary at a flow rate of 0.1 μL min-1 for 24 h. The product was collected from the opposing end and analysed by GC-FID.

5.5 References

1. Negishi, E-I. *Handbook of Organopalladium Chemistry for Organic Synthesis Volume I:* New York, **2002**.
2. Negishi, E-I. *Handbook of Organopalladium Chemistry for Organic Synthesis Volume II:* New York, **2002**.
3. Yin, L.; Liebscher J. *Chem. Rev.* **2007**, *107*, 133.
4. Garrett, C. E.; Prasad, K. *Adv. Synth. Catal.* **2004**, *346*, 889.
5. Welch, C. J.; Albaneze-Walker, J.; Leonard, W. R.; Biba, M.; Dasilva, J.; Henderson, D.; Laing, B.; Mathre, D. J.; Spencer, S.; Bu, X.; Wang, T. *Org. Process Res. Dev.* **2005**, *9*, 198.
6. Zapf, A.; Beller, M. *Top. Catal.* **2002**, *19*, 101.
7. de Vries, J. G. *Can. J. Chem.* **2001**, *79*, 1086.
8. Baumeister, P.; Meyer, W.; Oertle, K.; Seifert, G.; Steiner, H. *Chimia* **1997**, *51*, 144.
9. Blaser, H.-U.; Indolese, A.; Schnyder, A.; Steiner, H.; Studer, M. *J. Mol. Catal. A: Chem.* **2001**, *173*, 3.
10. Eisenstadt, A. *Chem. Ind. (Dekker)* **1998**, *75*, 415.
11. Bhanage, B. M.; Arial, M. *Catal. Rev.* **2001**, *43*, 315.
12. Tucker, C. E.; de Vries, J. G. *Top. Catal.* **2002**, *19*, 111.
13. Weck, M.; Jones, C. W. *Inorg. Chem.* **2007**, *46*, 1865.
14. Ley, S. V.; Baxendale, I. R.; Bream, R. N.; Jackson, P. S.; Leach, A. G.; Longbotom, D. A.; Nesi, M.; Scott, J. S.; Storer, R. I.; Taylor, S. J. *J. Chem. Soc., Perkin Trans. 1* **2000**, 3815.

15. Phan, N. T. S.; Van Der Sluys, M.; Jones, C. W. *J. Mol. Catal. A: Chem.* **2006**, *348*, 609.
16. Biffis, A.; Zecca, M.; Basato, M. *J. Mol. Catal. A: Chem.* **2001**, *173*, 249.
17. Leadbeater, N. E.; Marco, M. *Chem. Rev.* **2002**, *102*, 3217.
18. Köhler, K.; Kleist, W.; Pröckl, S. S. *Inorg. Chem.* **2007**, *46*, 1876.
19. Djakovitch, L.; Wagner, M.; Hartung, C. G.; Beller, M.; Köhler, K. *J. Mol. Catal. A: Chem.* **2004**, *219*, 121.
20. Heidenreich, R. G.; Krauter, J. G. E.; Pietsch, J.; Köhler, K. *J. Mol. Catal. A: Chem.* **2002**, *182-3*, 499.
21. Djakovitch, L.; Dufaud, V.; Zaidi, R. *Adv. Synth. Catal.* **2006**, *348*, 715.
22. Li, J.; Mau, A. W. H.; Strauss, C. R. *J. Chem. Soc., Chem. Commun.* **1997**, 1275.
23. Ramchandani, R. K.; Uphade, B. S.; Vinod, M. P.; Wakharhar, R. D.; Choudhary, V. R.; Sudalai, A. *Chem. Commun.* **1997**, 2071.
24. Merrifield, R. B. *J. Am. Chem. Soc.* **1963**, *85*, 2149.
25. Massa, D. J.; Robello, D.R. **2005**, www.chem.rochester.edu/~chem421/polymod3.htm, Department of Chemistry, University of Rochester, accessed 20/09/08.
26. Dörwald, F. Z. *Organic Synthesis on Solid Phase*; VCH-Wiley: Weinheim, Germany, **2000**.
27. Phan, N. T. S.; Brown, D. H.; Styring, P. *Green Chem.* **2004**, *234*, 1.
28. Altava, B.; Burguete, M. I,; García-Verdugo, E.; Karbass, N.; Luis, S. V.; Puzary, A.; Sans, V. *Tetrahedron Lett.* **2006**, *47*, 2311.
29. Lenaerts, P.; Driesen, K.; Van Deun, R.; Binnemans, K. *Chem. Mater.* **2005**, *17*, 2148.
30. Wang Q. C.; Svec F.; Fréchet J. M. J. *Anal. Chem.* **1995**, *67*, 670.
31. Peters, E. C.; Svec, F.; Fréchet, J. M. J. *Adv. Mater.* **1999**, *11*, 1169.
32. Buchmeiser, M. R. *Polymer*, **2007**, *48*, 2187.
33. Tripp, J.; Svec, F.; Fréchet, J. M. J. *J. Comb. Chem.* **2001**, *3*, 216.
34. Bolton K. *Honours Thesis*, University of Tasmania, **2005**.
35. Minakuchi, H.; Ishizuka, N.; Nakanishi, K.; Soga, N.; Tanaka, N. *J. Chromatogr. A* **1998**, *828*, 83.
36. Schweitz, L.; Andersson, L.; Nilsson, S. *J. Chromatogr. A* **1998**, *817*, 5.
37. Xie, S. F.; Svec, F.; Fréchet, J. M. J. *Chem. Mater.* **1998**, *10*, 4072.
38. Nikbin, N.; Ladlow, M.; Ley, S. V. *Org. Proc. Res. Dev.* **2007**, *11*, 4584.

39. Karbass, N.; Sans, V.; Garcia-Verdugo, E.; Burguete, M. I.; Luis S. V. *Chem. Commun.* **2006**, 3095.
40. Solodenko, W.; Wen, H.; Leue, S.; Stuhlmann, F.; Sourkouni-Argirusi, G.; Jas, G.; Schönfeld, H.; Kunz, U.; Kirschning, A. *Eur. J. Org. Chem.* **2004**, 3601.
41. Bolton, K. F.; Canty, A. J.; Deverell, J. A.; Guijt, R. M.; Hilder, E. F.; Rodemann, T.; Smith, J. A. *Tetrahedron Lett.* **2006**, *47*, 9321.
42. Canty, A. J.; Deverell, J. A.; Gömann, A.; Guijt, R. M.; Rodemann, T.; Smith, J. A. *Aust. J. Chem.* **2008**, *61*, 630.
43. Brown, J.F.; Krajnc, P.; Cameron, N. R. *Ind. Eng. Chem. Res.* **2005,** *44,* 8565.
44. Ehrfeld, W.; Hessel, V.; Löwe, H. *Microreactors: New Technology for Modern Chemistry*, Wiley-VCH, Weinheim, **2000**.
45. Jähnisch, K.; Hessel, V.; Löwe, H.; Baerns, M. *Angew. Chem. Int. Ed.* **2004,** *43*, 406.
46. Geyer, K.; Codée, J. D. C.; Seeberger, P. H. *Chem. Eur. J.* **2006,** *12*, 8434.
47. Brivio, M.; Verboom, W.; Reinhoudt, D. N. *Lab Chip,* **2006**, *6*, 329-344.
48. Watts, P.; Haswell, S. J. *Chem. Soc. Rev.* **2005**, *34*, 235.
49. Watts, P.; Wiles, C. *Chem. Commun.* **2007**, 443.
50. Haeberle, S.; Zengerle, R. *Lab Chip*, **2007**, *7*, 1094.
51. Hessel, V.; Löwe, H. *Chem. Eng. Technol.* **2005**, *28*, 267.
52. Ahmed-Omer, B.; Brandt, J. C.; Wirth, T. *Org. Biomol. Chem.* **2007**, *5*, 733.
53. Mason B. P.; Price K. E.; Steinbacher J. L.; Bogdan A. R.; McQuade D. T. *Chem. Rev.* **2007**, *107*, 2300.
54. Svec, F.; Fréchet, J. M. J. *J. Anal. Chem.* **1992**, *64*, 820.
55. Svec, F.; Fréchet, J. M. J. *J. Ind. Eng. Chem. Res.* **1999**, *38*, 34.
56. Svec, F.; Huber, C. G. *Anal. Chem.* **2006**, *78*, 2101.
57. Comer E.; Organ, M. G. *Chem. Eur. J.* **2005**, *11*, 7223.
58. Gömann, A.; Deverell, J. A.; Munting, K. F.; Jones, R. C.; Rodemann, T.; Canty, A. J.; Smith, J. A.; Guijt, R. M. *Tetrahedron*, **2009**, *65*, 1450.
59. Ghera, E.; Ben-David, Y.; Rapoport, H. *J. Org. Chem.* **1983**, *48*, 774.
60. Asimori, A.; Ono, T.; Uchida, T.; Ohtaki Y.; Fukaya, C.; Watanabe, M.; Yokoyama, K. *Chem. Pharm. Bull.* **1990**, *38*, 2446.
61. Malinowski, M.; Kaczmarek, L. *Synthesis* **1987**, 1013.
62. Kaczmarek, L.; Balicki, R.; Malinowski, M. *J. Prakt. Chem.* **1990**, *332*, 423.
63. Ryzhakov, A. V.; Andreev, V. P.; Rodina, L. L. *Heterocycles* **2003**, *60*, 419.
64. Maerker, G.; Case F. H. *J. Am. Chem. Soc.* **1958**, *80,* 2745.

65. van den Heuvel, M.; van den Berg, T. A.; Kellogg, R. M.; Choma, C. T.; Feringa, B. L. *J. Org. Chem.* **2004**, *69,* 250.

66. Canovese, L.; Visentin, F.; Uguagliati, P.; Chessa, G.; Pesce A. *J. Organomet. Chem.* **1998**, *566*, 61.

67. Davies, D. T. *Aromatic Heterocyclic Chemistry*: Oxford University Press, New York, **1999**.

68. Lozano,V.; Jones P. G. *Acta Cryst.* **2004**, *C60*, o653.

69. Jones P. G.; Vancea, F.; Herbst-Irmer, R. *Acta Cryst.* **2002**, *C58*, o665.

70. Kang, H.; Facchetti, A.; Jiang, H.; Cariati, E.; Righetto, S.; Ugo, R.; Zuccàccia, C.; Macchioni, A.; Stern, C. L.; Liu, Z.; Ho, S.-T.; Brown, E. C.; Ratner, M. A.; Marks, T. J. *J. Am. Chem. Soc.* **2007**, *129*, 3267.

71. Schulz, B.; Bricks, J.; Li, Y.-Q.; Resch-Genger. U.; Reck, G. *Acta Cryst.* **2004**, *C60*, o402.

72. Database of average bond-lengths in organic compounds: Allen, F. H.; Kennard, O.; Watson, D. G.; Brammer, L.; Orpen, A. G.; Taylor, R. *J. Chem. Soc., Perkin Trans. 2* **1987**, S1.

73. Würthner, F.; Yao, S.; Debaerdemaeker, T.; Wortmann, R. *J. Am. Chem. Soc.* **2002**, *124*, 9431.

74. Davies, P. J.; Veldman, N.; Grove D. M.; Spek, A. L.; Lutz, B. T. G.; van Koten, G. *Angew. Chem. Int. Ed.* **1996**, *35*, 1959.

75. Albrecht, M.; Lutz, M.; Schreurs A. M. M.; Lutz, E. T. H.; Spek, A. L.; van Koten, G. *J. Chem. Soc., Dalton Trans.* **2000**, 3797.

76. Mehendale, N. C.; Lutz, M.; Spek, A. L.; Klein Gebbink, R. J. M.; van Goten, G. *J. Organomet. Chem.* **2008**, *693*, 2791.

77. Cambridge Crystal Data base, **http://www.ccdc.cam.ac.uk/**, accessed 20/01/09.

78. Phan, N. T. S.; Khan, J.; Styring P. *Tetrahedron* **2005**, *61*, 12065.

79. Xie, S.; Svec, F. Fréchet J. M. J. *J. Polymer Sci., Part A, Polymer Chem.* **1997**, *35*, 1013.

80. Svec, F; Tennikova, T. B.; Deyl, Z. *Monolithic Materials: Preparation, Properties and Applications*: Elsevier, New York, **2003**.

81. Arvela, R. K.; Leadbeater, N. E.; Sangi, M. S.; Williams, V. A.; Granados, P.; Singer, R. D. *J. Org. Chem.* **2005**, *70*, 161.

82. He, P.; Haswell, S. J.; Fletcher, P. D. I. *Lab Chip* **2004**, *4*, 38.

83. Rohr, T.; Hilder, E. F.; Donovan, J. J.; Svec, F; Fréchet J. M. J. *Macromolecules*, **2003**, *36*, 1677.

84. Svec, F.; Fréchet, J. M. J. *Chem. Mater.* **1995**, *7*, 707.

85. Schwarz, J.; Böhm, V. P. W.; Gardiner, M. G.; Grosche, M.; Herrmann, W. A.; Hieringer, W.; Raudaschl-Sieber, G. *Chem. Eur. J.* **2000**, *6*, 1773.

Chapter Six

Dichloropalladium(II) Complexes Containing Heteroleptic Ligands in Sonogashira Reaction Conditions. Formation of Tetra-substituted Benzenes

6.1 Introduction

In view of positive outcomes from studies of complexes of *N,E* heteroleptic ligands as precatalysts in Heck and Suzuki catalysis, the dichloropalladium(II) complex $PdCl_2(pyCH_2SMe)$ was studied under Sonogashira reaction conditions, **Scheme 6.1**, for aryl halides and aryl acetylenes as substrates. Detailed mechanisms for both the copper co-catalysed and copper-free Sonogashira reactions can be found in **Chapter 1, Section 1.6.2.**

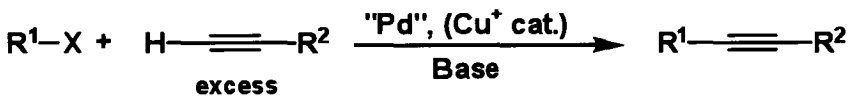

R^1 = aryl, heteroaryl, vinyl
R^2 = aryl, heteroaryl, alkenyl, alkyl, SiR_3
X = Halide, Triflate

Scheme 6.1 General catalytic scheme for the Sonogashira reaction. Cuprous iodide is optionally added as a co-catalyst.

In view of the unexpected results reported here which were uncovered at a late stage and a very comprehensive study required for full validation of results, the report in this Chapter is a preliminary exploration of this chemistry.

6.2 Results and Discussion

6.2.1 Preliminary Catalytic Testing Using an Activated Aryl Halide

Initial testing was conducted using an activated aryl halide (4-iodonitrobenzene) and excess phenylacetylene at the relatively high reaction temperature of 120 °C to enhance the potential for reaction, **Scheme 6.2.**

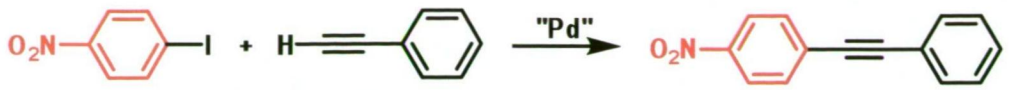

I

Scheme 6.2 First test reaction of 4-iodonitrobenzene and phenylacetylene, showing anticipated Sonogashira product.

Catalytic studies of copper-free Sonogashira reactions often use conditions similar to those typically used for the Suzuki reaction: a polar solvent such as DMF, or DMAc, bases such as metal carbonates or amines and tetrabutylammonium salts such as Bu^n_4NCl as phase transfer reagents with reaction duration usually no longer than 24 h. From these observations, the reaction conditions adopted for the Sonogashira chemistry in this study involved minor modifications from that used in the Heck reactions: The test was conducted under argon for 24 h with the reaction mixture containing Na_2CO_3 (base), Bu^n_4NCl (phase transfer reagent), and 1 mol% of the complex $PdCl_2(pyCH_2SMe)$ in anhydrous *N*,*N*-dimethylacetamide. Upon completion, the reaction solution had changed colour from yellow to dark red, from which an aliquot was taken and analysed by GC-MS. The analysis showed that the expected Sonogashira coupling product, **I**, had not formed, but indicated the presence of a sole unknown product with a molecular mass of 427.

Isolation and purification of the product was difficult using standard column chromatography techniques, with compound streaking evident using various solvent combinations. Isolation was finally achieved by means of HPLC purification techniques by Dr. Noel Davies (Central Science Laboratory, University of Tasmania) using an analytical C_{18} column (3.9 x 150 mm), an isocratic gradient of the eluent (90% MeOH and 10% of 2% acetic acid in H_2O) and UV detection. An analytical HPLC column was utilised as preparative size columns were not available. This process was repeated 55 times, collecting only the desired fraction, allowing the isolation of a pure unknown product as a pale yellow crystalline solid. The small quantity of the isolated material (< 0.4 mg), precluded identification by ^1H NMR techniques. The sample was dissolved in chloroform yielding yellow microcrystals (average crystal size 5 x 10 x 5 μm) which were analysed by X-ray diffraction techniques using a CCD area detector at Monash University (Dr. Craig Forsyth). However, due to the size and weak diffracting nature of the crystals, only a weak partial data set was obtained which did not allow positive identification.

Subsequently, the sample was analysed at the Australian Synchrotron by Dr. Tom Caradoc-Davies on the PX2 beamline, from which a structure was obtained identifying the isolated product as a tetrasubstituted benzene, 1,3,5-triphenyl-2-(4-nitrophenyl)benzene (**6a**), **Figure 6.1**.

Compound **6a** crystallises in the triclinic space group $P\square$ with the asymmetric unit comprised of one molecule. The overall structure of **6a** is similar to other tetrasubstituted benzenes such as 2,6-bis(4-iodophenyl)-4-(4-methoxyphenyl)-1-4-tolylbenzene[1] and 2,4,6,-2',4',6'-hexaphenyl-1,1'-biphenyl.[2] The central aromatic ring of **6a** is planar (rms of atoms = 0.0141 Å) with all aromatic rings attached to this central ring arranged in a propeller arrangement. The nitro functionalised aromatic ring **R(I)** forms a dihedral angle of 67.43(6) ° with the central ring, while the three phenyl rings, **R(II)**, **R(III)**, and **R(IV)** form dihedral angles of 43.33(8), 49.37(9), and 50.46(7) °, respectively, to the central ring. The nitro functionality is not planar with respect to **R(I)**, forming a dihedral angle of 16.7(21) °, typical for nitro-substituted aromatic molecules such as 4,4'-dinitrobiphenyl urea clathrate which displays a dihedral angle of 12.8_1.[3]

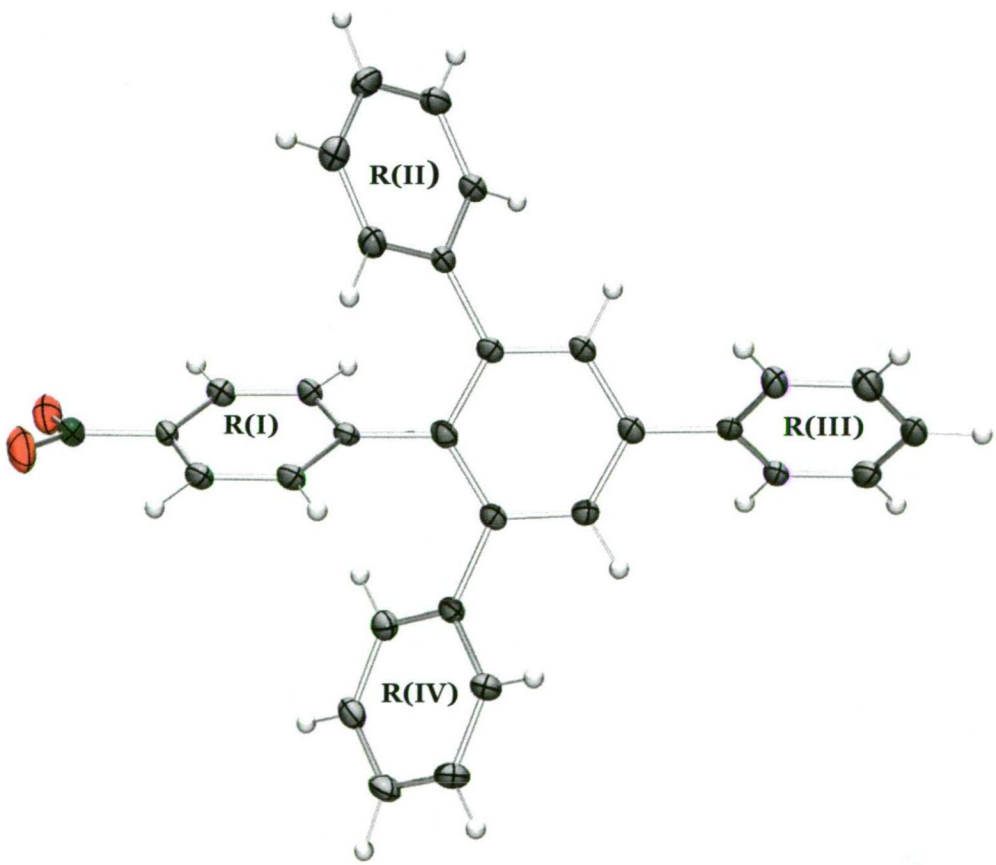

Figure 6.1 A rendered ORTEP of the molecular structure of tetrasubstituted benzene **6a**. Displacement ellipsoids are drawn at the 50% probability level and H atoms are represented by circles of arbitrary size.

Within the crystal lattice of **6a** (**Figure 6.2**) the molecules are orientated into a head-tail arrangement with its neighbours weakly stacked in the *b* direction, with no evidence of π-stacking or hydrogen bonding interactions between neighbouring molecules.

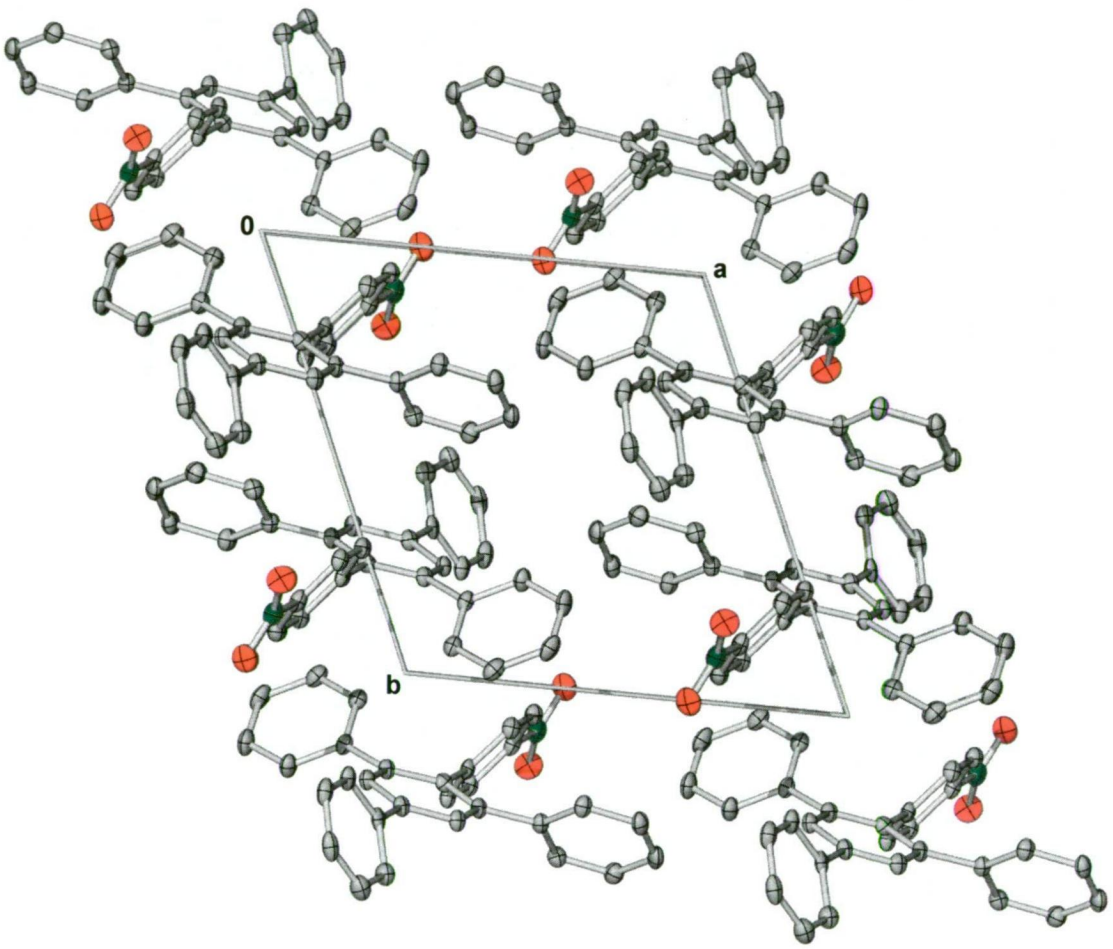

Figure 6.2 Unit cell contents of **6a** looking down *c*. Displacement ellipsoids are drawn at the 50% probability level. H atoms have been omitted for clarity.

Despite isolation and purification by HPLC, an evaluation of the yield has not been possible to date for **6a**. This is largely due to the difficulty in producing an appropriate standard with similar GC-MS characteristics. Currently, a synthetic method is being developed from which an appropriate structural analogue of **6a** will be produced. This will allow accurate calibration of catalytic runs using GC-MS.

The synthesis of **6a** is, apparently, the first reported synthesis of a tetrasubstituted benzene from common Sonogashira conditions (for general reviews see Chinchilla, Sonogashira and Brandsma).[4-6] However, before an extensive study into product formation was undertaken, a second catalytic reaction was tested in order to determine whether the formation of tetrasubstituted benzenes is limited to the use of 4-iodonitrobenzene as a substrate. The reaction explored used 4-iodotoluene and phenylacetylene as substrates, **Scheme 6.3**.

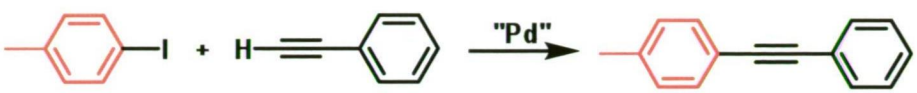

II

Scheme 6.3 Second test reaction of 4-iodotoluene and phenylacetylene, showing the anticipated Sonogashira product.

GC-MS analysis showed no indication of the formation of the Sonogashira product **II** but three product peaks with molecular masses of 396, **Figure 6.3**.

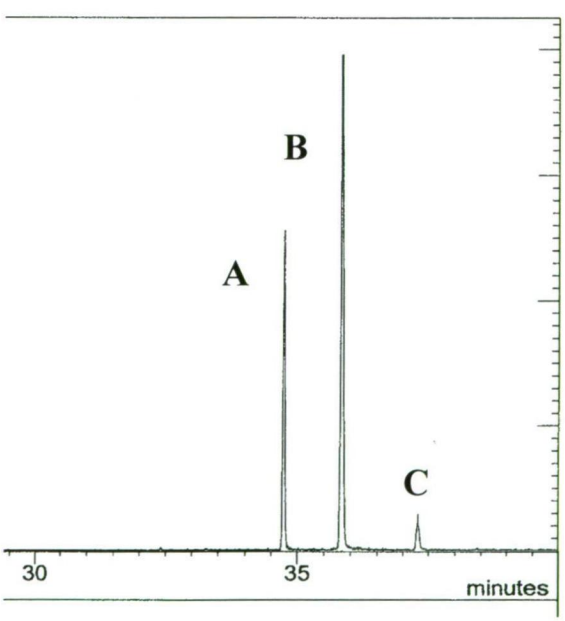

Retention Time

Figure 6.3 Part of a GC-MS trace of the reaction of 4-iodotoluene and phenylacetylene using $PdCl_2(pyCH_2SMe)$ as a precatalyst, indicating the products from the coupling reaction.

The structure of the products **A**, **B**, and **C** could not be determined, although high resolution mass spectrometry indicated a molecular formula of $C_{31}H_{24}$ (found

396.18768 calculated 396.18780) for all three products, consistent with $TolPh_3C_6H_2$. Column chromatography proved unsuccessful for the isolation of the compounds, while HPLC purification techniques were trialled but revealed that, under **A**, **B**, and **C**, more compound peaks were present which could not be separated by this technique. The complexity of **A**, **B**, and **C** was confirmed by extensive GC-MS analysis which also revealed multiple components to **A**, **B**, and **C**.

From this point forward, when a product distribution matching that of **Figure 6.3** is found, including variation in peak ratio, the notation **A**, **B**, and **C** is used for these components.

An approximate overall yield of the compounds (**A** + **B** + **C** = 32–45%) was determined using 1,2,4,5-tetraphenylbenzene (synthesised *via* Suzuki reaction of 1,2,4,5-tetrabromobenzene and phenylboronic acid)[7] as an internal standard for GC-MS analysis. Thus, products of molecular mass 396 having GC-MS characteristics similar to the standard 1,2,4,5-$Ph_4C_6H_2$ (retention time of ~32.8 minutes) are major products of the reaction and not low yield artefacts. Compounds **A**, **B**, and **C** may be structural isomers similar to 1,2,4,5-$Ph_4C_6H_2$, or may include other species such as Dewar benzenes. For simplicity throughout this preliminary study, the products with molecular mass corresponding to "tetraarylbenzenes" are assumed to have this general structure, although further analysis in a more extensive study is required.

In view of the observation of moderate to high yield of products differing from expected Sonogashira products, an extensive study has been commenced, *but not yet completed*, to explore the general applicability of the reaction and its mechanism.

6.2.2 Variation of Reaction Conditions

The first element of this study was an examination of the reaction of iodobenzene and phenylacetylene using the same conditions as the first two test reactions. Analysis of the completed reaction showed the presence of three product peaks matching the same pattern as **A**, **B**, and **C** with a molecular mass of 382 ($C_{30}H_{22}$, "$Ph_4C_6H_2$" in an approximate ratio of 35:60:5). Peak **A** matches that for 1,2,4,5-$Ph_4C_6H_2$ used as a standard for analysis of yield of products in **Figure 6.3**. A series of experiments were conducted in which the standard conditions were varied in order

to test whether selectivity of product formation can be varied, **Scheme 6.4**, and **Table 6.1**.

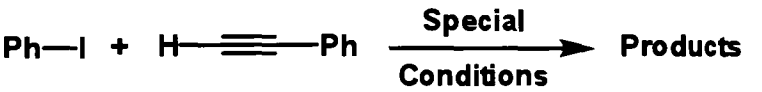

Scheme 6.4 Modification of reaction conditions using iodobenzene and phenylacetylene as substrates. Standard reaction conditions: 1 mol% Pd, 1.1 eq. of Bu^n_4NCl, 2 eq. of Na_2CO_3, 1.5 eq. of alkyne, under argon at 120 °C.

Entry	Special Conditions	Products
1	-	$C_{30}H_{22}$
2	10 mol% CuI (co-catalyst), NEt_3	$C_{30}H_{22}$
3	No Argon, reaction completed in air	$C_{30}H_{22}$
4	Reaction temperature 150 °C	$C_{30}H_{22}$
5	Reaction temperature 100 °C	20:80 mix*
6	Reaction temperature 80 °C	50:50 mix*
7	Reaction temperature 60 °C	80:20 mix*
8	Reflux in a sealed flask	$C_{30}H_{22}$
9	Ionic liquid as solvent (Bu^n_4NCl)	$C_{30}H_{22}$
10	No Bu^n_4NCl	$C_{30}H_{22}$
11	No Bu^n_4NCl, replaced with NaCl	$C_{30}H_{22}$
12	1:1 mixture of Bu^n_4NCl and NaCl	$C_{30}H_{22}$
13	No Na_2CO_3, replaced with NEt_3	$C_{30}H_{22}$
14	NaO_2CH present as catalyst reductant	$C_{30}H_{22}$

Table 6.1 GC-MS analysis of the products of reaction of iodobenzene and phenylacetylene using $PdCl_2(pyCH_2SMe)$ as a precatalyst, (*) denotes the formation of the Sonogashira product diphenylacetylene and "tetraryl benzene" (Ph_2C_2 : $Ph_4C_6H_2$), while the 3 unknown product peaks are denoted **A**, **B**, and **C** ($C_{30}H_{22}$, HRMS results for **A**, **B**, and **C**).

Products **A**, **B**, and **C** were obtained from all reactions. Presence of CuI, often present in Sonogashira reactions, did not affect the **A**:**B**:**C** product distribution (entry 2) nor did the absence of an argon atmosphere (entry 3), or raising the reaction temperature from 120 to 150 °C (4). Lowering of the temperature led to detection of the Sonogashira product diphenylacetylene (entries 5 – 7) until dominant at 60 °C (entry 7). Refluxing in a sealed flask gave the same products as obtained at 120 to

150 °C (entry 8), as did reaction in an ionic liquid at 120 °C (entry 9). The reaction was unaffected by the absence of Bu^n_4NCl (10), replacement of Bu^n_4NCl by NaCl (11), or the presence of a mixture of Bu^n_4NCl and NaCl (12). Temperature has a marked effect on the selectivity of product formation, indicating that the selectivity of "tetraaryl benzene" products and the Sonogashira product is tunable.

6.2.3 Variation of Aryl Halide

Various aryl halides (Ar^1–X) were reacted with phenylacetylene (Ar–C≡C–H) using the standard reaction conditions that are successful for the activated aryl halide 4-iodonitrobenzene; 1 mol% Pd, 1.1 eq. of Bu^n_4NCl, 2 eq. of Na_2CO_3, 1.5 eq. of alkyne, under argon, at 120 °C unless otherwise noted, **Table 6.2**.

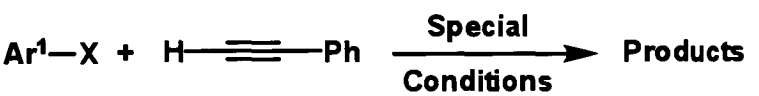

Entry	X	Ar^1	Special Cond.	Product
1	I	*p*-MeC_6H_4	-	$C_{31}H_{24}$[a]
2	I	*p*-$MeOC_6H_4$	-	$C_{31}H_{24}O$[a]
3	I	*p*-$F_3CC_6H_4$	-	$C_{31}H_{24}F_3$[a]
4	I	*p*-ClC_6H_4	-	$C_{30}H_{21}C$[a]
5	I	*m*-EtC_6H_4	-	$C_{32}H_{26}$[a]
6	Br	*p*-$MeCOC_6H_4$	-	Mostly m/z 306 ($Ph_3C_6H_3$), trace of $C_{32}H_{24}O$[a]
7	Br	*p*-$MeCOC_6H_4$	NEt_3	Mostly m/z 238 (Ar^1–C≡C–Ph)
8	Br	*p*-$MeCOC_6H_4$	CuI, NEt_3	$C_{32}H_{24}O$[a]
9	I	C_6F_5	-	Mostly m/z 306 ($Ph_3C_6H_3$)
10	Br	C_6F_5	-	Trace of $C_{30}H_{17}F_5$[a]
11	Br	C_6F_5	CuI, NEt_3	Mostly m/z 268 (Ar^1–C≡C–Ph), small amount of $C_{30}H_{17}F_5$[a]
12	Cl	*p*-$MeCOC_6H_4$	-	Mostly m/z 306 ($Ph_3C_6H_3$)
13	Cl	*p*-$MeCOC_6H_4$	CuI, NEt_3	Trace amount of $C_{32}H_{24}O$[a]

Table 6.2 GC-MS analysis of the products of reaction of various aryl halides and phenylacetylene using $PdCl_2(pyCH_2SMe)$ as a precatalyst. "Tetraaryl benzene" products denoted by molecular formulae, a denotes the presence of product peaks **A**, **B**, and **C**.

The results show that be "tetraaryl" substituted benzenes (denoted in the **Table 6.2** by **a**) are produced in most cases with little selectivity achieved. In the case of the aryl iodide substrates (entries 1 – 5, 9) three product peaks matching **A**, **B**, and **C** were identified with molecular masses corresponding to the presence of one moiety from the aryl halide and three acetylene moieties, as seen for **6a** and the results in **Table 6.1**.

However, when *p*-bromoacetophenone was used, a less reactive substrate in the Sonogashira reaction (entry 6), very little of the product peaks **A**, **B**, and **C** were observed, with the major product consisting of an unknown material with a molecular mass of 306 (believed to be an isomer of triphenylbenzene, a typical product in the [2 + 2 + 2] cyclotrimerisation of phenylacetylene). Consequently, this reaction combination was examined further with modifications including substitution of base for NEt_3 (entry 7), and the addition of CuI as a co-catalyst (entry 8). In the case of entry 7 the only product observed was an unknown compound with a molecular mass of 238 (corresponding to the homocoupling product of the aryl halide), but upon addition of 10 mol% of CuI (8) three product peaks matching **A**, **B**, and **C** were obtained.

For bromopentafluorobenzene (entry 10) a sole reaction product was observed with a molecular mass of 306. However, on addition of a catalytic amount of CuI (entry 11) two major products were identified, one at 268 corresponding to the expected Sonogashira coupling product, and products corresponding to the "tetraaryl" $C_{30}H_{17}F_5$. A similar observation was made in the case of entries 12 and 13, using standard conditions with the aryl chloride leading to a sole product with a molecular mass of 306, corresponding to triphenylbenzene. Addition of CuI (entry 13) led to the detection of one major peak with a molecular mass of 306 (triphenylbenzene), and three very minor peaks corresponding to "tetraaryl" species.

In general terms, the results indicate that "tetraaryl" products are more readily formed from aryl iodide reagents, except for C_6F_5I.

6.2.4 Variation of Alkyne

Standard conditions as described above were utilised unless otherwise noted, **Table 6.3**.

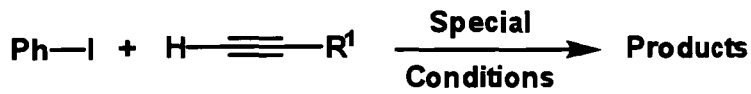

Entry	R^1	Special Cond.	Product
1	$PhCH_2$	-	$C_{31}H_{24}$, five "tetraaryl" peaks
2	Bu^t	-	$C_{28}H_{26}$, multiple "tetraaryl" peaks, and 240
3	Bu^t	CuI, NEt_3	$C_{28}H_{26}$, multiple "tetraaryl" peaks, and 240
4	*o*-MeC_6H_4	-	Mostly m/z 348 ($Tol_3C_6H_3$) and biphenyl
5	*o*-MeC_6H_4	CuI, NEt_3	Mostly m/z 348 ($Tol_3C_6H_3$) and biphenyl
6	H-C≡C-C_6H_4-C≡C-H	-	Plastic polymeric solid

Table 6.3 GC-MS analysis of the products of reaction of various alkynes with iodobenzene using $PdCl_2(pyCH_2SMe)$ as a precatalyst. "Tetraaryl" products denoted by molecular formulae.

In the reaction of iodobenzene and benzylacetylene (entry 1) "tetraaryl" products were detected. For *t*-butylacetylene under standard conditions, and with the addition of CuI (entries 2, 3 respectively), two unknown products were formed in each case, with molecular masses of 240 (unknown species) and a "tetraaryl" benzene. With the addition of CuI (entry 3) the proportion of "tetraaryl" product increased. In the reaction of iodobenzene and *o*-tolylacetylene under standard conditions and upon addition of CuI (entries 4 and 5), the major products of the reaction were biphenyl (produced from homocoupling) and an unknown compound with a molecular mass of 348 (corresponding to a tritolylbenzene product from the cyclotrimerisation of the alkyne) and a very small amount of a "tetraaryl" species. Addition of CuI resulted in a higher percentage of "tetraaryl" being formed. In the case of the reaction of 1,4-diethynylbenzene and iodobenzene (entry 7), a plastic like polymeric solid was obtained which could not be analysed using conventional techniques (this polymeric product is not obtained in other systems where iodobenzene and 1,4-diethynylbenzene are reacted using $PdCl_2(PPh_3)_2$ as a precatalyst).[8]

6.2.5 Comparison with Classical Sonogashira Catalysts and Other Bidentate Ligands

The precatalysts chosen were traditional phosphine containing catalysts for the Sonogashira reaction $Pd(PPh_3)_4$, $PdCl_2(PPh_3)_2$, $PdCl_2$(dmpe) (dmpe = 1,2-bis(dimethylphosphino)-ethane) (dmpe) as a representative of precatalysts containing a bidentate phosphine, together with $PdCl_2$(bipy) and $PdCl_2(MeSCH_2CH_2SMe)$ containing homoleptic ligands closely related to $pyCH_2SMe$, and the *N,Se* analogue $PdCl_2(pyCH_2SeMe)$.

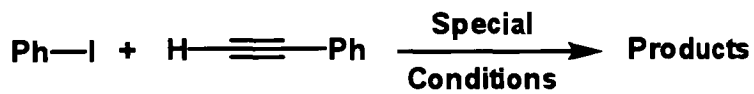

Entry	Special Conditions	Product
1	$Pd(PPh_3)_4$	Ph-C≡C-Ph, $C_{30}H_{22}$[a] (< 1%)
2	$PdCl_2(PPh_3)_2$	Ph-C≡C-Ph only
3	$PdCl_2$(dmpe)	Ph-C≡C-Ph and $C_{30}H_{22}$[a]
4	$PdCl_2(MeSCH_2CH_2SMe)$	Ph-C≡C-Ph and $C_{30}H_{22}$[a]
5	$PdCl_2$(bipy)	$C_{30}H_{22}$[a]
6	$PdCl_2(pyCH_2SeMe)$	$C_{30}H_{22}$[a], Ph-C≡C-Ph (< 5%)

Table 6.5 GC-MS analysis of the products of reaction of phenylacetylene with iodobenzene using various precatalysts, in the standard conditions described previously. "Tetraaryl" products are denoted by molecular formulae, a denotes the presence of product peaks **A**, **B**, and **C**.

In the case of the triphenylphosphine containing precatalysts (entries 1 and 2) the major product of the reaction was diphenylacetylene with, in the case of $Pd(PPh_3)_4$ only, a trace amount of a compound corresponding to a "tetraaryl" product. In the case of the bidentate phosphine ligand dmpe and the dithioether complex (entries 3 and 4), diphenylacetylene was produced, together with 3 products matching **A**, **B**, and **C**. In the case of the homoleptic bidentate *N*-donor ligand (entry 5), no diphenylacetylene was produced, with the sole products corresponding to three peaks matching **A**, **B**, and **C**. In the case of the selenium containing heteroleptic ligand

(entry 6), a small portion of diphenylacetylene was produced (< 5%) together with three peaks matching **A**, **B**, and **C**.

6.3 Conclusion

"Tetraaryl" products are synthesised in the catalytic reaction of aryl iodides and terminal aryl acetylenes at 120 °C using $PdCl_2(pyCH_2SMe)$ as a palladium(II) precatalyst, *apparently* the first reported case of such products synthesised using Sonogashira conditions. Although a full and extensive study of the identity of the formed products, and possible mechanism for the reaction, are yet to be undertaken.

For aryl iodides as substrates, lowering of the temperature from 120 °C results in the formation of typical Sonogashira products (diaryl acetylenes) together with "tetraaryl" products. Aryl bromides and aryl chlorides were observed to provide low, trace, or complete absence of "tetraaryl" products, and absence of diarylacetylenes.

Other precatalysts such as $PdCl_2(bipy)$ and $PdCl_2(pyCH_2SeMe)$ also produce "tetraaryl" products, while the traditional phosphine precatalyst $Pd(PPh_3)_4$ and $PdCl_2(PPh_2)_2$ show little to no indication of the formation of these compounds.

However, the formation of trace, or low, quantities of "tetraaryl" products using $Pd(PPh_3)_4$ and $PdCl_2(dmpe)$ indicate that these products may well be frequently obtained as minor by-products in Sonogashira catalysis, and thus are not being reported in the literature.

The moderate yield of "tetraaryl" products established for one system (iodobenzene and phenylacetylene) and confirmation by crystal structure analysis of the single product 1,3,5-triphenyl-2-(4-nitrophenyl)benzene (from 4-iodonitrobenzene and phenylacetylene), indicate that the $pyCH_2SMe$ system is suitable for further studies of this system.

It is anticipated that further studies may lead to elaboration of the mechanism, new methodologies for the synthesis of tetraarylbenzenes and related compounds, and

potential improvements in procedures to give typical diorganoacetylene Sonogashira products.

6.4 Experimental

6.4.1 General Experimental

The palladium precatalysts $PdCl_2(pyCH_2SMe)$ and $PdCl_2(pyCH_2SeMe)$ were prepared according to the procedure outlined in Chapter 3. Other complexes used in this study ($Pd(PPh_3)_4$,[9] $PdCl_2(PPh_3)_2$,[10] $PdCl_2(dmpe)$,[11] $PdCl_2(MeSCH_2CH_2SMe)$,[12] $PdCl_2(bipy)$[13]) and the "tetraaryl" standard 1,2,4,5-tetraphenylbenzene[7] were synthesised as reported. All other reagents used are commercially available from the Aldrich Chemical Co. and were used as received unless noted. Ultra high purity argon was purchased from BOC Gases. Gas chromatographic-mass spectrometry was conducted by Dr. Noel Davies of the Central Science Laboratory using a Varian 1200 triple quadrupole benchtop GC-MS.

6.4.2 Experimental Procedures

General procedure for reactions under Sonogashira conditions:

Standard Conditions:

The aryl halide (1.5 mmol) was added to a solution of alkyne (2.25 mmol, 1.5 eq.), Na_2CO_3 (2.0 eq.), catalyst (5.0 mg) and Bu^n_4NCl (1.5 eq.) in anhydrous *N,N*-dimethylacetamide (5 mL) under argon. The resulting mixture was then stirred at 120 °C for 24 h under Ar. Once cooled to room temperature an aliquot (1.50 mL) was taken and diluted with CH_2Cl_2, then washed three times with an aqueous solution saturated with NaCl. The organic layer was extracted, dried over $MgSO_4$, filtered and the sample analysed by GC-MS.

6.5 References

1. Hoger, S.; Rosselli, S.; Ramminger, A.–D.; Enkelmann, V. *Org. Lett.* **2002**, *4*, 4269.
2. Tong, L.; Lau, H.; Ho, D. M.; Pascal Junior, R. A. *J. Am. Chem. Soc.* **1998**, *120*, 6000.
3. Thaimattam, R.; Reddy, D. S.; Xue, F.; Mak, T. C. W.; Nagia, A.; Desiraju, G. R. *J. Chem. Soc., Perkin Trans. 2* **1998**, 1783.
4. Chinchilla, R.; Nájera, C. *Chem. Rev.* **2007**, *107*, 874.
5. Sonogashira, K. *J. Organomet. Chem.* **2002**, 653, 46.
6. Brandsma, L. *Synthesis of Acetylenes, Allenes and Cumulenes: Methods and Techniques;* Elsevier: Oxford, **2004**; 293.
7. Li, Z. H.; Wong, M. S.; Tao, Y. *Tetrahedron*, **2005**, *61*, 5277.
8. Songkram, C; Takaishi, K.; Yamaguchi, K.; Kagechika, H.; Endo, Y. *Tetrahedron Lett.* **2001**, *42*, 6365.
9. Crawforth, C.M.; Fairlamb, I.J. S.; Kapdi, A. R.; Serrano, J. L.; Taylor, R. J. K.; Sanchez, G. *Adv. Synth. Catal.* **2006**, *348*, 405.
10. Hahn, F. E.; Luegger, T.; Beinhoff, M. *Z. Naturforsch. B* **2004**, *59*, 196.
11. Gray, L. R.; Gulliver, D. J.; Levason, W.; Webster. M. *J. Chem. Soc., Dalton. Trans.* **1983**, 133.
12. Asanin, D. P.; Rajkovic, S.; Molnar-Gabor, D.; Djuran, M. I. *Monatsh. Chem.* **2004**, *135*, 1445.
13. Wehman, P.; Dol, G. C.; Moorman, E. R.; Kamer, P. C. J.; van Leeuwen, P. W. N. M.; Fraanje, J.; Goubitz, K. *Organometallics*, **1994**, *13*, 4856.

Appendix A

Publications Arising From Work in This Thesis

The candidate performed all synthetic chemistry for publications **1** and **3**, and a minor contribution ~15% made in the synthesis of functionalised monoliths in publication **2**. All publications involve Prof. Allan Canty and Dr. Michael Gardiner as the main supervisors who played a major role throughout the project. Further publications will arise from Chapters 2 – 4 to give publications on the synthesis of *N,E* heteroleptic ligands, their complexes and subsequent testing in Heck chemistry. A further publication is expected from Chapter 6 on the formation of tetrasubstituted benzenes.

Publications:

1) Jones, R. C.; Skelton, B. W.; Tolhurst, V.-A.; White, A. H.; Wilson, A. J.; Canty, A. J. *Polyhedron*, **2007**, *26*, 708.

2) Gömann, A.; Deverell, J. A.; Munting, K. F.; Jones, R. C.; Rodemann, T.; Canty, A. J.; Smith, J. A.; Guijt, R. M. *Tetrahedron*, **2009**, *65*, 1450.

3) Jones, R. C.; Canty, A. J.; Deverell, J. A.; Gardiner, M. G.; Guijt, R. M.; Smith, J. A.; Rodemann, T.; Tolhurst, V.-A. *Tetrahedron,* Supported Palladium Catalysis Using a Heteroleptic 2-Methylthiomethylpyridine –*N,S*-Donor Motif for Mizoroki-Heck and Suzuki-Miyaura Coupling, Including Organic Monolith in Capillary Microscale Flow-Through Mode, *Tetrahedron,* **2009**, submitted.